

# Sheffield Hallam University

*Molecular genetics and microbiology of bioremediation using methane-oxidising bacteria*

AL-LUAIBI, Yasin Y. Y.

Available from the Sheffield Hallam University Research Archive (SHURA) at:

<http://shura.shu.ac.uk/17361/>

## A Sheffield Hallam University thesis

This thesis is protected by copyright which belongs to the author.

The content must not be changed in any way or sold commercially in any format or medium without the formal permission of the author.

When referring to this work, full bibliographic details including the author, title, awarding institution and date of the thesis must be given.

Please visit <http://shura.shu.ac.uk/17361/> and <http://shura.shu.ac.uk/information.html> for further details about copyright and re-use permissions.

# **Molecular genetics and microbiology of bioremediation using methane-oxidising bacteria**

Yasin Y Y AL-Luaibi

A thesis submitted in partial fulfilment of the requirements of  
Sheffield Hallam University  
for the degree of Doctor of Philosophy

December 2015

## **Dedication**

**To Imam Ali and his sons**

**To all of my family**

<b>Table of contents</b>	<b>ii</b>
<b>List of figures</b>	<b>viii</b>
<b>List of tables</b>	<b>xi</b>
<b>Acknowledgements</b>	<b>xii</b>
<b>Declaration</b>	<b>xiii</b>
<b>Abbreviations</b>	<b>xiv</b>
<b>Abstract</b>	<b>xvii</b>

## Table of Contents

---

1	Introduction .....	1
1.1	Methanotrophic bacteria .....	1
1.1	The role of methane in the environment .....	6
1.2	Bioremediation of toxic substances by methane monooxygenase.....	8
1.3	Methanotrophs in Biotechnology.....	13
1.4	Methane monooxygenase enzyme .....	15
1.4.1	Particulate methane monooxygenase .....	16
1.4.2	Soluble methane monooxygenase (sMMO) .....	25
1.4.3	Components of sMMO .....	28
1.5	Copper effect in switching between pMMO and sMMO .....	39
1.6	Soluble diiron monooxygenase (SDIMO).....	45
1.6.1	Butane monooxygenase (BMO) .....	47
1.6.2	Toluene ortho- monooxygenase.....	50
1.6.3	Toluene/o-Xylene Monooxygenase (ToMO).....	53
1.6.4	Toluene 4-Monooxygenase (T4MO).....	58
1.6.5	T4MO from <i>Bradyrhizobium</i> sp. BTAi1 (T4MO.BTAi1).....	63
1.6.6	Toluene 3- Monooxygenase from <i>Ralstonia pickettii</i> PKO1 (T3MO) . .....	66
1.6.7	Ribonucleotide reductase (RNR).....	68

1.6.8	Deoxyhypusine hydroxylase (DOHH).....	73
1.6.9	Stearoyl ACP desaturase .....	75
1.7	Aims of the present study .....	78
2.1	Bacterial strains and growth conditions.....	80
2.1.1	Bacterial strains and plasmids.....	80
2.1.2	Culturing the isolates and mutants .....	81
	Chemical reagents and media for bacterial cultures growth .....	83
2.2	General DNA methods.....	83
2.2.1	QIAprep spin plasmid miniprep protocol.....	84
2.2.2	QIAprep spin plasmid maxiprep protocol.....	85
2.2.3	QIAquick gel extraction protocol.....	86
2.2.4	QIAEX II gel extraction kit .....	86
2.2.5	Phenol/ Chloroform/ Isoamyl alcohol extraction .....	87
2.2.6	Electrophoresis of DNA .....	88
2.2.7	Digestion by restriction enzymes.....	88
2.2.8	DNA phosphatase .....	89
2.2.9	DNA ligation .....	89
2.3	DNA template preparation and PCR manipulation conditions.....	90
2.3.1	Colony template preparation .....	90
2.3.2	Genomic DNA extraction using Qiagen genomic tip-20 kit.....	90
2.3.3	Genomic DNA preparation using Qiagen QIAamp DNA Mini kit ...	91
2.4	Preparation of <i>E. coli</i> S17.1 CaCl <sub>2</sub> competent cells .....	92
2.4.1	Transformation of CaCl <sub>2</sub> competent cells .....	93
2.4.2	Transforming <i>Methylosinus trichosporium</i> SMDM by conjugation .	93
2.4.3	Conjugation procedure .....	94
2.5	Sequences of primers used in the study.....	95
2.5.1	Standard PCR protocol .....	96
2.5.2	Four primeroverlap PCR .....	97

2.5.3	Ligation of mutant <i>mmoX</i> genes into pJET 1.2.....	99
2.5.4	Double digestion of purified mutated <i>mmoX</i> gene with <i>Bam</i> HI and <i>Nde</i> I .....	101
2.5.5	Cloning the constructed mutants into the His-tag expression plasmid pT2MLY.....	101
2.6	Cell preparation for protein purification .....	103
2.6.1	Preparation of the hydroxylase and reductase for purification.....	103
2.6.2	Purification of the hydroxylase .....	104
2.6.3	Purification of the reductase.....	105
2.6.4	Purification of protein B .....	106
2.7	Protein quantification .....	107
2.8	Protein visualization via SDS-PAGE .....	108
2.9	Cell preparation and substrates oxidation assay .....	109
2.9.1	Whole cell oxidation test.....	109
2.9.2	Soluble extract assay .....	109
2.9.3	Colorimetric naphthalene test.....	110
2.10	Oxidation of mono-, di- and tri-aromatic compounds by <i>Ms. trichosporium</i> OB3b (wild type), wild type with His-tag and mutants. ....	111
2.11	Propylene oxidation assay.....	112
2.11.1	Propylene oxidation assay for whole cell.....	112
2.11.2	Propylene oxidation assay for soluble extract .....	113
2.12	Statistical analysis .....	115
3	Protein purification .....	116
3.1	Purification of sMMO componenets by anion exchange chromatography .....	116
3.2	His-tag affinity system.....	117
3.3	GST-fusion affinity system.....	118
3.4	Solid phase microextraction (SPME) .....	119
3.5	Experimental work and Results .....	120

3.5.1	Purification of the His-tagged hydroxylase (MMOH).....	120
3.5.2	Purification of protein B (MMOB).....	124
3.5.3	Purification of the reductase (MMOR) .....	127
3.6	Enzyme activity .....	130
3.6.1	Growth of mutant F282L.....	130
3.6.2	Propylene assay for soluble extract.....	132
3.7	Discussion .....	137
Chapter 4: The role of C151 .....		140
4	Investigating the role of Cysteine 151 in MMOH $\alpha$ -subunit in providing free radicals during the catalytic cycle of sMMO .....	140
4.1	Introduction .....	140
4.1.1	Residues corresponding to Thr 213 and Cys 151 in other diiron enzymes .....	142
4.1.2	Mutagenesis of residues Cys151 and Thr213 .....	143
4.2	Investigation of mutant C151S in the $\alpha$ -subunit of sMMO .....	145
4.3	Site-directed mutagenesis .....	146
4.3.1	Characterization and naphthalene test for C151S.....	148
4.4	Investigating the role of C151S in oxidation of aromatic compounds.152	
4.4.1	The C151S mutant showed regioselectivity in oxidation of the monoaromatic hydrocarbon toluene .....	152
4.4.2	Oxidation of ethyl benzene by C151S yields regiospecific products different from OB3b and His-tag wt.....	155
4.4.3	Oxidation and product distribution from naphthalene by C151S .158	
4.4.4	C151S showed no detectable activity toward mono-aromatic mesitylene, the di-aromatic hydrocarbon biphenyl, and tri-aromatics anthracene and phenanthrene.....	160
4.4.5	Propylene oxidation assay for the C151S mutant showed the production of propylene oxide.....	160
4.5	Discussion .....	163

Chapter 5: Investigating the role of hydrophobic and hydrophilic residues within and outside the hydroxylase active site.....	166
5.1 Introduction .....	167
5.2 Construction of C151Y E114D and E114D .....	168
5.3 Mutagenesis of the proposed substrate gating residue Phe 188 .....	170
5.4 Mutants R98L, R98A and R98A S4G .....	172
5.4.1 Construction and cloning of mutants E114D C151Y, E114D, R98A and R98A S4G using vectors pTJS175 and pT2MLY .....	174
5.4.2 Ligation of mutant <i>mmoX</i> genes into pJET 1.2.....	175
5.4.3 Double digestion of purified mutated <i>mmoX</i> gene with <i>Bam</i> HI and <i>Nde</i> I .....	178
5.4.4 Cloning of mutant into His-tag expression plasmid pT2MLY .....	179
5.4.5 Purification of His-tagged mutant hydroxylases .....	183
5.4.6 No detectable naphthalene product in GC-MS for naphthalene positive E114D on NMS plates .....	185
5.4.7 Oxidation of toluene by the E114D mutant.....	185
5.4.8 E114D produced 1-phenyl ethanol from ethyl benzene.....	187
5.4.9 Mutant E114D showed no activity towards the di-aromatic or tri-aromatic substrates in GC assays. ....	188
5.5 Transformation of <i>E. coli</i> S17.1 with pT2MLY F188W and R98L and then conjugation with <i>Ms. trichosporium</i> SMDM.....	189
5.5.1 Purification of the His-tag hydroxylase from mutants R98A and R98A S4G.....	190
5.5.2 Oxidation of naphthalene by mutant R98L and product distribution ..	192
5.5.3 Oxidation of ethyl benzene by the R98L mutant results in increased activity. ....	193
5.5.4 No recognizable activity could be seen for R98L towards the tri-aromatic compound anthracene or phenanthrene .....	197
5.6 Discussion .....	198

5.6.1	Sequential ligation by using two plasmids for the mutated overlap PCR .....	198
5.6.2	Mutation of C151Y mutant to double mutant E114D C151Y .....	198
5.6.3	Mutation of glutamic acid 114 to aspartic acid (mutant E114D) ..	199
5.6.4	Activity of transconjugated R98L, F188W, R98A and R98A S4G .....	201
	Chapter 6: General discussion, summary and future work .....	203
6.1	Protein purification .....	204
6.1.1	Purification of hydroxylase .....	204
6.1.2	Purification of protein B .....	206
6.1.3	Purification of protein C .....	207
6.1.4	Activity of purified protein .....	208
6.2	Mutants construction.....	211
6.2.1	Using two cloning steps to facilitate cloning of mutants and minimise PCR-derived errors.....	211
6.3	Mutation of Cys151 to Ser proved that the thiol group from cysteine is not essential for the oxidation of substrates tested in the present study .....	212
6.4	Mutants R98L, R98A and R98A S4G .....	213
6.5	Mutants E114D C151Y and E114D .....	215
6.6	Summary and future work.....	218
	Preparation of 1 x NMS Medium .....	221

---

# List of figures

---

Figure 1.1 Two distinct arrangement of intercellular membrane in methanotrophs shown by electron microscopy. ....	4
Figure 1.2 Structure of pMMO from <i>Methylococcus capsulatus</i> (Bath). ....	19
Figure 1.3 Structure of single protomer from pMMO purified from <i>Mc. capsulatus</i> Bath. ....	21
Figure 1.4 Soluble methane monooxygenase from three different methanotrophs. ....	27
Figure 1.5 The structure and the geometry of active site within the hydroxylase from <i>Methylococcus capsulatus</i> Bath. ....	29
Figure 1.6 Hydroxylase cavities and some changing during MMOH-MMOB complex formation. ....	32
Figure 1.7 Structure of protein B from <i>M. capsulatus</i> . ....	35
Figure 1.8 Conformational changes in the formation of complex MMOH-MMOB. ....	36
Figure 1.9 Structure of reductase protein from <i>M. capsulatus</i> Bath. ....	38
Figure 1.10 The suggested role of methanobactin and <i>mmoD</i> gene in copper regulation by Semrau <i>et al.</i> , (2013) in <i>Methylosinus trichosporium</i> OB3b. ....	44
Figure 1.11 Mutation of amino acids in ToMO active site centre. ....	56
Figure 1.12 The two proposed route for substrate migration into the active site in T4MO. ....	61
Figure 1.13 Crystallographic structure of Diiron centre in R2 of ribonucleotide reductase. ....	70
Figure 1.14 Three dimensional schematic showing the hydrogen bond connection of residue Asp 237 with Trp 48 and His 118 in the radical transfer pathway. ....	71
Figure 2.1 Construction of mutant by using overlap PCR. ....	97
Figure 2.2 Cloning steps for introduction of the mutated <i>mmoX</i> gene into vector pJET1.2. ....	99
Figure 2.3 Diagram showing the construction of the His-tagged expression system pT2MLY and the cloning steps to introduce the mutated <i>mmoX</i> gene into this plasmid. ....	101
Figure 2.4 Solid Phase microextraction (SPME) apparatus ....	113

Figure 3.1 Purification of sMMO hydroxylase and reductase by Anion Exchange chromatography.....	121
Figure 3.2 SDS-16%PAGE showing the His-tagged hydroxylase purified by Anion exchange and Ni-NTA affinity column from wild type with His-tag soluble extract, and the attempted purification of the reductase ..	123
Figure 3.3 SDS-12% PAGE showing the His-tagged hydroxylase purified from the wild type with His-tag soluble extract by using different concentrations of histidine dissolved in phosphate buffered saline.....	123
Figure 3.4 Agarose (1%) gel electrophoresis showing restriction and analysis of pGEX-2T <i>mmoB</i> using <i>Bam</i> HI and <i>Eco</i> RI in pGEX-2T in <i>E.coli</i> BL-21.....	124
Figure 3.5 Time course of IPTG induction of protein B fused with GST expressed	124
Figure 3.6 Purification of protein B fused with the GST affinity tag from <i>E. coli</i> BL-21 by GSTrap affinity column chromatography. ....	126
Figure 3.7 Purification of protein C in gel filtration column (Superdex 75). ....	128
Figure 3.8 SDS-PAGE for soluble extract and purified His-tagged hydroxylase subunits from mutant F282L. ....	131
Figure 3.9 traces showing the activity of the whole cells and soluble extract containing the wild type His-tagged hydroxylase toward propylene .....	133
Figure 3.10 Propylene assay by using Solid phase microextraction (SPME) under various conditions. ....	135
Figure 4.1 The position of Cys151 and Thr213 near the diiron centre of sMMO where the proposed binding site for methane and other substrates lies. ....	140
Figure 4.2 Diagram explaining the order of the genes <i>mmoXYBZDC</i> in the sMMO operon. ....	146
Figure 4.3 <i>mmoX</i> gene detection for <i>M. trichosporium</i> parental strain OB3b, wild type with His-tagged hydroxylase and mutant C151S.....	149
Figure 4.4 <i>mmoX</i> gene sequencing for C151S comparing to OB3b and His-tag wild type.....	151
Figure 4.5 The significant difference of toluene oxidation products between C151S comparing to OB3b and wt. His-tag. ....	153
Figure 4.6 Comparing the raw data for Ethyl benzene oxidation by C151S, OB3b and wt. His-tag showing no significant difference between them at $p < 0.05$ , 0.01, and $p < 0.001$ .....	157

Figure 4.7 Product distribution percentages from naphthalene oxidation by mutant C151S.....	159
Figure 4.8 Propylene oxidation assay by C151S whole cells.....	162
Figure 5.1 The diiron centre of sMMO.and the position of residues E114 and C151. ....	168
Figure 5.2 The oxidation and reduction form of the active site showing the movement of residues L110 and Phe 188. ....	171
Figure 5.3 sMMO hydroxylase showing the position of R98 .....	172
Figure 5.4 PCR with four primers to construct new mutants. ....	175
Figure 5.5 Representative agarose gels showing cloning steps for mutated <i>mmoX</i> gene R98A, E114D in pJET1.2.....	176
Figure 5.6 Double digestion of amplified R98A and E114D mutant genes. ...	177
Figure 5.7 Naphthalene oxidation assays for the new mutants.....	180
Figure 5.8 Deduced sequences of amino acid for the new mutants compared to wild type OB3b and C151S.....	181
Figure 5.9 The soluble extract and His-tagged hydroxylase for the mutants E114D and E114D C151Y, compared to the His-tagged wild type hydroxylase. ....	184
Figure 5.10 Detection of <i>mmoX</i> gene for mutants R98L and F188W.....	190
Figure 5.11 The soluble extract and purified His-tagged hydroxylase for the mutants R98A and R98A S4G compared to the His-tagged wild type hydroxylase.....	191
Figure 5.12 GC trace showing peaks of products from ethyl benzene oxidation by mutant R98L.....	194
Figure 5.13 Comparing the original data for three triplicate samples for mutants R98L with OB3b and His-tagged wt. ....	196
Figure 5.14 Soluble methane monooxygenase hydroxylase showing the position of the S4G mutant. ....	203

## List of tables:

---

Table 1.1 Classification of aerobic methanotrophic bacteria.....	5
Table 1.2 The most common substrates oxidized by sMMO and the oxidation products.....	10
Table 1.3 Operon organization of soluble methane monooxygenase and other diiron enzymes.....	46
Table 1.4 Product distribution of hydroxylation of benzene (165 $\mu$ M) to phenol, catechol, and 1, 2, 3-THB by T4MO, TOM, and T3MO (Tao <i>et al.</i> , 2004).....	62
Table 2.1 Plasmids used in the present study.....	80
Table 2.2 Sequences of primers used in construction of the mutants in the present study .....	94
Table 2.3 Table shows the substrates, substrate concentrations, incubation period, and the internal standard (if used in the assay) to estimate the ability of sMMO in oxidation mono-, di- and tri-aromatic compounds.....	111
Table 4.1 Product distribution percent of toluene oxidation by C151S.....	152
Table 4.2 Distribution of products from oxidation of the monoaromatic ethyl benzene by parental methanotrophs OB3b, His-tag wild type and mutant C151S.....	156
Table 4.3 Distribution of products 1-naphthol and 2-naphthol from naphthalene oxidation by mutant C151S.....	159
Table 5.1 Distribution of toluene oxidation product by E114D comparing to OB3b and His-tag wild type. ....	186
Table 5.2 Oxidation of ethyl benzene by mutant E114D, OB3b and His-tagged wild type.....	188
Table 5.3 Oxidation of naphthalene by mutant R98L and product distribution percentages.....	192
Table 5.4 Distribution of products from ethyl benzene oxidation by OB3b, His-tag wild type and mutant R98L.....	195

## **Acknowledgements**

Firstly I am very grateful to my supervisor Professor Thomas J. Smith (Sheffield Hallam University) for all the advice and support he has given me during my PhD, without his encouragement this thesis would not have been possible. I would also like to thank my collaborator Professor J. Colin Murrell (University of East Anglia) who has given me support throughout my time working on sMMO; and thanks to my second supervisor Karen N. Stanley who also given me advice help go through this work.

I would also like to thank Professor Nicola Woodroffe and the BMRC (Sheffield Hallam University) for allowing me to carry out this PhD.

I am very indebted Dr. Tim Nichol (Sheffield Hallam University) for his help all the time in the microbiology lab. Thanks most go for Khaled AL-Shamaki, Mariam and all other, past and recent PhD student for their continued support.

I would also like to thank the technical staff here at Sheffield Hallam University, particularly Dan English in the internal store, Michael Cox and Dan Kinsman for help with the GC and GC-MS.

Outside of the laboratory I would like to thank my family in Iraq: my mother, brothers and sisters and small family here with me particularly my wife Zahraa who has shown complete patience and understanding at all times and for my three Angels Mohammed, Hussein and Nerjiss.

I would like finally give special thanks for the Iraqi government represented by the Ministry of Higher Education and Scientific Research and the University of Basra for founding my scholarship.

## **Declaration**

I declare that the work described herein to study the soluble methane monooxygenase enzyme using mutagenic methods was conducted by me under the supervision of Prof. Thomas J. Smith, Dr. K. N. Stanley Sheffield Hallam University, and Prof Collin J. Murrell, University of East Anglia and none of the work has been previously submitted for any other degree. Contribution from others has been specifically acknowledged.

The construction of mutant C151S and C151Y in the system pTJS175 was done by Prof. Thomas J. Smith when he was working at University of Warwick.

The construction of the new His-tag system and creation of plasmid pT2MLY were performed by Dr. Malcolm Lock and Dr. Tim Nichol from Sheffield Hallam University.

Part of this work in Chapter 4 and part of Chapter 5 will be prepared to publish in a paper with proposed title: Mutagenesis studies to probe the stability and substrate-enzyme interactions in soluble methane monooxygenase

All sources of information have been referenced

Yasin Y Y AL-Luaibi

December 2015

# Abbreviations

---

ATP	adenosine triphosphate
BLAST	basic local alignment search tool
BMO	butane monooxygenase
bp	base pair
CD spectroscopy	Circular dichroism spectroscopy
CBM	copper binding molecules
DEAE	diethyl amine ethylene
DNA	deoxyribonucleic acid
DNase	deoxyribonuclease
DOHH	deoxyhypusine hydroxylase
EDTA	ethyldiaminetetraacetic acid
EPR	electron paramagnetic resonance
g	gram
GST	glutathione S-transferase
IPTG	isopropyl $\beta$ -D-thiogalactopyranoside
kDa	kilo Daltons
LB	Luria-Bertani
mb	methanobactin
MDH	methanol dehydrogenase
mg	milligram
ml	millilitre
$\mu$ l	micro litre
$\mu$ g	microgram
mM	milli molar
mRNA	messenger RNA
MS	mass spectrometry

m/z	mass-to-charge ratio in GC chart
ng	nanogram
nmol	nanomole
NCBI	National Centre for Biotechnology Information
NIST	National Institute for Standards and Technology
Ni-NTA	Nickel-nitrilotriacetic acid
NMR	nuclear magnetic resonance
NMS	nitrate mineral salts
OD	optical density
ORF	open reading frame
<i>ori</i>	origin of replication
<i>oriT</i>	origin of transfer
PAGE	polyacrylamide gel electrophoresis
PCR	polymerase chain reaction
pMMO	particulate methane monooxygenase
ppm	part per million
RNA	ribonucleic acid
RNase	ribonuclease
RNR	ribonucleotide reductase
RuMP	ribulose monophosphate
SCP	single cell protein
SDS	sodium dodecyl sulphate
sMMO	soluble methane monooxygenase
SPME	solid phase microextraction
TAE	tris acetate EDTA
TCE	trichloroethylene
TEMED	N, N, N, N-tetramethyl-ethane-1, 2-diamine

TOM	toluene monooxygenase
T4MO	toluene 4-monooxygenase
ToMO	toluene <i>ortho</i> -monooxygenase
v/v	volume/volume
w/v	weight to volume

## Abstract

Methanotrophic bacteria can grow on methane as their sole source of carbon and energy. *Methylosinus trichosporium* OB3b is a Gram negative, methanotrophic bacterium, which can convert methane to methanol by either particulate (pMMO) or soluble (sMMO) methane monooxygenase. The sMMO comprises three polypeptides; hydroxylase ( $\alpha\beta\gamma$ )<sub>2</sub>, regulator/coupling protein (protein B), and reductase. The hydroxylase contains the diiron active site.

The three components of sMMO are found to be indispensable for full enzyme activity. In the present study, the sMMO hydroxylase was purified by anion exchange chromatography and protein B fused with GST was purified by using affinity chromatography. Attempts to purify the reductase were unsuccessful although the reductase was detected during the purification steps. To shorten the long purification protocol of the hydroxylase and minimize the loss of its activity during multiple purification steps, a new system was developed by inserting a His-tag in the wild type hydroxylase  $\beta$ -subunit. The His-tag hydroxylase was then purified in one step by using an affinity column. The new His-tag system yields hydroxylase with detectable activity when it was tested toward propylene. Solid phase microextraction (SPME) was used for the first time in the present study to detect the product propylene oxide from propylene oxidation for the wild type His-tagged hydroxylase.

Crystallographic studies have suggested roles for a number of amino acids within and around the active site. The present study used site-directed mutagenesis to create four new mutants in addition to performing further characterization of another two. The mutation C151S preserved activity toward a range of substrates, and indicated that radical chemistry at this position is not

essential for monooxygenase activity toward a number of aliphatic and aromatic hydrocarbons. Results from other mutations included stabilising a previously unstable mutant (C151Y) with a secondary mutation to gain the double mutant E114D C151Y. The mutant R98L showed activity toward the monoaromatic substrate ethyl benzene and the diaromatic substrate naphthalene. Mutation of one of the diiron site coordinating residues E114D resulted in a stable hydroxylase with activity toward naphthalene. In terms of the oxidation of the triaromatic hydrocarbons anthracene and phenanthrene, no activity could be detected for the mutants tested in the present study or the wild type.



# Chapter 1: Introduction and literature review

---

## 1 Introduction

### 1.1 Methanotrophic bacteria

The term methanotroph refers to bacteria that can grow on methane as their sole source of carbon and energy. Currently known methanotrophs are gram negative that show substantial diversity. Various examples are mesophilic, neutrophilic, psychrophilic, thermophilic, halophilic and moderate acidophilic (Hanson and Hanson, 1996). Methanotrophs are rod or cocci shaped; in addition, two filamentous methanotrophs have also been described *Crenothrix polyspora* (Stoecker *et al.*, 2006) and *Clonothrix fusca* (Vigliotta *et al.*, 2007). A facultative methanotroph *Methylocella silvestris*, which can grow on either methane or multicarbon compounds, has also been isolated (Theisen *et al.*, 2005). Methanotrophs have been isolated from various sites including; soils, peat lands, rice paddies, sediments, fresh water and marine, acidic hot springs, mud pots, alkaline soda lakes, cold environments and tissues of higher organisms (Smith and Murrell, 2009), as well as from even more extreme environments, since three thermoacidophilic methanotrophs belonging to the phylum Verrucomicrobia named *Methylacidiphilum inferorum* V4T (Dunfield *et al.*, 2007), *Methylacidiphilum fumariolicum* SolV (Polet *et al.*, 2007) and *Methylacidiphilum kamchatkense* Kam1 (Islam *et al.*, 2008), were isolated from an environment with pH 1.5 and 65°C.

Methanotrophic bacteria were also detected from animal tissues, though they have not been grown on culture media (Cavanaugh, 1993). There is considerable evidence that methanotrophs can form a symbiotic relationship with other organisms. For example, Luo *et al.* (2007) found that up to 99% of phenol at a concentration 600 mg/ L could be oxidized during the first 11 h of growth of a consortium including *Methylosinus trichosporium* (OB3b) and methane as unique source for carbon and energy.

Although, pure cultures capable of anaerobic methane oxidation have not been obtained, there is a strong evidence to support the presence of such bacteria in environments rich with sulphate which suggests sulfate as the terminal acceptor of electrons (Dalton 2005).

The high diversity of places where the methanotrophic bacteria have been identified may indicate that there are many other methanotrophs that have not been isolated yet.

The isolation of over 100 new methane-utilizing bacteria as pure cultures by Whittenbury *et al.* (1970) established the fundamental construction of current classification of these organisms. Whittenbury *et al.* divided methanotrophic bacteria initially into two types depending on the cell morphology and intracytoplasmic membrane structure; type I and type II methanotrophs. Type 1 methanotrophs have intracytoplasmic membrane arranged in a vesical like form (Figure 1.1A). This type can assimilate formaldehyde into biomass through the ribulose monophosphate pathway (RuMP). This type includes the genera: *Methylococcus*, *Methylobacter* and *Methylomonas*, which belong to gamma proteobacteria. Type II methanotrophs contain intracellular membrane organised as peripheral concentric layers (Figure 1.1B). This group contains the

genera *Methylosinus* and *Methylocystis*, which belong to the alphaproteobacteria. The pathway this group uses in assimilation of formaldehyde into biomass is the serine pathway (Hanson and Hanson, 1996). Type X was added to include the methanotrophs which can assimilate the formaldehyde into biomass via the RuMP and sometimes by the serine pathway such as *Methylococcus capsulatus* (Bath) (Whittenbury, 1981; Whittenbury and Dalton 1981; Whittenbury and Krieg, 1984).

Cultured methanotrophs from the phylum Verrucomicrobia as mentioned above, are able to oxidize methane under extreme conditions (pH 1.5 and temperature 65°C) suggesting that these bacteria should be a third group of methanotrophs. Dunfield *et al.*, (2007) have found that the verrucomicrobial *Methylacidiphilum inferorum* constitute a sac like structure inside the cell containing a tubular membrane. In addition it contains intracytoplasmic membranes arranged in parallel layers which are similar to that in other methanotrophs. The intracytoplasmic membrane may accommodate the particulate methane monooxygenase (pMMO), which is produced, by almost all methanotrophic bacteria except *Methylocella*. The other enzyme in methanotrophs named soluble methane monooxygenase (sMMO) which is produced by a sub-set of methanotrophic bacteria such as *Methylococcus capsulatus* (Bath), *Methylosinus trichosporium* (OB3b) and others (Dalton, 2004).

The filamentous methanotrophs *Crenothrix polyspora* (Stoecker *et al.*, 2006) and *Clonothrix fusca* (Vigliotta *et al.*, 2007) were classified as a new subgroup of methanotrophs belonging to the Gammaproteobacteria. They are able to oxidize methane with an inner membrane arrangement similar to that in  $\gamma$ -proteobacteria methanotrophs. The other details about the methanotrophs can be found in (Table 1.1).

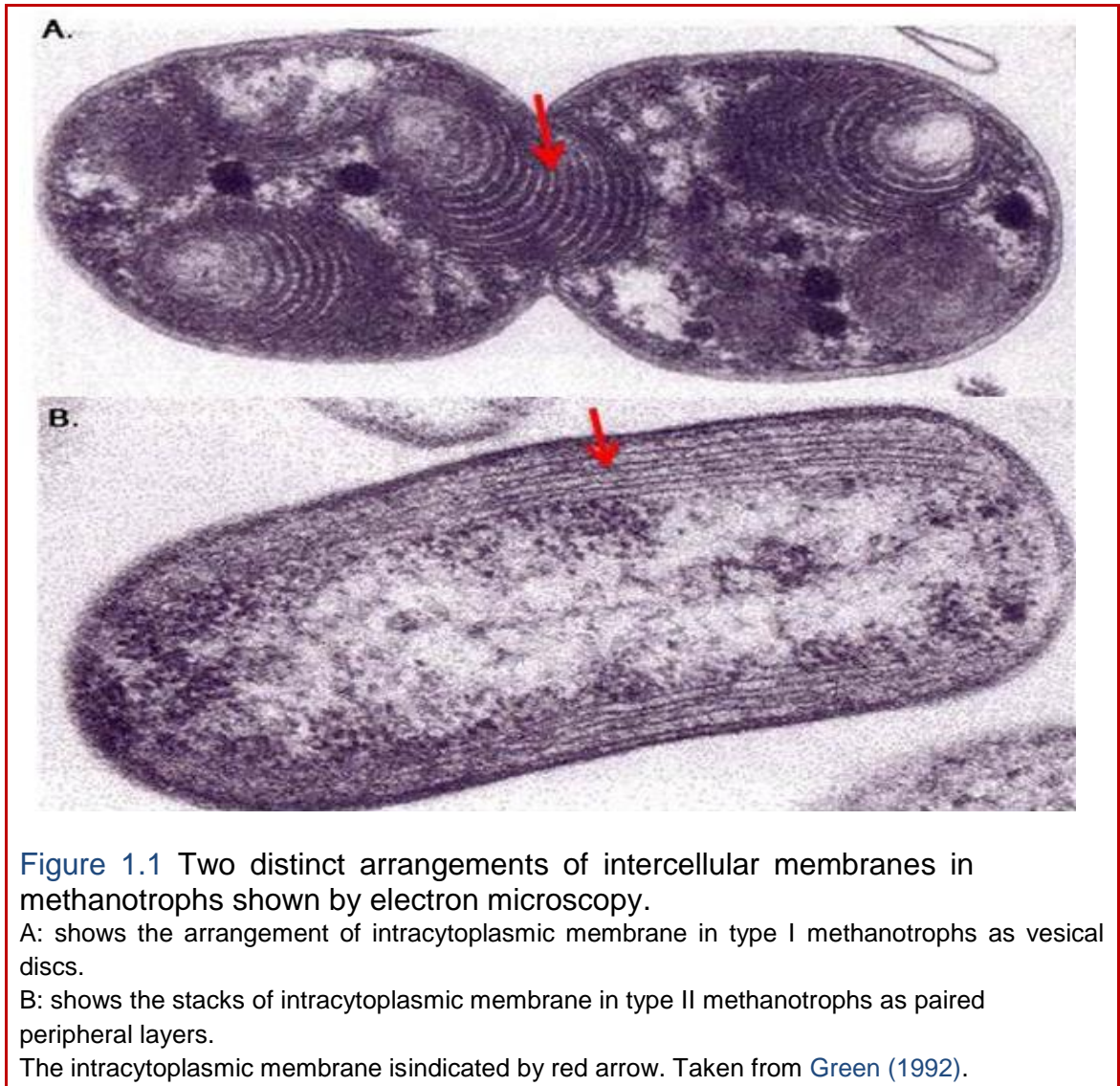


**Table 1.1** Classification of aerobic methanotrophic bacteria.

Type	Phylum	Genus	C1 assimilation	MMO type	Tropic niche
Type I	γ-Proteobacteria	<i>Methylobacter</i>	RuMP	pMMO	some psychrophilic
		<i>Methylomonas</i>	RuMP	pMMO+/-sMMO	some psychrophilic
		<i>Methylosoma</i>	not known	pMMO	not extreme
		<i>Methylochromium</i>	RuMP	pMMO+/-sMMO	Halotolerant; alkaliphilic
		<i>Methylothermus</i>	RuMP	pMMO	thermophilic
		<i>Methylohalobius</i>	RuMP	pMMO	halophilic
		<i>Methylosarcina</i>	RuMP	pMMO	not extreme
		<i>Methylosphaera</i>	RuMP	pMMO	psychrophilic
Type II	α-Proteobacteria	<i>Methylcystis</i>	Serine	pMMO+/-sMMO	some acidophilic
		<i>Methylosinus</i>	Serine	pMMO+/-sMMO	not extreme
		<i>Methylocapsa</i>	Serine	pMMO	acidophilic
		<i>Methylocella</i>	Serine	sMMO	acidophilic
Type X	γ-Proteobacteria	<i>Methylococcus</i>	RuMP/Serine	pMMO+/-sMMO	thermophilic
		<i>Methylocaldum</i>	RuMP/Serine	pMMO	thermophilic
Others	γ-Proteobacteria	<i>Crenothrix polyspora</i>	RuMP/Serine?	pMMO	not extreme
	γ-Proteobacteria	<i>Clonothrix fusca</i>	RuMP/Serine?	pMMO	not extreme
	Verrucomicrobia	<i>Methylacidiphilum</i>	RuMP/Serine?	pMMO	acidophilic

RuMP: Ribulose mono phosphate, pMMO: particulate methane monooxygenase, sMMO: soluble methane monooxygenase.

Adapted from [Smith and Murrell, \(2010\)](#) and [Jiang et al., \(2010\)](#)

## 1.1 The role of methane in the environment

Methane, a one-carbon compound with a formula CH<sub>4</sub>, is one of the most important gases in atmosphere. It causes a global warming due to its high ability to absorb the infrared and then re-emitt radiation causing reduction of the ozone layer leading to global warming (Lelieveld *et al.*, 1993). During the last 320 years, the concentration of methane has increased from 0.75 to 1.75 ppm and it may reach to 4.0 ppm by 2050 (Ramanathan *et al.*, 1985). The global warming potential of methane which is 25 times more than CO<sub>2</sub>, makes methane more severe global warming factor (IPPC Fourth assessment report: Climate Change 2007: 2.10.2). The methane arrives to the atmosphere via many sources including natural, anthropogenic sources, wetlands, rice paddies, intestines of ruminants, lakes, oceans, soils, oil and even termites (Dalton 2005).

The unique step of the CH<sub>4</sub> oxidation pathway is the conversion of methane to methanol by methane monooxygenase (MMO) from methanotrophic bacteria. Methanotrophs oxidize methane to methanol via two important enzymes; particulate methane monooxygenase and soluble methane monooxygenase by incorporation of an oxygen molecule across the C-H bond to produce methanol (Dalton, 1980; Feig & Lippard, 1994; Lipscomb, 1994; Wallar & Lipscomb, 1996; Merx *et al.*, 2001) as in the equation below:



This important reaction has attracted considerable interest from many researchers for many reasons; methane can serve as a source for energy and

as a chemical feedstock in industry Smith and Dalton, 2004). The major problem with methane is the difficulty of transport since methane is a gas. This problem can be overcome by converting methane to more easily transportable liquid methanol (Periana *et al.*, 1993). The conversion of methane (which has a very unreactive C-H bond) to methanol chemically needs a high energy  $>100 \text{ kcal mol}^{-1}$ , hence the conversion of methane to methanol by methane monooxygenase makes this enzyme potentially interesting commercially (Rosenzweig *et al.*, 1997). Also an understanding of how MMO can oxidize methane could inform the design of small-molecule catalysts to perform the reaction more effectively on an industrial scale. It is known that methane causes an increasing in global warming; methanotrophs via their methane monooxygenase can be considered as one of the most important natural routes for decreasing global warming (Dalton 2005). The widespread occurrence of methanotrophic bacteria is believed to help in minimizing the amount of methane released to the atmosphere (Semrau *et al.*, 2010; Jiang *et al.*, 2010). The improvement of methane monooxygenase in oxidation of methane to methanol has become the aim of many studies to enhance the removal of methane from the environment and in oxidation of other toxic substances, as will be explained in more detail in below.

## 1.2 Bioremediation of toxic substances by methane monooxygenase

It is known that methane monooxygenases (MMOs) from methanotrophs have the ability to co-oxidize many hydrocarbons ranging from simple molecules such as methane including alkanes, alkenes, heterocyclic compounds. Trichloroethylene (TCE), which is considered as a toxic and carcinogenic pollutant in water is also one of the substrates that can be oxidized by MMO (Smith and Dalton 2004). It has been found that MMO can oxidize hydrocarbons other than methane even though they do not use them as a source for carbon and energy. The oxidation of methane or the other diverse hydrocarbons by MMO takes place by the action of one of the two MMO; either pMMO or sMMO (Smith and Dalton 2004; Jiang *et al.*, 2010).

Yoon *et al.* (2011) showed that pMMO from the facultative methanotroph, *Methylocystis* strain SB2 was able to oxidize chlorinated ethanes. Im and Semrau (2011) also found that *Methylocystis* strain SB2 has the ability to oxidize chlorinated hydrocarbons such as vinyl chloride (VC), *trans*-dichloroethylene (*t*-DCE), TCE, 1,1,1,-trichloroethene (1,1,1,TCA) and chloroform (CF), when they grow on methane. sMMO was found to have a wider range of substrates extending to involve large di- and triaromatic compounds such as naphthalene, biphenyl, but not anthracene and phenanthrene (Colby *et al.*, 1997; Fox *et al.*, 1990; Smith and Dalton 2004), more details about sMMO substrates can be seen in Table 1.2. Many studies have attempted to increase its ability to oxidize larger toxic hydrocarbons by molecular modification of this enzyme. The rationale of these studies is to

understand the mechanism of this enzyme and if possible construct modified enzymes that can be employed in industry.

In addition to hydrocarbons, chromium VI which is a highly toxic, mutagenic, soluble metal that has been widely used in tanning and paper making (Cervantes *et al.*, 2001; Zayed and Terry, 2003) has been found to be reduced by methanotrophic bacteria. *Methylococcus capsulatus* (Bath) has been able to reduce the toxic form of chromium VI to the less toxic, more easily adsorbed by soil, form of chromium III across a wide range of concentrations which extend the list for the substrates of group of bacteria (Al-Hasin *et al.*, 2010).

**Table 1.2** The most common substrates oxidized by sMMO and the oxidation products.

Adapted from Smith and Dalton 2004; Jiang *et al.*, 2010

Substrate	Major detected products; relative molar proportions of multiple products are shown in brackets	Specific activity (nmol of product min <sup>-1</sup> mg <sup>-1</sup> ) <sup>1</sup>	Reference (type of assay) <sup>2</sup>
<b>1- Alkanes</b>			
Methane	Methanol	84	1 (SE)
Ethane	Ethanol	68	1 (SE)
Propane	Propan-1-ol (39); propan-2-ol (61)	69	1 (SE)
Butane	Butan-1-ol (54); butan-2-ol(46)	77	1 (SE)
Pentane	Pentan-1-ol (28); pentan-2-ol (72)	73	1 (SE)
Hexane	Hexan-1-ol (63); hexan-2-ol (37)	40	1 (SE)
Heptane	Heptan-1-ol (22); heptan-2-ol (78)	27	1 (SE)
Octane	Octan-1-ol (9); octan-2-ol (91)	9	1 (SE)
2- Methylpropane	2-Methylpropan-1-ol (70); 2-methylpropan-2-ol (30)	33	2 (PP)
2,3-Dimethylpentane	3,4-Dimethylpentan-2-ol	20	2 (PP)
<b>2- Alkenes</b>			
Ethene	Epoxyethene	148	1 (SE)
Propene	Epoxypropene	83	1 (SE)
But-1-ene	1,2-Epoxybutane	49	1 (SE)
<i>cis</i> -But-2-ene	<i>cis</i> -2,3-Epoxybutane (47); <i>cis</i> -2-butane-1-ol (53)	33	2 (PP)
<i>trans</i> -But-2-ene	<i>trans</i> -2,3-Epoxybutane (27); <i>trans</i> -2-butane-1-ol (73)	39	2 (PP)
<b>3- Alicyclic hydrocarbons</b>			
Cyclohexane <sup>3</sup>	Cyclohexanol	25	3 (SE)
Methylenecyclohexane	1-Cyclohexane-1-methanol (13.7)methylene cyclohexane oxide (75.8); 4- hydroxymethylene cyclohexane (10.5)	3	2 (PP) 2 (PP)

Substrate	Major detected products; relative molar proportions of multiple products are shown in brackets	Specific activity (nmol of product min <sup>-1</sup> mg <sup>-1</sup> ) <sup>1</sup>	Reference (type of assay) <sup>2</sup>
β-Pinene Adamantane <i>cis</i> -1, 4- Dimethyl cyclohexan <i>cis</i> -1,3-dimethyl cyclohexane	6,6-Dimethylbicyclo [3.1.1] hept-2-ene-2-methanol (72.3); β-pinene oxide (27.7) 1- Adamantol (50); 2-adamantol (50). 1-ci-4-Dimethylcyclohexanol (35); 1-trans-4-dimethylcyclohexanol (61); <i>cis</i> -2, 5-dimethylcyclohexaneol (4). 3,5-Dimethylcyclohexanol (80); 1-trans-3-dimethylcyclohexanol (6).		2 (PP)
4- <i>Halogenated aliphatics</i> Vinyl chloride <sup>3</sup> Trichloroethylene <sup>3</sup>  1,1-Dichloroethene <sup>3</sup> Trifluoroethene <sup>3</sup>  Chlorotrifluoroethylene <sup>3</sup> Tribromoethylene <sup>3</sup>	Formate (35); CO (53); glyoxylate (5); dichloroacetate(5); chloral (6)  Glycolate (80); dichloroacetaldehyde (3) Glycolate (53); difluoroacetate (43); fluoral (5)  Oxalate Formate (80); bromal (5)	748 682  684 79 179	4 (PP) 4 (PP)  4 (PP) 4 (PP) 4 (PP) 4 (PP)
5- <i>Monoaromatic</i> Benzene Toluene Ethylbenzene <sup>3</sup> Styrene <sup>3</sup> Pyridine	Phenol Benzyl alcohol; 4- cresol 1-Phenyl ethanol (30); 4- hydroxyethylbenzene (70) Styrene oxide Pyridine N-oxide	74 53 18.7 82 29	3 (SE) 1 (SE) 3 (SE) 3 (SE) 3 (SE)

Substrate	Major detected products; relative molar proportions of multiple products are shown in brackets	Specific activity (nmol of product min <sup>-1</sup> mg <sup>-1</sup> ) <sup>1</sup>	Reference (type of assay) <sup>2</sup>
6- <i>Diaromatics</i> Naphthalene Biphenyl <sup>3</sup> 2- Hydroxybiphenyl <sup>3</sup> 2- Methylbiphenyl <sup>3</sup> 2- Chlorobiphenyl <sup>3</sup> 2- Bromobiphenyl <sup>3</sup> 2- Iodobiphenyl	1- Naphthol; 2-naphthol 2- Hydroxybiphenyl (9); 3-hydroxybiphenyl(1); 4-hydroxybiphenyl (90) Dihydroxybiphenyls Ring (56) and side chain(44) hydroxylated products Hydroxychlorobiphenyls Hydroxybromobiphenyls (41); 2-hydroxybiphenyl (59) Hydroxyiodobiphenyl (18); 2-hydroxybiphenyls (82)		5 (W) 6 (W) 6 (W) 6 (W) 6 (W) 6 (W) 6 (W)
7- <i>Substituted methane derivatives</i> Chloromethane Dichloromethane Chloroform Bromomethane Nitromethane Methanethiol Methanol		84 82 35 66 45 64 246	1 (SE) 1 (SE) 1 (SE) 1 (SE) 1 (SE) 1 (SE) 1 (SE)
8- <i>Others</i> Diethyl ether Carbon monooxide	Ethanol (47); acetaldehyde (53) Carbon dioxide	61	1 (SE) 1 (SE)

<sup>1</sup> Specific activities are as reported in the original publications. <sup>2</sup> Type of enzyme preparation used for assay: PP, purified protein; SE, soluble extract; W, whole cells. <sup>3</sup> sMMO of *Ms. trichosporium*OB3b; other entries refer to *Mc. capsulatus* Bath.

**References:** 1; Colby *et al.*, 1977. 2; Green and Dalton 1989. 3; Burrows *et al.*, 1984. 4; Fox *et al.*, 1990. 5; Brusseau *et al.*, 1990. 6; Lindner *et al.*, 2000

### 1.3 Methanotrophs in Biotechnology

Methanotrophs have also been used in biotechnology, since methane monooxygenase from methanotrophs has been proposed as a biocatalyst to produce methanol from methane. Methanol has been used as an important bulk chemical and solvent in industry for a long time (Dalton 2005). It has been used as an alternative to methane as a carbon source for food production in the form of Single Cell Protein (SCP) (Dalton and Stirling, 1982; Davies and Whittenbury, 1970; Hanson, 1992; Large and Bamforth 1988). Methanol is widely available, readily stored and transported, safer to utilize than methane and there are biotechnologically versatile bacteria which can use methanol as their sole source of carbon and energy. This has led to research to enable production of methanol from methane, derived from either fossil or biological sources (Anthony 1986; Dijkhuizen *et al.*, 1992; Large and Bamforth.1988; Lidstrom, 1991; Lidstrom and Stirling 1990). Zuniga *et al.* (2011) used methanotrophs to produce the bioplastic polyhydroxybutyrate (PHB) from methane. These authors isolated and identified *Methylobacterium organophilum* from a PHB-producing consortium and then described its ability to use methane as a carbon source to produce PHB, both in the consortium and as the isolated *Mlb. organophilum* strain.

Pfluger *et al.* (2011), found that when a laboratory-scale fluidized bed reactor was inoculated with a *Methylocystis*-like strain (type II methanotroph, producing polyhydroxybutyrate), as the starter culture under conditions of dissolved oxygen 9 mg/L, pH of 6.2-6.5 with nitrate as the N-source, a *Methylobacter*-like

type I methanotrophs that did not produce PHB became prevalent within biofilms in the reactor. Re-inoculating with another type II methanotroph culture (*Methylosinus*), providing dissolved N<sub>2</sub> as the nitrogen source and keeping dissolved oxygen (DO) at a low level (2.0 mg/L) resulted in a biofilm dominated by type II methanotrophs that produced PHB and contained at the same time some type I organisms. It was concluded that provision of N<sub>2</sub> as the nitrogen source was a limiting factor for growth of type I methanotrophs that did not produce PHB whereas it enhanced growth of type II methanotrophs that produced PHB.

Astaxanthin is a type of carotenoid which is added to the diet of farmed salmon to improve the colour of the fish produced (Torrissen and Christiansen 1995). In addition carotenoids such as astaxanthin have antioxidant activity (Hussein *et al.*, 2006). Ye *et al.* (2007) have constructed a genetically modified *Methylomonas* sp. strain known as strain 16a to produce the carotenoid astaxanthin which established proof of concept for employing molecular engineering to synthesise new small-molecule products by methanotrophic bacteria.

The ability to use a combination of a tractable genetic system and a cheap carbon source such as methane may motivate researchers toward use of methanotrophs for production of pharmaceutical precursors, enzymes for bioremediation and other valuable products (Smith and Murrell, 2009). Site-directed mutagenesis has been employed previously in this research group and also that of J. Collin Murrell (currently at the University of East Anglia) to engineer the hydroxylase component of sMMO from *Methylosinus trichosporium* OB3b.

## 1.4 Methane monooxygenase enzyme

It was well known that the *Methylosinus trichosporium* OB3b and *Methylococcus capsulatus* Bath can produce sMMO or pMMO (Hanson and Hanson, 1996). Until a few years ago, the methanotrophs belonging to the genus *Methylocystis* were believed to be obligate methanotropic bacteria. Two new facultative methanotrophs were isolated which produced both pMMO and sMMO. These bacteria are able to grow on methane and methanol when other C1 substrates are not available in addition to slow growth on acetate and ethanol in the absence of the other C1 source. They were classified as *Methylocystis bryophila* sp. strains H2sT and S2854. Each of these, like the other methanotrophs, was found to produce pMMO enzyme in two forms named as pMMO1 and pMMO2. The identity of the *pmoA2* DNA sequence of strains H2sT and S2854 with *pmoA2* from other methanotrophs was 89.0-91.8% respectively (Belova *et al.*, 2011; Im *et al.*, 2011; Belova *et al.*, 2012). It was also found that some *Methylomonas* species produce sMMO, since Ogiso *et al.* (2012) were able to characterize an obligate methanotroph from Japan that can grow on methane and methanol as a sole source for carbon; it was named as *Methylomonas koyamae*. Recently in 2015, Smith's group were able to isolate *Methylomonas koyamae* that also produces sMMO in addition to being able to reduce chromium VI to chromium III. The sMMO enzyme was also found to be produced by the marine methanotrophic bacteria, *Methylomicrobium* (Fuse *et al.*, 1998). Unlike the sMMO which is produced by certain species of methanotrophic bacteria as it was explained above, it is well known that pMMO is produced by almost all methanotrophs except the genus *Methylocella* and

*Methyloferula* (Hanson and Hanson, 1996; Theisen *et al.*, 2005; Vorobev *et al.*, 2011).

Despite the fact that both pMMO and sMMO oxidize methane to methanol; there is no detectable significant amino acid sequence similarity between them and metal content at the active site (Smith and Dalton, 2004; Dalton 2005). The pMMO is membrane associated whereas sMMO is soluble in the cytoplasm. There are also major differences in the substances which they can oxidize and their requirements for electron donors (Dalton 2005). Stanley *et al.* (1983) proved that the production of MMO in the methanotrophs which contains both types of MMO, such as *Methylosinus trichosporium* and *Methylococcus capsulatus*, depends on copper-to-biomass ratio since pMMO is expressed when the ratio of copper to biomass is high whereas sMMO is produced when the copper starts to deplete from the medium and the ratio of copper to the biomass becomes low.

#### **1.4.1 Particulate methane monooxygenase**

##### **1.4.1.1 Purification and structure of pMMO**

The major catalyst in bioconversion of methane to methanol in the environment is the particulate methane monooxygenase (pMMO) from methanotrophic bacteria (Stanley *et al.*, 1983; Hakemian and Rosenzweig, 2007).

DNA sequencing studies showed that pMMO is encoded by three genes *pmoC*, *pmoA*, and *pmoB* organised as an operon *pmoCAB*. The genes *pmoC*, *pmoA*, and *pmoB* encode for pMMO  $\gamma$  (22 kDa),  $\beta$  (24 kDa), and  $\alpha$  (45 kDa) subunits respectively (Semrau *et al.*, 1995).

The precise crystal structure for pMMO was not available until 2005 owing to difficulties with obtaining the enzyme in a suitable purified form. The purification was complicated owing to problems with solubilizing the pMMO from lipid bilayer in the membrane without complete loss of activity (Smith and Dalton, 2004; Kühlbrandt, 1988; Michel, 1991). Among many non denaturing detergents tested for solubilization of pMMO, Dodecyl- $\beta$ -D-maltoside was found to be most effective whilst minimising loss of activity, and most subsequent work with isolated pMMO has relied on this detergent (Smith and Dalton, 1989; Liberman and Rosenzweig, 2004). A number of different groups have reported somewhat different conditions as optimal for purification of pMMO; Choi *et al.* (2003) found that to keep the enzyme active, the purification is better in the absence of oxygen, whereas Nguyen *et al.* (1998) indicated that aerobic circumstances are acceptable and Basu *et al.* (2003) found the oxygen is actually advantageous in pMMO purification. Liberman *et al.* (2003) were able to purify active pMMO from *Methylococcus capsulatus* (Bath) with molecular mass about 200 kDa which may correspond to  $\alpha_2\beta_2\gamma_2$  subunits of pMMO hydroxylase. The purified enzyme from the same study contained  $4.8 \pm 0.8$  copper ions and  $1.5 \pm 0.7$  Fe ions (Figure 1.2). Analysis of the pMMO complex by electron paramagnetic resonance spectroscopy showed that 40-60% of the total copper corresponded to mononuclear type 2 Cu sites. In the same study X-ray absorption spectroscopy of the pMMO complex revealed the presence of both Cu (I) and Cu (II) oxidation state. Choi *et al.* (2003) improved the purification of pMMO by changing the growth conditions to stabilize pMMO and the amount of detergent used to maintain the metal composition of the pMMO. It was found that addition of type 2 NADH: quinone oxidoreductase complex (NADH dehydrogenase [NDH]), keeping a high ratio between duroquinol/ duroquinone, led to a highly

active purified pMMO with an activity of  $130 \text{ nmol min}^{-1} \text{ mg of protein}^{-1}$  compared to  $< 50 \text{ nmol min}^{-1} \text{ mg of protein}^{-1}$  obtained by Basu *et al.* (2003) from partially purified pMMO. By using electron microscopy in combination with single-particle analysis (SPA), Kitmitto *et al.* (2005) were able to characterise the three dimensional structure of the pMMO hydroxylase and show that it was a trimer.

The purification of pMMO was also achieved by other studies from *Mc. capsulatus* Bath (Nguyen *et al.*, 1994; Zahn and DiSpirito, 1996) and *Ms. trichosporium* OB3b (Miyaji *et al.*, 2002; Takeguchi *et al.*, 1998). All these studies agreed that pMMO contains copper at the active site, although there has been a considerable controversy about the number and nature of the metal ions. One model suggested that pMMO contained up to 10-15 Cu atoms and 2 iron atoms. In this model, it was found that 8-13 Cu atoms were attached to a small peptide (1,218 Da) which named as copper binding compound (cbc) that appeared in the purified pMMO (DiSpirito *et al.*, 1998; Zahn and DiSpirito, 1996). The second proposed model is an enzyme with 15-21 copper atoms, in this model 5-7 copper atoms arranged in trinuclear copper atom cluster, in which 2-3 cluster are catalytic and 3-4 transfer an electron from NADH to the active site centre (Nguyen *et al.*, 1994; Nguyen *et al.*, 1996; Nguyen *et al.*, 1998). The last model suggested the presence of 2 copper atoms and 1-2 iron atoms in the active centre of the pMMO enzyme (Basu *et al.*, 2002; Lieberman *et al.*, 2003; Tikhvatullin *et al.*, 2000).

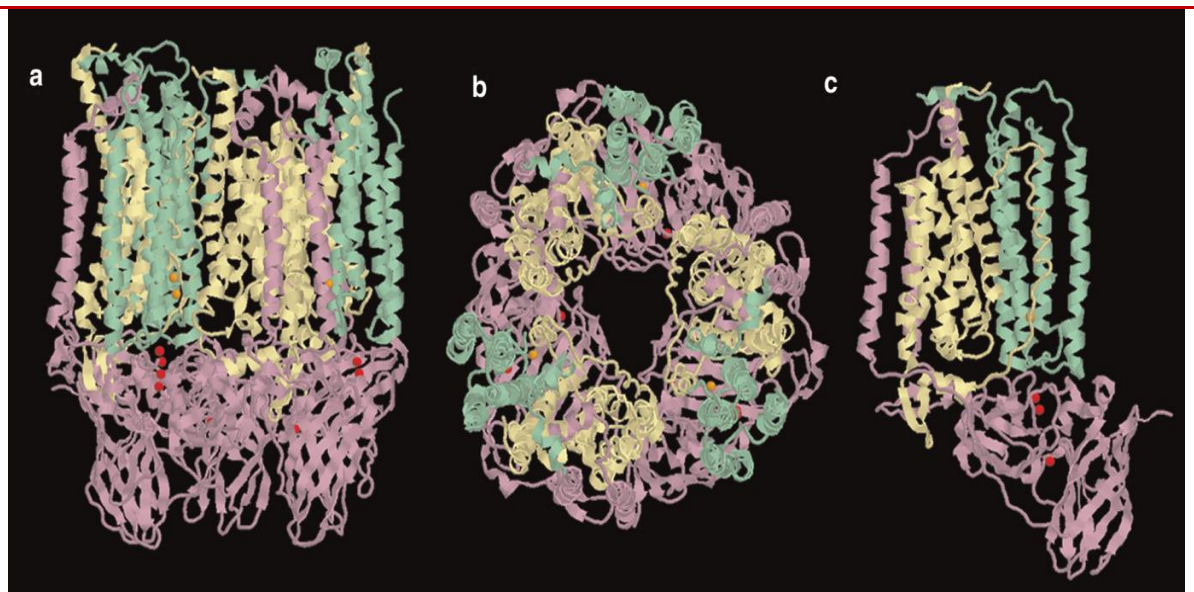
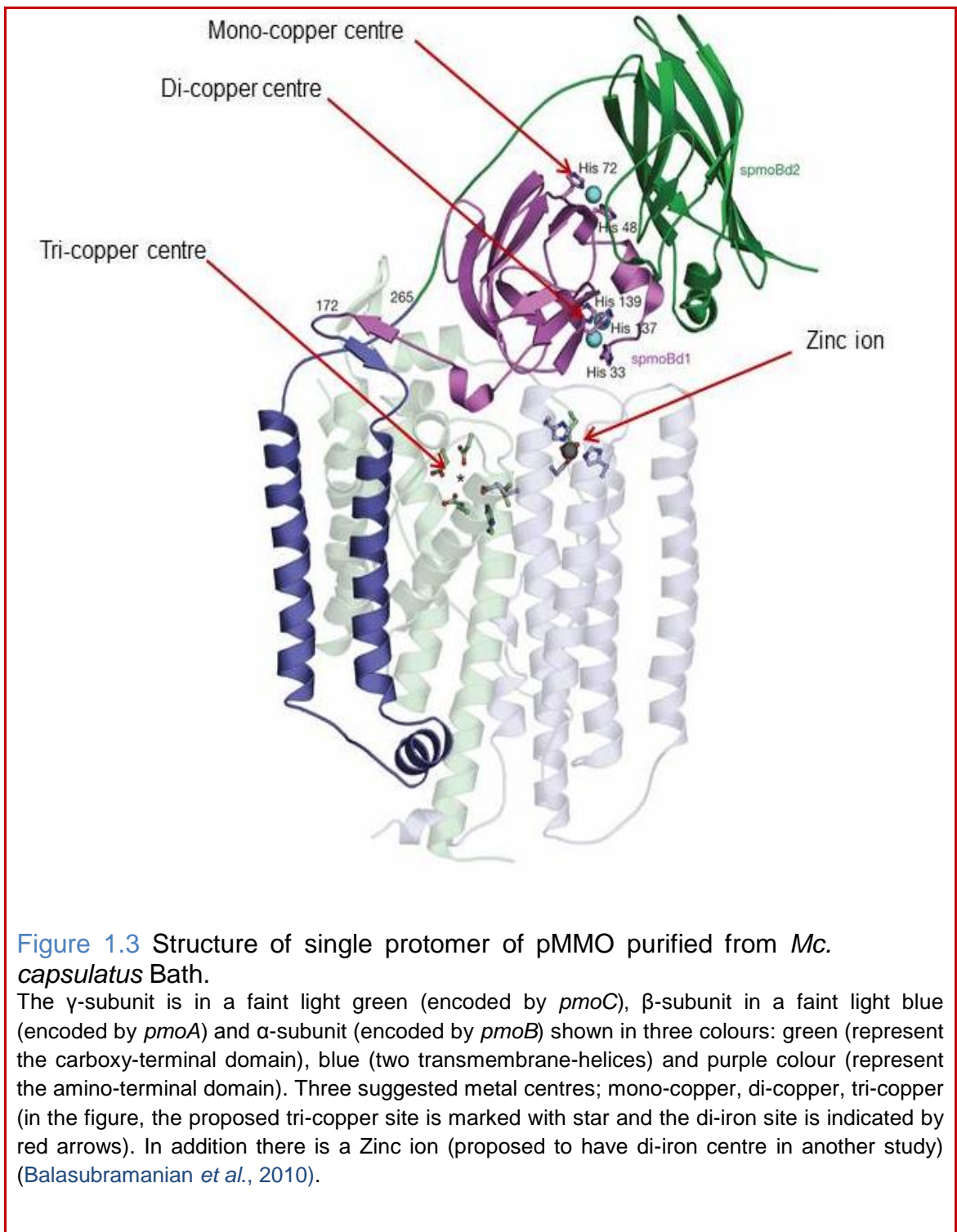


**Figure 1.2** Structure of pMMO from *Methylococcus capsulatus* (Bath). The  $\alpha$ -subunit (PmoA),  $\beta$ -subunit (PmoB), and  $\gamma$ -subunit (PmoC) are coloured lilac, yellow, and green, respectively. Metal atoms shown as spheres, copper red, and zinc orange. (a)  $(\alpha\beta\gamma)^3$  enzyme; (b) view looking down on (a) from above; (c) one promoter showing the mononuclear and dinuclear copper and zinc (Smith and Murrell, 2010).

In other studies (Lieberman and Rosenzweig, 2005; Balasubramanian and Rosenzweig, 2007) three different metal centres positions were proposed for particulate MMO of *Ms. trichosporium*. In the first metal position, a dicopper centre lies in the soluble domain of PmoB subunit (spmoB), with shortened Cu-Cu stretch of 2.5-2.7 Å accompanied with highly conserved residues (histidines) (Hakemian and Rosenzweig, 2007; Hakemian *et al.*, 2010). In the second position, one copper centre lies alongside the conserved residues, His48 and His72. The third metal centre, which in this crystal structure appears to be occupied by zinc, lies attached to the membrane and coordinated with two residues from pmoB, one from pmoC and probably one from pmoA (Figure 1.3) (Lieberman and Rosenzweig, 2005). In a study by Hakemian *et al.* (2008)

where pMMO was purified from *Methylosinus trichosporium* OB3b, it was found that the mononuclear copper centre in *Mc. capsulatus* Bath was absent in *Ms. trichosporium* OB3b and a third copper centre in the latter replaced the zinc in *Mc. capsulatus* pMMO. This indicates that there is a difference in function between the two enzymes from the bacteria or maybe the difference came from the preparation of the two enzymes. By using the suicide substrate acetylene in a radiolabelled form, the copper active site was proposed to lie in PmoB or between PmoB and PmoA subunits (Zahn *et al.*, 1996; Prior and Dalton, 1985), which was then confirmed by a molecular study where a recombinant fragment of soluble part of PmoB which was able to bind copper and have activity toward propylene (Balasubramanian *et al.*, 2010). In addition to the pMMOH (pMMO hydroxylase), Dalton and co-workers purified another protein which they proposed to be pMMOR (pMMO reductase), which consisted of 63 and 8 kDa polypeptides (Basu *et al.*, 2003). It was found that the pMMOR and pMMOH did not give activity when they were tested separately towards propylene. However, mixing them together resulted in an active enzyme with  $2.6 \text{ nmol min}^{-1} \text{ mg}^{-1}$ . The N-terminal sequences for the 63 kDa subunit was then shown to be a methanol dehydrogenase by Adeosun *et al.* (2005). Myronova *et al.* (2006) were able to purify and characterise a complex between pMMO-H and methanol dehydrogenase (MDH). In this study it was suggested that MDH can play a role as a reductase.



### 1.4.1.2 Molecular genetics of pMMO

Two copies of the *pmoCAB* operon with approximately identical structures have been identified in *Methylosinus trichosporium* OB3b, *Methylocystis* sp. strain M (Gilbert *et al.*, 2000) and in *Methylococcus capsulatus* Bath (Semrau *et al.*, 1995). The two copies were found to be indispensable for reliable activity for pMMO by applying chromosomal insertion mutations (Stoylar *et al.*, 1999). In addition to a third copy of *pmoC* (*pmoC3*) was identified in *Mc. capsulatus* Bath with a different sequence in each the N-terminal and C-terminal from the other two *pmoC* copies in the same bacterium. A proposed role in growth on methane was suggested for *pmoC3*, since a mutant was not able to grow on media with methane (Stoylar *et al.*, 1999). It was known that pMMO from cultured methanotrophic bacteria oxidizes methane only when it is in a high concentration >600 ppmv in the environment and not in low concentration. In a study by Yimga *et al.* (2003) using newly designed primers, a second copy of *pmoA* encoding the active polypeptide was characterized in *Methylocystis* sp. strain SC2. It was then referred to as *pmoA2* to distinguish it from the *pmoA1*. By using the same primers, they were able to characterise *pmoA2* in a wide range of type II methanotrophic bacteria such as *Methylosinus-Methylocystis* group. Further study by Ricke *et al.* (2004) showed that *pmoA1* and *pmoA2* belong to different operons referred to as *pmoCAB1* and *pmoCAB2*. The DNA analysis showed that the identity between these two gene clusters was 67.4-70.9%. The first copy was able to oxidize methane in a high level >600 ppmv. The second copy *pmoCAB2* encodes for a different pMMO (called as pMMO2) that has a higher affinity for methane and is able to oxidise methane at lower concentration (< 1.75 ppmv) than any other pMMO investigated (Baani and Liesack 2008).

Interestingly, three different copies of the *pmoCAB* operons were isolated from the extremophilic verrucomicrobial, *Methyloacidophilum kamchatkense* kam1. Each operon codes for the  $\alpha\beta\gamma$  subunits of the pMMO. In addition to the above operons, this bacterium possesses a *pmoCA* cluster, i.e. a third operon encoding only the alpha and beta subunits (Dunfield *et al.*, 2007; Pol *et al.*, 2007; Op den Camp *et al.*, 2009). By using qPCR analysis, Islam *et al.* (2008) were able separately to measure the expression of the four *pmoA* genes. One gene named *pmoA2* was transcribed 35 times more than any one of the other *pmoA*. Changing temperature and pH was found not affect the rate of expression of this gene whereas altering the carbon source from methane to methanol reduced the transcription of *pmoA2* ten times. This may refer to a specific role for substitution carbon source in gene regulation (Erikstad *et al.*, 2012).

As mentioned earlier, by using molecular genetic methods Balasubramanian *et al.* (2010) were able to prove that pMMO activity relies on copper and not iron. These authors firstly detected an activity for purified pMMO towards propylene. No detectable activity was obtained when purified pMMO was treated with cyanide. Reapplying 2-3 equiv. of copper per 100 kDa pMMO protomer led to restoration of nearly 70% of pMMO activity towards propylene oxidation and more than 90% as measured by methane oxidation activity. In contrast, when they applied iron, there was no effect on recombinant pMMO activity, which indicates that Cu is at the active site of pMMO. The position of the Cu active-site was then identified in the soluble part of the recombinant  $\alpha$ -subunit expressed in *E. coli*, which was called *spmoB*, rather than in bacterial cell membrane (Balasubramanian *et al.*, 2010; Smith *et al.*, 2011). By site directed

mutagenesis it was also shown that the di-copper centre is responsible for substrate oxygenation, since the disruption by mutagenesis of the putative ligands for the mono-copper, di-copper and tri-copper centres separately resulted in lost the enzyme activity towards propylene and methane only for the eliminated dicopper in *spmoB* of pMMO enzyme, whereas the mutants with removal of the mono- and tri-copper were active. However, Chan's group have suggested based on biophysical and biochemical studies that the tri-copper site (Figure 1.3) which lies between PmoA and PmoC may have a role in hydrocarbon oxidation activity (Chan *et al.*, 2008; Chan *et al.*, 2004; Chan *et al.*, 2013), since PmoA and PmoC were able to oxidise methane and propene oxidation at room temperature (Chan *et al.*, 2013). By combining high-resolution mass spectrometry with computational studies, Chan's group were able to confirm that pMMO oxidizes acetylene to ketene ( $\text{CH}_2=\text{C}=\text{O}$ ) which then interacts with an amino acid within the PmoC subunit leading to covalent modification of amino acid that resulted in loss of enzyme activity. Further analysis of the digested peptide from in-gel proteolysis by using labelled acetylene and high resolution mass spectrometry showed that K196 of PmoC is the position that is modified. No evidence was found for chemical changes in the PmoB or PmoA subunits (Chan *et al.*, 2015). In same study, it was suggested a putative role for PmoC in controlling the entry and egression of hydrophobic substrates to and from the active site. Zinc was also implicated as an inhibitor of pMMO by replacing the copper in the active site or altering the copper at another site implicated in providing a proton to the active site to initiate the catalytic cycle (Chen *et al.*, 2004; Cook and Shiemke, 1996; Takeguchi *et al.*, 1999). Sirajuddin *et al.* (2014), in a study on pMMO from *Methylococcus capsulatus* and *Methyocystis* species strain Rockwell, found via

crystallography that there are two putative site for zinc binding in PmoC; the first sites is in the PmoC subunit, it was found that when zinc binds here, ten residues were rearranged which may lead to conformational changes. These conformational changes might affect the binding site for the quinol that (acts as the reductant for pMMO) consequently led to release of a proton to start the catalytic cycle. The second zinc site was found in the soluble part of PmoC.

Although controversy remains about the the exact role for the copper, iron and zinc in pMMO, substantial progress in purification of active pMMO, identification of the active site and other functional features have been made recently.

#### **1.4.2 Soluble methane monooxygenase (sMMO)**

sMMO is among the most important diiron active site monooxygenase enzymes that can incorporate molecular oxygen to methane and convert it to methanol. As in the case of methanotrophs growing using pMMO, the methanol produced from oxidation of methane by sMMO is then further oxidized by methanol dehydrogenase to formaldehyde which either is used to build cell mass or further oxidized. The sMMO also has ability to oxidize a wide range of other substrates (for more information, see [Table 1.2](#)) ([Woodland \*et al.\*, 1986](#); [Myronova \*et al.\*, 2006](#)).

The sMMO enzyme from two methanotroph model organisms have been identified and investigated in detail. One is produced by *Mc. capsulatus* Bath ([Colby and Dalton, 1978](#)) that works at 45°C and the second is produced by *Ms. trichosporium* OB3b ([Fox \*et al.\*, 1989](#)) which has optimal activity at 30°C. The

previous studies showed that sMMO from *Ms. trichosporium* and *Mc. capsulatus* are comparable in their subunit and prosthetic group composition, catalytic properties and the substrates which they oxidize (Smith and Dalton, 2004). The sMMO enzyme consists of three components “hydroxylase, the regulatory/coupling protein and the reductase”. These components of sMMO are sometimes referred to as proteins A, B, and C respectively. The sMMO operon is made up of six genes, *mmoXYBZDC*. The structure and function of the sMMO enzyme components will be explained in greater detail in the next section.

The sMMO gene cluster also harbours two additional genes known as *mmoG* and *mmoR* (Figure 1.4) encoding a GroEL homologue and a  $\sigma^{54}$ - specific transcriptional regulator. *mmoX*, *Y*, *Z*, *B* and *C* are the structural genes that encode the sMMO enzyme. The *mmoD* gene codes for protein of previously unknown function (Csaki *et al.* 2003; Scanlan *et al.* 2009).

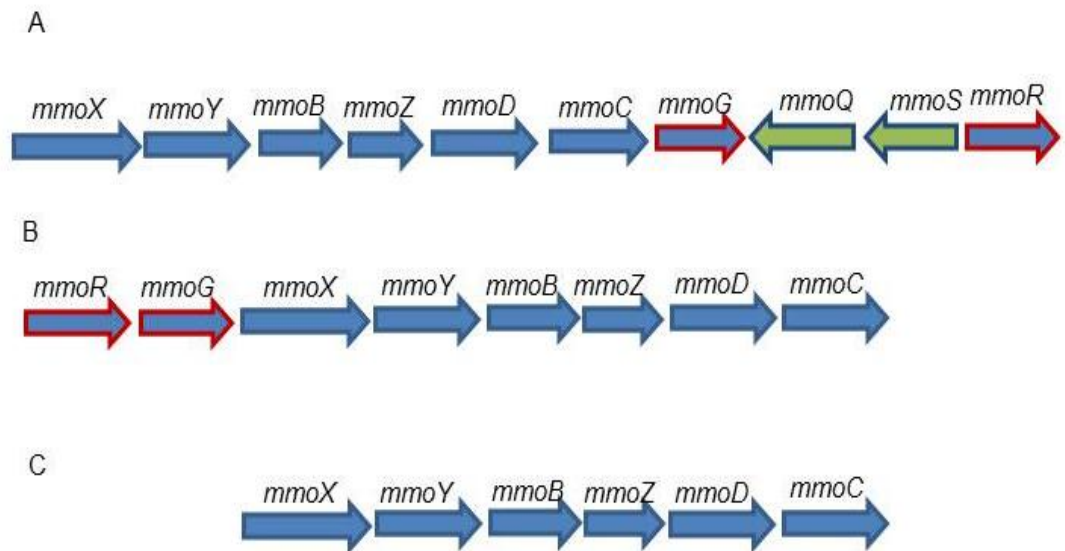


**Figure 1.4** Soluble methane monooxygenase gene cluster from three different methanotrophs; *Methylococcus capsulatus* (Bath) (A), *Methylosinus trichosporium* OB3b (B) and *Methylocystis* sp (C).

A) sMMO operon from *Methylococcus capsulatus* (Bath) showing the sMMO-encoding genes in addition to genes *mmoR* and *mmoG*, *mmoS* and *mmoQ*. B) sMMO operon from *Methylosinus trichosporium* OB3b showing genes *mmoR* and *mmoG* in different positions from those recognized in Bath. No *mmoS* and *mmoQ* were identified in OB3b strains while C) shows the sMMO operon from *Methylocystis* sp. strain M which does not have genes *mmoR* and *mmoG*, *mmoS* and *mmoQ*.

### 1.4.3 Components of sMMO

#### 1.4.3.1 Hydroxylase (Protein A)

The hydroxylase may be considered to be the most important and critical part of sMMO, a part of group of active versatile hydrocarbon oxygenases with binuclear iron centres. The family also includes hemerythrin, the R2 subunit of class I ribonucleotide reductase, purple acid phosphatase (Que Jr and True., 1990), and others (Rosenzweig *et al.*, 1999). The hydroxylase component (250 kDa) which comprises  $\alpha_2 \beta_2 \gamma_2$  subunits arranged in a heart shape (Figure 1.5 A), is encoded by *mmoX*, *Y* and *Z* and contains the active site in the  $\alpha$ -subunit.

The active site contains two iron atoms connected by  $\mu$ -(hydro) oxo-bridge buried deeply in the  $\alpha$ - subunit, where the oxygen is activated, surrounded by four glutamic acid and two histidine side chains in addition to the bridging OH, a terminal H<sub>2</sub>O ligand, and an acetate at 4°C swapped with a H<sub>2</sub>O molecule at -160°C (Figure 1.5) (Rosenzweig *et al.*, 1999). It has been found from the study of Elango *et al.* (1997) that there are substantial differences in the active site structure in various redox states of the diiron centre.

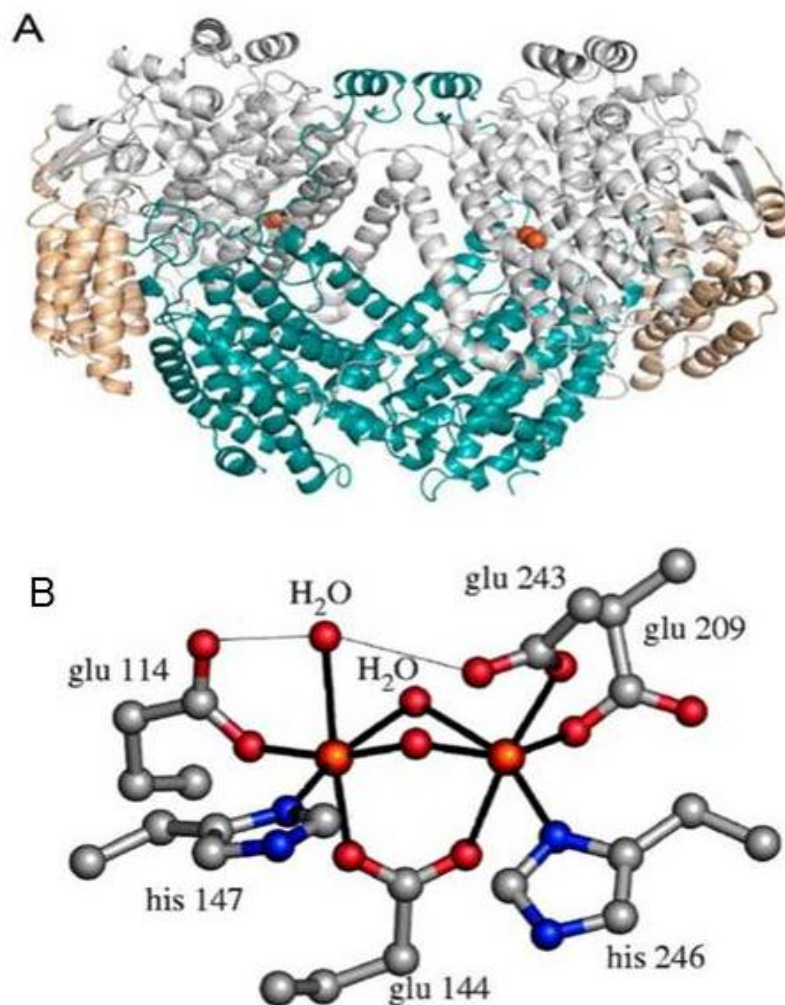


**Figure 1.5** The structure and the geometry of active site within the hydroxylase from *Methylococcus capsulatus* Bath.

A) hydroxylase (MMOH), gray:  $\alpha$  subunit, teal:  $\beta$  subunit, wheat:  $\gamma$  subunit and orange spheres: diiron centre. The structure of MMOH was determined by single crystal X-ray diffraction

B) The image shows the diiron centre surrounded with four Glutamates 114, 144, 209, 243, two histidines 147 and 246 (A; taken from Sirajuddin and Rosenzweig, 2015 and B; from Lippard 2005).

Crystallography studies of MMOH have indicated that there are a number of cavities that form a potential route from the upper surface of the enzyme toward the active site, but no direct evidence for the role for any of them in substrate entry and product exit (McCornick and Lippard, 2011). Molecules ranging in size from methane to 2, 2-diphenyl-1-methylcyclopropane can reside in cavity one (Liu *et al.*, 1993). The proposed function of large cavities, 3 and 4, is a pathway for entrance of the substrates to the active site, egression of the product via these cavities, or could be both (Figure 1.6) (Rosenzweig *et al.*, 1997). In addition to that there is a pore region between the protein exterior and the active site, the presence of this route was first observed by (Rosenzweig *et al.*, 1997; Rosenzweig *et al.*, 1993; Matthew *et al.*, 2006; Murray and Lippard 2007). According to these studies it might have a role in proton shuttling or dioxygen activation in the active site (Murray and Lippard 2007; Song *et al.*, 2010; Tinberg and Lippard, 2009; Lee and Lipscomb, 1999). Another role was suggested for these cavities in allowing substrate entrance to the active site of phenol hydroxylase enzyme (PHH) which has considerably bigger pore region than the other monooxygenase enzymes (Sazinsky *et al.*, 2004; Sazinsky *et al.*, 2006).

Also a channel has been found between cavities one and two in toluene/ o-xylene monooxygenase (ToMOH), when protein B attaches to the hydroxylase, this causes a conformational change leading to plugging of the channel (Bailey *et al.*, 2008). In MMOH a channel of this type could not be identified. A number of amino acids with hydrophobic side chains were found such as F188, F236, and L110 preventing the formation of an analogous channel and this might have a role in providing a hydrophobic ambient environment to facilitate the accommodation of hydrophobic hydrocarbon substrates in sMMO (Tinberg *et*

*al.*, 2009; Lee *et al.*, 1999; Song *et al.*, 2011; Song *et al.*, 2010). As such, a role for Leu110 was suggested in controlling the access or egression of the substrates and product in and out from the active site (Rosenzweig *et al.*, 1997). This hypothesis was investigated by site directed mutagenesis by Borodina *et al.* (2007). It was shown that this residue is important in controlling the regioselectivity more than access of substrate to the active site. Also, there are specific cavities with certain characteristics and specific side chains that form a route for passage of dioxygen to the active site of sMMO and other bacterial multi-component monooxygenases (Song *et al.*, 2011). Crystallographic studies in which xenon was used as a surrogate for methane substrate were consistent with the previously proposed location of the substrate-binding site in both sMMO and toluene/o-xylene monooxygenase (Song *et al.*, 2011; McCormick and Lippard, 2011).

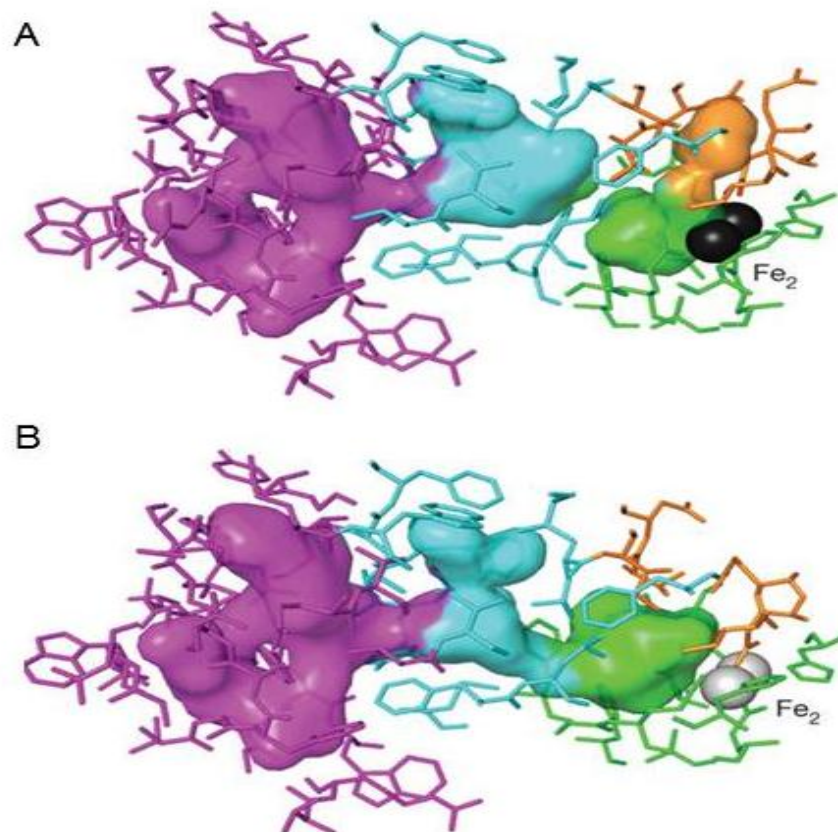


**Figure 1.6** Hydroxylase cavities and some changing during MMOH-MMOB complex formation.

The diagram shows the cavities from outside toward the active site of MMOH; Cavity 3 (magenta), cavity 2 (blue) and cavity 1 (green). The orange colour represents the pore region. Amino acids residues corresponding to each cavity depicted as sticks with the same colour for the contributed cavity. The diiron centre represented with black and gray colour. The image is for the diiron centre in oxidation and reduction state; A and B respectively. In the reduction state where the MMOH-MMOB complex formed, the pore region become completely plug and cavity one as a consequence is open access to allow the entrance of  $\text{CH}_4$  (other substrates) and oxygen to start the catalytic cycle.

(Lee *et al.*, 2013)

### 1.4.3.2 Coupling/ Regulator protein (protein B)

The protein B (effector/ regulator) component is a single polypeptide of 16 kDa with no metal group (Green and Dalton 1985). Many roles also have been proposed for protein B involving regulating electron transfer to the sMMO hydroxylase from the reductase to start the catalytic cycle of the sMMO enzyme (Green and Dalton 1985; Fox *et al.*, 1991). In addition, the formation of a complex between protein B and the hydroxylase changes the activity and regioselectivity of the enzyme (Lee *et al.*, 1993; Paulsen *et al.*, 1994; Kazlauskaite *et al.*, 1996).

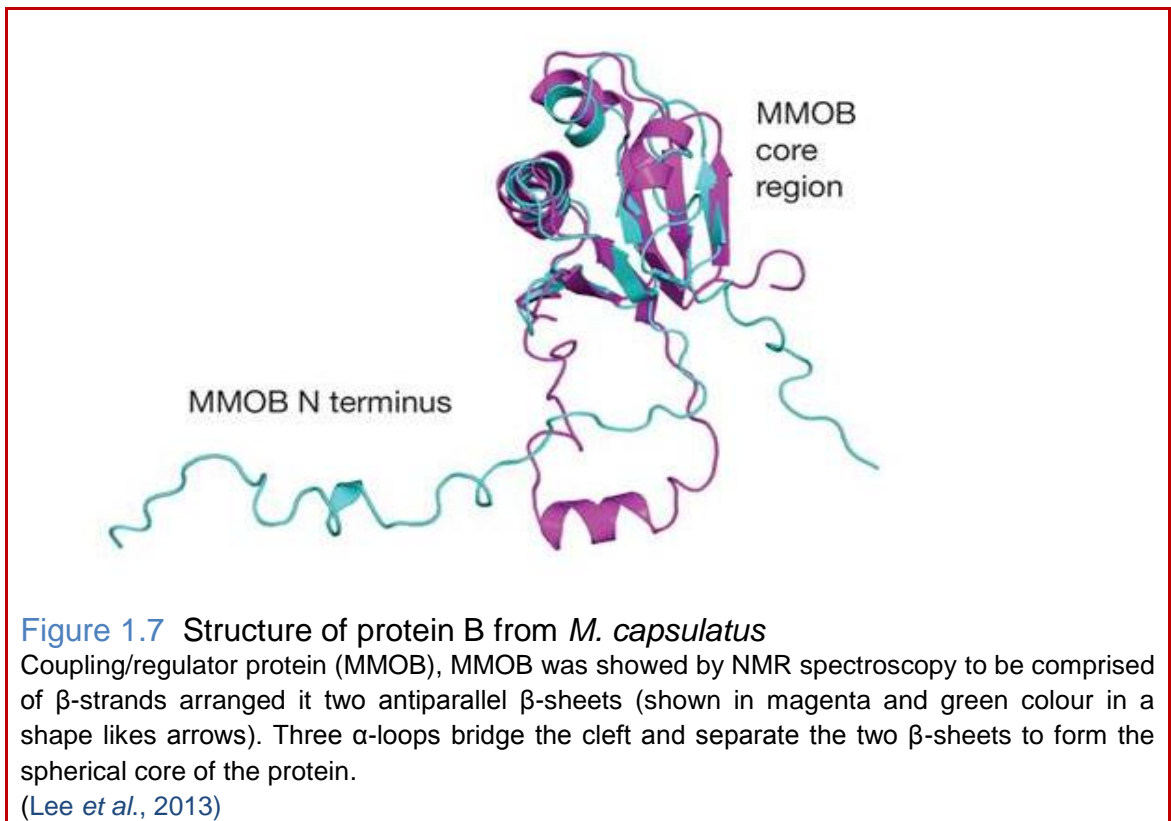
Chang *et al.* (1999) and Walters *et al.* (1999), demonstrated by NMR spectroscopy the structure of protein B from both *Ms. trichosporium* and *Mc. capsulatus*, the core of MMOB, residual 35-127 in *Mc. capsulatus*, comprised of 7  $\beta$ -strands arranged in two antiparallel  $\beta$ -sheets organised almost perpendicular to each other. Three  $\alpha$ -loops bridge the cleft and separate the two  $\beta$ -sheets to form the spherical core of the protein. Although, NMR could not identify the first 35 and the last 12 amino acids of the regulatory protein, NMR and CD experiments showed that section of the N- terminus might form a helical construction (Figure 1.7).

It has been suggested that interaction between protein B and the hydroxylase opens the blocked active site allowing entrance of oxygen and methane (Brazeau & Lipscomb 2000; Chang *et al.*, 2001). Many other roles have been proposed for protein B in the sMMO complex. Astier *et al.* (2003) revealed that H<sub>2</sub>O<sub>2</sub> was being created in their experiment, but when the protein B was added, H<sub>2</sub>O<sub>2</sub> disappeared, this result provided evidence for an additional role for

protein B namely by preventing  $\text{H}_2\text{O}_2$  formation as an accidental by-product when dioxygen reacts with the sMMO diiron- centre. The exact role for the protein B during the formation of a complex between MMOH and MMOB was unclear, largely due to the lack of crystallographic study data for the MMOH-MMOB complex. A crystal structure of this complex has now been obtained and reveals that MMOB has a core region (Asp36-Leu129), that binds to the canyon between the  $\alpha$  and  $\beta$  subunits of MMOH, and a disordered N-terminal tail which forms a regular ring-shape structure after connecting with  $\alpha$ -subunit. Both these structural features have been shown to be indispensable in MMO activity (Lee *et al.*, 2013). The important role for the N-terminal region was firstly discovered by (Green *et al.*, 1985; Brandstetter *et al.*, 1999; Chang *et al.*, 2001) and proved recently by mutation study which revealed a decrease in the activity of mutated MMOB ( $\Delta 1-8$ ,  $\Delta 1-17$  and  $\Delta 1-33$ ) comparing to the activity of non-mutated MMOB (Lee *et al.*, 2013).

It has been found also that the ring shaped structure interacts with the  $\alpha$ -subunit of MMOH via the  $\alpha$ -helix (Gly17-Phe 25) from MMOB that could make the complex difficult to reduce by MMOR. The interaction also leads to a structural changes in certain residues within the  $\alpha$ -subunit around the active site such as Thr 213 and Glu 240 leading to closure of the pore region which is implicated in proton supply during the catalytic cycle (some of the conformational changes will be explained in more detail later) (Tinberg *et al.*, 2009; Wallar and Lipscomb, 1996; Merx *et al.*, 2001). Another important role of the formation of the MMOB-MMOH complex is that when this complex forms in the diferric oxidation state of MMOH, the cavities 2 and 3 become connected and presumably are able to allow dioxygen and methane to pass to the active site, whereas in the absence of MMOB these two cavities are separate. This opening

of the channel between cavities 1 and 2 is brought about by movement of a number of residues including Phe188 and L110 which then allow passage of substrates, O<sub>2</sub> and protons to the diiron active site (Figure 1.8) (Lee *et al.*, 2013).



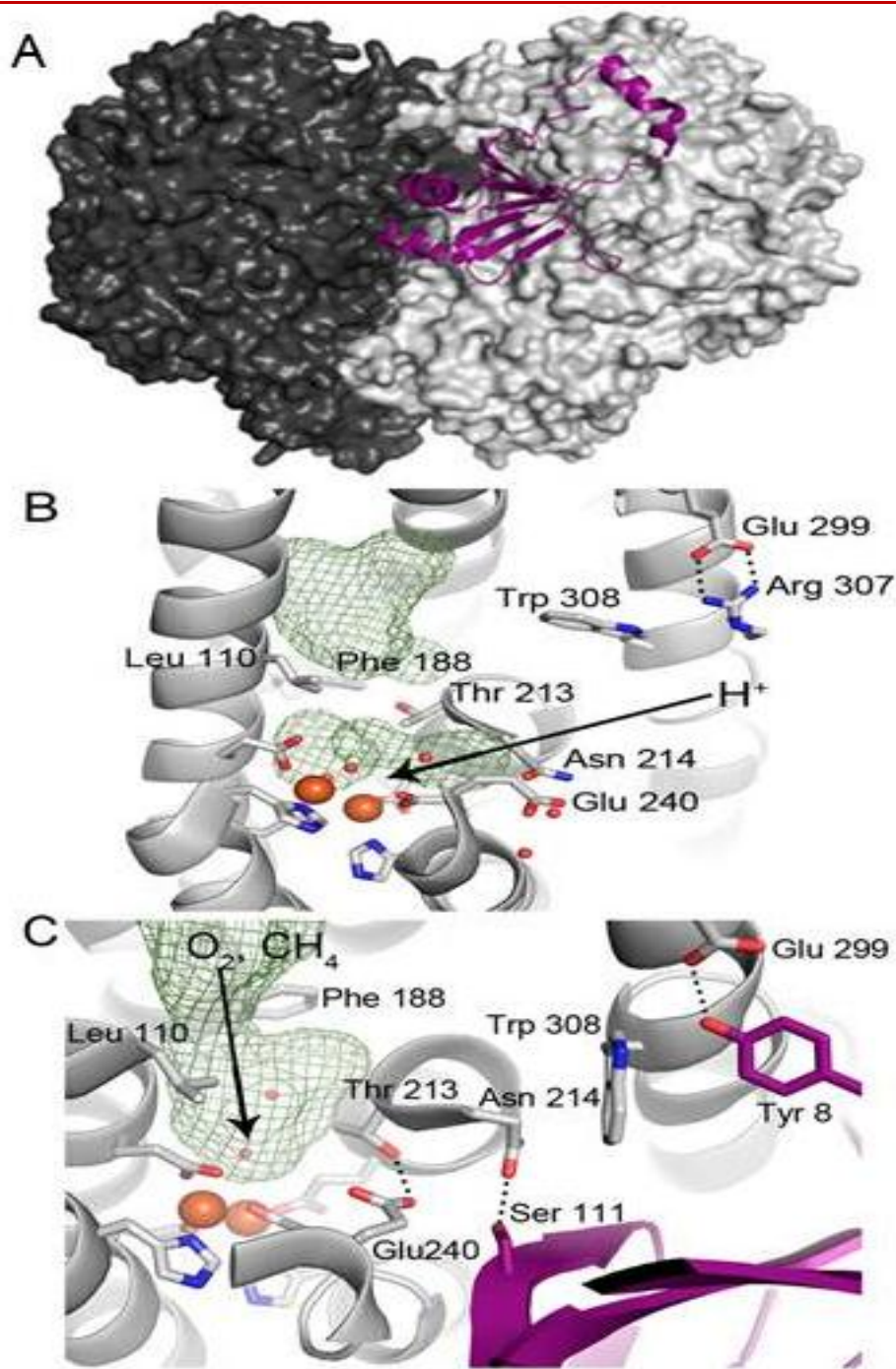


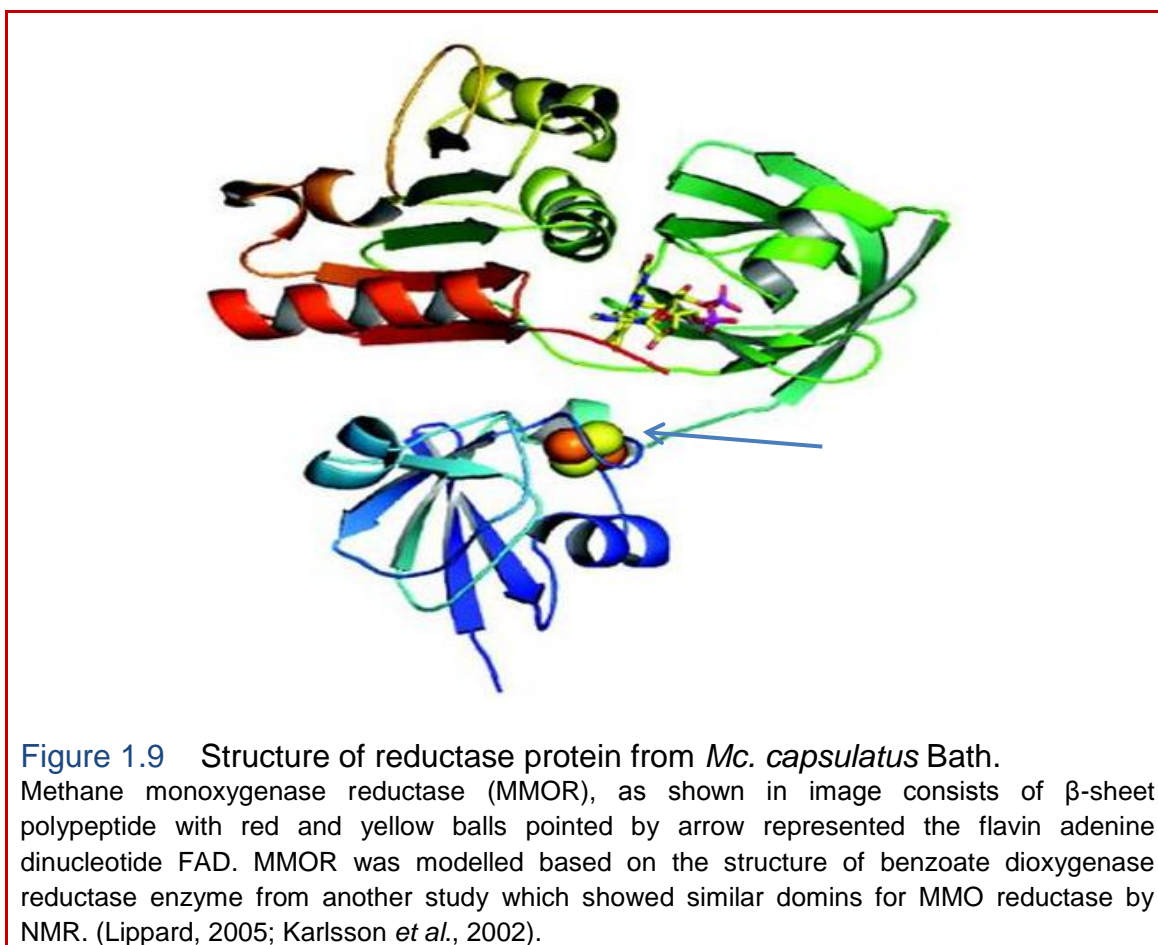
**Figure 1.8** Conformational changes in the formation of complex MMOH-MMOB.

A; Protein B in magenta attached in the canyon between MMOH protomers, B; the diiron centre in the  $\alpha$ -subunit of MMOH and the pore region is open for solvent and cavities 1&2 are disconnected by Phe 188 and L110. C; The pore region is closed and geometry alteration leads to open cavities 1&2 to allow substrate to enter the active site. Cavities are represented in a green net (Sirajuddin and Rosenzweig, 2015).

### 1.4.3.3 Reductase (protein C)

The third component of the sMMO, responsible for electron transfer from NADH to the hydroxylase is known as protein C or the reductase (MMOR) (Smith and Dalton, 2004). The reductase from *Mc. capsulatus* is a single polypeptide of 38.5 kDa with an Fe<sub>2</sub>S<sub>2</sub> prosthetic group and FAD (Flavin adenine dinucleotide) (Colby and Dalton 1979). The existence of the Fe<sub>2</sub>S<sub>2</sub> prosthetic group was proved by means of electron paramagnetic resonance (EPR) (Figure 1.9), and NADH was suggested as the electron donor. Protein C was found to be inactivated by copper ions that disrupt the Fe<sub>2</sub>S<sub>2</sub> centre, inhibiting the electron transfer from the reductase to the hydroxylase (Green *et al.*, 1985). Also it was shown that the reductase attached to the β-subunit of MMOH, suggesting other roles for protein C in sMMO activity: (i) The formation of a complex between MMOR and MMOH causes changes in product distribution (Froland *et al.*, 1992); (ii) protein C could be attached to MMOH in various positions with different affinity, which make it a competitor to MMOB (Fox *et al.*, 1991); and (iii) the redox potential of the diiron centre in MMOH are changed (Paulsen *et al.*, 1994; Liu *et al.*, 1997). There is a strong functional analogy between sMMO and cytochrome P450, since P450 is also a complex of monooxygenases utilizing NAD (P) H and oxygen to catalyse the oxygenation of various C-H compounds). It was found in cytochrome P450 that hydrogen hydroxide H<sub>2</sub>O<sub>2</sub> can substitute for O<sub>2</sub> as an oxidant in the absence of the reductase component (White & Coon 1980). In later studies it was found that methane oxidation was observed when H<sub>2</sub>O<sub>2</sub> was added to the MMOH components of methane monooxygenase from *Ms. trichosporium* (Andersson *et al.*, 1991) or *Mc.*

*capsulatus* (Jiang *et al.*, 1993), even in the absence of the other two components of sMMO.



Although some studies revealed that reductase binds in the  $\beta$ -subunit as just mentioned above, it is still unclear where the reductase binds to the MMOH. In an investigation on sMMO from *Ms. trichosporium* by using 1-ethyl-3-(3-(dimethylamino) propyl) carbodiimide (EDC) it was suggested that MMOR adheres to the MMOH  $\beta$ -subunit whereas MMOB appeared to attach to the  $\alpha$ -subunit (Fox *et al.*, 1991). In contrast, a study on *Mc. capsulatus*, also using EDC suggested that MMOR binds to the  $\alpha$ -subunit of MMOH (Kopp *et al.*, 2003). Recently, it has been found by using hydrogen-deuterium exchange coupled to mass spectrometry (HDX-MS) that MMOR attaches to the canyon between the  $\alpha$  and  $\beta$  subunits of MMOH where protein B was shown via x-ray

crystallography to bind (Wang *et al.*, 2014). The crystallographic study by (Wang *et al.*, 2014) also suggested that due to competition between MMOB and MMOR on the binding site, MMOB may inactivate electron transfer to the active site when it displaces MMOR from the MMOH.

As detailed above, many studies have proved that all parts of sMMO are indispensable and critical for the enzyme activity *in vivo* and *in vitro*. As such an attempt to purify the three components of soluble methane monooxygenase was performed in the present study to achieve the full activity of the enzyme.

## **1.5 Copper effect in switching between pMMO and sMMO**

As mentioned above some species of methanotrophic bacteria produce two types of methane monooxygenase, pMMO and sMMO. For these methanotrophs, switching between pMMO and sMMO takes place depending on the amount of copper in the media or in the environment. The pMMO is expressed in the cell when the ratio of copper to biomass is high, whereas sMMO is elaborated at low copper to biomass ratio (Stanley *et al.*, 1983; Hanson and Hanson, 1996). It was found that pMMO activity is enhanced by the presence of Cu outside the bacterial cell, and more activity was observed when more copper was added (Nguyen *et al.*, 1994). However, there is an effect of Cu on sMMOR which inhibits the sMMO reductase and inactivates the sMMO enzyme (Green *et al.*, 1985). Understanding the effect of copper in methanotrophic bacteria that produce pMMO and sMMO is valuable in biotechnology and bioremediation. For instance, due to its wide substrate range, sMMO has a wide potential role in oxidation of toxic substances in the

environment but is not expressed in high copper conditions which may exist frequently in nature. Many proposals for regulation of pMMO and sMMO by copper have been suggested as the precise mechanism for the copper switch is not well understood. [Murrell \*et al.\* \(2000\)](#) proposed a model for this switching between pMMO and sMMO in *Methylosinus trichosporium* OB3b depending on the presence of a regulator protein as described below; according to this model there is a putative regulator protein called copper binding regulator protein (CBR) that binds to a putative repressor molecule (R). The complex CBR-R-Cu then binds to a putative sMMO activator protein (A). When the copper ratio is high, this complex is formed and holds the repressor protein and activator protein to allow the transcription of the *pmo* genes and production of pMMO. In the opposite condition namely when the copper to biomass ratio is low, the complex containing CBR-Cu, as well as the activator (A) and repressor (R), cannot be established. This leaves the R protein to suppress transcription of *pmo*. Meanwhile, the activator protein will bind to the upstream-activating sequence of *mmoX* and initiate sMMO transcription. The initiation of sMMO transcription in *Methylosinus trichosporium* OB3b starts from a  $\sigma^N$  promoter upstream of *mmoX*. As was mentioned previously, the sMMO operon contains *mmoX*, *mmoY*, *mmoZ* which encode for  $\alpha$ ,  $\beta$ ,  $\gamma$  subunit of sMMO hydroxylase. *mmoB* encode for protein B and *mmoC* encode for protein C. In addition to *mmoD* (*OrfY*) with a proposed role for MmoD in assembly of the diiron centre in soluble methane monooxygenase was suggested by [Merkx and Lippard \(2002\)](#).

Initiation of transcription from the promoter upstream from the *mmoX* gene requires the presence of the  $\sigma^N$  subunit of RNA polymerase and the enhancer-binding-proteins (EBPs) which activate the start of transcription from a specific enhancer area upstream from the promoter ([Merrick 1993](#)).

In another model suggested by [Stafford et al. \(2003\)](#) on *Methylosinus trichosporium* OB3b, two more genes were included, which were, identified upstream from the sMMO operon named as *mmoR* and *mmoG*. These two genes were implicated in the regulation of operon by copper. According to the model hypothesised by [Stafford et al. \(2003\)](#); at the low copper to biomass ratio, the transcription of *mmoR* and *mmoG* will take place. The MmoR protein is thought to work as an enhancer binding protein which binds to  $\sigma^N$  (encoded by the *rpoN* gene) to start transcription of the sMMO operon from the  $\sigma^N$  dependent promoter. The role of MmoG was believed to work as a chaperon (GroEL) to help in folding of the MmoR protein or other polypeptides responsible for inhibition of MmoR. By mutagenesis of the *rpoN*, *mmoR* and *mmoG* genes, the sMMO expression under the low copper conditions was abolished, which may reflect an important role for these genes.

In another study by [Cśaki et al. \(2003\)](#) on *Methylococcus capsulatus* Bath another model was proposed involving two additional proteins. Sequencing of 9.5 kb near to the sMMO operon resulted in identification of the *mmoR* and *mmoG* genes down stream from the sMMO operon (), unlike the upstream location for *Ms. trichosporium* OB3b mentioned above. In addition, two more genes; *mmoS* and *mmoQ* were identified in the opposite direction to *mmoR* and *mmoG* in *Mc. capsulatus*. A hypothetical model in *Mc. capsulatus* was suggested in this study as below; in the low ratio of copper to biomass, MmoS protein senses the Cu to induce MmoQ by phosphorylation. The MmoQ protein was found to bind the enhancing protein MmoR, which, as described above, binds to  $\sigma^N$  to initiate the sMMO operon transcription. The roles proposed for *mmoR* and *mmoG* are the same as those described in *Ms. trichosporium*. Similar to the result from *Ms. trichosporium* the *mmoR* and *mmoG* genes were

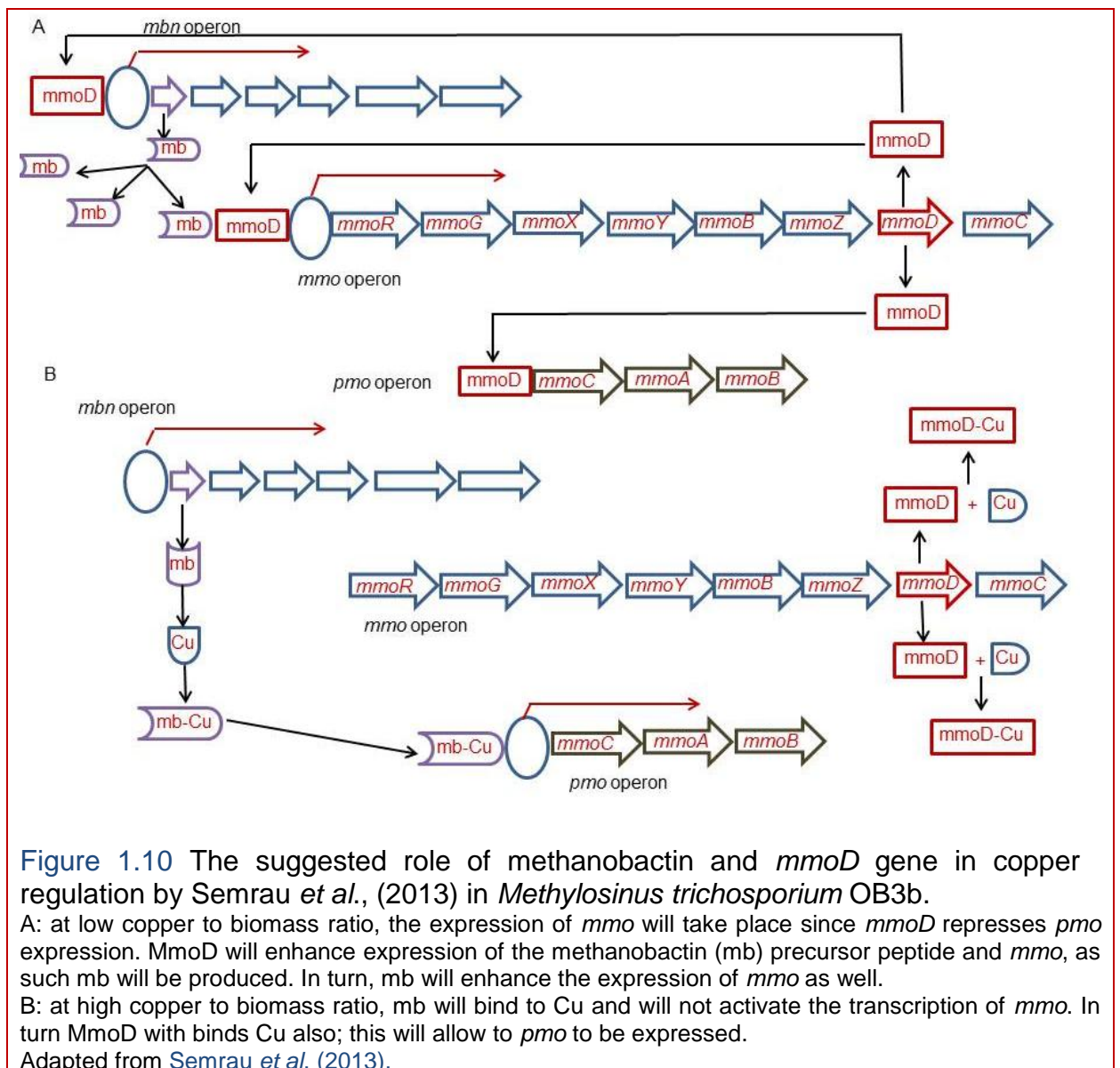
found to be indispensable for sMMO expression in addition to another proposed role for the putative chaperon protein MmoG in producing sMMO as a final well folded mature protein. No sequence motifs MxCxxC (which these authors expected to be metal binding residues) were identified in MmoS. This suggests either that MmoS detects copper indirectly or that it binds copper in a different way.

From previous studies, the presence of molecules that mediated the effect between the copper and MMO enzyme has been suggested. Copper-binding compounds (cbcs) were proposed to have such role (Choi *et al.*, 2003; Zhan and DiSpirito, 1996). Kim *et al.* (2004) identified a molecule from *Methylosinus trichosporium* OB3b similar to a siderophore and named as methanobactin (mb) (a siderophore is a molecule that binds iron which is able to transfer it into bacterial cells). The mb was implicated in scavenging and transport of copper into methanotrophic bacteria in the environment or in cells growing in a medium with added copper. Also it was suggested that CBCs are a small degraded fragment from mb. The crystal structure of mb was solved (Kim *et al.*, 2004); it is a chromopeptide of 1216 Daltons (C<sub>45</sub> N<sub>12</sub> O<sub>14</sub> H<sub>62</sub> Cu); it consists of a tetrapeptides composed of seven amino acids, with two 4-thionyl-5-hydroxyimidazole chromophores which acquire copper. By using mass spectrometry, X-ray crystallography and NMR, Behling *et al.* (2008) confirmed the crystal structure for mb by indicating the chemical formula and chemical construction as described above but suggested the presence of alkylidene oxazolone moieties rather than the hydroxyimidazolate rings which were suggested by the earlier study by Kim *et al.* (2004) in addition to proposing a biosynthetic pathway for mb in methanotrophs.

El Ghazouani *et al.* (2011) identified two types of mb from *Ms. trichosporium* OB3b; the full length form (FL-mb) and the truncated form (mb-Met), which lost the C-terminal Met residue. The removal of Met was found to have a small effect on the structure of the Cu (I) site. Both FL-mb and mb-Met have an effect on switching between sMMO and pMMO in *Ms. trichosporium* OB3b. Since the discovery of mb, a number of studies have concentrated on the role of these molecules in copper switching in methanotrophs that produce both pMMO and sMMO. By molecular genetics, Semrau *et al.* (2013) were able to identify the gene that is responsible for methanobactin precursor expression; deletion of this gene resulted in inactivation of mb production. Also they suggested another model for regulating the copper switch between pMMO and sMMO under copper variation in the environment or media for *Ms. trichosporium* OB3b. The model (Figure 1.10) includes the *mmoD* gene which encodes for a protein with previously unknown function. The model proposed that; under the low ratio of copper: biomass *mmoD* is transcribed to produce a protein MmoD which was found to suppress the transcription and expression of *pmo* and upregulate the expression of the sMMO operon and mb gene. It was proposed that the copper free mb enhances the expression of sMMO operon which includes *mmoD* and consequently the increased level of MmoD leads to strict repression of *pmo*. Under the high copper: biomass ratio, the mb will engage with Cu and as such the activation of *smo* will decrease which results in less MmoD being produced. Decreasing MmoD results in less production of mb and alleviates suppression of *pmo* by MmoD. Addition of more mb in the same study was found to increase the expression of *mmo* operon which was consistent with this hypothesis.

In a recent study, Al-Haque *et al.* (2015) revealed that mb from *Methylocystis* sp. strain SB2 can regulate expression of *mmo* in *Methylosinus trichosporium*

OB3b which indicates that mb from different methanotrophs have similar structures/functions. When *Ms. trichosporium* OB3b was grown at a high copper medium, the expression of the *mmoX* gene which encodes the  $\alpha$ -subunit from the sMMO hydroxylase was very low. When the mb from *Methylocystis* was added to the medium, the expression of *mmoX* in *Ms. trichosporium* was raised.

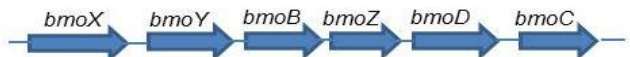
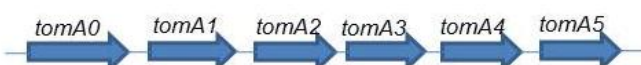
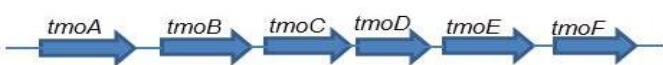
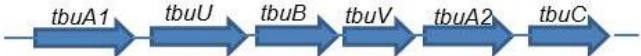
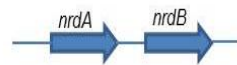


**Figure 1.10** The suggested role of methanobactin and *mmoD* gene in copper regulation by Semrau *et al.*, (2013) in *Methylosinus trichosporium* OB3b.  
 A: at low copper to biomass ratio, the expression of *mmo* will take place since *mmoD* represses *pmo* expression. *MmoD* will enhance expression of the methanobactin (*mb*) precursor peptide and *mmo*, as such *mb* will be produced. In turn, *mb* will enhance the expression of *mmo* as well.  
 B: at high copper to biomass ratio, *mb* will bind to Cu and will not activate the transcription of *mmo*. In turn *MmoD* with binds Cu also; this will allow to *pmo* to be expressed.  
 Adapted from Semrau *et al.* (2013).

## 1.6 Soluble diiron monooxygenase (SDIMO)

Soluble methane monooxygenase is one of important member of large family of soluble enzymes which contains a carboxylate-bridged diiron centre that activate dioxygen to oxidize C-H bonds (Leahy *et al.*, 2003) which are called the soluble diiron monooxygenases (SDIMOs). This family includes other enzymes such as butane monooxygenase (BMO), toluene-*ortho*-monooxygenase (TOM), toluene-4- monooxygenase (T4MO), toluene o-xylene monooxygenase (ToMO), and deoxyhypusine hydroxylase (DOHH). The SDIMOs are homologous to other proteins that are not monooxygenases such as hemerythrin, the R2 protein of ribonucleotide reductase (Qur and True, 1990; Vincent *et al.*, 1990; Nordlund and Ekland 1995) rubrerythrin (deMare *et al.*, 1996), and stearyl-acyl carrier protein (ACP)  $\Delta^9$ -desaturase (Nordlund and Ekland 1995; Fox *et al.*, 1993). Investigation and study of the molecular genetics of the SDIMOs and understanding their mechanism may help in exploiting them in industry, biotechnology and bioremediation of pollutants such as hydrocarbons.

**Table 1.3** Operon organization of soluble methane monooxygenase and other diiron enzymes

Diiron enzyme	Source organism	operon organization	Reference (s)
soluble methane monooxygenase (sMMO)	<i>Methylosinus trichosporium</i> OB3b		1, 2, 3
butane monooxygenase (BMO)	<i>Thauera butanivorans</i>		4
toluene-ortho-monooxygenase (TOM)	<i>Burkholderia cepacia</i> G4		5,6
toluene/ o-xylene monooxygenase (ToMO)	<i>Pseudomonas stutzeri</i> OX1		7
toluene-4-monooxygenase T4MO	<i>Pseudomonas mendocina</i> KR1		8
toluene-3-monooxygenase (T3MO)	<i>Ralstonia pickettii</i> PKO1		9, 10
Ribonucleotide reductase (RNR)	<i>Escherishia coli</i> K-12		11
deoxyhypusine hydroxylase (DOHH)	<i>Homo sapiens</i>		12, 13, 14
Stearoyl-ACP-desaturase	<i>Ricinis communis</i>		15

**References:**

- |                                  |                               |                                 |                                  |                                     |
|----------------------------------|-------------------------------|---------------------------------|----------------------------------|-------------------------------------|
| 1- Stafford <i>et al.</i> , 2003 | 4- Sluis <i>et al.</i> , 2002 | 7- Newman and Wackett, 1995     | 10- Byrne <i>et al.</i> , 1995   | 13- Kim <i>et al.</i> , 2006        |
| 2- Scanlan <i>et al.</i> , 2009  | 5- Yen <i>et al.</i> , 1991   | 8- Bertoni <i>et al.</i> , 1998 | 11- Carlson <i>et al.</i> , 1984 | 14- Abbruzzese <i>et al.</i> , 1986 |
| 3- Stein <i>et al.</i> , 2010    | 6- Yen and Karl 1992          | 9- Oslen <i>et al.</i> , 1994   | 12- Park <i>et al.</i> , 2006    | 15- Shanklin and Somerville, 1991   |

#### 1.4.4 Butane monooxygenase (BMO)

Butane monooxygenase is produced by the Gram-negative bacterium *Thauera butanivorans* (formerly *Pseudomonas butanovora*) (Dubbels *et al.*, 2009). The main substrate for BMO is butane in addition to its ability to oxidize alkanes, alcohols, organic acids (Takahashi *et al.*, 1980) and co-oxidation of chlorinated hydrocarbons (Hamamura *et al.*, 1997). Butane is oxidized at the terminal position by BMO to produce 1-butanol, which is then further oxidized to butyraldehyde by butanol dehydrogenase (Vangnai *et al.*, 2002). The butyraldehyde is then converted to butyrate (Arp, 1999), which is probably metabolized further via the fatty acid  $\beta$ -oxidation pathway to be used in building cell biomass and providing energy. As compared with the methane oxidation pathway, the steps of oxidation of butane are considered as very similar to the sMMO oxidation pathway. Cloning and sequencing of the BMO genes (Miriam *et al.*, 2002) showed that the BMO operon consists of six genes; *bmoX*, *bmoY*, and *bmoZ* encode a multimeric hydroxylase ( $\alpha_2 \beta_2, \gamma_2$ ) of 61, 45, 19 kDa respectively. The *bmoC* gene encodes the BMO reductase (40 kDa). The *bmoB* gene encodes a small protein of 15 kDa molecular mass considered as a regulator protein. The remaining gene in BMO operon, called *bmoD*, encodes a 9.6 kDa protein similar to MmoD, which has a proposed role in assembling the metal centre in sMMO (Table 1.3). As with sMMO operon there is also a gene encoding a putative initiation factor  $\sigma^{54}$  for transcription upstream from the *bmo* genes (Miriam *et al.*, 2002). In a study by Dubbels *et al.* (2007), BMO was purified and the properties of the purified protein confirmed the previous information about the composition of BMO and proved that the purified BMO

has activity towards ethene with H<sub>2</sub>O<sub>2</sub> as the oxidant via the peroxide shunt reaction, although the activity towards ethene was three orders of magnitude less than the hydroxylase of sMMO of *Methylosinus trichosporium* OB3b.

#### 1.6.1.1 Site directed mutagenesis studies on BMO

As it was mentioned previously about the sMMO, it is likely that there are a number of cavities implicated in allowing the entrance of substrate or egressing of product. Cavity 1 in the active site of sMMO is lined with hydrophobic side chains and cavity 2 forms a path from the active site to the enzyme surface (Rowsenzweig *et al.*, 1997). Also as mentioned above, the interaction between MMOH and MMOB changes the conformation of the residues in the active site which influences the flexibility of the active site toward substrates. Comparing the sequence of the  $\alpha$ -subunit of the hydroxylase of BMO with six strains of methanotrophs led to the conclusion that there is a high similarity between BMO and sMMO (Leahy *et al.*, 2003). In addition, there is a similarity in the versatility of substrates they oxidize. However, BMO has only a trace activity towards methane (Halsey *et al.*, 2006).

Exploiting the high similarity between BMO and sMMO, Halsey *et al.* (2006) designed five mutants in the  $\alpha$ -subunit of BMO hydroxylase. The mutated amino acids were converted to the corresponding amino acids in the active site of the sMMO, near to the active site and in the place in the hydroxylase of the BMO where regular protein proposed to bind to establish a complex with BMOH. *T. butanivorans* which expressing G113N and L279F were found to grow slowly on butane compared to the wild type. Also these mutants revealed a 277- and 5.5 fold increase respectively in the ratio of 2-butanol to 1-butanol produced

compared to the wild type. All the five mutants were shown to be capable of oxidizing methane although the methanol inhibited the enzyme. The maximum concentration of the methanol produced by the wild type was 23  $\mu\text{M}$ , whereas it was 83  $\mu\text{M}$  for mutant G113N.

There was a significant change in regioselectivity of this enzyme when the mutant G113N was constructed. This mutant oxidized propane subterminally to produce acetone that was not further oxidized; this activity mimicked the activity of sMMO towards this substrate, which also produces acetone as the sole final product, unlike wild-type BMO, which gives a mixture of terminal and subterminal oxidation products.

The ability of mutants G113N, L279F, and F321Y from *T. butanivorans* to oxidize dichloroethene (DCE) and trichloroethene (TCE) was also investigated by Halsey *et al.* (2007). It was found that the oxidation of three chloroethenes was lower in G113N mutant as was the rate of butane oxidation. A change in regioselectivity and products distribution was also observed in this study when the mutants were tested towards the same substrates. Unlike the wild type which was able to produce chloride stoichiometrically from CE oxidation, the mutant G113N yielded 14-25 % of available chloride from DCE and 56% from TCE oxidation. The F321Y mutant produced 40% of available chloride from the oxidation of both 1, 2-*cis*-DCE and TCE. The oxidation of 1, 2-*cis*-DCE by mutants L279F, F321Y and *T. butanivorans* wild type resulted in production of 1, 2-*cis*-DCE epoxide whereas G113N yielded only 50% of the oxidized 1, 2-*cis*-DCE. Mutant F321Y and wild type were also found to be able to produce epoxide from TCE oxidation whereas mutants G113N and L279F were not. The production of less than 40% of the available chloride from 1, 2-*cis*-DCE oxidation by all mutants and production of a new product epoxide may be an

example how the regioselectivity could be changed by site directed mutagenesis through substitution of one or more amino acids to make BMO or other diiron enzymes more active towards toxic substances. Also, this may indicate the value of such a study to obtain a mutant(s) able to be exploited in bioremediation, biotechnology and in industry.

### 1.6.2 Toluene *ortho*- monooxygenase

One of the SDIMOs which is able to oxidize aromatic compounds such as toluene and phenol is toluene *ortho* monooxygenase (TOM) from *Burkholderia cepacia* G4. TOM is able to oxidize toluene in the *ortho* position. The oxidation pathway of toluene by this enzyme takes place via converting toluene to *o*-cresol which is then further oxidized to catechol (Shields *et al.*, 1989; Worsey and Williams 1975). TOM is encoded by a 4.6 kb operon of six genes (*tom012345*); a 40-kDa NADH dependent oxidoreductase (encoded by *tomA5*), a protein encoded by *tomA2* (10.4-kDa) that transfers electrons from the reductase into the third component, the hydroxylase (211 kDa). The hydroxylase is composed of three subunits  $\alpha_2\beta_2\gamma_2$  encoded by three genes *tomA1*, *tomA3*, and *tomA4* respectively and contains a diiron centre within the  $\alpha$ -subunit (Table 1.3) (Shields and Francesconi, 1997).

### 1.6.2.1 Mutagenesis studies on Toluene *ortho*-monooxygenase (TOM)

Shields *et al.* (1995) showed that the TOM genes are carried on a plasmid (TOL), since a mutant of *Burkholderia cepacia* G4 without the putative TOM harbouring plasmid (TOL) resulted in no growth for this mutant on toluene or phenol. The reconstituted mutant with the TOL plasmid resulted in restoration of the enzyme activity in oxidizing toluene and phenol. The 36% amino acid sequence similarity between TOM and sMMO led to the suggestion of a similar role for equivalent amino acids in the two enzymes. A DNA shuffling technique was employed by Canada *et al.* (2002) to investigate the role of residue V106 (corresponding to L110 in sMMO which was suggested to have a role as a substrate gate) in playing similar role as substrate gate in the  $\alpha$ -subunit of TOM. Another aim for this study was to increase the ability of TOM to produce 1-naphthol from naphthalene oxidation and in degradation of trichloroethylene (TCE). Mutation of V106 to Ala (variant named TOM-Green), was expressed in *E. coli*. The activity of this mutant in oxidation of naphthalene to 1-naphthol was increased up to sixfold compare to the wild type. No alteration of enzyme regioselectivity was seen with 1-naphthol representing more than 97% of the product. Also the ability of TOM-Green to degrade 1, 1-dichloroethylene was increased to about 2.5-fold compared to that of the wild type and nearly 1.4-fold more active than the wild type in oxidation of *trans*-dichloroethylene. In addition, the TOM-Green mutant was able to oxidize triaromatic compounds; anthracene, phenanthrene, and fluorene more rapidly than the wild type. In a study by Rui *et al.*, (2004), saturation mutagenesis was used to create mutants A106E and A106F within TOM, which led to an increase in the activity in converting naphthalene to 1- naphthol by about 2-fold more than the wild type

without any change in regioselectivity. Mutant A106E was found to oxidize the main substrate toluene 63% more rapidly than the wild type does with a shift in regioselectivity to produce (50%) *o*-cresol, (25%) *p*-cresol and (25%) *m*-cresol, compared to 98% *o*-cresol being yielded from the wild type. Also nearly the same result was obtained from A106F which oxidized toluene 62% faster than the wild type. The regioselectivity for A106F was different from A106E, since A106F yielded (54%) *p*-cresol, (28%) *o*-cresol, and (18%) *m*-cresol. The expression of TOM was found to be raised in mutant A106E as shown by SDS-PAGE, whereas A106F showed similar expression level to the wild type. The ability of the A106F mutant to degrade chloroform was found to be 2.8 fold more than the wild type. The mutant V106A was showed a different colouration from oxidation of indole which may indicate a different product distribution from the wild type, since the V106A mutant produced a green colour whereas the wild type produced brown. Taking advantage of this observation, [Rui \*et al.\* \(2005\)](#) used saturation mutagenesis at positions A113 and V106 to create a library of mutants and study their properties in indole oxidation. These mutants showed novel products with various colours such as green, purple and orange. Characterization of the mutant enzymes revealed that, with indole as substrate, A113V produced indigo, A113I produced indirubin, and A113H as well as the C106A/A113G double mutant produced isatin. The wild type produced isoindigo through the insertion an OH group into the C-2 position in the indole pyrrole ring. A113G did not produce any of the compounds listed above; instead it oxidized indole to 4-hydroxyindol and an uncharacterized yellow product. The double mutant A113G/V106A was able to oxidize indole at the C-3 position. The study revealed the important role for these amino acids in TOM enzyme. The resulting compounds are potentially valuable in industry, for example indigo,

which is used as a dye in textiles (Maugard *et al.*, 2002). Also indirubin is important as a pharmaceutical since it is a cyclin-dependent kinase inhibitor, and it is one of a promising group of anticancer compounds (Hoessel *et al.*, 1999; Buolamwini 2000).

In addition to the ability of TOM to oxidize toluene, it was found that TOM is able to oxidize phenol and benzene which also enhance the expression of TOM, so they were used to activate TOM expression in bioremediation of TCE (Landa *et al.*, 1994; Lee *et al.*, 2006; Kim *et al.*, 2010). In a large area contaminated with TCE, it is unacceptable to add such an inducer as toluene, phenol or benzene which will lead to further contamination with toxic substances in addition of being expensive. An alternative approach was used by Kang and Doty (2014) by adding a ground poplar leaf (which is known to contain phenol and other phytochemical compounds) to the media used to grow *Burkholderia cepacia* G4 as the carbon and energy source and also an inducer for TOM enzyme. Kang and Doty (2014) were able to detect activity in degradation of TCE by *Burkholderia cepacia* grown using the poplar leaf material. qRT-PCR showed that the expression of the TOM enzyme genes were upregulated, which confirms the activation of gene expression by these poplar derived compounds and the expression is higher than the wild type by 1.8 times.

### **1.6.3 Toluene/o-Xylene Monooxygenase (ToMO)**

Toluene/ o-Xylene monooxygenase (ToMO) from *Pseudomonas stutzeri* OX1 is a four-component monooxygenase which is able to oxidize aromatic hydrocarbons such as toluene, xylene and phenol. In addition, it can co-

metabolise a wide range of substrates at various positions. The oxidation of xylene by ToMO takes place in a pathway in which an intermediate compound results from primary oxidation of toluene and xylene such as 2, 3-dimethylphenol (2, 3-DMP) and 3, 4-DMP. These intermediates subsequently will be further oxidized to produce dimethylcatechol (Bertoni *et al.*, 1996). Cloning and sequencing of the ToMO genes transferred to *E. coli* showed that ToMO is encoded by an operon of six genes; *touABE* which encodes the  $\alpha$ ,  $\beta$ , and  $\gamma$  subunits of the ToMO hydroxylase. *touD* encodes the regulator protein, *touF* encodes an oxidoreductase and *touC* encodes a Rieske type ferredoxin component (Table 1.3). Knocking out the genes that encode the regulator protein or the genes that encode the ToMO hydroxylase  $\alpha\beta\gamma$  subunits led to complete abolition of enzyme activity. However, in the same study, knocking out the reductase encoding genes (ToMOC and F) did not abolish the whole enzyme activity (Bertoni *et al.*, 1998). A crystallographic study by Sazinsky *et al.* (2004) in which crystals of ToMO hydroxylase were soaked with the surrogate product 4-bromophenol yielded a structure at 2.3 Å resolution that showed that there is a close similarity between the substrate binding sites within sMMO and ToMO. A wide channel with 6-10 Å width and ~35 Å in length crosses the distance between the enzyme surfaces and the active site within the hydroxylase. The detection of 4-bromophenol inside this channel led to the suggestion that this channel is the route for entrance of substrate or egressing of product. Although there is a high structural similarity between ToMOH and sMMO hydroxylase, ToMO is not able to oxidize methane like sMMO (Merks *et al.*, 2001).

There are a number of studies that have focused on engineering ToMO to produce di- and tri-hydroxy aromatic compounds. Such di- and tri-hydroxy

aromatic compounds for example, catechol, resorcinol, and hydroxyquinone are valuable in industry (Davis *et al.*, 1991). Catechols are used as starting materials in the pharmaceutical industry, and also in the food industry, whereas hydroquinone has been used as developer during processing of medical and industrial X-ray film (Davis *et al.*, 1991; Gillner *et al.*, 1994). 1, 2, 3- THB (trihydroxybenzene) has been used in the manufacture of hair dye and pharmaceuticals, whereas 1, 2, 4-THB has been used as an anti-corrosion substance (Davis *et al.*, 1991)

Vadar and Wood (2004) used DNA shuffling and saturation DNA mutagenesis in the  $\alpha$ -subunit of ToMO hydroxylase focusing on the important residues identified by previous studies such as that of Canada *et al.* (2002). I110 in ToMO was mutated because it corresponded to V106 in toluene *ortho*-monooxygenase. New mutants were also created in ToMO at residues Q141, T201, and F205. Novel regioselectivity was obtained during the oxidation of *o*-cresol by mutant F205G of ToMO when expressed in *E. coli* TGI/pBS (kan). The mutant yielded three products: 4-methylcatechol, 3-methylcatechol and methylhydroquinone, compared to one product 3-methylcatechol yielded by ToMO wild type. Also mutant F205G oxidized phenol to a mixture of catechol, resorcinol and hydroquinone, compared to wild type which yielded only catechol. Mutants I100Q and M180T/E284G (Figure 1.11) converted *o*-cresol to methylhydroquinone and 3-methylcatechol. These mutants also oxidized phenol to a mixture of hydroquinone and catechol.

The I100Q mutant was able to further oxidize catechol to 1, 2, 4-trihydroxybenzene (THB) whereas the wild type produced 1, 2, 3-THB from the same substrate, which showed a marked change in regioselectivity. It was reported that there was an altered regioselectivity for I100Q even with the

original substrate of ToMO, toluene, since the I110Q mutant oxidized toluene to *o*-cresol, *m*-cresol, and *p*-cresol (reported as 22%, 44%, and 34% respectively) whilst the wild type produced the same products with different proportions (reported as 32%, 21%, and 47% respectively).

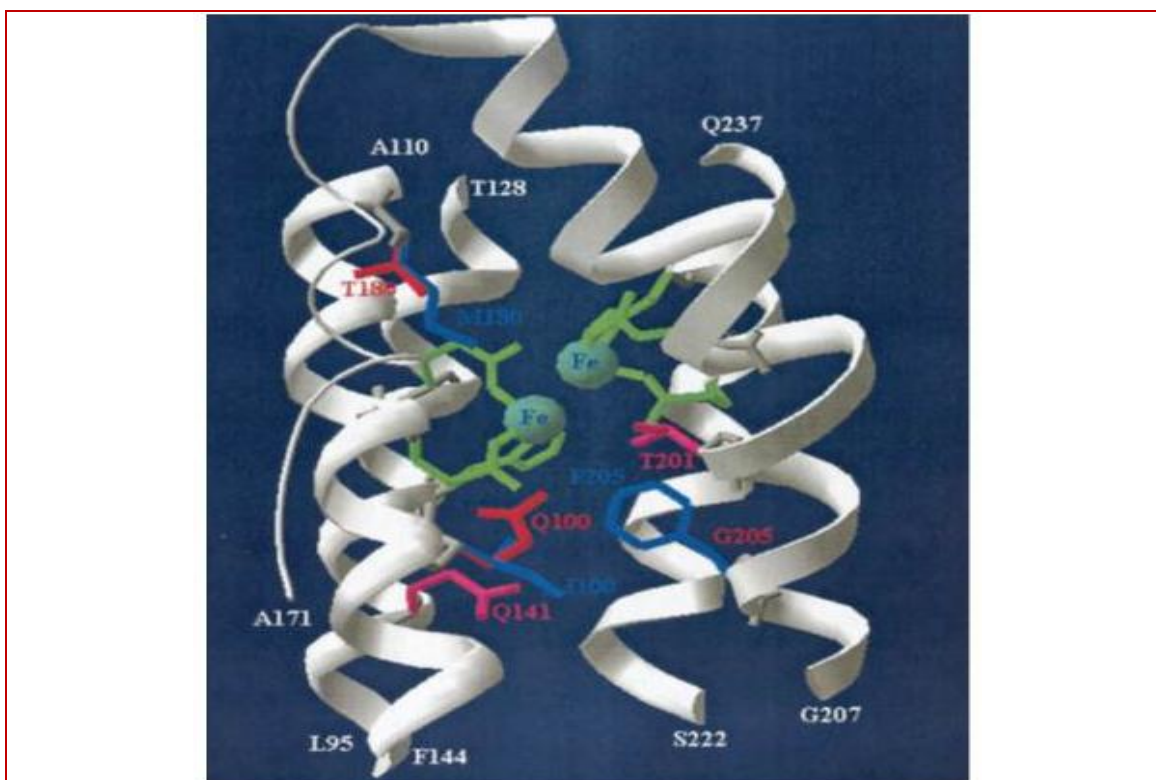


**Figure 1.11** Mutation of amino acids in ToMO active site centre.

The three dimensional model was constructed based on sMMO from *Methylococcus capsulatus*. The diiron centre is represented as a green sphere, I100Q, F205G and M180T (showed regioselectivity), Q141C, and T201 (no noticed regioselectivity) shown in red. The wild type I100, F205, and M180 shown in blue (Vardar and Wood, 2004).

The wild type ToMO was able to oxidize nitrobenzene (NB) to produce *m*-nitrophenol (*m*-Np) and *p*-nitrophenol (*p*-Np). The *m*-Np and *p*-Np were found to be further oxidized by ToMO to produce 4-nitrocatechol (4-NC), whereas 3-NC and nitrohydroquinone (NHQ) were the products from the oxidation of *o*-NP. DNA shuffling and saturation mutagenesis were employed by Vardar *et al.* (2004) to improve the activity of the ToMO enzyme or to alter its regioselectivity.

Random mutation in residues I100, Q141, T201 and F205 in the active site of ToMO was made and the products expressed in *E. coli*. Mutants M180T/E284G and E214G/D312N/M399V were able to produce 4-NC from oxidation of *p*-NP 4.5 and 20 times respectively faster than the wild type ToMO. Oxidation of NB by mutant A107T/E214A showed a large regioselectivity alteration by producing 79% from *p*-NP compared to 28% of the same product produced by ToMO wild type. Mutant A107T/E214A showed a strong regioselectivity towards toluene by yielding 93% *p*-cresol unlike the wild type which produced 32%, 21%, and 47% of *o*-, *m*-, and *p*-cresol respectively with 2.3fold activity for the mutant higher than the wild type. Most of the chemical products from the new mutants have a substantial advantage either in industry or in medicine, since it was found that nitroaromatic compounds are used as dyes, pesticides, and solvents (Spain and Gibson, 1991), whereas the nitrocatechol derivatives are used as pharmaceutical precursors, since it was used as inactivator for catechol-*o*-methyltransferase and then could be used to treat Parkinson's disease (Borgulya *et al.*, 1989; Learmonth and Freitas, 2002; Learmonth *et al.*, 2002). NHQ is used as a precursor for manufacturing compounds such as dephostain with an inhibitory activity for tyrosine phosphatase, which has been suggested for use in treatment of diabetes mellitus and neurodiseases such as Alzheimer's and Parkinson's diseases (Hamel and Girard, 1994; Umezawa *et al.*, 2003).

The role of the highly conserved T201 in providing a proton during the dioxygen activation in the catalysis cycle was further investigated in ToMO active site. Song *et al.* (2010) created four mutants in this residue by using point mutation; T201S, T201G, T201C, and T201V. The role of T201 was found to be indispensable in proton shuttling in ToMO. However, the substrate specificity was decreased for mutants T201C, T201G, and T201V which was attributed to

the loss of OH the group in these mutants which were suggested to have a role in the catalytic cycle. Ethylene oxide is an important compound, used to produce polyester and automotive antifreeze (Dever *et al.*, 2004). Ethylene (which is an alkene) was found to be oxidized by alkene monooxygenase (Small and Ensign, 1997). ToMO from the other side was found to be able to oxidize wide range of aromatic compounds producing an epoxide as an intermediate (Whited and Gibson, 1991). Carlin *et al.* (2014) supposed that the ToMO or mutated TOM might have the ability to oxidize ethylene to ethylene oxide in *E. coli*. Based on work done by Wood's group eleven mutants were designed by changing amino acids with small side chains to amino acids with larger side-chains which may have an effect on substrate size and restrict activity to small substrate such as ethylene; one of these mutants (V106) was found the best in oxidation of trichloroethylene. Since the ethylene is a small molecule, the best investigated mutants towards ethylene oxidation were found with the larger side chain mutants; A113F and V106F. A113F was able to oxidize ethylene to produce >99% ethylene oxide within the four incubation hours and V106F was found to have >170-fold higher activity than ToMO wild type.

#### **1.6.4 Toluene 4-Monooxygenase (T4MO)**

##### **1.6.4.1 Structure of toluene 4-monooxygenase**

T4MO from *Pseudomonas mendocina* KR1 is one of the most important aromatic hydroxylase enzymes due to its specificity in oxidation of toluene to produce *p*-cresol as the main product in addition to oxidization of a wide range of other substrates including phenol and trichloroethylene (TCE) (Yen *et al.*,

1991; van Beilen *et al.*, 2003). The T4MO is a four component enzyme with an operon comprising six genes named *tmoABCDEF*. Genes *tmoABE* encode the T4MO hydroxylase  $\alpha$ ,  $\beta$ ,  $\gamma$  subunits respectively (212 kDa). The diiron active centre is in the  $\alpha$ -subunit of the T4MO hydroxylase. The *tmoC* gene encodes a Rieske-type (2Fe-2S) ferredoxin (12.5 kDa). A small regulator protein (11.6 kDa) is encoded by *tmoD*. The fourth component is an NADH-dependent oxidoreductase protein (33 kDa) encoded by *tmoF* gene (Table 1.3) (Pikus *et al.*, 2000; Fishman *et al.*, 2004; Tao *et al.*, 2004).

#### 1.6.4.2 Mutagenesis of T4MO enzyme

One of T4MO's substrates is *p*-xylene, which when oxidized yields 4-methyl benzyl alcohol as the main product. This indicates the ability of T4MO to catalyse benzylic hydroxylation (Pikus *et al.*, 1997). Site-directed mutagenesis was employed to investigate the role of several residues within the  $\alpha$ -subunit of the hydroxylase; namely Q141 (corresponding to C151 in sMMO which is investigated in the current study), I180 and F205 (corresponding to F192 and I217 in sMMO respectively). A change in regioselectivity was observed in mutants Q141C and F205I in oxidation of toluene, with an increase in the proportion of *m*-cresol in the product from 2.8% from the wild type to 14.5% produced by the F205I mutant. When Q141C mutant was tested toward *p*-xylene, the results showed a change from benzylic oxidation by the T4MO wild type to ring hydroxylation by mutant Q141C. In contrast, mutant F205I oxidized *p*-xylene to produce an almost equimolar mixture of the benzylic and phenolic monohydroxylation products. However little or no shift in regioselectivity was observed with mutant I180F with either substrate. These results together with crystallographic studies on the similar diiron enzyme methane monooxygenase

(Rosenzweig *et al.*, 1997; Elango *et al.*, 1997), led to the hypothesis that the residues Q141 and F205 are in a position close to Fe<sub>A</sub> in the active site and residue I180 is on the opposite side to them and near the Fe<sub>B</sub> atom. The mutagenic studies on T4MO suggested that the amino acids in the hydrophobic cavity near the active site influence the orientation of substrates and so change the regioselectivity of the enzyme. As mentioned previously, SDIMOs generally have a series of cavities extending from the enzyme outer surface toward the active site to form a channel for substrate entry and product exit. Hosseini *et al.* (2014), by using mutagenesis combined with computational modelling, to dock two substrates; 2-phenylethanol (PEA) and *p*-tyrosol into the structure, identified two cavities in the T4MO hydroxylase. These cavities were described as the long and the short cavity both of which were found to have a role in substrate egression. The short channel that terminates with D285 and E214 was suggested to be responsible for hydrophilic product egression. The long cavity, which terminates with S395, was found to be important in determining substrate orientation by mutation of the serine to cysteine at this position. In addition another important role was proposed for residue F269 which lies at the junction between the short and long channels (Figure 1.12). Possible role for this residue include controlling regioselectivity and controlling the route taken by substrate and product entering and leaving the active site. Elsen *et al.* (2009) used X-ray crystallography to investigate the interaction between the oxidized and reduced form of the T201A mutant T4MO hydroxylase with, the regulator protein (T4moD). It was shown that in the complex which formed between the mutant T201A T4MO hydroxylase and the T4MOD, several residues within the hydroxylase active site adopted different orientations compared to the same side chains in the a complex of the wild type T4moH with T4moD.

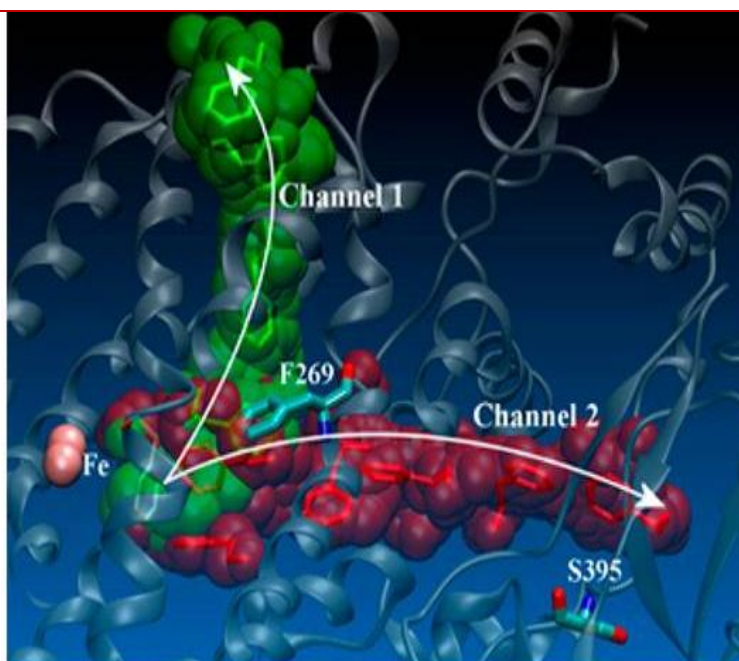


Figure 1.12 The two proposed routes for substrate migration out of the active site in T4MO. Short channel in green colour and long channel in red colour (Hosseini *et al.*, 2014).

#### 1.6.4.3 Production of industrial and pharmaceutical precursor compounds by T4MO

A large number of monooxygenase products are valuable even though many of them are harmful. The monooxygenase substrate benzene is able to cause anaemia and leukemia in cases of long exposure (Korte *et al.*, 2000; Smith, 1999). The oxidation of benzene gives phenol which is also known as harmful and polluting. One of benzene's double hydroxylation derivatives is catechol, which is valuable as an intermediate in pharmaceutical manufacture in addition to uses in the synthesis of agrochemicals, flavours, polymerization inhibitors, and antioxidants (Draths and Frost 1991; Draths and Frost 1995). Tao *et al.* (2004) expressed the operons encoding T4MO, TOM and T3MO in *E. coli* TG1/pBS (Kan) controlled by the *lac* promoter. This study showed that

recombinant T4MO, TOM and T3MO were able to hydroxylate benzene to produce catechol, which was then further oxidized to 1, 2, 3-trihydroxybenzene (1, 2, 3-THB). The hydroxylation products were identified by high-pressure liquid chromatography and mass spectrometry. The rate of hydroxylation varied between the three tested enzymes as detailed in (Table 1.4).

**Table 1.4** Product distribution of hydroxylation of benzene (165  $\mu$ M) to phenol, catechol, and 1, 2, 3-THB by T4MO, TOM, and T3MO (Tao *et al.*, 2004).

Enzyme	bacteria	phenol nmol/min/mg protein	catechol nmol/min/mg protein	1,2,3-THB nmol/min/mg protein
T4MO	<i>P. mendocina</i>	19 $\pm$ 1.6	13.6 $\pm$ 0.3	2.5 $\pm$ 0.5
TOM	<i>B. cepacia</i> G4	0.89 $\pm$ 0.07	1.5 $\pm$ 0.3	1.7 $\pm$ 0.3
T3MO	<i>Ralstonia pickettii</i> PKO1	3 $\pm$ 1	3.1 $\pm$ 0.3	0.26 $\pm$ 0.09

#### 1.6.4.4 Changing the regioselectivity of T4MO

Nitrocatechols are considered as important compounds due to their role as intermediates in manufacturing of pharmaceutical compounds e.g. Flesinoxan; which is antihypertensive drug (Hartog and Wouters, 1988; Scharrenburg and Frankena, 1996). Also an application has been suggested for nitrocatechol as an inhibitor of the enzyme catechol-o-methyltransferase, which has been investigated as a target for treatment for Parkinson's disease and other neurological diseases (Learnmonth and Freitas, 2002; Learnmonth *et al.*, 2002). Work in Wood's lab showed that T4MO was able to oxidize nitrobenzene to 4-nitrocatechol at a low rate. Fishman *et al.* (2004) have improved this ability by protein engineering using saturation mutagenesis. Mutations were introduced by using error-prone PCR in the  $\alpha$ - and  $\beta$ - subunits of T4MOH. The mutants

were expressed in *E. coli* TG1/pBS (Kan). Six mutants (TmoA Y22N, I84Y, S95T, I100S, S400C; TmoB D79N) yielding nitrocatechol were selected from 550 tested variants. Based on previous work in the same group on the ToMO enzyme, it was proposed that the I100 position has an important role in the catalytic properties of T4MO. Two more mutants were identified at position I100 after saturation mutagenesis; I100A and I100S. Mutant I100A was found to hydroxylate nitrobenzene to 4-nitrocatechol more than 16-fold more quickly than the wild type T4MO. Mutants I100A and I100S were found to hydroxylate nitrobenzene to *m*-nitrophenol and then to 4-nitrocatechol, unlike the T4MO wild type which hydroxylates nitrobenzene directly to *p*-nitrophenol with a very small amount of nitrocatechol. In addition, the regioselectivity is also shifted in toluene oxidation; the wild type produced 96% *p*-cresol from the oxidation of toluene whereas both mutants yielded a mixture of 20% *m*-cresol and 80% of *p*-cresol. Also the rate of toluene oxidation by mutant I100A was 65% higher than the wild type T4MO. The authors suggested that the change of a large residue near the active site in the  $\alpha$ -subunit into a smaller one makes the space wider to accommodate a larger substrate and changes the substrates orientation.

### **1.6.5 T4MO from *Bradyrhizobium* sp. BTAi1 (T4MO.BTAi1)**

A novel T4MO from *Bradyrhizobium* sp. BTAi1 was found to have similarity with members from the TMO family. It has 35%, 36%, and 38% similarity with ToMO, T4MO (*Pseudomonas mendocina*), and TpMO (toluene *p*-monooxygenase) respectively. It was classified as a T4MO due to its specificity in hydroxylation of the natural substrate toluene at the *para* position to produce *p*-cresol, like T4MO and TpMO (Yanik-Yildirim and Vardar-Schara, 2014). However the T4MO from

*Bradyrhizobium* sp. BTAi1 showed markedly different regioselectivity with other substrates. When it oxidized phenol, the products were 88% catechol and 12% hydroquinone compared to only catechol formed by the other TMO's. In addition, the toluene 4-monooxygenase from *Bradyrhizobium* sp. BTAi1 (T4MO.BTAi1) was found also to oxidize trichloroethylene (TCE) like the other TMOs. *Bradyrhizobium* sp. BTAi1 isolated and characterized from the nodules of *Aeschynomene indica* and is a photosynthetic rhizobacterium (Giraud *et al.*, 2007). The TMO gene-cluster from *Bradyrhizobium* sp. BTAi1 was cloned and sequenced in *E. coli* TG1, which showed that the TMO is encoded by an operon of six genes (*tmoABCDEF*) (Yanik-Yıldırım and Vardar-Schara, 2014). Like T4MO (i.e. the enzyme from *Pseudomonas mendocina*), the  $\alpha$ ,  $\beta$ , and  $\gamma$  hydroxylase subunits of T4MO.BTAi1 are encoded by the genes *tmoABE* respectively. The regulator protein TmoD.BTAi1 is encoded by *tmoD*. *tmoC* encodes TmoC.BTAi1 ferredoxin and TmoF.BTAi1 is an NADH oxidoreductase.

#### 1.6.5.1 Mutagenesis studies on T4MO.BTAi1

From previous mutagenesis studies (Vardar *et al.*, 2005; Sönmez *et al.*, 2014; Tao *et al.*, 2004; Fishman *et al.*, 2004) and crystallographic studies (Baily *et al.*, 2008; Baily *et al.*, 2012) an important role was suggested for a number of amino acids in the hydrophobic pocket of the  $\alpha$ -subunit around the active site. These residues are almost same in most of the TMO family apart from positions 101, 103, 180, and 214 in T4MO.BTAi1. The position 101 is occupied by proline in T4MO.BTAi1 unlike ToMO, T4MO, and TpMO which have alanine. The site 103 also has proline in T4MO.BTAi1 unlike ToMO which has glutamic acid

whereas T4MO and T $\rho$ MO both have the amino acid glycine. Mutagenesis studies showed an important role for these residues in enzyme activity and regioselectivity (Vardar *et al.*, 2005; Fishman *et al.*, 2005; Notomista *et al.*, 2001; Tao *et al.*, 2004). Site-directed mutagenesis in T4MO at position E214 (analogous to H214 in T4MO.BTAi1) showed an 11fold increase in the rate of the hydroxylation of 2-phenylethanol (Brouk *et al.*, 2010). There are different amino acids in these positions in T4MO.BTAi1 compared to the other TMOs. Saturation and site directed mutagenesis were employed to investigate the role of these amino acids in T4MO.BTAi1 in the oxidation of aromatic hydrocarbons and TCE (Yanik-Yildirim and Vardar-Schara, 2014). Eight mutants were created at positions P101, P103 and H214 in the  $\alpha$ -subunit of the T4MO.BTAi1 hydroxylase designated as H214:P101T/P103A, P101S, P101N/P103T, P101V, P103T, P101V/P103V, H214G, and H214G/D278N. Phenol, nitrobenzene and naphthalene were chosen as substrates to evaluate these mutants. Both residues P101 and P103 were found to have an important role in controlling the enzyme conformation. The main product from oxidation of phenol was resorcinol (60%), unlike the wild type which was inactive toward phenol. Mutant P103T produced *m*-nitrophenol from nitrobenzene with 4-times higher rate than the wild type. Using naphthalene as substrate, mutants P101T/P103A and P101S also showed altered regioselectivity by producing 2.3 times more 2-naphthol than the T4MO.BTAi1 wild type. The same mutants gave 1.6 times less 1-naphthol than the T4MO.BTAi1 wild type in the same reaction. The study confirmed the important role of these residues in holding the substrates in the active site in these enzymes because mutation of these residues changed the regioselectivity.

## 1.6.6 Toluene 3- Monooxygenase from *Ralstonia pickettii* PKO1 (T3MO)

Another member of the SDIMOs, which belongs to the toluene monooxygenase family, is toluene 3-monooxygenase (T3MO) from *Ralstonia pickettii* PKO1. The T3MO can oxidize toluene to produce *m*-cresol and co-oxidizes benzene and many other alkylaromatic hydrocarbons. It is a four component enzyme encoded by the *tbu* operon, which showed more than 60% amino acid sequence identity with T4MO (Leahy *et al.*, 1997); *tbuA1A2U* encode the three subunits of the  $\alpha_2 \beta_2 \gamma_2$  of the hydroxylase of T3MO. *tbuC* encodes an NADH dependent oxidoreductase. *tbuV* encodes a regulator protein without prosthetic group. *tbuB* encodes a Rieske-type ferredoxin protein (Table 1.3) (Kahng *et al.*, 2000; Fishman *et al.*, 2004). In addition to the *tbu* operon, a gene downstream of *tbu* operon was identified (*tbuX*) which has been found to be expressed in a low level in the cell. This expression was found to be increased when the cell was exposed to toluene such that more TbuX was produced than the T3MO enzyme. The way that this gene was induced led to the suggestion that it has a role as facilitator in toluene entry into the bacterial cells in addition to taking part in toluene metabolism (Kahng *et al.*, 2000).

### 1.6.6.1 Molecular studies on T3MO

The commercial importance of the hydroxylation products of benzene and its derivatives as mentioned previously led to the investigation of T3MO in oxidation of benzene. It was found that like T4MO and TOM, when T3MO was

expressed in *E. coli* TG1/pBS (Khan), it was able to hydroxylate benzene to phenol and then catechol, which was then hydroxylated to 1, 2, 3-trihydroxybenzene (1, 2, 3-THB). The rate of oxidation of each substrate to the subsequent product is shown in (Table 1.4). The formation of catechol by T3MO and T4MO, and the formation of 1, 2, 3-trihydroxybenzene by TOM were found to occur at a similar rate to that at which cresols were formed from toluene oxidation by these enzymes (Fishman *et al.*, 2004). As was mentioned previously, T3MO oxidizes toluene at the *meta* site to produce *m*-cresol. Olsen *et al.* (1994) and Fishman *et al.* (2004) found that T3MO expressed in *E. coli* TG1/pBS (Khan) oxidized toluene with an activity of  $11.5 \pm 0.33 \text{ nmol}^{-1} \text{ min}^{-1} \text{ mg}^{-1}$  of protein to give the unexpected product distribution of 90% *p*-cresol and 10% *m*-cresol. Further oxidation subsequently yielded 4-methylcatechol. The reaction rate was similar to that produced from the original plasmid pRO1966 containing T3MO that was expressed in *Pseudomonas aeruginosa*, which yielded *m*-cresol and *p*-cresol in the proportion 97% and 3% respectively. Also, *E. coli* TG1/pBS (Kan) harbouring T3MO oxidized nitrobenzene to form 66% and 34% of *p*-nitrophenol and *m*-nitrophenol respectively, whereas methoxybenzene was oxidized to 100% *p*-methoxyphenol by the native enzyme. Naphthalene was also oxidized by this recombinant enzyme to yield 1-naphthol (62%) and 2-naphthol (38%). The *tbu* genes were sequenced from the original plasmid pRO1966 alongside pBS (Kan) T3MO to exclude any unwanted mutations during the recombination steps which showed no sequencing difference. The similarity of T3MO with T4MO and TOM may allow researchers to identify the roles of candidate residues in the  $\alpha$ -subunit that are implicated in oxidation or product regioselectivity.

## 1.6.7 Ribonucleotide reductase (RNR)

Another diiron enzyme is the ribonucleotide reductase (RNR) which catalyses the reduction of ribonucleotides to deoxyribonucleotides which is then used in DNA synthesis (Climent and Sjöberg, 1992). RNR has been isolated from many organisms. One of the best characterized RNR is from *E. coli* which consists of two non-identical subunits named as R1 and R2. The R1 component comprises two subunits designated as the  $\alpha$  and  $\alpha'$  subunits, which are encoded by gene *nrdA*. The R2 subunits ( $\beta$  and  $\beta'$ ) are encoded by the *nrdB* gene. The R2 subunits contain the diiron centre and the free radical supplying, tyrosine residue (in the past, the R2 subunits were known as B1 and B2) (Table 1.3)

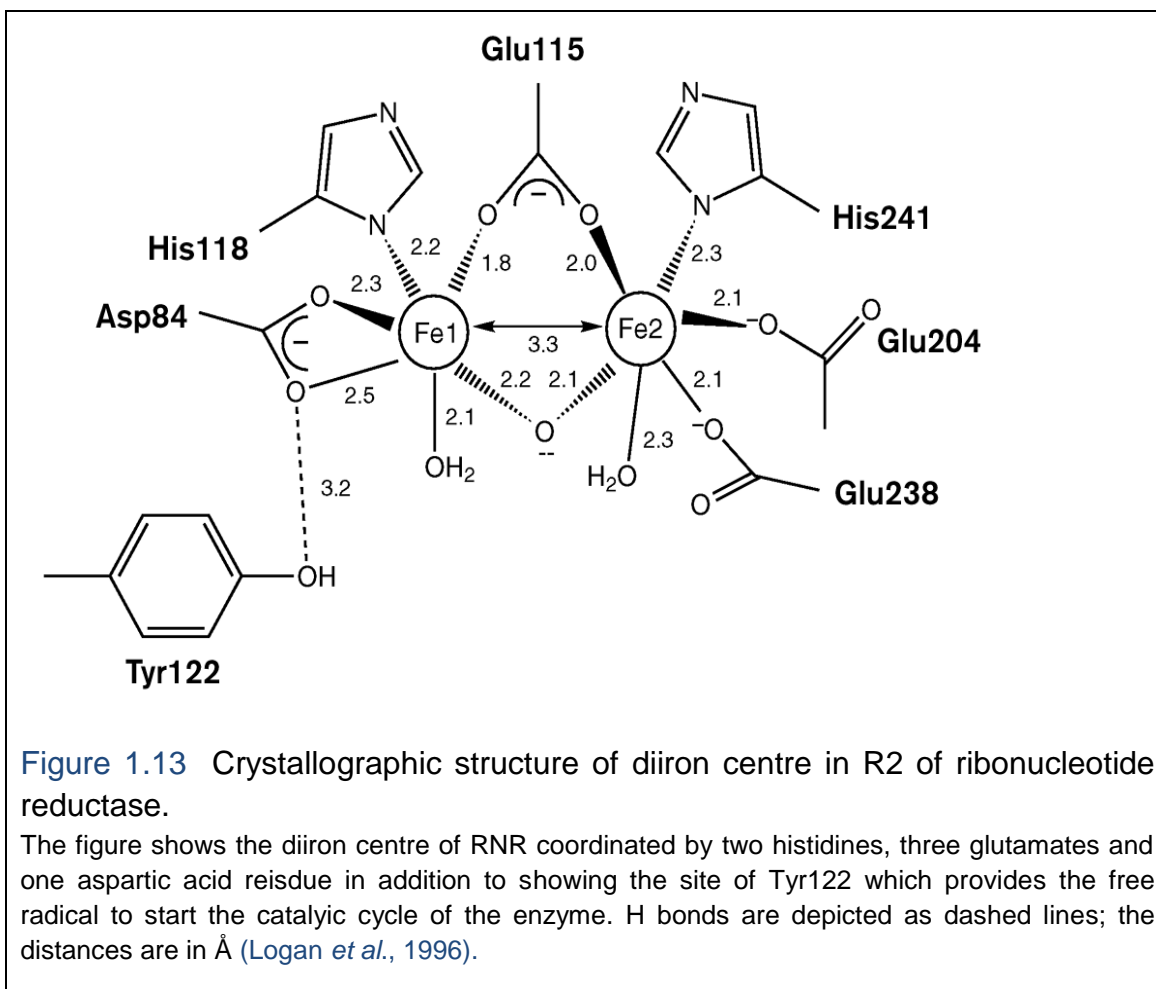
(Climent and Sjöberg, 1992; Carlson *et al.*, 1984). The diiron centre is coordinated by three glutamic acid residues, two histidines and two water molecules (Figure 1.13) (Logan *et al.*, 1996). R1 is implicated in accommodating the substrate and contains the catalytically important cysteine residues (Richard, 1988; Albert *et al.*, 1989). The role of R2 is to supply a free radical from the conserved tyrosine residue 122 to the R1 subunit through a conserved cysteine residue to start the enzyme catalytic cycle.

### 1.6.7.1 Crystallographic and mutagenesis studies on RNR

The tight interaction between the R1 and R2 subunits in RNR has been investigated by mutagenesis. The effect of deletion of 30 amino acids in the C-terminal of R2 showed an affect on the enzyme. The substitution of E350 and Y356 to alanine (both are along the pathway between the tyrosine122 and the

active site and as such implicated in transferring the electron from the Tyr122 to the active site via C-terminal), resulted in high effect on catalytic activity. However, no change in the strong interaction between R2 and R1 was observed. There was a decrease in E350A mutant activity (240-fold lower than that for the native protein) whereas the whole activity was abolished for mutant Y356A. The results suggested a catalytic role for these residues rather than a structural role.

Logan *et al.* (1996) has suggested a model in which a stable radical from Y122 in the R2 component oxidizes C439 in the RNR  $\alpha$ -subunit of the R1 component to produce a thyl radical. The distance between Y122 and C439 is about 35 Å which is considered to be too long a distance. This has led to the suggestion that there is a different pathway that can mediate this electron transfer including the presence of several amino acids along the way to facilitate this transfer; Y122, W48, Y356 in  $\beta$  2, Y731, Y730, and C439 in the  $\alpha$ 2 subunit. The role of tyrosine in producing the free radical for catalysis in the RNR reaction is well investigated by site-directed mutagenesis.



Another pathway was suggested by different research groups based on the crystal structure of the enzyme. The transfer of the free radical formed by tyrosine in R2 to the active site in R1 takes place through a series of hydrogen bonds including residues; Tyr 122, Asp 84, His118, Asp 237, Trp 48, and Tyr 356 in the R2 subunit and Tyr 730, Tyr 731, and Cys439 in the R1 subunit (Nordlund *et al.*, 1990; Nordlund and Sjöberg, 1993; Nordlund and Eklund, 1993; Uhlin and Eklund, 1994; Eriksson *et al.*, 1997). Asp 237 is implicated in connecting three helices through the residues His118, Trp 48 and Gln 43 (Figure 1.14). This residue (Asp 237) was mutated to an asparagine or glutamate. The mutation D237E resulted in an enzyme with a comparable activity to the wild type. However, mutant D237N lost its activity due to an unstable tyrosyl radical (Ekberg *et al.*, 1998), which support the hypothesis for

needing a chain of suitable amino acids to form a pathway to transfer the radical to the active site of the R1 component in order to achieve substrate catalysis.

Due to the similarity of RNR with sMMO, it has been suggested from the crystallographic studies of sMMO a same role for the corresponding amino acids to tyrosine (C151). This hypothesis has been investigated in the present study by designing a mutant at this site to investigate the role of this residue in providing a free radical during the sMMO oxidation catalytic cycle.

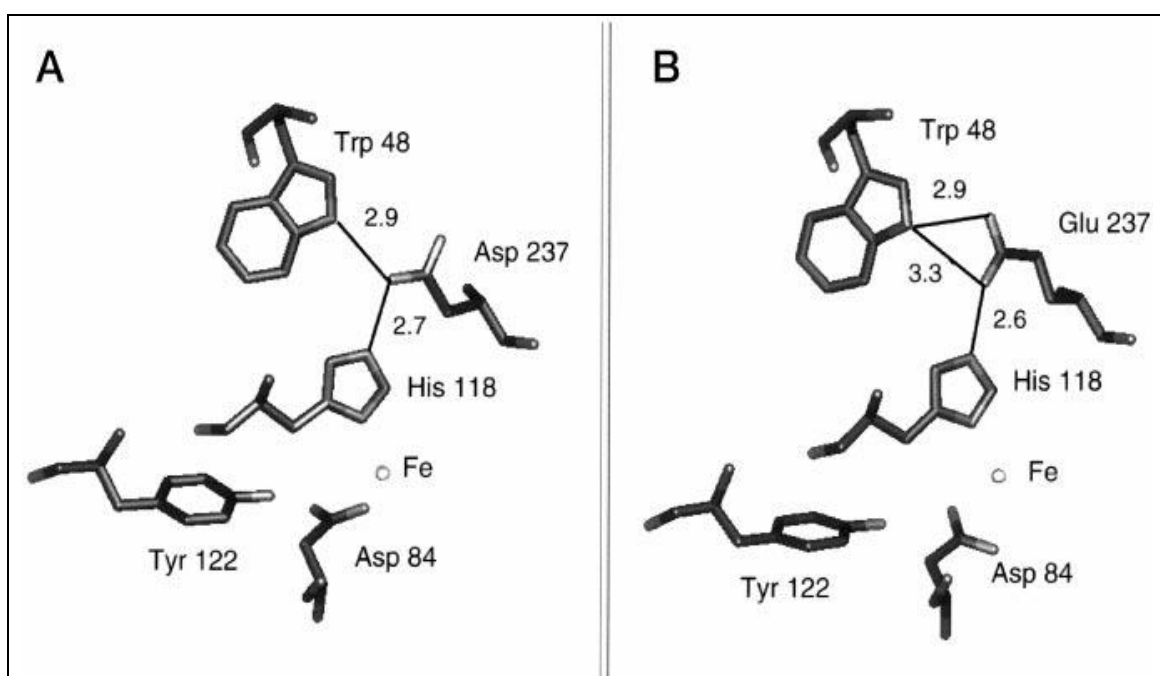


**Figure 1.14** Three dimensional schematic diagram showing the hydrogen bond connection of residue Asp 237 with Trp 48 and His 118 in the radical transfer pathway.

**A:** wild type shows the distance between the residue Asp 237 and the other two residues Trp48 and His118 which are proposed to transfer the electron to the active site.

**B** shows the change in the distance between residue 237 and the neighbouring residues Trp48 and His118 in D237E mutant (Ekberg *et al.*, 1998).

### 1.6.7.2 RNR as a target for anticancer drugs

Cancer is a main cause for death over the world, in the United States more than 500,000 deaths due to cancer are recorded every year. Most of the current anti-cancer drugs have a serious side effects or lead to tumour resistance (Jordan and Reichard, 1998; Kolberg *et al.*, 2004; Cerqueira *et al.*, 2007). Due to the critical role of RNR in DNA synthesis, it is considered as a target for anticancer medications. Inhibiting of activity of RNR, which supplies the cell with DNA precursors prevents the cell from synthesizing DNA (Tanaka *et al.*, 2000). The human RNR comprises two subunits designated as (RRM1 ~85 kDa) which contains the catalytic site where the substrates accommodate (analogous to R1 in *E. coli*) and RRM2 ~ 45kDa which contains the diiron active site (analogous to R2 in *E. coli*) (Larsson and Sjöberg, 1986; Ekberg *et al.*, 1998). It was found that reducing the activity of RRM2 in cancer cells *in vitro* minimized drug resistance and slowed cancer cell division, which led to the proposal to investigate it as a drug target (Zhou *et al.*, 1995; Goan *et al.*, 1999; Zhou *et al.*, 1998; Liu *et al.*, 2007). As mentioned for RNR from *E. coli* the C-terminal was found to be responsible for interaction between RRM1 and RRM2 and radical transfer. In a study conducted in the National Cancer Institute (NCI), a new ligand-binding cavity was identified close to the C-terminal in the RRM2 by computer modelling and confirmed by site directed mutagenesis. Based on this result, this pocket was suggested as a place for targeting by a new anticancer drug (Zhou *et al.* 2013). The drug CHO29, which binds in this position, was found to be effective in inactivation a number of neoplastic cell lines, especially ovarian and leukemia cancer cell lines.

## 1.6.8 Deoxyhypusine hydroxylase (DOHH)

### 1.6.8.1 Structure of deoxyhypusine hydroxylase

Deoxyhypusine hydroxylase (DOHH) from human is also one of the diiron hydroxylase enzymes, which catalyses the hydroxylation of a specific amino acid lysine in spermidin (an eIF5A precursor) in two steps to produce the unusual amino acid called hypusine (Kim *et al.*, 2006 a). The lysine is hydroxylated to an intermediate compound called deoxyhypusine by deoxyhypusine synthase (Wolff *et al.*, 1995; Joe *et al.*, 1995) which is then hydroxylated by deoxyhypusine hydroxylase to yield hypusine in eukaryote initiation translation factor 5A (eIF5A) (Park *et al.*, 2006; Abbruzzese *et al.*, 1986). Although DOHH is a non-heme diiron enzyme like methane monooxygenase, toluene monooxygenase and stearyl acyl carrier protein  $\Delta^9$ -desaturase, there is no statistically significant similarity with these enzyme (Kim *et al.*, 2006 b). Vu *et al.* (2009), by using Mössbauer and XAS spectroscopic on recombinant DOHH hydroxylase, were able to confirm that the active site is contains diiron and the enzyme was able to activate oxygen to produce an intermediate compound ( $\mu$ -1, 2-peroxo) diiron (III) during the transformation of eIF5A precursor to mature eIF5A which is similar to the methane monooxygenase.

### 1.6.8.2 Mutagenesis studies on DOHH

Like the other non-heme diiron enzymes, the diiron active site for DOHH is coordinated by His and Glu residues. The role of these residues was investigated in a study by [Kim \*et al.\* \(2006\)](#) who showed that the mutation of the diiron coordinating residues in DOHH resulted in inactive enzymes. Six of these eight mutants namely; H56A, H89A, E90A, H207A, H240A, and E241A showed less iron content compared to the wild type whereas the other two had comparable iron content. This study indicated that the binding ligands Glu and His are important for enzyme activity and to hold the Fe in the active site of the DOHH. An enzyme similar to human DOHH was characterized from *Saccharomyces cerevisiae* named Lia1 encoded by gene *LIA1* ([Thompson \*et al.\*, 2003](#)) which hydroxylates deoxyhypusine to hypusine ([Park \*et al.\*, 2006](#)). Mutagenesis studies on the Lia1 active site showed a change in interaction with the substrate. This was added additional important role in conserving the diiron centre in the active site, the structure of the protein and catalysis the transformation of deoxyhypusine to hypusine ([Cano \*et al.\*, 2010](#)). The crystal structure was also solved for DOHH, which revealed the presence of the intermediate compound peroxo-diiron (III) in the DOHH hydroxylase active site; after the reduced diiron centre had reacted with oxygen. These results were confirmed by UV/Vis and Mössbauer spectroscopy ([Han \*et al.\*, 2015](#)). The understanding of the active site properties may enable more studies into the importance of this enzyme. Inhibitors of the two enzymes deoxyhypusine synthase and deoxyhypusine hydroxylase are candidates for treatment of HIV/AIDS, chronic myeloid leukemia, and diabetes ([Kaiser, 2012](#)).

### 1.6.9 Stearoyl ACP desaturase

A family of diiron enzymes was isolated from plants that are able to catalyse the transformation of plant saturated fatty acids to unsaturated fatty acids, known as stearoyl acyl-carrier protein (ACP) desaturases (Lindqvist *et al.*, 1996). Each enzyme from this family catalyses the introduction of a double bond in a particular site in the fatty acid. One of these enzymes is the soluble  $\Delta^9$  stearoyl-ACP desaturase which inserts a double bond between carbons 9-10 in an 18 carbon fatty acid chain. The crystal structure revealed similar motifs to those present in the monooxygenase. The diiron in the active site in the stearoyl ACP desaturase is coordinated by glutamate and histidine residues in addition to two glutamic acids within the coordination space of both Fe ions. In addition, a long channel was identified starting from the enzyme surface and continuing towards the active site, which is thought to be appropriate in size for a fatty acid substrate to be oxidized at position 9.

#### 1.6.9.1 Site directed mutagenesis studies on stearoyl ACP desaturase

Although there is little similarity in amino acid sequence between the  $\Delta^9$  stearoyl-ACP desaturase and the diiron monooxygenase (Guy *et al.*, 2006),  $\Delta^9$  stearoyl-ACP desaturase has a similarity with the other ACP desaturases within the same family. Site-directed mutagenesis was performed on  $\Delta^6$  palmitoyl-ACP desaturase based upon a comparison to  $\Delta^9$  stearoyl-ACP desaturase to investigate the regiospecificity of these enzymes in desaturation of fatty acid

(Cahoon *et al.*, 1997). Five amino acids lining the hydrophobic cavity around the diiron centre of  $\Delta^6$  palmitoyl-ACP desaturase were substituted with the analogous residues in  $\Delta^9$  stearoyl-ACP desaturase; A181T/ A200F/ S205N/ L206T/ G207A. The result showed that mutated  $\Delta^6$  palmitoyl-ACP desaturase was able to behave like  $\Delta^9$  stearoyl-ACP desaturase, since it could introduce double bonds at either the  $\Delta^6$  or  $\Delta^9$  position. Based on crystallographic and previous mutagenic studies the replacement of two residues L118F/ P179I in  $\Delta^9$  stearoyl-ACP desaturase was performed. This led to a change in the specificity of  $\Delta^9$  stearoyl-ACP desaturase to that of  $\Delta^6$  palmitoyl-ACP. Whittle *et al.* (2008) designed a triple mutant T117R/ G188L/ D280K that was able to convert the stearoyl-ACP substrate into an allylic alcohol. This change in catalytic properties was attributed to a change in the substrate binding site around the diiron centre that may have led to the substrate being held in a different way. Liu *et al.* (2015) designed a mutant T104K/ S202E in soluble castor  $\Delta^9$  stearoyl-ACP desaturase to introduce a salt bridge to block one of the substrate-binding cavities of the enzyme. After the mutant was expressed, the protein was purified and characterized by X-ray crystallography, activity assay and size exclusion chromatography. It was shown that the one of the substrate cavities was occluded and mutant T104K/ S202E enzyme had an activity comparable to wild type full activity.

### 1.6.9.2 Mutagenesis of stearoyl-ACP desaturase converts the desaturation to oxidation activity

A comparison between  $\Delta^9$  stearoyl-ACP desaturase from castor with the diiron ruberythrin peroxidase showed a large similarity in the conformation and residues around the diiron centre, apart from at position 199 of the  $\Delta^9$  stearoyl-ACP desaturase. The residue 199 is threonine in  $\Delta^9$  stearoyl-ACP desaturase whereas the corresponding residue is a glutamic acid in the ruberythrin peroxidase. The carboxylate group at this site was implicated in catalysis the oxidase activity of ruberythrin peroxidase by providing a proton to bound oxygen due to its close position to diiron centre. Substitution of threonine to glutamic acid in  $\Delta^9$  stearoyl-ACP desaturase (mutant T199D) resulted in an enzyme which was capable of accommodating the substrate, but a decrease in desaturation activity was about  $2 \times 10^3$  times. A change in peroxide-dependent oxidase activity was increased by more than 31 times comparing to the wild type enzyme. This mutation in  $\Delta^9$  stearoyl-ACP desaturase altered the enzyme activity to become more similar to ruberythrin peroxidase enzyme (Guy *et al.*, 2006).

## 1.7 Aims of the present study

As illustrated by the mutants that have been made in the aromatic monooxygenases, mutagenesis has answered a number of questions about the role of specific amino acids in these enzymes. Changing some of these amino acids by mutagenesis has resulted in a substantial difference in yield of products with value to industry or uses as pharmaceutical precursors, and proof or disproof of hypotheses about how the enzymes function. It would be valuable to identify mutants of sMMO which may be used as alternative methods for synthesis of high value compounds from cheaper starting materials and with less toxic side products. In addition it may be possible to construct mutants to produce molecules for which no adequate chemical synthesis is available

- It was intended in the present study to use this approach to investigate the role of selected residues in the  $\alpha$ -subunit of soluble methane monooxygenase hydroxylase where the active site is situated. Residue C151 was chosen to investigate its possible role in radical chemistry in the sMMO catalytic cycle.
- Residue (R98), which has not been hypothesized from previous crystallographic studies to have a role in the sMMO hydroxylase  $\alpha$ -subunit is also one of the candidate residues that has been investigated as one of the aims in the present study. The function of this residue was probed in the formation of an ionic network which was proposed to restrict the size of the substrate entering the active site. It was intended by changing this residue, to reduce the ionic network, which may make the protein more flexible to allow large substrates to enter and be oxidized by sMMO.

- A new mutant was also designed to investigate the role of one of the glutamate residues (E114), which ligates the diiron centre, with the intention of stabilizing the previously designed unstable mutant (C151Y) to allow further characterization of the role of this position in enzyme activity.
- Finally, analysis of recombinant enzyme requires the purification of the three components of the soluble methane monooxygenase. In the present study it was aimed to purify and test the activity of a new affinity His-tagged hydroxylase created in this group, which was intended to minimize the long purification protocol into a one step method by using an affinity column.

# Chapter 2: Materials and Methods

---

## 2.1 Bacterial strains and growth conditions

### 2.1.1 Bacterial strains and plasmids

All methanotrophs and *E. coli* strains that were not constructed during this project were supplied by the microbiological laboratory of Biomedical Research Centre, Sheffield Hallam University. The methanotrophs strains used in this work were *Methylosinus trichosporium* OB3b (wild type), the recombinant wild type with His-tag, and three other mutants; SMDM (soluble methane monooxygenase deleted mutant), SMDM pT2MLY C151S, SMDM pT2MLY F282L, pT2MLY C151Y. The mutants SMDM pT2MLY R98A, double mutant SMDM pT2MLY R98A S4G, SMDM pT2MLY E114D C151Y and SMDM pT2MLY E114D were constructed in the present study.

The competent strains *E. coli* S17.1 and *E. coli* BL21 were from Invitrogen and *E. coli* XL-10 gold ultra-competent cells were from Agilent technologies.

Plasmids that were used in this study are described in Table 2.1.

**Table 2.1** Plasmids used in the present study.

Plasmids	Main features	References
pTJS 175	Methanotroph expression vector, pTJS140 containing 10.1 kb insert including the sMMO operon. Ap <sup>r</sup> Sp <sup>r</sup> Sm <sup>r</sup>	Smith <i>et al.</i> , (2002)
pTJS175 C151Y	Same as above in addition to mutation of the C151Y.	Smith <i>et al.</i> , (2002)
pT2MLY	It is a modified pTJS140 by removing <i>Nde</i> I, two <i>Bam</i> HI and 516 bp to create pT2ML which then became pT2MLY by inserting His-tag into the $\beta$ -subunit of the hydroxylase	Nichol, (2011) and Lock <i>et al</i> (unpublished)
pT2MLY R98L	Same as above in addition to mutation in R at 98 position to L.	Lock <i>et al</i> (unpublished)
pT2MLY F188W	Same as above in addition to mutation in F at 188 position to W.	Lock <i>et al</i> (unpublished)
pGEX <i>mmoB</i>	Plasmid with the gene encoding for protein B of sMMO and GST affinity tag.	Lloyd <i>et al.</i> , 1997
pJET1.2	It is a 2974 bp plasmid with Ap <sup>r</sup> and Multiple Cloning Site (MCS) to clone blunt end inserts.	Thermo scientific

### 2.1.2 Culturing the isolates and mutants

Methanotrophs were grown on Nitrate Mineral Salt (NMS) (Appendix 1) liquid or agarat 30°C with methane as the sole source of carbon and energy. When the growth was in NMS liquid, the methanotrophs were grown in a 250 ml Quickfit flask with a subaseal and 50 ml of the headspace replaced with methane. The flasks were incubated at 30°C with shaking at 180 rpm. Methane was provided every 3-5 days. Plate cultures were incubated in sealed anaerobic jars with 50/50 oxygen air to methane. After 2-3 weeks the methanotrophs were ready

for naphthalene test, which confirmed the production of sMMO when it was positive. Antibiotics were used when needed at concentration of 20  $\mu\text{g ml}^{-1}$  for streptomycin and spectinomycin, 50-100  $\mu\text{g ml}^{-1}$  for ampicillin, 5  $\mu\text{g ml}^{-1}$  for gentamycin and 25  $\mu\text{g ml}^{-1}$  for nalidixic acid. Growth of large-volume cultures of wild-type or mutant methanotrophic strains was performed as described by Lloyd *et al.* (1999), with modifications as follows; A New Brunswick Bioflo 101 fermentor fitted with an additional rotameter to provide a continuous air/methane gas with a flow rate 750  $\text{ml min}^{-1}$  and 55  $\text{ml min}^{-1}$  respectively at 30 °C. Copper sulfate was added to the NMS at 0.1 mg of  $\text{CuSO}_4 \cdot 5\text{H}_2\text{O}$  litre<sup>-1</sup> in the first batch, whereafter NMS without copper was used, antibiotics were not added except for the first batch of medium (Smith *et al.*, 2002). The optical density was measured at 600 nm using a spectrophotometer at regular periods to observe growth of the culture. Cells harvested from the fermenter were pelleted by centrifugation for 20 min at 10,000  $\times g$ , washed once with 25 mM MOPS (pH 7.0), 1 mM benzamidine, 1 mM dithiothreitol (DTT) and resuspended in a minimum amount of the same buffer. The cells were drop frozen drop wise into liquid nitrogen and stored at -80 °C.

Luria bertani (LB) or Nutrient broth/agar (Oxoid) (Appendix 1) was used for cultivation of *E. coli* at 37°C. LB cultures were incubated with shaking at 180-220 rpm. Both liquid and nutrient agar cultures were incubated at 37°C overnight.

### **2.1.2.1 Chemical reagents and media for bacterial culture growth**

All chemical reagents used for growing bacterial cultures in the present study were supplied by Sigma Aldrich and Melford Labs. Gases were supplied by BOC and Air liquid (formerly Scott gas).

## **2.2 General DNA methods**

All restriction enzymes, phosphatase, ligase, and the high fidelity Phusion master mix were supplied by New England Biolabs unless otherwise stated.

All the work concerning DNA purification, analysis and cloning in *E. coli* was done following the protocols from Sambrook *et al.* (1989). Plasmid DNA (pDNA) mini, midi and maxi preparations were performed using the Qiagen mini, midi and maxi prep kits and the supplier's instructions. The composition of DNA manipulation and analysis buffers are provided in Appendix 2. For extraction of plasmid DNA in a small amount ( $<50 \text{ ng } \mu\text{l}^{-1}$ ), the QIAprep spin miniprep kit (QIAGEN) was used following the manufacturer's instructions. For high DNA plasmid amount ( $>100 \text{ ng } \mu\text{l}^{-1}$ ), Qiagen maxiprep kit was used. For preparing intermediate amount of pDNA, the Qiagen midi prep kit was used.

### 2.2.1 QIAprep spin plasmid miniprep protocol

This is a modification of the alkaline lysis method of Birnboim and Doly (1979). A single colony of plasmid-containing bacteria was grown overnight in (5 ml) LB with an appropriate antibiotics at 37°C. The culture was then centrifuged at high speed (17170 x g) in a bench centrifuge for 1 min to pellet the cells. The pellet was resuspended in 250 µl from buffer P1 was and moved to a sterilized Eppendorf tube. A 250 µl of lysis buffer P2 was added and mixed by inverting the tube 4-6 times until clear solution could be seen. The suspension was not allowed to stand more than 5 min before adding neutralization buffer N3. The tube was again inverted 4-6 times. The suspension was then centrifuged at a high speed (17,170 x g) for 10 min at 4°C to remove all chromosomal DNA, cell debris, denatured proteins and SDS. The supernatant was then applied to the column provided with the kit and centrifuged for 1 min at room temperature in at high speed to bind plasmid DNA. The flow through was discarded. The bound plasmid was washed with 500 µl buffer BP and centrifuged at 17170 x g (room temperature) for 1 min. Plasmid was washed again with 750 µl PE and centrifuged for one min. Flow through was discarded and the column was centrifuged for one more minute. The column was transferred to a clean sterilized Eppendorf tube. The plasmid DNA was eluted by 30-50 µl buffer EB (10 mM Tris-HCl, pH 8.5) or distilled water, then the column was allowed to stand for one min and centrifuged for one min at a high speed (13330 rpm) at 4°C. The purified plasmid was kept at -20°C. P1, P2, N3, PB, PE and EB were supplied in QIAgen miniprep kit.

## 2.2.2 QIAprep spin plasmid maxiprep protocol

A single colony was used to inoculate a 5 ml LB to grow for 8 hat 37°C with shaking at 300 rpm. The bacteria were used to inoculate a flask with 500 ml LB broth with appropriate antibiotics. The flask was incubated overnight at 37°C with shaking at 200 rpm. The bacteria were pelleted by centrifugation at 5000 x *g* for 15 min at 4°C. The pelleted cells were resuspended in 10 ml buffer P1 and mixed properly. An equal volume of buffer P2 was added and the suspension was inverted 4-6 times and left at the room temperature for 5 min. 10 ml of prechilled buffer P3 was added to the mixture and mixed by inverting to stop the lysis reaction. The suspension incubated on ice for 20 min and then centrifuged at  $\geq 15000$  x *g* for 30 min at 4°C to remove all chromosomal DNA, denatured protein and SDS. The clear lysate supernatant was centrifuged again for 15 min as above in a new sterilized tube to remove any other residues. QIAGEN-tip 500 column was equilibrated with 10 ml of equilibration buffer QBT and left to pass through the column by gravity. The supernatant was applied to the equilibrated column and left to pass through also by gravity. The column was washed with 2x30 ml buffer QC. The DNA was eluted from the column by buffer QF and precipitated by 10.5 ml isopropanol at room temperature and centrifuged at  $\geq 15000$  x *g* for 30 min at 4°C. The plasmid DNA pellet was washed then with 5 ml of 70% ethanol (v/v): air dried and resuspended with 1 ml of 10 mM Tris-HCl (pH 8.5). The plasmid DNA then kept at -20°C. P1, P2, P3, QBT, QB, and QF were supplied in QIAGEN Maxi prep kit.

Pure DNA fragments for DNA sequencing, digestion, ligation and PCR amplification were obtained by running in 1% Agarose gel and the desired band

was excised and purified from the gel by using gel extraction gel. QIAquick gel extraction kit was used to purify the DNA < 10 kb, and QIAclean Gen II for DNA > 10 kb (QIAGEN).

### **2.2.3 QIAquick gel extraction protocol**

The desired DNA fragments were excised from gels using a scalpel and weighed to estimate the volume (1 mg=1 µl). The excised band was transferred to an Eppendorf tube. Three times volume of buffer QG was added and incubated in a hot plate at 50°C for 10 min or until the agarose had completely dissolved. One volume of isopropanol then was added and mixed. The mixture was carefully applied to QIAquick gel extraction column and centrifuged for 1 min at a high speed in a bench-top centrifuge. Flow through was discarded and the column was washed with 750 µl buffer PE and centrifuged for 1 min. The column was centrifuged for one more min to remove all residues. Finally, the column was transferred to a clean Eppendorf tube and the product eluted in 30-50 µl EB buffer. QG and EB were provided with QIAquick gel extraction kit (QIAGEN).

### **2.2.4 QIAEX II gel extraction kit**

QIAEX kit was used to purify plasmid larger than 10kb. The desired band was excised using a clean scalpel blade and weighed in a clean Eppendorf tube as above to estimate the volume. Three volumes of buffer QX1 and two of distilled

water were added to the gel slice. QIAEXII was mixed by vortexing before adding 30 µl to the sample and mixing. The sample was incubated at 50°C or until the gel completely dissolved and the DNA was bound to the matrix. The sample was centrifuged for 30 s and the supernatant carefully removed. The pellet was washed with 500 µl of buffer QXI and centrifuged for 30 s to remove all traces from the sample. The pellet was washed twice with buffer PE and centrifuged for 30 s each time. The pellet was air dried for 30 min or until the colour was white. DNA was eluted after that by adding 20 µl distilled water and re-suspended, incubated at 50°C for 10 min and centrifuged for 30 s. The supernatant which contains the DNA was carefully transferred to a clean tube. Buffer QXI and QXII were supplied in the QIAEXII gel extraction kit.

### **2.2.5 Phenol/ Chloroform/ Isoamyl alcohol extraction**

An equal volume of Phenol/ Chloroform/Isoamyl alcohol 25: 24: 1 (Sigma) was added to the DNA sample. This was mixed gently on rocking platform for 5 min and then centrifuged at maximum speed for 30 min at room temperature. The aqueous solution (upper layer) was carefully transferred to a clean tube. An equal volume of sterile distilled water (s.d.w.) was added; the sample was mixed gently for 5 min and centrifuged as above. The upper phase was carefully added to the previous aqueous phase. Same volume of Chloroform: Isoamyl alcohol 24:1) was added and mixed for 2 min and centrifuged at high speed for 1 min in a benchtop centrifuge. The top layer was removed to a new clean tube (containing DNA). Then 0.1 µl volume of 3M sodium acetate (pH 5.5) and three volumes from ice cold ethanol (99-100%) were added to the aqueous

phase. The sample was mixed gently and incubated at  $-20^{\circ}\text{C}$  overnight or at  $-80^{\circ}\text{C}$  for one h. The sample was then centrifuged at maximum speed by using a bench top centrifuge for 30 min at  $4^{\circ}\text{C}$ . The DNA pellet was washed with pre chilled 70% ethanol ( $50\mu\text{l}$ ), mixed and centrifuged for 15 min. The ethanol was carefully aspirated off using a Pasteur pipette. The DNA was then air dried for 15 min and resuspended in  $50\mu\text{l}$  distilled water.

### **2.2.6 Electrophoresis of DNA**

Where necessary to separate DNA band, DNA was run in an agarose gel 1% (w/v) with TAE buffer (40 mM Tris-acetate, 10 mM EDTA) containing ethidium bromide  $5\mu\text{g ml}^{-1}$ . The gels were run for 45-60 min at 95-110 V and visualized under UV light.

### **2.2.7 Digestion by restriction enzymes**

Digestion reactions were set up in  $50\mu\text{l}$  reaction volumes. In each reaction,  $1\mu\text{g}$  of DNA sample was used together with the desired restriction enzyme (1-10 units), 1x digestion buffer and  $1\mu\text{l}$  of BSA ( $\text{mg ml}^{-1}$ ) when the supplied buffer did not contain BSA. The reactions were incubated between 1-4 h in a water bath at the supplier's recommended temperature, mostly  $37^{\circ}\text{C}$ .

### **2.2.8 DNA phosphatase**

The digested vector was de-phosphorylated using Antarctic alkaline phosphatase (AP) to avoid re-ligation. Digested DNA was purified from agarose gels by QIAEX II gel extraction kit or heat inactivated. Reactions were set up in 50  $\mu$ l including 1  $\mu$ g DNA, 1  $\mu$ l AP enzyme and 5  $\mu$ l enzyme buffer (10 x), the volume made up to 50  $\mu$ l of s.d.w.. The reactions were incubated for 30 min at 37°C. Then the enzyme was inactivated at 65°C for 5 min according to the supplier's instructions. Most of the time the dephosphorylation was performed after digestion and before running the agarose gel.

### **2.2.9 DNA ligation**

DNA ligation was performed to join two DNA molecules. When a DNA inserts into the vector, the ratio between the vectors: insert should be 1:1 or 1:3. Ligation reaction was performed either in 50  $\mu$ l or 20  $\mu$ l volumes according to the supplier's instructions: 50  $\mu$ l reaction including 1  $\mu$ l concentrated DNA ligase and 5  $\mu$ l of 10 x enzyme buffer. The reaction was incubated in 4°C overnight or 60-90 min at 16°C. Then the enzyme was inactivated at 65°C for 20 min. For the 20  $\mu$ l reaction tube, 10  $\mu$ l master mix buffer was used with 1  $\mu$ l DNA ligase, the reaction was mixed up and down by micropipette for 4-6 times and then stopped by putting on ice if it was not to be used or transformed directly.

## **2.3 DNA template preparation and PCR manipulation conditions**

### **2.3.1 Colony template preparation**

*E. coli* or transformed SMDM colonies were resuspended in 20  $\mu$ l s.d.w. and boiled for 10 min. This suspension was used as a DNA template for PCR amplification in colony PCR.

### **2.3.2 Genomic DNA extraction using Qiagen genomic tip-20 kit**

An Eppendorf tube contains 1 ml liquid culture ( $OD_{600}$ : 0.5-1) or loopfull of plate culture in 1 ml resuspended in Phosphate Buffer Saline (PBS) was centrifuged at 7100 rpm (5000  $\times$   $g$ ) for 5 min to pellet the cells. The pellet was resuspended in 1 ml buffer B1 containing 2  $\mu$ l of RNase by vortexing. 20  $\mu$ l lysozyme (100 mg  $ml^{-1}$ ) and 45  $\mu$ l of 20 mg  $ml^{-1}$  proteinase K were added. The content was mixed and incubated at 37°C for 30 min. Then 0.35 ml of buffer B2 was added and incubated at 50°C for 30 min. The lysed cell- containing sample was applied to pre-equilibrated genomic tip-20 with 2 ml of buffer QBT, the lysate was allowed to pass through by gravity. The column was then washed with 3  $\times$  1 ml Qiagen QC buffer and left to flow through by gravity. The genomic DNA was eluted by using 2  $\times$  1 ml Qiagen QF buffer then precipitated with 1.4 ml isopropanol at room temperature and centrifuged at 9100 rpm (8000  $\times$   $g$ ) for 20 min at 4°C to pellet the DNA. The DNA was washed with 1 ml cold 70% ethanol, centrifuged at 9100 rpm (8000  $\times$   $g$ ) for 10 mins at 4°C and allowed to dry for 10 min. Air

dried DNA was then resuspended in 50-100  $\mu$ l of 10 mM Tris-Cl, pH 8.5 and placed in shaker incubator at 30°C overnight or at 55°C for 1-2 h to be dissolved and then kept at -20°C. Buffer B1, B2, QBT, QC and QF were prepared in the lab according to supplier's instructions (Appendix 2). Proteinase K and lysozyme were supplied by Sigma.

### **2.3.3 Genomic DNA preparation using Qiagen QIAamp DNA Mini kit**

An Eppendorf tube containing 1 ml liquid culture ( $OD_{600}$ : 0.5-1) or loopfull of plate culture was resuspended in 1 ml phosphate buffer saline (PBS). The suspension was centrifuged at 2400  $\times g$  for 5 min to pellet the cells. Supernatant was removed and 180  $\mu$ l from Buffer ATL was added. 20  $\mu$ l proteinase K (20 mg ml<sup>-1</sup>) was added, the content was mixed by vortexing and then incubated at 56°C for 1 h (tube was mixed 2-3 times during the incubation to assure efficient lysis). The tube briefly centrifuged and 200  $\mu$ l of Buffer AL was added, the mixture was vortexed for 15 s and then incubated at 70°C for 10 min. Again, the sample was briefly centrifuged and 200  $\mu$ l of ethanol (95-100%) was added and the content was mixed by pulse vortexing for 15 s and, centrifuged briefly. The sample was applied carefully to QIAamp spin column and centrifuged at 8000  $\times g$  for 1 min. Flow through was discarded and 500  $\mu$ l from buffer AW1 was added and centrifuged at 6200  $\times g$  for 1 min. The flow through was discarded and 500  $\mu$ l from buffer AW2 then added, centrifuged at a full speed at bench-top centrifuge for 3 min. The QIAamp spin column was placed in a clean 1.5 Eppendorf tube, 150  $\mu$ l buffer AE was added and incubated at room temperature for 1 min and then centrifuged for 1 min at 6200

x g. This step was repeated by adding AE but this time sample was incubated for 5 minutes at room temperature before centrifugation to elute all DNA. All buffers in this kit were supplied by Qiagen.

## **2.4 Preparation of *E. coli* S17.1 CaCl<sub>2</sub> competent cells**

This method was adapted from that of [Sambrook \*et al.\* \(1989\)](#). LB (10 ml) was inoculated with a fresh single colony from an *E. coli* S17.1 culture plate and incubated overnight at 37°C. The culture was used as an inoculum for 500 ml of LB broth with MgCl<sub>2</sub> [10 mM], MgSO<sub>4</sub> [10 mM] and incubated at 37 °C with shaking at 200 rpm until the culture reached an OD<sub>600</sub> of 0.5 - 0.6 (mid log phase). The cells were chilled on ice for approximately 15 min and then pelleted by centrifugation at 5000 × g for 10 min (4°C). Pelleted cells were resuspended in 25 ml ice cold, filter sterilized 0.1 M MgCl<sub>2</sub> and pelleted by centrifugation as above. The cells were washed in 5 ml filter sterilized CaCl<sub>2</sub>, incubated on ice for 45 min and then, pelleted again and resuspended in 25 ml 0.1 M MOPS, 50 mM CaCl<sub>2</sub>, 20% glycerol. The cells were drop frozen in 200 µl aliquots in liquid nitrogen and stored at -80°C. Using this method cells could be store for several years.

#### 2.4.1 Transformation of CaCl<sub>2</sub> competent cells

An aliquot of 200 µl of CaCl<sub>2</sub> competent cells were thawed on ice. The thawed *E.coli* S17.1 CaCl<sub>2</sub> competent cells were transformed with 1-5 µl of DNA and incubated for 30 min on ice. The cells were heat shocked for 90 s in a water bath at 42°C and then incubated for more two min on ice. When other commercial competent cells were used such as *E. coli* BL-21 “One-Shot” (Invitrogen) and XL-10 Golden ultra-competent cells (Agilent technologies), the transformation was performed according to the supplier’s instructions. The appropriate volume of medium was then added to the cells to complete the volume to 1 ml. LB was used with CaCl<sub>2</sub> competent cells *E. coli* S17.1, NZY was used with XL-10 gold ultra-competent cells and SOC (Super optimal broth with catabolite repression) (Appendix 1) was used with *E. coli* BL-21 “One-Shot” competent cells. The sample was then incubated at 37°C with shaking at 200 rpm for one h. Aliquots of 50-200 µl were then cultured on LB agar with appropriate antibiotic(s).

#### 2.4.2 Transforming *Methylosinus trichosporium* SMDM by conjugation

To express recombinant *Methylosinus trichosporium* MMO genes in a homologous expression system, plasmids were used to transform *E. coli* S17.1 (Simon *et al*, 1983) and then were transferred by conjugation to a soluble methane monooxygenase deleted *Methylosinus trichosporium* mutant (SMDM) (Borodina *et al.*, 2007).

### 2.4.3 Conjugation procedure

*E. coli* S17.1 harbouring the recombinant vector containing the desired mutation was grown in LB broth overnight at 37°C in a shaker incubator. Meanwhile, SMDM was grown in 50 ml culture in NMS liquid medium to an optical density  $OD_{600} \sim 0.2$ . Both cultures were mixed together and centrifuged for 10 min at 5000 x g to pellet the cells. The pelleted cells were resuspended in 50 ml NMS. The suspension was collected on a nitrocellulose filter membrane with 0.22 µm pore size. The filter membrane was then cultured on NMS agar containing 0.02% protease peptone, the plate being incubated for 24 h in anaerobic jar with 50/50 air: methane. The growing bacteria on the filter paper were resuspended in 10 ml NMS medium and centrifuged as above. The pellet was resuspended in 1 ml NMS medium. Aliquots (100 µl) were then cultured on NMS agar with four antibiotics; streptomycin (20 µg ml<sup>-1</sup>), spectinomycin (20 µg ml<sup>-1</sup>), gentamycin (5 µg ml<sup>-1</sup>) and nalidixic acid (25 µg ml<sup>-1</sup>). The plates were incubated in a methane/air atmosphere at 30°C for 2-3 weeks or until colonies could be seen. Then selected colonies were cultured on NMS agar with three antibiotics; streptomycin, spectinomycin and gentamycin with same concentration as above. The pure colonies containing *mmoX* gene with a desired recombinant were further confirmed by positive naphthalene test or colony PCR for the negative colonies.

## 2.5 Sequences of primers used in the study

The sequences of the primers which were used in the present study are shown in [Table 2.2](#).

**Table 2.2** Sequences of primers used in the construction of the mutants in the present study.

Primer	Sequence 5' -3'	Description
<i>mmoX</i> - p1	ATT CGA GCT CAA ACG TTC GAA C	Forward/ Upstream external primer for <i>Bam</i> HI
<i>mmoX</i> - p4	GGG CTC TCG ACG CCA TAT TTG	Reverse/ Downstream external primer for <i>Nde</i> I
E114D-f (p2)	CGA GGT CGG <b>CGA</b> CTA TAA CG	Forward/ E114D mutagenic primer
E114D-r (p3)	CGT TAT <b>AGT</b> <b>CGC</b> CGA CCT CG	Reverse/complement of primer E114D-f.
R98A-f (p2)	ATC <b>CCG</b> <b>CCT</b> GGG GCG AGA C	Forward/ R98A mutagenic primer
R98A-r (p3)	GTC TCG CCC <b>CAG</b> <b>GCG</b> GGA T	Reverse/complement of primer R98A-f.
Seq-f	CGG TCC GAA ACA AAA GAA AA	Primer to bind downstream of <i>mmoX</i> - p1. This primer was used to sequence the area around the active site that contains the mutations in the present study
Seq-r	ATC GGT GTT GAG GAA CTT GG	Primer to bind downstream of <i>mmoX</i> - p4. This primer was used to sequence the area around the active site that contains the mutations in the present study

The reverse mutagenic primers (r) are complementary to the corresponding forward primers (f). The bold letters indicate the nucleotide bases being changed. *mmoX*- p1, p2, p3 and *mmoX*- p4 refer to the role that the primer played in overlap-extension PCR mutagenesis as described below (Figure 2.4).

## 2.5.1 Standard PCR protocol

PCR was run using *Taq* DNA polymerase (Invitrogen), or *Pfu* proofreading polymerase (Agilent technologies) or Phusion High-fidelity PCR Master Mix or Hot start Master Mix (Fisher scientific). The melting temperatures  $T_m$  for primers were calculated by using:  $T_m$  (°C) =  $2(N_A + N_T) + 4(N_G + N_C)$  since  $N_A$ ,  $N_T$ ,  $N_C$  and  $N_G$  are the number of adenosine, thymine, cytosine and guanine bases present respectively.

The standard PCR reaction was run for 95°C for 2 minutes to denature the DNA and then the DNA was amplified for 30-35 cycles of: 95°C 30 sec  $kb^{-1}$ , ( $T_m - 5$ ) °C for 30 sec  $kb^{-1}$ , 72 °C for 1 min  $kb^{-1}$  with final extension time for 10 min at 72°C and then held at 4-8°C. For colony PCR the colony was heated in 20  $\mu$ l s.d.w. for 10 minutes at 100°C and then 5  $\mu$ l was used as a template or the colony was heated at 95°C for 10 minutes before use. When PCRs were set up using individual reaction components, the following recipe was used:

### PCR Recipe 1:

- dNTPs (25 mM each dNTP) 0.5  $\mu$ l
- 10 x buffer 5  $\mu$ l
- primer 1 (100-200 ng) 1  $\mu$ l
- primer 2 (100-200 ng) 1  $\mu$ l
- DNA template 1 - 5  $\mu$ l
- *Taq* polymerase or *Pfu* turbo 1  $\mu$ l
- 50 mM  $MgCl_2$  (not added for *Pfu* Turbo) 2  $\mu$ l
- BSA (colony and culture template only) 1  $\mu$ l
- s.d.w. up to 50  $\mu$ l

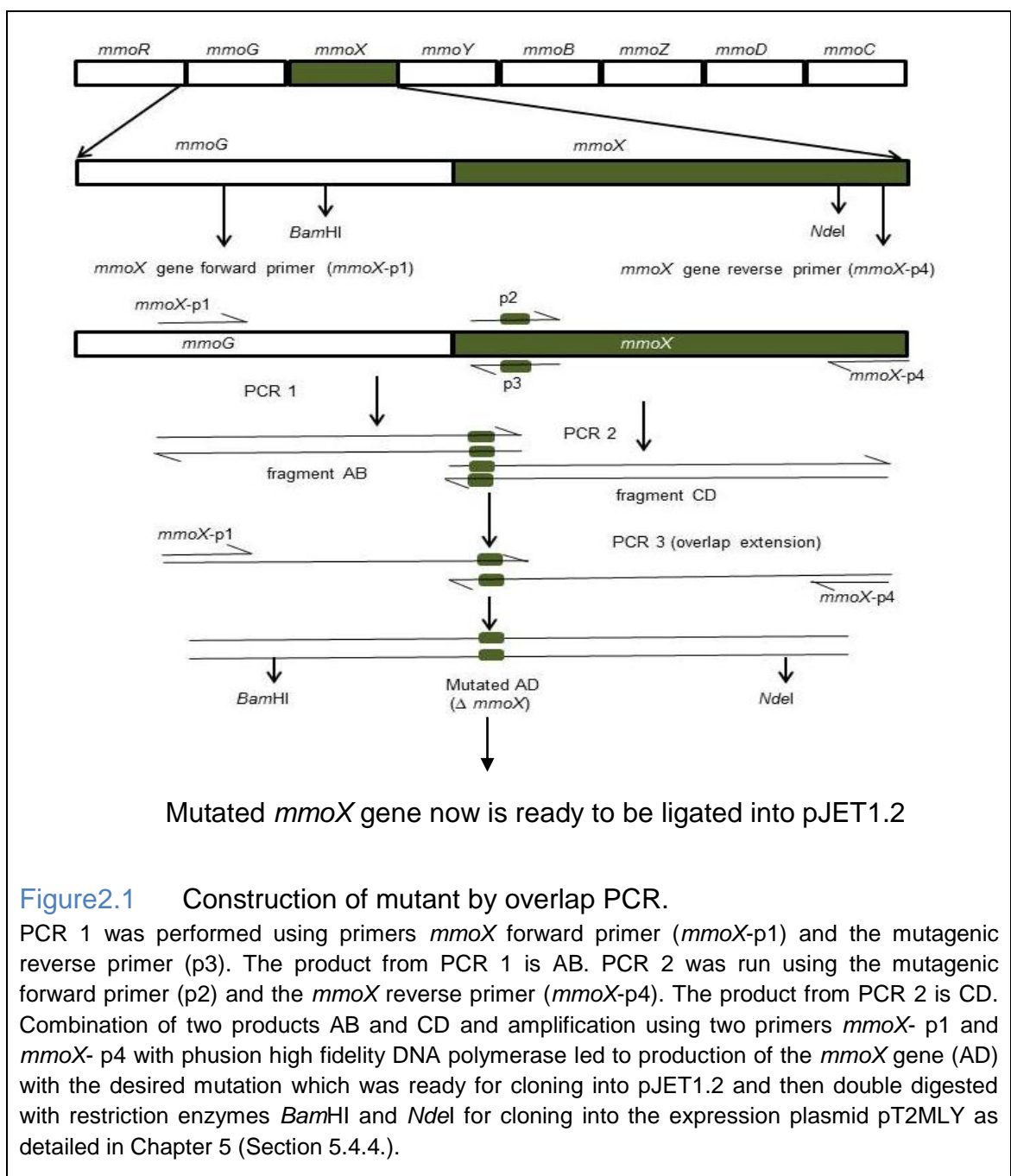
PCRs using Master Mix were set up as follows (Recipe 2):

Master Mix	25 $\mu$ l
Forward primer (100-200ng)	2.5 $\mu$ l
Reverse primer (100-200ng)	2.5 $\mu$ l
DNA template	1-5 $\mu$ l
Sterile distilled water (s.d.w.)	up to 50 $\mu$ l

## 2.5.2 Four primeroverlap PCR

For each of the two mutations created, overlap PCR was used to perform the mutagenesis. Two PCRs were set up according to recipe 2 (Section 2.4.1.); the first PCR (PCR 1 in [Figure 2.1](#)) was performed by using the external forward primer (*mmoX*- p1) with the appropriate internal mutagenic primer (p3) to create the product AB. The second PCR (PCR 2 in [Figure 2.1](#)) was performed by using the reverse external primer (*mmoX*- p4) and the appropriate internal mutagenic primer (p2) which is complementary to p3 to create product CD. ). These two gel purified products were mixed and used as the DNA template for the subsequent combinatorial follows PCR (PCR 3 in [Figure 2.4](#).). An equimolar amount of each product was mixed and incubated at 96°C for two minutes and then left for 10 minutes to cool. The High fidelity Phusion Master Mix, was then added to the reaction, together with primers *mmoX*- p1 and *mmoX*- p4 (volume as indicated in recipe 2 in Section 2.1). The tube was then replaced into the

heating block of the PCR apparatus, which had been pre-heated to 98°C for 2 minutes., then the PCR was run under the conditions recommended by the supplier which was as follows; an initial denaturation temperature 98°C for 30 s, 35 cycles of denaturation at 98°C for 30 s, annealing temperature at 52°C for 30 s and extension at 72°C for 30 s kb<sup>-1</sup> with final extension at 72°C for 10 minutes and hold at 4°C.



### 2.5.3 Ligation of mutant *mmoX* genes into pJET 1.2

The overlap PCR product from the previous steps was ligated into the high efficiency pJET1.2 cloning vector (Life technology) to produce pYYL1 (Figure 2.2). Laboratory prepared competent cells of *E. coli* S17.1 were transformed with the ligation reaction. Colony PCR was performed to detect the putative mutated *mmoX* gene by using primers *mmoX*- p1 and *mmoX*- p4.

The transformed *E. coli* S17.1 which showed a band in the colony PCR with primers *mmoX*- p1 and *mmoX*- p4 was then recultured in LB broth with the appropriate antibiotic (ampicillin  $100 \mu\text{g}^{-1} \text{ml}^{-1}$ ). A miniprep was done for the progeny plasmids (pYYL1) isolated from these transformed *E. coli* S17.1. The *mmoX* gene was then amplified by PCR using primers *mmoX*-p1 and *mmoX*-p4 to confirm its presence in the purified plasmid.

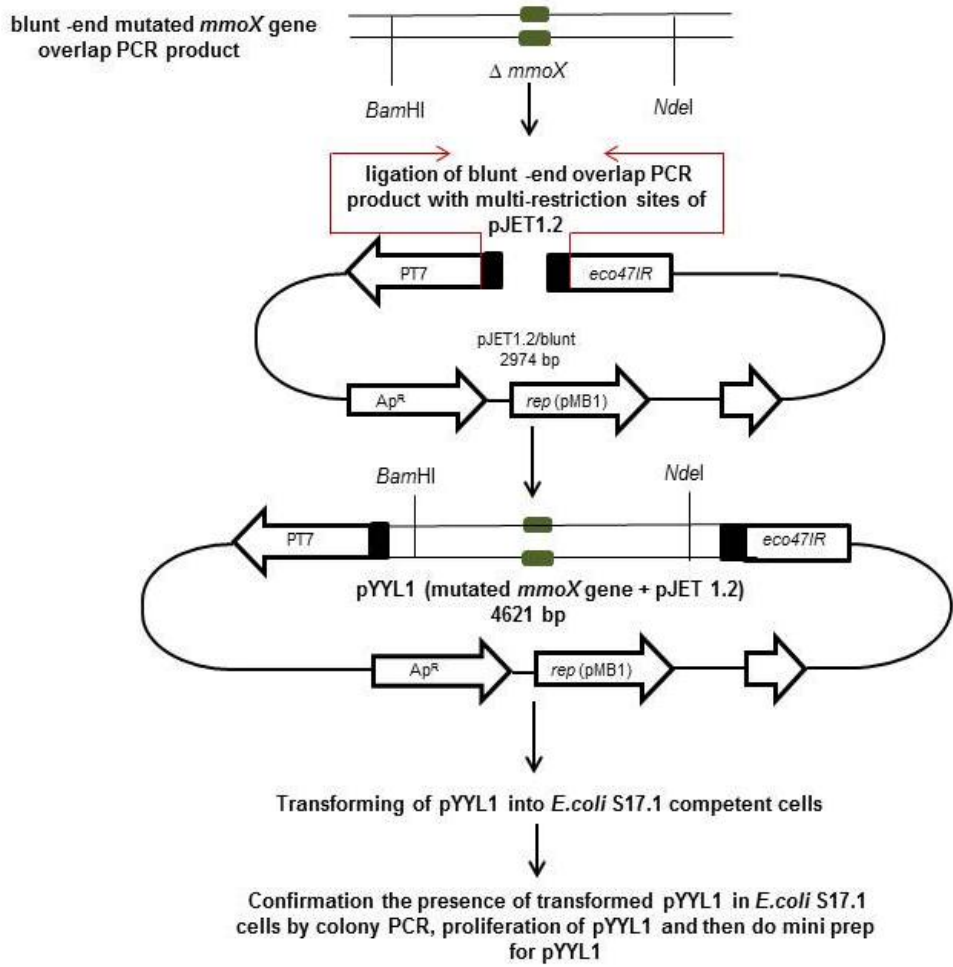


**Figure 2.2** Cloning steps for introduction of the mutated *mmoX* gene into vector pJET1.2

Scheme describes the cloning of the overlap PCR product containing the desired mutation in the *mmoX* gene into the vector pJET1.2 and transformation into competent cell *E. coli* S17.1 to create pYYL1.

*rep*(pMB1): Replicon (*rep*) from the pMB1 plasmid responsible for the replication of pJET1.2, *eco47/R* lethal gene *eco47/R* enables positive selection of recombinant plasmid, PT7:T7 RNA polymerase promoter for *in vitro* transcription of the cloned insert, Ap<sup>R</sup>: Ampicillin resistance.

#### **2.5.4 Double digestion of purified mutated *mmoX* gene with *Bam*HI and *Nde*I**

The mutated *mmoX* gene that was amplified from pYYL1 by PCR was gel purified by using the gel extraction kit (Qiagen) and then double digested with *Nde*I and *Bam*HI. The desired band was then excised from the gel and purified for ligation with pT2MLY double digested with the same restriction enzymes *Bam*HI and *Nde*I (Figure 2.3).

#### **2.5.5 Cloning the constructed all mutants in the present study into the His-tag expression plasmid pT2MLY**

After purification of the band that contained the desired mutation from the double digested *mmoX* gene, the purified double digested gene was ligated by using the Quick Instant Ligation Kit (NEB) into pT2MLY that had been digested with same restriction enzymes (*Nde*I and *Bam*HI). The *E. coli* XL-10 gold ultra-competent cells were transformed with the ligation reaction as described in Section 2.5.1. Colony PCR was performed and the resulting plasmid containing the putative mutated gene was purified from the transformants and then sent for sequencing from four primers *mmoX*- p1, *mmoX*- p4, Seq-f and Seq-r (Table 2.2). After the sequencing, the purified mutated plasmids were transferred into *E. coli* S17.1 and then the mutated plasmids transferred from *E. coli* S17.1 into SMDM by conjugation as described in Section 2.5.2. The transconjugants were grown for three weeks on NMS agar plates with four antibiotics (streptomycin, spectinomycin, gentamicin and nalidixic acid) and methane as a source for

carbon and energy. The mutants were then tested for oxidation of naphthalene. Colony PCR was run for the *mmoX* gene for the exconjugant strains and then the PCR product was purified and sent for sequencing. The mutants were further characterized by growing on NMS medium with low copper to induce the production of sMMO, which was then assayed by the naphthalene oxidation plate test again.

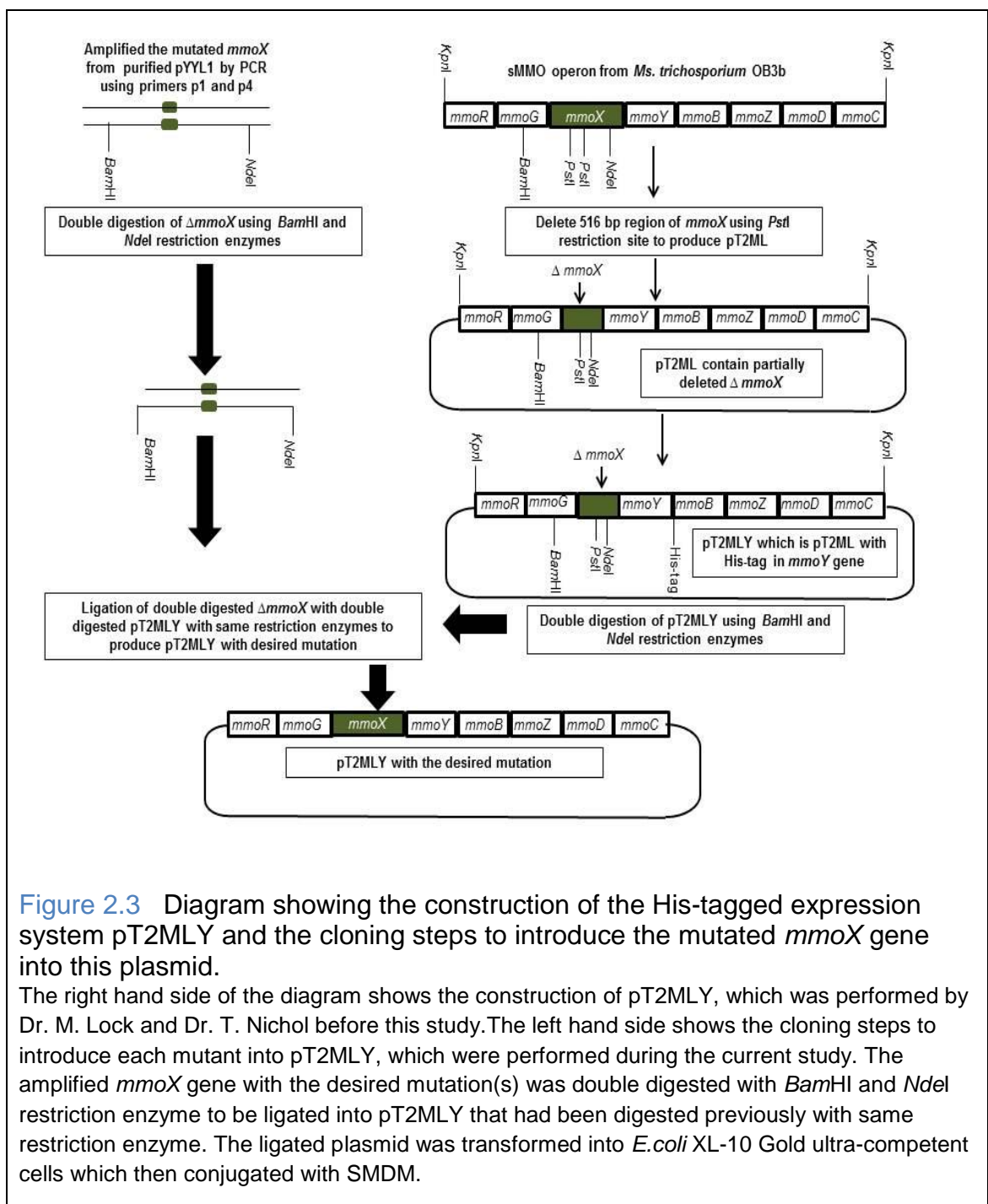


**Figure 2.3** Diagram showing the construction of the His-tagged expression system pT2MLY and the cloning steps to introduce the mutated *mmoX* gene into this plasmid.

The right hand side of the diagram shows the construction of pT2MLY, which was performed by Dr. M. Lock and Dr. T. Nichol before this study. The left hand side shows the cloning steps to introduce each mutant into pT2MLY, which were performed during the current study. The amplified *mmoX* gene with the desired mutation(s) was double digested with *Bam*HI and *Nde*I restriction enzyme to be ligated into pT2MLY that had been digested previously with same restriction enzyme. The ligated plasmid was transformed into *E. coli* XL-10 Gold ultra-competent cells which then conjugated with SMDM.

## **2.6 Cell preparation for protein purification**

### **2.6.1 Preparation of the hydroxylase and reductase for purification**

Frozen cells were harvested by centrifugation (8900  $\times g$ , room temperature) then 30 g of whole frozen cells were resuspended in equal volume of 25 mM (MOPS)-NaOH (pH 7.2) containing 2 mM dithiothreitol (DTT) and 1 mM benzamidine, 200  $\mu\text{M}$  Fe (NH<sub>4</sub>)<sub>2</sub> (SO<sub>4</sub>)<sub>2</sub>, 2  $\mu\text{M}$  cysteine, 2 unit ml<sup>-1</sup> of DNaseI (Sigma, Aldrich), and 0.5 mM MgCl<sub>2</sub> (buffer A). Cells were disrupted by passing them three times through a French pressore cell (Thermo) at 20,000 mPa (pressure achieved in the French press cell disrupter, 4°C) or for smaller amounts ( $\leq$  5 ml) using a Sonics vibracell VCX 750 sonicator on ice using 10  $\times$  30 s bursts at 40 % maximum amplitude with 30 s on ice between each burst to allow cooling. Cells were centrifuged in pre-chilled Oakridge tubes at 10000  $\times g$  for 5 min to remove the majority of the cell debris. The supernatant was then transferred to ultracentrifuge tubes and centrifuged for 90 min at 50000  $\times g$  at 4 °C. The debris was excluded and supernatant was aliquoted in prechilled Eppendorf tubes and kept in -80°C until needed.

## **2.6.2 Purification of the hydroxylase**

### **2.6.2.1 Anion exchange chromatography**

The supernatant from the broken cell suspension described above was loaded onto an anion exchange column (DEAE Sepharose CL-6B anion exchange matrix (Amersham-Pharmacia; 80 ml of settled bed) pre-equilibrated with 25 mM MOPS, pH 7.0, 8 mM sodium thioglycolate, 200  $\mu$ M Fe (NH<sub>4</sub>)<sub>2</sub> (SO<sub>4</sub>)<sub>2</sub> and 2 mM DTT (buffer B). After that the column was washed with 600 ml of buffer B. The hydroxylase and reductase were then eluted by a linear gradient of NaCl from 0 to 0.4 M in buffer B. The MMOH-containing samples were concentrated by ultra-filtration with an XM50, 50 kDa molecular mass cut-off membrane (Millipore- Amicon). Further purification was performed as described below. SDS-PAGE (16% and 12%) was used to analyse all protein samples of hydroxylase and reductase.

### **2.6.2.2 His-tagged MMOH purification**

A Ni-NTA QIAGEN His-tag affinity column with 2 ml collection tube was equilibrated with 600  $\mu$ l phosphate buffered saline (PBS) at 800 x g for 2 min. Then 600  $\mu$ l of hydroxylase-containing soluble extract were loaded onto the column and centrifuged at 200 x g for 5 min (flow through was saved) The column washed with 600  $\mu$ l of 1 mM histidine in PBS buffer (2 min 800 x g) followed by washing twice with 600  $\mu$ l of 10 mM histidine in PBS buffer for 2 min at 800 x g. Finally the MMOH was eluted with 600  $\mu$ l of 100 mM histidine in PBS buffer 2 min at 800 x g.

### 2.6.3 Purification of the reductase

The MMOC (reductase) protein containing samples were concentrated by ultra-filtration with an XM50, 10 kDa molecular mass cut-off membrane (Millipore-Amicon). Further purification of MMOC was achieved by loading the concentrated fraction from DEAE Sepharose chromatography containing protein C onto a Superdex 75 (Amersham-Pharmacia) column (26 mm by 60 cm) and eluting with buffer A (mentioned in hydroxylase purification). MMOC purification was conducted in a cool and dark room to avoid inactivation since it is light sensitive (Smith *et al.*, 2002).

#### 2.6.3.1 NADH oxidase assay for MMOR

The assay for NADH oxidase activity was performed for the putative purified reductase by measuring the decrease in NADH absorbance at a wavelength of 340 nm ( $\epsilon=6.22 \times 10^3 \text{ M}^{-1} \text{ cm}^{-1}$ ) at 25°C using a Jenway 6715 UV/Vis spectrophotometer. Reaction mixture (1 ml) contained 50 mM sodium phosphate buffer (pH7.0), 0.016  $\mu\text{M}$  NADH (ethanol free), 0.05 mM cytochrome *c* as alternative electron acceptor in place of sMMO, and 0.10  $\text{mg}^{-1}\text{ml}^{-1}$  of enzyme (reductase). The concentration of protein in the reductase sample was measured by using Bradford reagent with bovine serum albumin (BSA) as a standard.

## **2.6.4 Purification of protein B**

### **2.6.4.1 Transformation of *E. coli* BL-21 with pGEX-2T *mmoB***

Firstly, *E. coli* BL-21 was transformed with pGEX-2T*mmoB* plasmid following the Invitrogen protocol, as mentioned in Section 2.6.1 in the Materials and Methods Chapter. The plasmid was then purified using the QIAmini prep plasmid kit (Qiagen) and analysed by gel electrophoresis. After that, plasmids were digested using two restriction enzymes (*EcoRI* and *BamHI*) to confirm the presence of the gene *mmoB*.

### **2.6.4.2 Induction and expression of protein B**

Induction and expression of protein B was performed by following the Invitrogen Expression Guidelines. Three to four transformed colonies were cultured overnight in 5 ml LB broth containing ampicillin  $100 \mu\text{g ml}^{-1}$  with shaking until the  $\text{OD}_{600}$  was 0.6-1.0. This overnight culture was used to inoculate LB with ampicillin to an  $\text{OD}_{600}$  of 0.05-0.1 (~1:50 dilution of the overnight culture) to allow the cell growth to return to the logarithmic phase. The cells were left to grow for a further 2-3 h to an  $\text{OD}_{600}$ ~0.4. Cells were induced by adding IPTG to a concentration of 0.5 mM of the bacterial culture and incubated under the same conditions for a further 2-3 h. Samples were taken at time zero (when IPTG was added) and after two and three h of incubation to detect protein production. Samples from different time points were centrifuged at  $17000 \times g$  for 20 min and resuspended with 200  $\mu\text{l}$  of PBS, and recentrifuged at  $17000 \times g$  for 20 min. The supernatant from the last step was discarded and the cells from

each sample were resuspended in 200 µl of PBS. The suspension was mixed with an equal volume of SDS-loading dye, boiled for ten minutes and then analyzed by SDS-PAGE.

#### **2.6.4.3 Purification of protein B**

Protein B with the glutathione S-transferase (GST) fusion was purified from *E. coli* according to [Lloyd \*et al.\* \(1997\)](#) and the GE Healthcare protocol, as follows. The culture was centrifuged and then the cells were resuspended in 25 mM MOPS pH 6.8 with DTT and benzamidine. The cells were disrupted by passing them three times through a French pressure cell (Thermo) at 20,000 mPa (pressure achieved in the French press cell disrupter, 4°C). Supernatant containing soluble extract was obtained after centrifugation at 50400 x *g* for 90 min at 4°C. Supernatant was loaded onto a 5 ml GSTrapHP (GE Healthcare) column pre-equilibrated with 140 mM NaCl, 2.7 mM KCl, 10 mM Na<sub>2</sub>HPO<sub>4</sub>, 1.8 mM KH<sub>2</sub>PO<sub>4</sub>, pH 7.3 (buffer A). After protein adsorption for 2 min, the column was washed with approximately five column volumes of buffer A. Fusion protein was eluted with freshly prepared 50 mM Tris-HCl, 10 mM reduced glutathione, pH 8.0.

## **2.7 Protein quantification**

A standard curve was made by dissolving different concentrations of BSA in MOPS 25 mM pH 7.0. Then 100 µl from each concentration of BSA was mixed

with 3 ml of Bradford reagent (Bio- Rad), the mixture was then incubated for 5 min at room temperature. Absorbance of the samples at 595 nm was measured in a Jenway 6715 UV/Vis spectrophotometer. The concentration of BSA was read by comparing to a negative control from Bradford reagent without BSA. The protein concentration was estimated according to BSA standard curve.

## **2.8 Protein visualization via SDS-PAGE**

Gels for SDS-PAGE were prepared as two layers; separating and stacking gel. The full formulations for the buffers and other solution used in SDS-PAGE can be found in Appendix 3. 12 or 16% SDS-PAGE was used in this study. The separating gel was prepared by mixing 4.5 ml or 6 ml 40% (acrylamide: bisacrylamide) 37:5:1 for (12% and 16% PAGE respectively), 3 ml of 2 M Tris HCl pH 8.8 and 6 ml or 7.5 ml D.W. (distilled water) for (12% and 16% PAGE respectively). The separating gel was set up finally by adding 75  $\mu$ l of 1% ammonium persulfate, 150  $\mu$ l from 10% of sodium dodecyl sulfate and 10  $\mu$ l TEMED and poured in the cassette. The gel was overlaid with isopropanol and left for 30 min to set before removing the isopropanol. Stacking gel was prepared by adding 0.6 ml (acrylamide: bisacrylamide) 37:5:1, 0.7 ml of 0.5 M Tris HCl pH 6.8 and 3.6 ml D.W. The stacking gel was set up finally by adding 50  $\mu$ l of 1% ammonium persulfate, 25  $\mu$ l from 10% of sodium dodecyl sulfate and 5  $\mu$ l TEMED and poured in the cassette. The comb was then added and the gel was left until set. The gel was run for 130 V for 1 hour or until the first band in the protein marker reached the end of the gel. The gel was stained in 0.1% Coomassie blue dissolved in methanol, glacial acetic acid and water (Appendix

3) with gentle shaking for 1 hour and then washed off, overlaid in destaining solution (30% methanol, 10% glacial acetic acid) overnight or until clear protein bands could be seen.

## **2.9 Cell preparation and substrates oxidation assay**

### **2.9.1 Whole cell oxidation test**

To test the enzyme, frozen cells were resuspended in a minimum volume of 25 mM MOPS pH 7.2 to a final OD<sub>600</sub> of 5-10. As sMMO can oxidize aromatic compounds and these substrates could not be oxidized by pMMO, an aromatic compound assay was performed with the whole cell suspension. Aliphatic compounds can serve as pMMO and sMMO substrates; analysis of these compounds was performed with the soluble extract to exclude the membrane attached pMMO enzyme.

### **2.9.2 Soluble extract assay**

Frozen cells were thawed in an equal volume of 25 mM MOPS (e.g: 25 g of frozen cells were thawed in 25 ml of MOPS) buffer pH 7- 7.2 on ice with 5 mM DTT (dithiotheritol), 2 mM benzamidine chloride and DNase I (1.5 - 2  $\mu\text{l ml}^{-1}$ ) (Sigma). Cells were then disrupted by either passing them through the French

pressure disruptor or sonication for 10 x 30 sec at amplitude at 40% (SONICS vibra-cell). Then the sample was centrifuged at 10000 x g to remove the debris and then the supernatant was clarified using a prechilled ultracentrifuge at 50000 x g for 90 mins at 4°C. The soluble extract was then kept in -80°C until needed.

### **2.9.3 Colorimetric naphthalene test**

The colorimetric naphthalene oxidation test was performed for liquid and solid cultures. A few crystals were added to the liquid culture (1 ml of liquid culture) or on the lid of a plate with growing culture on solid medium. In both types of culture, the reactions were incubated for one hour at 30°C, with shaking for the liquid culture at 180 rpm. The result was positive when the colour was dark pink to purple after adding the indicator tetrazotized *o*-dianisidine (TOD). The coloured diazo dye complex forms during the contact of TOD with hydroxylated product from the reaction. For the solid cultures, colonies were flooded with the TOD reagent (5 mg ml<sup>-1</sup>). For the liquid cultures, 100 µl ml<sup>-1</sup> of TOD (5 mg ml<sup>-1</sup>) was added to the liquid culture.

## **2.10 Oxidation of mono-, di- and tri-aromatic compounds by *Ms. trichosporium* OB3b (wild type), wild type with His-tag and mutants.**

The ability of the wild type of *Ms. trichosporium* OB3b (wild type), wild type with His-tag and mutants in the present study to oxidise a range of mono-, di- and tri-aromatic compounds was assayed in the present study. A universal tube with 5 ml of bacteria suspended in MOPS buffer was prepared with different substrates (toluene, mesitylene, ethyl benzene, biphenyl, naphthalene, anthracene and phenanthrene) (Table 2.2) at different concentrations. The assayed cultures were incubated at 30°C with shaking at 180 rpm for different incubation periods as explained in Table 2.2. The reaction was stopped on ice for 5 minutes and then tubes were centrifuged at 17000 x g for 2 min, the supernatant was then extracted into 1ml diethyl ether and evaporated into  $\geq 50\mu\text{l}$ . 1 $\mu\text{l}$  of the resulting concentrated solution was then analysed in an Agilent GC-MSD 7890A/5975C. The GC was fitted with a Hewlett Packard HP-5 MS column with a (5% phenyl) methyl polysiloxane coating (30 m x 0.25 mm; coating thickness 0.25  $\mu\text{m}$ ) and operated with a carrier gas (Helium) flow rate of 1.5 ml min<sup>-1</sup>. The separation was performed without split with a column temperature starting at 50°C with holding for 2 min, and then ramped to 150°C at 10°C/ min. The temperature was then ramped from 150°C to 250°C at 5°C/min and held for 5 minutes.

**Table 2.3** Table shows the substrates, substrate concentrations, incubation period, and the internal standard (if used in the assay) to estimate the ability of SMMO in oxidation mono-, di- and tri-aromatic compounds.

	tested substrate	amount in 5 ml of bacterial culture	incubation time	internal standard
1-	Toluene	5 $\mu$ l toluene	48 hours	25 $\mu$ mol of naphthol
2-	Mesitylene	5 $\mu$ l of mesitylene	72 hours	None
3-	Ethyl benzene	5 $\mu$ l of ethyl benzene	48 hours	None
4-	Biphenyl	~ 5 mg of biphenyl	24, 48, 72, and 96 hours	25 $\mu$ l of <i>p</i> -cresol
5-	Naphthalene	~ 5 mg of	48 hours	25 $\mu$ l of <i>p</i> -cresol
6-	Phenanthrene	~ 5 mg of phenanthrene	48 hours	None
7-	Anthracene	~ 5 mg of anthracene	48 hours	None

None- no internal standard was used in this assay. Incubation of all assays was run in shaker incubator at 180 rpm.

## 2.11 Propylene oxidation assay

### 2.11.1 Propylene oxidation assay for whole cell

GC vials each containing 2 ml of culture were prepared as in previous assays (Section 2.11); DTT was added to a final concentration 5 mM. The tube was equilibrated in water bath at 30°C for 1 min. To test the strains toward propylene, 2 ml of propylene was added and incubated for 20 minutes at 30°C. The reactions were put on ice for 5 min and then the cells separated by centrifugation in a benchtop centrifuge in a maximum speed for 1 min. Extraction of the product was performed by using CCl<sub>4</sub> which was then evaporated to  $\geq$  50  $\mu$ l. To analyse the product, 1  $\mu$ l was injected into an Shimadzu GC-AOC 2010 fitted with a column connected to a RTX-5 column

with flame ionisation detector. The GC was fitted with a Restek RTX-5 column with a 5% diphenyl/ 95% dimethyl polysiloxane coating (50 m x 0.32 mm; coating thickness 0.25  $\mu\text{m}$ ) and operated with a carrier gas (nitrogen) flow rate of 1.5 ml  $\text{min}^{-1}$ . Also the samples were analysed by GC-MS.

### **2.11.2 Propylene oxidation assay for soluble extract**

Soluble extract for the wild type with His-tag and mutant F282L was prepared as described in Section 3.5.1. A negative naphthalene test on the F282L mutant-expressing cells (done before preparation of the soluble extract) confirmed that this strain lacks active sMMO. The His-tagged hydroxylase was purified from the appropriate wild type as explained in Section 3.5.2.2. 600  $\mu\text{l}$  from the wild type His-tagged hydroxylase preparation was mixed with 400  $\mu\text{l}$  from F282L soluble extract as a source for protein B and C (this mutant contains inactive hydroxylase). 2 ml of headspace was replaced with 2 ml propylene gas. The tube was equilibrated in a water bath with a 30°C; the reaction was started by addition of 100  $\mu\text{l}$  of 100 mM ethanol free NADH (Appendix 4). The reaction was incubated for 20 min and then quenched on ice for 5 minutes. The product was extracted into 150  $\mu\text{l}$   $\text{CCl}_4$  and then 1  $\mu\text{l}$  from the extracted sample was injected into the GC. In the case of samples extracted via the SPME method, the reaction tube was warmed and agitated on a magnetic stirrer to evaporate the propylene oxide which then became adsorbed onto the solid phase micro extraction apparatus. The solid phase microextraction apparatus consists of a modified syringe (Figure 2.4) consisting of a fibre holder and fibre assembly. The fibre assembly comprises a 1-2 cm long retractable

SPME fibre which in turn contains a thin fused-silica optical fibre, coated with a delicate polymer film such as polydimethylsiloxane. In order to load the sample, the 1  $\mu\text{l}$  from the extracted sample in  $\text{CCl}_4$  or saturated SPME needle was injected into a Shimadzu GC2010 fitted with a RTX-5 column with a flame ionisation detector. The Restek RTX-5 column, which had a 5% diphenyl / 95% dimethyl polysiloxane coating (50 m x 0.32 mm; coating thickness 0.25  $\mu\text{m}$ ) was operated with a carrier gas (nitrogen) flow rate was 30  $\text{ml min}^{-1}$  and a split ratio of 30:1. The inlet temperature was 250°C. The temperature was ramped to 40°C, held at 40°C for 8  $\text{min}^{-1}$ , and then ramped to 100°C and held at 100°C for 5 min.

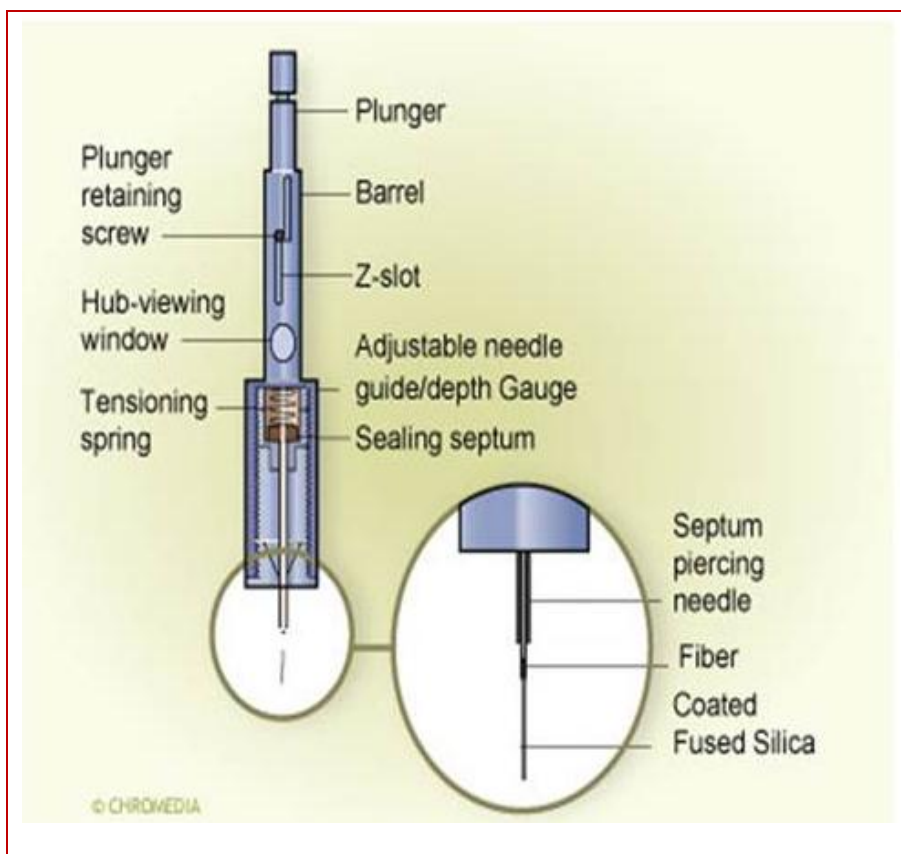


**Figure 2.4** Solid Phase Microextraction (SPME) apparatus. The enlargement of the injection part shows fused silica-coated fibers which adsorb the product from the reaction to be injected into gas chromatography. The fibres are retractable and protected by the septum piercing needle. Image is taken from (Vas and Vèkey, 2004)

## 2.12 Statistical analysis

Statistical analysis of results was performed by applying the Kruskal-Wallis test (Conover-Inman). Data are presented as (Mean  $\pm$  S.E.M).

# Chapter 3: Purification and assay of soluble methane monooxygenase components

---

## 3 Protein purification

### 3.1 Purification of sMMO components by anion exchange chromatography

Unlike pMMO, sMMO was purified many years ago and consequently its biochemistry and the crystal structure are well investigated. Active sMMO has been purified to homogeneity from different methanotrophic bacteria such as *Methylocystis* sp.W114, *Methylosinus trichosporium* OB3b, *Methylocystis* sp. M, *Methylococcus capsulatus* Bath, *Methylomonas* sp. GYJ13, *Methylobacterium* sp. CRL-26, and *Methylosinus trichosporium* IMV3011 (Fox and Lipscomb 1988; Nakajima *et al.*, 1992; Woodland and Dalton, 1984; Grosse *et al.*, 1999; Patel and Savac, 1987; Rosenzweig *et al.*, 1997; Elango *et al.*, 1997; McDonald *et al.*, 1997; Smith *et al.*, 2002; Shaofeng *et al.*, 2007). The sMMO hydroxylase and reductase have previously been purified by using anion exchange chromatography followed by gel filtration (Smith *et al.*, 2002). During previous studies, optimizations of protein purification conditions were made to obtain an active purified protein. Shaofeng *et al.* (2007) found that using iron, DTT at concentrations up to 20 mM, 15% glycerol and 5 mM sodium dithionite improved the purified hydroxylase activity and stability. However, purification of the sMMO hydroxylase or reductase by using an affinity column was not attempted in previous studies.

## 3.2 His-tag affinity system

During previous studies in this research group, a homologous expression system for sMMO was developed in which recombinant sMMO genes carried on plasmids pTJS175 or pT2ML could be expressed in sMMO-minus mutants of *Ms. trichosporium* OB3b known as SMDM. More details of this expression system can be found later in this thesis (Section 4.3.)(Lloyd *et al.*, 1999; Smith *et al.*, 2002; Borodina *et al.*, 2007; Nichol 2011). In order to further improve the expression system for sMMO, a poly histidine-tag was inserted into the sMMO hydroxylase. A His-tag is a structure of six histidine amino acids attached to each other (6x His-tag or histidine hexa tag in the present study it will be referred to as His-tag). The His-tag was inserted in the  $\beta$ -subunit of sMMO hydroxylase in the cloning vector system pT2ML to form a new system named as pT2MLY (Lock *et al.*, manuscript in preparation). The His-tag forms an affinity tag on the hydroxylase to be used to purify it using an affinity column. The system pT2MLY was used in the present study to manipulate new mutants aiming to minimize the cloning steps and facilitate purification of sMMO hydroxylase, both wild type and mutants, in the homologous expression system in *Ms. trichosporium* SMDM.

In addition, the His-tag was inserted to the sMMO reductase and cloned into the vector pET by a member in this group (M. Lock, personal communication). Although attempts in the current study were made to express and purify the His-tagged reductase from the heterologous expression system *E. coli*, these did not result in purification of the reductase. More investigation is needed to achieve this goal.

### 3.3 GST-fusion affinity system

As mentioned in the introduction, protein B has many critical roles in sMMO activity during oxidation of methane and other substrates. Unlike the hydroxylase, protein B could be expressed and purified from a heterologous expression system from *E. coli* (West *et al.*, 1992). It has been noticed that during the purification of protein B from *Ms. capsulatus*, it loses its activity due to cleavage that occurs between Met12 and Gly13, and Gln29 and Val30, resulting in formation of the truncated forms B' and B'' respectively (Lloyd *et al.*, 1997; Callaghan *et al.*, 2002). It was found that fusion of protein B with Glutathione-S-transferase (GST) at the N-terminus of protein B resulted in more resistant protein against truncation, in addition to which this protein was active with the GST attached (Lloyd *et al.*, 1997; Callaghan *et al.*, 2002). In the same studies, it was found that changing the *E. coli* expression host to strains either lacking *ompT* or being *lon*-deficient, or addition of protease inhibitors did not result in any change in truncation, which suggested that the truncation was auto catalytic. Mutation of Gly12 to Gln stabilized the protein but truncation still occurred, whereas the triple mutant G10A/G13Q/G16A resulted in a more stable protein with no activity (Brandstetter *et al.*, 1999). Lloyd *et al.* (1997) found that protein B fused to GST had high activity when it was expressed and then purified from *E. coli*. Although truncation of protein B has not been observed *in vivo* in *Ms. trichosporium* OB3b, it is possible that such truncation may happen *in vitro*. To avoid this possibility, protein B that was used for purification in the present study was fused with GST in the pGEX-2T vector, which was also constructed by this group research previously.

### 3.4 Solid phase microextraction (SPME)

The propylene assay has been widely used to assay purified sMMO activity. Usually the product from propylene oxidation, propylene oxide, is detected in a GC or GC/MS after being extracted by using suitable solvent. CCl<sub>4</sub> was used as a solvent to extract propylene oxide from reaction mixtures in the present study. As an alternative to solvent extraction, a new solventless method known as solid phase microextraction (SPME) was used for the first time to detect propylene oxide in the present study. SPME decrease sample preparation steps, which may have led to loss of product (Vas and Vekey 2004). SPME can be used with gas chromatography (GC), GC/mass spectrometry (GC-MS) and high performance liquid chromatography (HPLC) in addition to being used for volatile and semi-volatile organic compounds from food, environmental, and other biological samples (Vas and Vekey 2004).

Many studies have demonstrated that all parts of sMMO are indispensable and critical for enzyme activity *in vivo* and *in vitro*. This Chapter will concentrate on (i) purification of the native sMMO reductase from *Ms. trichosporium* by using anion exchange chromatography (ii) affinity purification of protein B fused to GST from *E. coli* and (iii) purification of the His-tag hydroxylase by affinity chromatography from the recombinant methanotrophs. The activity of the purified His-tagged hydroxylase was tested in assays with the other sMMO components.

## 3.5 Experimental work and Results

### 3.5.1 Purification of the His-tagged hydroxylase (MMOH)

#### 3.5.1.1 Anion Exchange chromatography

The sMMO hydroxylase and reductase were purified from His-tagged OB3b wild type according to the protocols from (Fox *et al.*, 1989; Pilkington and Dalton 1990; Smith *et al.*, 2002; Shaofeng *et al.*, 2007) and the soluble extract was prepared as described in Section 2.6.1. The purification of the His-tagged hydroxylase by anion exchange chromatography comprised three steps: after cell disruption and centrifugation, the soluble extract was loaded onto DEAE-Sephacel CL-6B anion exchange column and then eluted by gradient of NaCl (0-0.4 M NaCl). The hydroxylase containing fractions that gave a peak at 0.12 M NaCl (Figure 3.1) were pooled together and then concentrated with an XM50-50, 50 kDa, The pooled hydroxylase-containing fractions were then purified further by using His-tag affinity column, as detailed below. Samples were taken and separated by SDS-PAGE which revealed three bands corresponding to the hydroxylase  $\alpha$ ,  $\beta$ , and  $\gamma$  subunits with approximate sizes 58, 46, 25 kDa respectively (Figure 3.1), in addition to a few other faint bands.

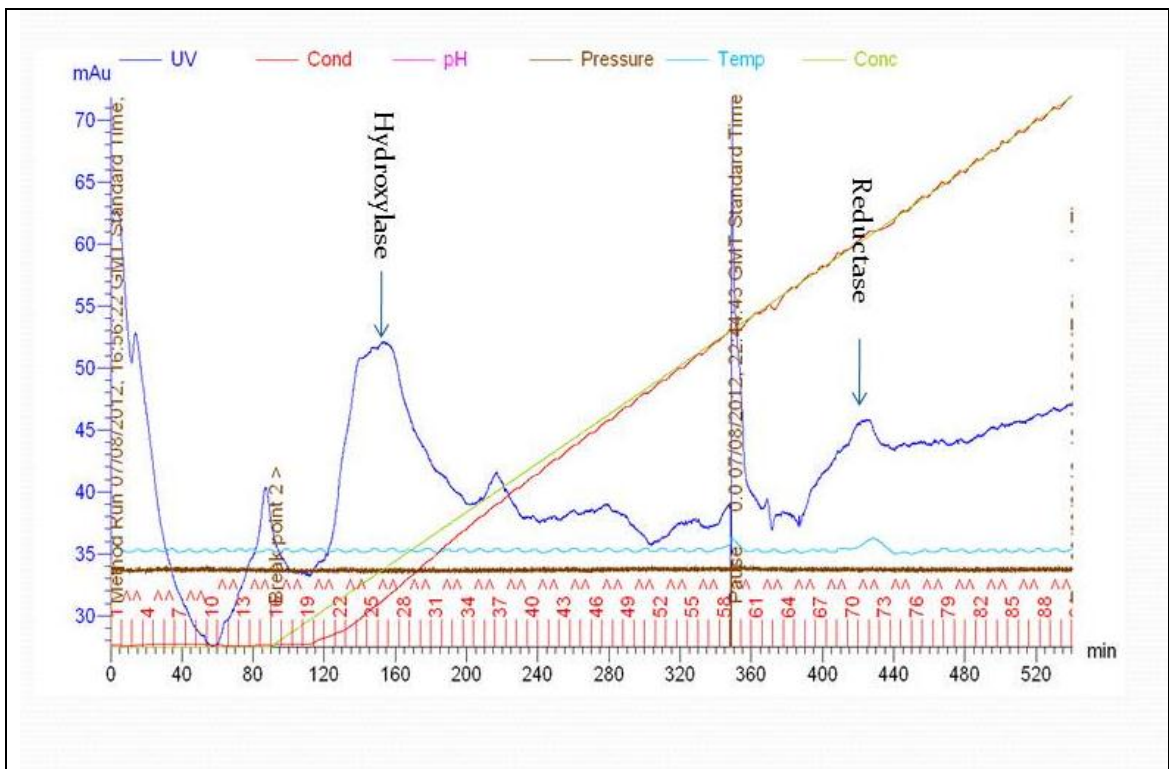


**Figure 3.1** Purification of sMMO hydroxylase and reductase by anion exchange chromatography.

After cell breakage, the soluble extract which contained the sMMO components was loaded onto the anion exchange chromatography column DEAE-Sepharose CL-6B attached to the AKTA purification system. The proteins bound to the DEAE column were eluted by a linear gradient of NaCl. The hydroxylase eluted first whereas the reductase eluted at high salt concentration. The peaks (dark blue coloured line) representing the MMOH and MMOR are indicated by arrows. The green line represents the salt concentration increasing during the elution and the red line represents the conductivity.

### 3.5.1.2 His-tag affinity column purification

Samples taken from the concentrated pooled purified sample after anion exchange chromatography were purified using Ni-NTA affinity chromatography as described in Materials and Methods (Section 2.6.2.2.). The affinity purified His-tagged hydroxylase was run on SDS-PAGE alongside a sample of His tagged hydroxylase partially purified by anion exchange chromatography to compare them and to confirm that the affinity step enriched the hydroxylase

subunits. This revealed three bands corresponding to the  $\alpha$ ,  $\beta$ , and  $\gamma$  subunits with approximate sizes of 58 kDa, 46 kDa, and 25 kDa respectively, exactly as with the anion exchange column purified samples (Figure 3.2). In addition there was another faint band with size approximately 20 kDa. A separate sample of the His-tagged hydroxylase also purified directly by affinity chromatography from the soluble extract without the anion exchange step as detailed in Section 2.6.2.2. The protein was eluted by using different concentrations of histidine with a larger Ni-NTA column (5-10 ml). The result also showed three bands corresponding to the three subunits of the hydroxylase in addition to fourth faint band as in the Anion exchange method (Figure 3.3).

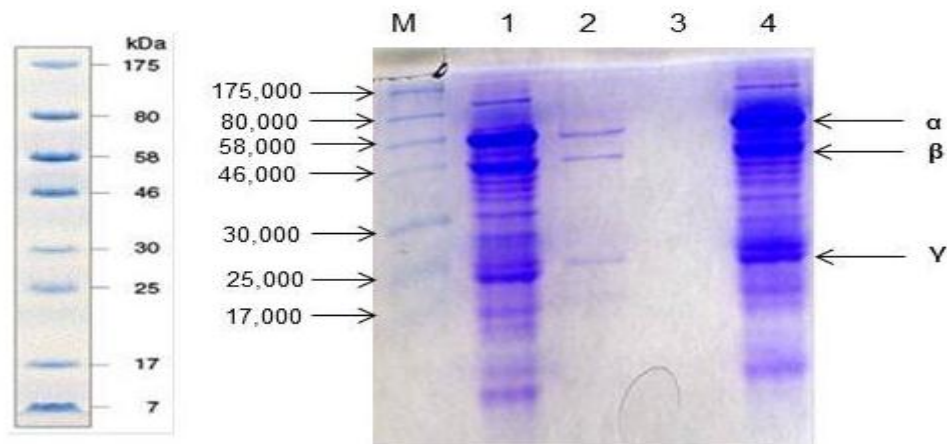


**Figure 3.2** SDS-16% PAGE showing the His-tagged hydroxylase purified by Anion exchange and Ni-NTA affinity column from wild type with His-tag soluble extract, and the attempted purification of the reductase .

**M**=Prestained protein marker, broad range (7-175 kDa) (New England Biolabs), **lane 1 and 4**= His-tagged hydroxylase purified by anion exchange chromatography. These show many bands including three bands representing MmoX, MmoY and MmoZ, i.e. the  $\alpha$ ,  $\beta$ , and  $\gamma$  subunits respectively. **Lane 2**= His-tagged hydroxylase purified by anion exchange chromatography and Ni-NTA affinity column which shows three bands representing the  $\alpha$ ,  $\beta$  and  $\gamma$  subunits of the hydroxylase. **Lane 3**= putative purified reductase fraction from anion exchange chromatography, which showed no band.

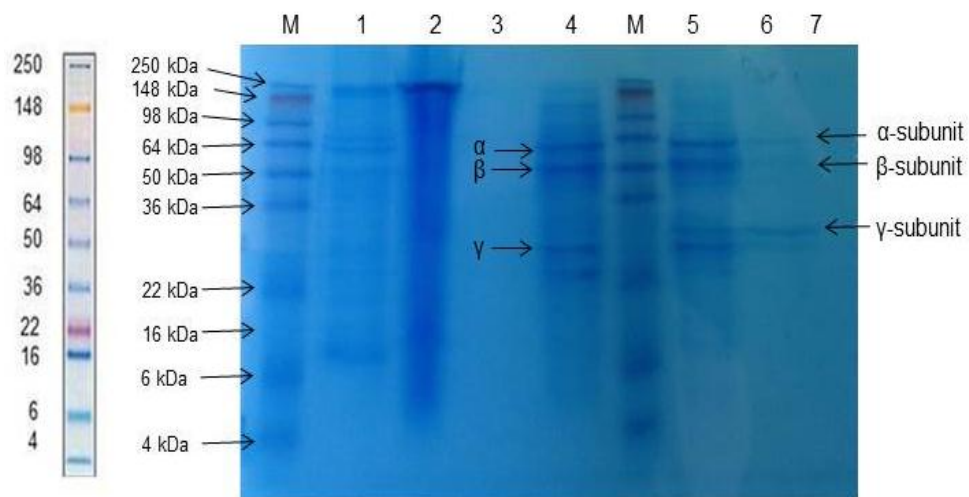


**Figure 3.3** SDS-12% PAGE showing the His-tagged hydroxylase purified from the wild type with His-tag soluble extract by using different concentrations of histidine dissolved in phosphate buffered saline.

**M**= SeeBlue® Plus2 Pre-stained protein marker (Invitrogen). **Lane 1** the run through of soluble extract. **Lane 2**= wash with phosphate buffered saline (PBS) only. **Lanes 3, 4 and 5**= elution with 1 mM, 10 mM, and 20 mM histidine respectively. **Lane 6**= protein eluted with 50 mM histidine. **Lane 7**= protein eluted with 100 mM histidine (the different washing and elution concentrations were prepared by dissolving the appropriate amount of histidine in PBS).

### 3.5.2 Purification of protein B (MMOB)

#### 3.5.2.1 Gene detection in pGEX-2T *mmoB*

*E. coli* BL21 One shot was transformed with pGEX-2T *mmoB* as described in Section 2.6.1. The transformed *E. coli* (one colony) was grown on LB broth with ampicillin. The plasmid was purified from the *E. coli* by using Qiagen minipep as described in the Materials and Methods Chapter, Section 2.2.1. The purified plasmid was then digested with two restriction enzymes *Bam*HI and *Eco*RI to confirm the presence of *mmoB* gene that encodes for protein B (*mmoB* was originally cloned into pGEX-2T using two restriction enzyme *Bam*HI and *Eco*RI).The result from the digestion showed that there is a band with size approximately 500 bp representing the *mmoB* and 4900 bp corresponding to the vector pGEX-2T (Figure 3.4).

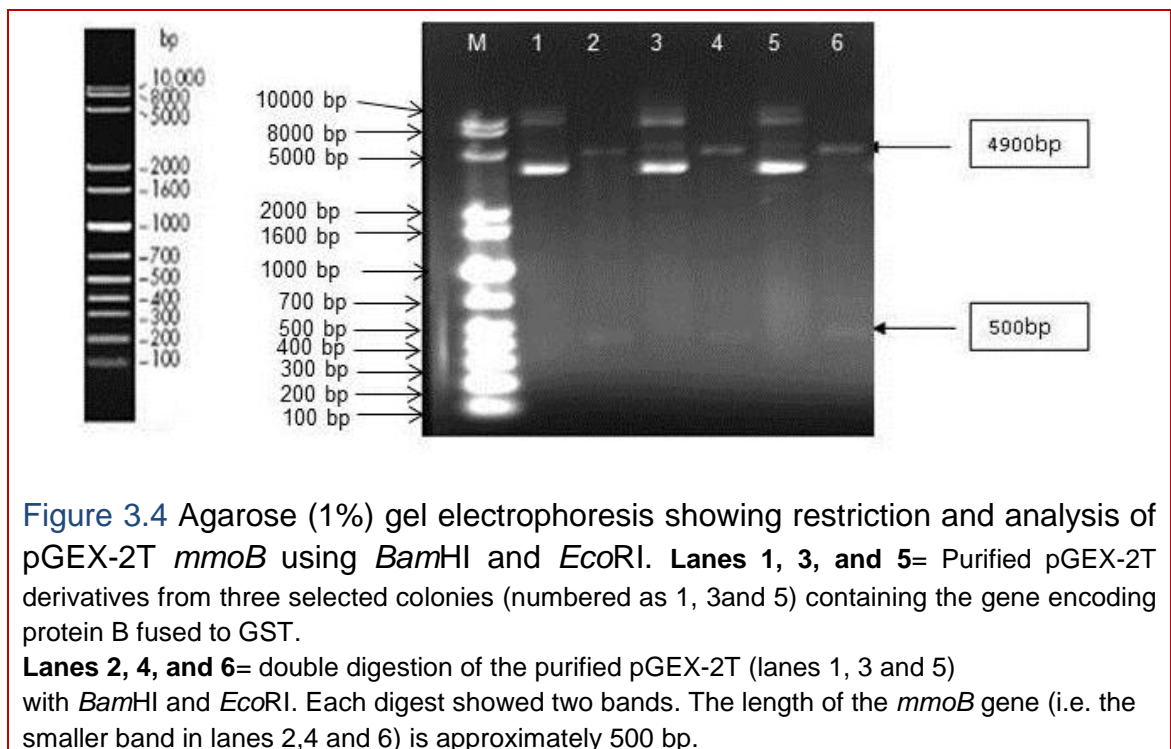
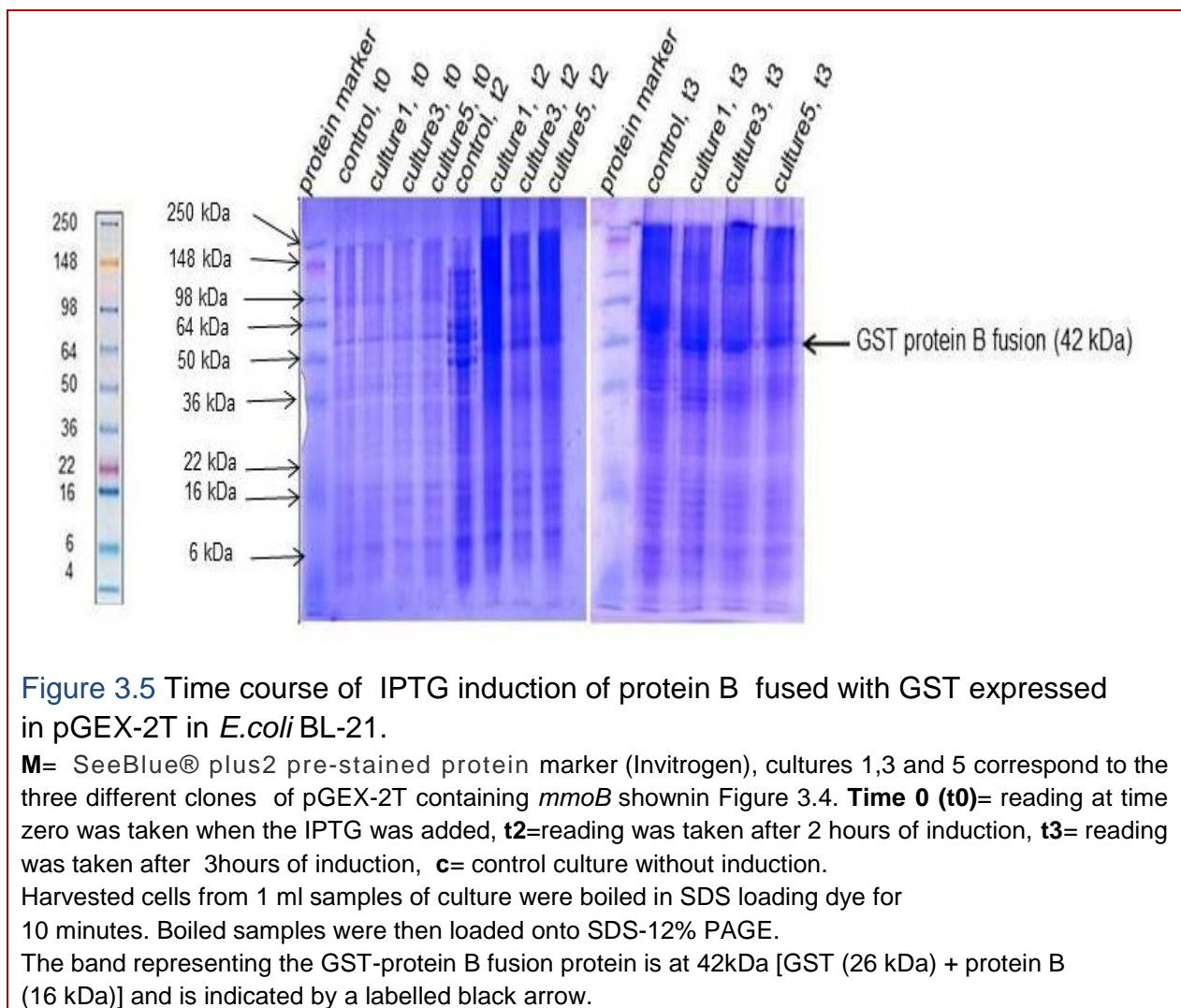


**Figure 3.4** Agarose (1%) gel electrophoresis showing restriction and analysis of pGEX-2T *mmoB* using *Bam*HI and *Eco*RI. **Lanes 1, 3, and 5**= Purified pGEX-2T derivatives from three selected colonies (numbered as 1, 3 and 5) containing the gene encoding protein B fused to GST.

**Lanes 2, 4, and 6**= double digestion of the purified pGEX-2T (lanes 1, 3 and 5) with *Bam*HI and *Eco*RI. Each digest showed two bands. The length of the *mmoB* gene (i.e. the smaller band in lanes 2,4 and 6) is approximately 500 bp.

### 3.5.2.2 Induction and expression of protein B

Expression of the GST-protein B fusion was induced by adding IPTG (0.5 mM) to a culture of *E. coli* harbouring pGEX-*mmoB* and incubating the culture of *E. coli* for further 2-3 hours. It can be seen from the SDS-PAGE that at time zero when IPTG was just added, there was no band with size equal to GST (26 kDa) plus protein B (16 kDa). This band started appearing 2-3 h after induction, with size approximately equal to that expected for the GST-protein B fusion (26 kDa + 16 kDa = 42 kDa) (Figure 3.5).



### 3.5.2.3 Purification of the GST-protein B fusion

Purification of the GST-protein B fusion was performed by using a GSTrap HP column manually with a slow flow rate ( $5-10 \text{ ml}^{-1} \text{ min}^{-1}$ ), which gave an effective purification as shown by SDS-PAGE. The gel shows a band with expected size after the elution step (Figure 3.6).

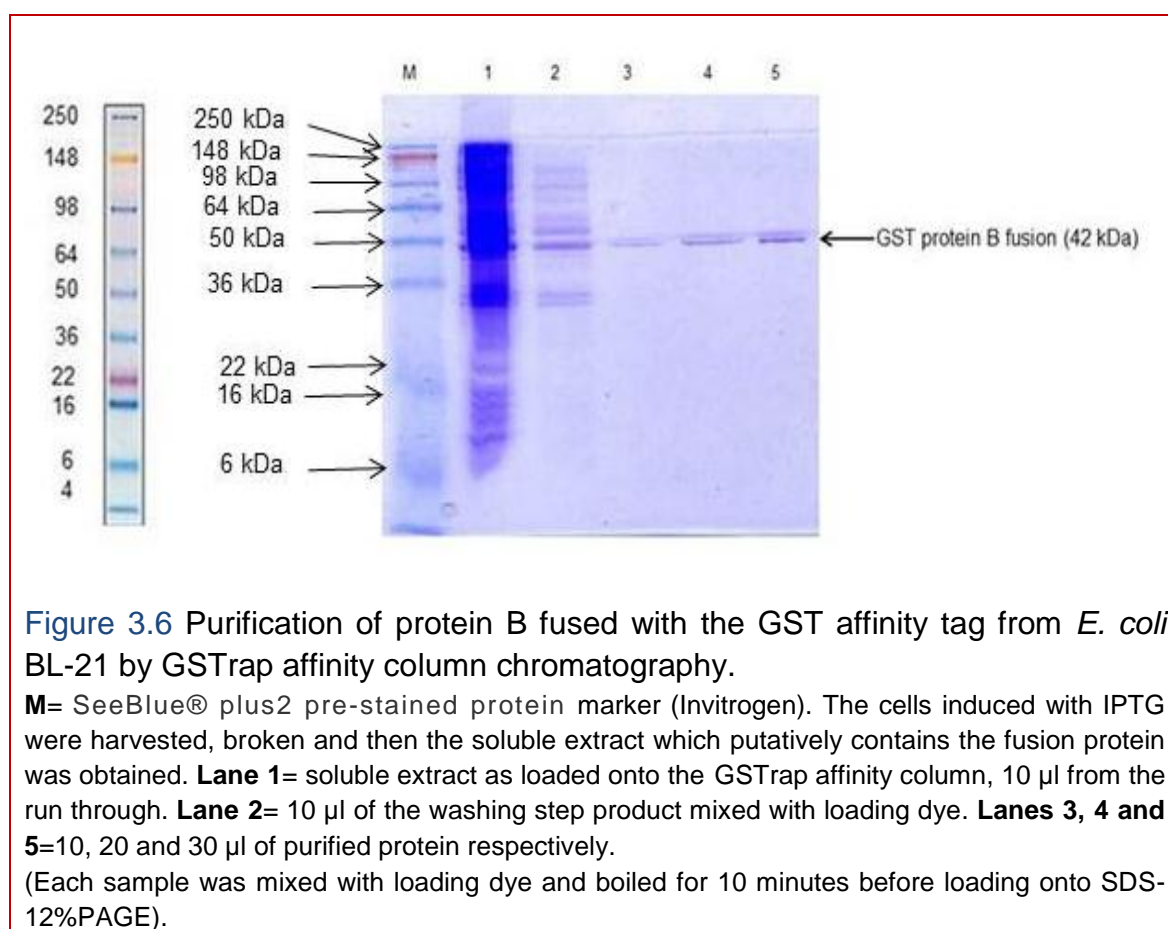


**Figure 3.6** Purification of protein B fused with the GST affinity tag from *E. coli* BL-21 by GSTrap affinity column chromatography.

**M**= SeeBlue® plus2 pre-stained protein marker (Invitrogen). The cells induced with IPTG were harvested, broken and then the soluble extract which putatively contains the fusion protein was obtained. **Lane 1**= soluble extract as loaded onto the GSTrap affinity column, 10 µl from the run through. **Lane 2**= 10 µl of the washing step product mixed with loading dye. **Lanes 3, 4 and 5**=10, 20 and 30 µl of purified protein respectively.

(Each sample was mixed with loading dye and boiled for 10 minutes before loading onto SDS-12%PAGE).

### 3.5.3 Purification of the reductase (MMOR)

The attempted reductase purification like the hydroxylase purification comprised three steps. After breaking the cells the soluble extract was loaded onto a DEAE- Sepharose CL-6B anion exchange column. The putative reductase containing fractions, which (as described previously [Smith *et al.*, 2002]) gave a peak at 0.35 M NaCl, were pooled together and then concentrated by ultrafiltration with an XM50, 10-kDa molecular mass cut-off membrane (Millipore-Amicon). The concentrated sample was then further purified by using a Superdex 75 gel filtration column. A possible protein peak was observed in the elution trace (Figure 3.7), but no band could be detected for these samples in SDS-PAGE (Figure 3.2). In an attempt to improve detection of the protein, samples eluted from the gel filtration column were concentrated with a 10 kDa cut-off membrane. SDS-PAGE of the concentrated samples did not reveal any bands after Coomassie staining. Silver staining method, which can detect a very low amount of protein, showed a number of bands which may reflect the degradation of reductase into small fragments during the purification procedure (data not shown).

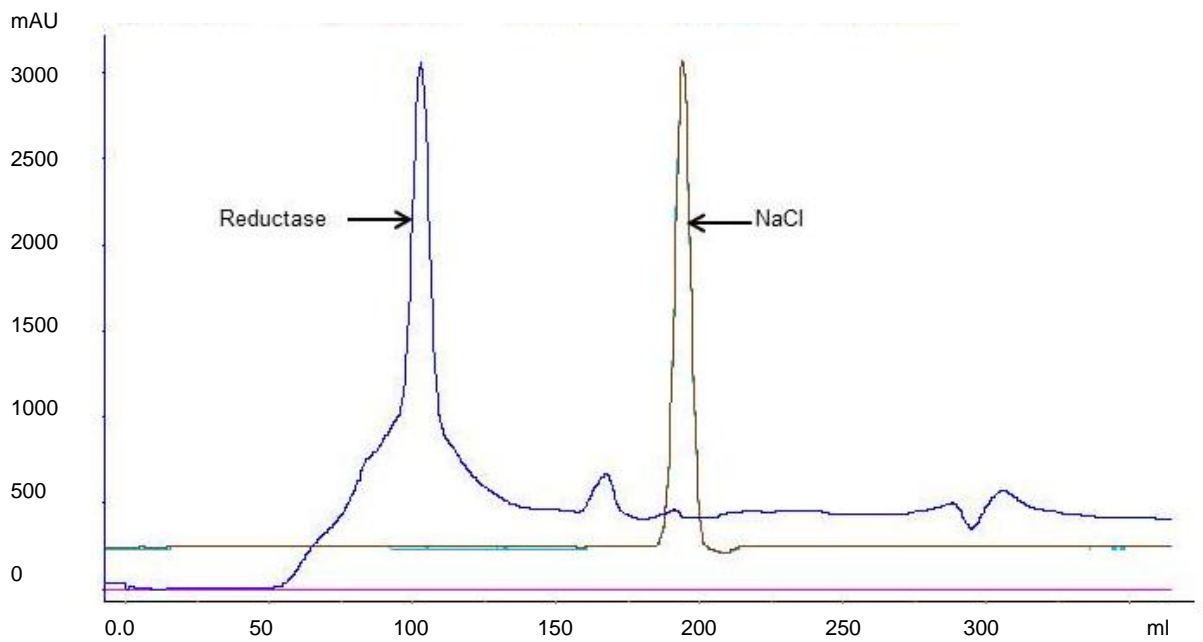


**Figure 3.7** Purification of protein C in gel filtration column (Superdex 75).

The reductase was initially loaded onto the DEAE anion exchange column and the putative eluted reductase was concentrated using a 10 kDa cut-off membrane. The concentrated sample was loaded onto a Superdex 75 column (trace shown above). Blue trace: represents the absorbance at a wavelength 280 nm showing the elution of the protein from the column, brown trace: electrical conductivity showing the elution of the NaCl present in the loaded sample.

### 3.5.3.1 NADH oxidase activity

It has been found previously that the sMMO reductase shows NADH oxidase activity, which can be used to assay the reductase in the absence of the other sMMO components (Lund *et al.*, 1985). The NADH oxidase activity of the putative reductase was tested in the presence of cytochrome *c* as the electron acceptor. The amount of putative reductase was measured by using Bradford reagent with BSA as standard. The concentration of the putative reductase was 0.10 mg ml<sup>-1</sup>. The result of the NADH oxidase assay showed that NADH was oxidized by the reductase to shuttle electrons to cytochrome *c* without presence of substrate such as propylene. The rate of NADH oxidation was found 1.27 nmol min<sup>-1</sup> (mg of reductase)<sup>-1</sup>.

## **3.6 Enzyme activity**

### **3.6.1 Growth of mutant F282L**

Since the purification of the wild type reductase protein was irreproducible in the present study, an alternative method was used to test mutated His-tagged MMOH. Soluble extract containing protein B, reductase and the inactive F282L hydroxylase was used in place of purified protein B and reductase. The mutant F282L was constructed in a previous mutagenesis study in this research group. The hydroxylase of this mutant was inactive even though it is expressed when the Cu to the biomass ratio was low. F282L was grown in a large batch in fermentor as described in the Materials and Methods Chapter. The OD<sub>600</sub> was measured at intervals. The cells were harvested when the growth rate began to slow down, which may represent the point at which production of the inactive sMMO began and the bacteria stopped using the pMMO enzyme to gain their carbon and energy. The presence of MMOH for F282L was further confirmed by SDS-PAGE and the cells then were kept at -80°C (Figure 3.8). Soluble extract was obtained as described in Materials and Methods Chapter.

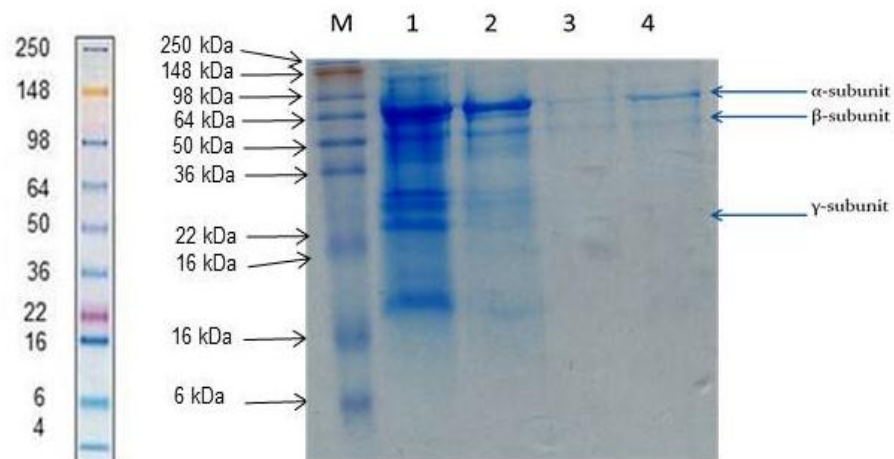


**Figure 3.8** SDS-PAGE for soluble extract and purified His-tagged hydroxylase subunits from mutant F282L.

**M**= SeeBlue® plus2 pre-stained protein marker (Invitrogen),

**lane 1**=soluble extract containing His-tagged wild type hydroxylase showing the three hydroxylase subunits which was used as a control, **lane 2**= His-tagged F282L soluble extract obtained via the same procedure used for the His-tagged wild type in lane 1, **lanes 3 and 4**= 10 and 20 µl respectively of the purified His-tagged hydroxylase preparation from affinity chromatography. The three subunits of the hydroxylase are indicated.

Samples were run on SDS-12%PAGE.

## 3.6.2 Propylene assay for soluble extract

### 3.6.2.1 Propylene assay by solvent extraction

To confirm the activity of the wild type with His-tagged hydroxylase in whole cells, naphthalene was used as a substrate. After being positive for the naphthalene test, whole cells were tested towards propylene.  $\text{CCl}_4$  was used to extract the propylene oxide as a product from the mixture which showed a peak at a retention time 3.27 minutes for the whole cell of the wild type with His-tag compared to the negative control (Figure 3.9 A). The rest of the cells were then broken by French press to obtain cell free soluble extract. A propylene assay was run for the soluble extract alone (Figure 3.9 B). The His-tagged wild-type MMOH was then purified from the soluble extract by using His-tag affinity column and soluble extract from mutant F282L was used as a source for protein B and C in an sMMO assay using propylene as the substrate. The propylene assay was performed for His-tagged MMOH under various conditions: mixture of MMOH with protein B, C and propylene at time zero, mixture of MMOH, proteins B, C and NADH without propylene, F282L soluble extract with propylene, and finally for wild-type purified His-tagged MMOH. Except for the time zero control, all assays were incubated for 20 minutes. The wild-type His-tagged MMOH with F282L soluble extract (at  $t = 20$  min) showed a peak at retention time about 3.25-3.27 min, corresponding to propylene oxide. None of the other assays showed a peak at this retention time. All experiments were run alongside negative controls. The retention time for propylene oxide was compared to standard of pure propylene oxide.

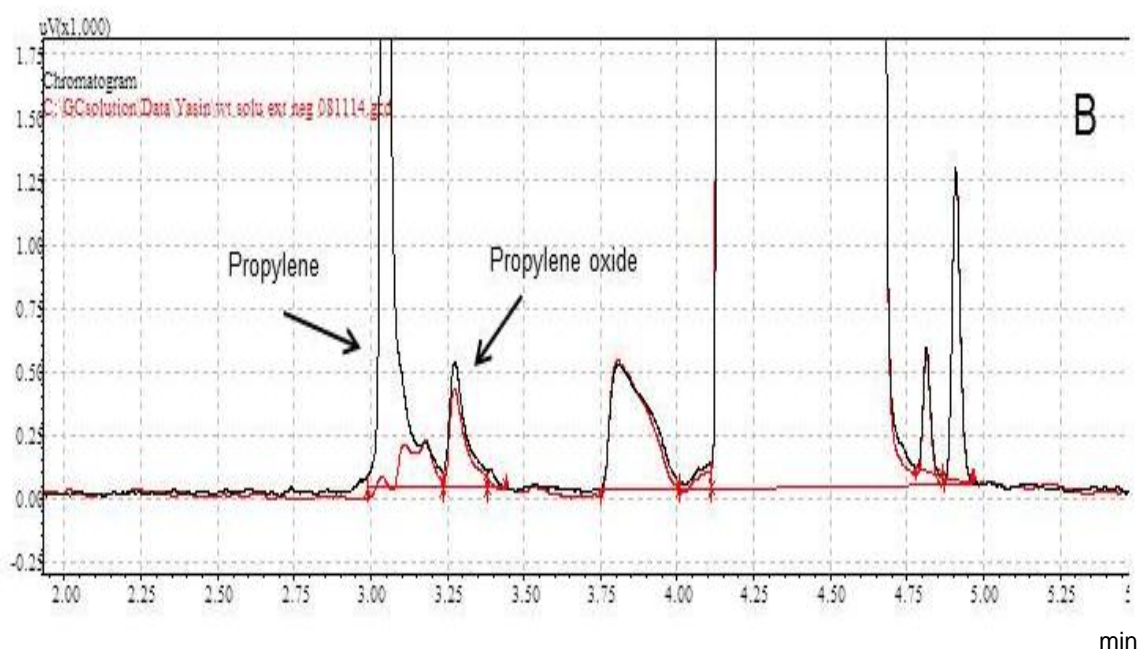
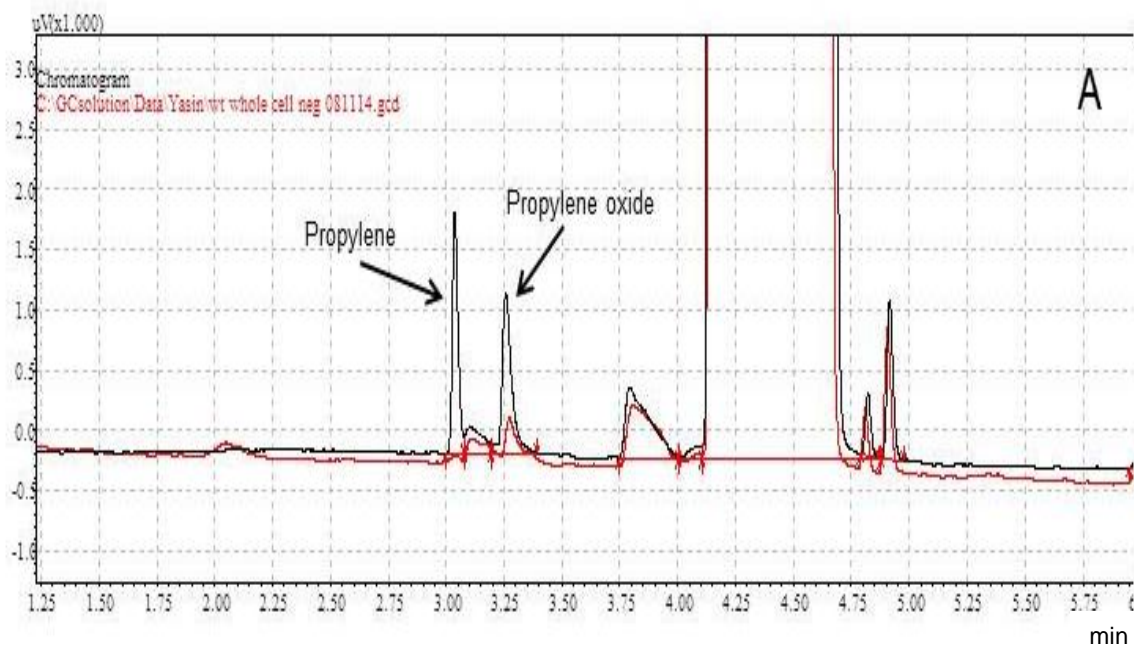


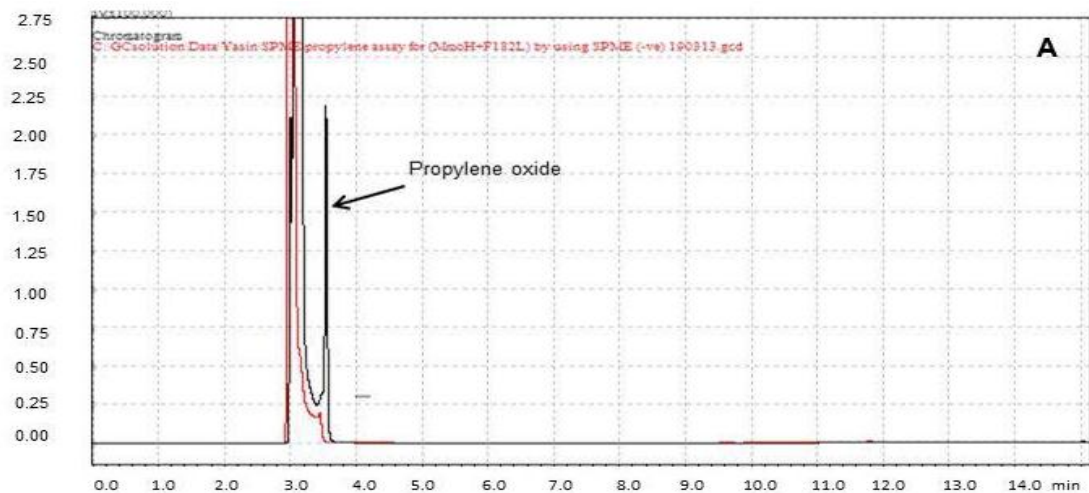
**Figure 3.9** GC traces showing the activity of the whole cells and soluble extract containing the wild type His-tagged hydroxylase toward propylene.

**A:** Whole cells. The peak corresponding to the propylene oxide product is indicated by an arrow at retention time (RT) 3.27 minutes (black line) compared to the whole cells without propylene as a negative control (red line).

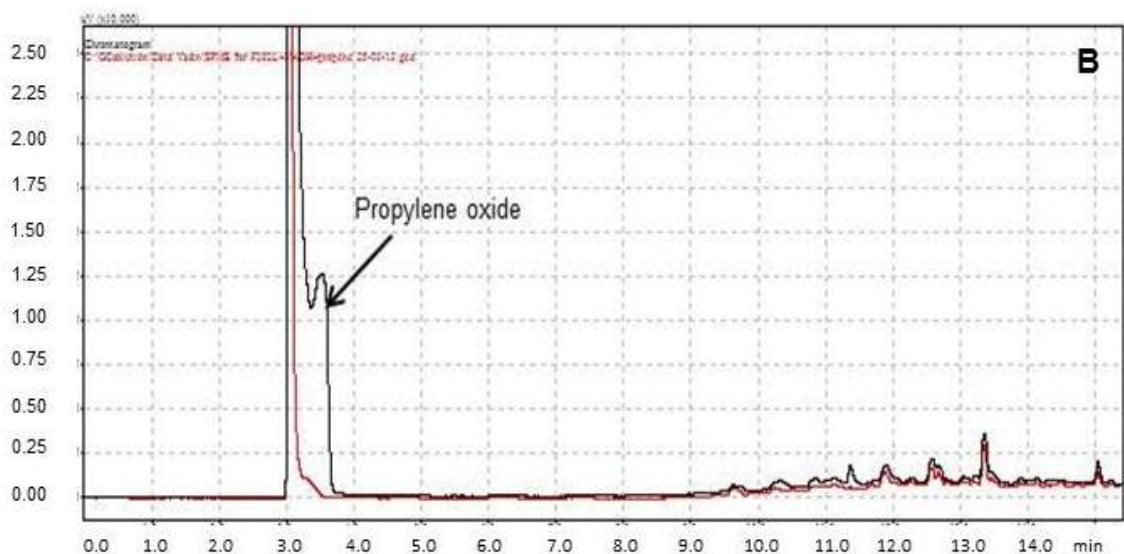
**B:** Soluble extract. The peak corresponding to the propylene oxide product was smaller than that obtained with whole cells and is indicated by an arrow at retention time (RT) 3.27 minutes (black line) compared to the soluble extract without propylene as a negative control (red line).

### **3.6.2.2 Propylene assay by using Solid Phase Microextraction (SPME)**

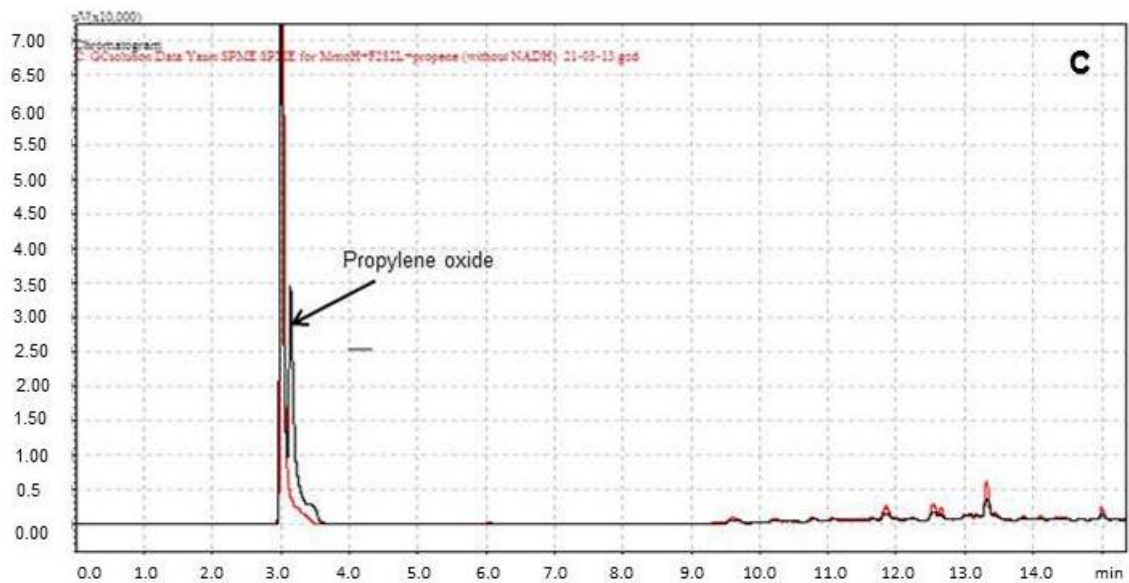
Propylene assay was also performed by using the solventless method called solid phase microextraction (SPME). For these assays, protein B and C were supplied by adding soluble extract from F282L mutant and the hydroxylase was the purified His-tagged form. GC analysis after SPME of the products revealed a peak at the retention time of propylene oxide after incubation with propylene gas for 20 min (Figure 3.10 A). This was compared to an authentic standard of propylene oxide, whereas there was no peak corresponding to propylene oxide from F282L soluble extract with NADH and propylene gas without His-tagged hydroxylase (Figure 3.10 B), His-tagged MMOH and F282L soluble extract and propylene oxide without NADH (Figure 3.10 C). Also a mixture of wild type His-tagged MMOH, F282L, NADH and propylene gas at time zero comparing to the same mixture after 20 minutes, all compared with different negative controls (Figure 3.10 D). It is now suggested that the affinity-purified hydroxylase is active by combining it with the other two components of sMMO and assessing it has similar monooxygenase activity to the native enzyme.



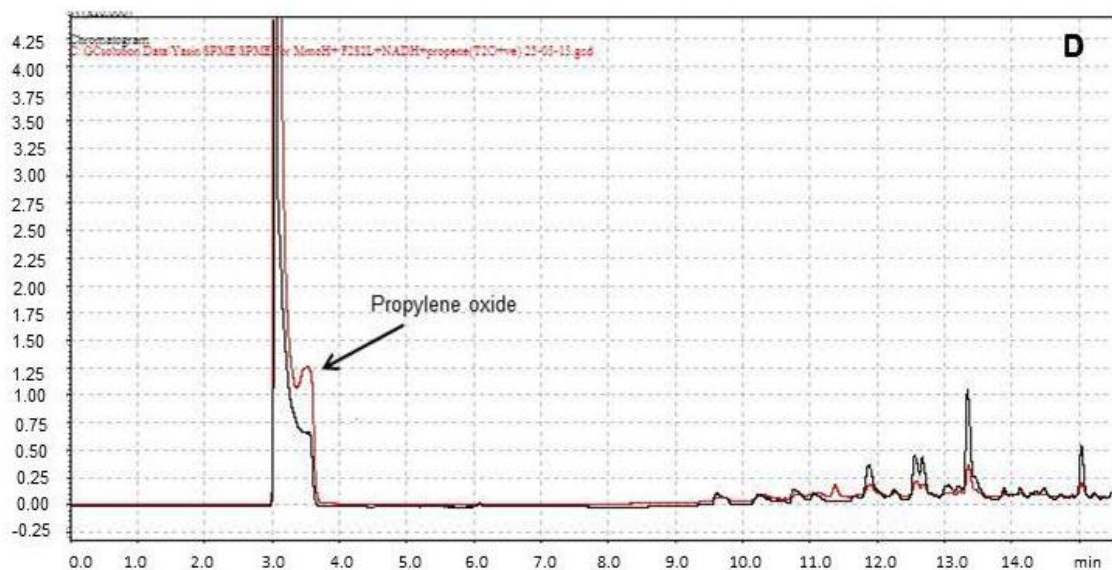
Propylene oxidation assay for affinity purified His-tagged wild type hydroxylase. The assay also contained F282L soluble extract as a source of protein B and C, NADH and 2 ml propylene gas. The GC trace shows a peak of propylene oxide indicated by arrow (black trace) which has the same RT 3.40-3.50 minutes as authentic sample of propylene oxide (data not shown). The red trace represents the negative control without propylene. This trace shows no peak corresponding to propylene oxide.



Control to show that F282L soluble extract has no activity without addition of purified wild type His-tagged hydroxylase. A control assay was set up the same as the assay in A except that the purified wild type His-tagged hydroxylase was omitted. This gave no peak corresponding to propylene oxide (red line). A parallel positive control assay containing all the reaction components gave a peak that could be assigned to the propylene oxide product (black line).



Control to show that added NADH is necessary for the reaction. A control assay was set up the same as the assay in A except that NADH was omitted. This gave no peak corresponding to propylene oxide (red line). A parallel positive control assay containing all the reaction components gave a peak that could be assigned to the propylene oxide product (black line).



The amount of propylene oxide was increased by the increasing the time of reaction. Two identical assays were set up containing all reaction components as in A. Product from one reaction (black line) were analysed at t=0 whereas those from the other assay (red line) were analysed after a reaction time of 20 minutes.

**Figure 3.10** Propylene assay by using Solid phase microextraction (SPME) under various conditions.

- A:** Full assay with negative control lacking propylene.
- B:** Control to show that the F282L soluble extract does not have a hydroxylase activity.
- C:** Control to show that the reaction required NADH.
- D:** Control to show that the amount of propylene oxide increases with reaction time.

### 3.7 Discussion

The purification of the hydroxylase component of sMMO, which is a prerequisite for detailed enzymological studies and many practical applications, is challenging because of the large size of the protein (250 kDa) and the fact that multiple chromatographic steps must be used (Pilkington & Dalton, 1990; Fox *et al.*, 1989; Smith *et al.*, 2002). The genetic manipulation of the hydroxylase to introduce an affinity tag to facilitate purification is also challenging because the genetic system needed to express the hydroxylase in active form requires the genetic manipulation of methane-oxidising bacteria, for which genetic systems are still rather cumbersome (Borodina *et al.*, 2007; Smith and Murrell 2011). As part of a previous project (Lock *et al.*, manuscript in preparation), a 6His tag was added to the beta subunit of sMMO and introduced into the methanotroph expression system. The activity of sMMO in whole cells confirmed that the tag did not prevent catalysis or the functionality necessary for interactions of the hydroxylase with the other component of sMMO. During the current study, the affinity purification of the 6His tagged hydroxylase has been optimised.

In order to determine whether the His-tag system afforded a workable expression system for preparation of pure and active hydroxylase, the affinity-purified His-tagged hydroxylase was tested in sMMO activity assays in the presence of the other sMMO components and using propene as a substrate. The result in the present study revealed that the hydroxylase, with the His-tag inserted in the  $\beta$ -subunit, was active when it was purified by using an affinity column. The remaining components of sMMO, protein B (the coupling/gating protein) and protein C (the reductase) are known to be active when expressed

in *E. coli* (Lloyd *et al.*, 1997; West *et al.*, 1992). Affinity purification of protein B from a GST-fusion construct (Smith *et al.*, 2002) has already been achieved during the current project. Affinity purification of protein C had not been attempted previously. During the current project a number of attempts to purify it using the GST system have been ineffective and so a His-tag fusion system is currently under investigation. Also attempts to express active His-tagged reductase were not reproducible and need to be further investigated.

In a previous work by Smith's group, it has been found that mutant F282L contains inactive hydroxylase which motivated us to use this mutant as a source for protein B and C in the present study, as long as protein C purification was not available, to test the protein activity. The propylene oxidation assay was performed to detect the activity of the purified His-tagged wild type hydroxylase with the F282L soluble extract to provide the protein B and C components. Propylene oxide was extracted by solvent carbon tetrachloride (CCl<sub>4</sub>) which some batches showed for some instance another peak with the same retention time as the propylene oxide. Many other solvents (up to 12 solvents) were investigated for product extraction; all of the tested solvents had a peak in the same retention time for propylene oxide. Propylene oxidation method was swapped with solventless solid phase microextraction (SPME) method that revealed a clear and sharp peak of propylene oxide compared to the negative control and other method. The investigated sample needs to be warm on hot plate and most researchers prefer warming with shaking to allow evaporation of the product which will be adsorb by the fibre in the SPME apparatus, then the needle will inject into GC and analysed. Due to the uncontrolled conditions in this method during the warming on hot plate which led to different results,

optimization is useful in developing this method in future for propylene assay especially for few number of samples.

During the current project, several mutants have been introduced into the His-tag expression system with a view toward purifying and characterising them when the system has been implemented with the wild-type enzyme. The purification of these hydroxylases does not need go through anion exchange chromatography. Also, the fact that it has been shown in the present study that the active recombinant His-tagged hydroxylase can be purified by means of affinity chromatography suggests that the His-tag system will offer an improved way to purify mutant and wild-type hydroxylase in future.

Pure protein is needed to test the hypothesis behind the mutation of the wild type, because methane oxidation assays are unsatisfactory in whole-cell methanotroph systems due to the presence of particulate form of MMO (actually a completely different enzyme from sMMO), which is able to oxidise methane. Also, the methanol produced from methane oxidation by either sMMO or pMMO is removed by methanol dehydrogenase, the next enzyme after MMO in the methane oxidation pathway in methanotrophs. However, a new method to test sMMO directly by adding inhibitors to pMMO is under development (will be more discussed in next chapters)

It is also anticipated that the affinity purification system under development currently in large scale (10 ml column since the column used in the present study can purify only 600  $\mu$ l of the His-tagged hydroxylase) will be valuable in characterising and testing additional mutants of sMMO in the future.

# Chapter 4: The role of C151

---

## 4 Investigating the role of Cysteine 151 in MMOH $\alpha$ -subunit in providing free radicals during the catalytic cycle of sMMO

### 4.1 Introduction

As mentioned previously, the diiron centre of the active site is buried deeply in the  $\alpha$ -subunit of the hydroxylase where the methane and other substrates can be oxidized (Rosenzweig *et al.*, 1997; Cardy *et al.*, 1991). This diiron centre is ligated with four glutamates, two histidines and surrounded by a number of amino acids with hydrophobic residues forming a hydrophobic cavity on the way of the substrate to the diiron centre (Elango *et al.*, 1997). Like the MMO, the cytochrome P-450 monooxygenase enzyme can oxidize very kinetically unreactive C-H bonds. During the oxidation, they both activate oxygen as a substrate to produce a water molecule and a high valent iron compound which catalyses breakage of the inert C-H bonds (Ortiz de Montellano, 1986; McMurry & Groves, 1986; Lipscomb, 1994). In the cytochrome P-450 enzyme, the cleavage of the O-O bond happens with the aid of a non-ligating residue which transfers a proton to the active site. The similarity of MMO to Cytochrome P-450 has led to the suggestion by Fox's group (Fox *et al.*, 1989; Fox *et al.*, 1991) that the same mechanism operates and the only non-ligating residues that may be implicated in formation a hydrogen bond to provide a proton, are Cys151 and Thr213 (Figure 4.1). In addition to the roles of protein B which have been explained previously, before formation a complex with MMOH, Glu240 and Asp214 in MMOH both are occupied with water or a hydronium ion in a

hydrogen bond and in a position to allow free passage of solvent through to the active site. During the formation of the complex between protein B and the hydroxylase in the sMMO, the Glu240 carboxylate side chain undergoes a conformational change to make a hydrogen bond with the Thr213 hydroxyl group. Consequently, the change at Glu240 may result in proton delivery to active site of the sMMO (Lee *et al.*, 1999; Tinberg *et al.*, 2009; Lee *et al.*, 2013).

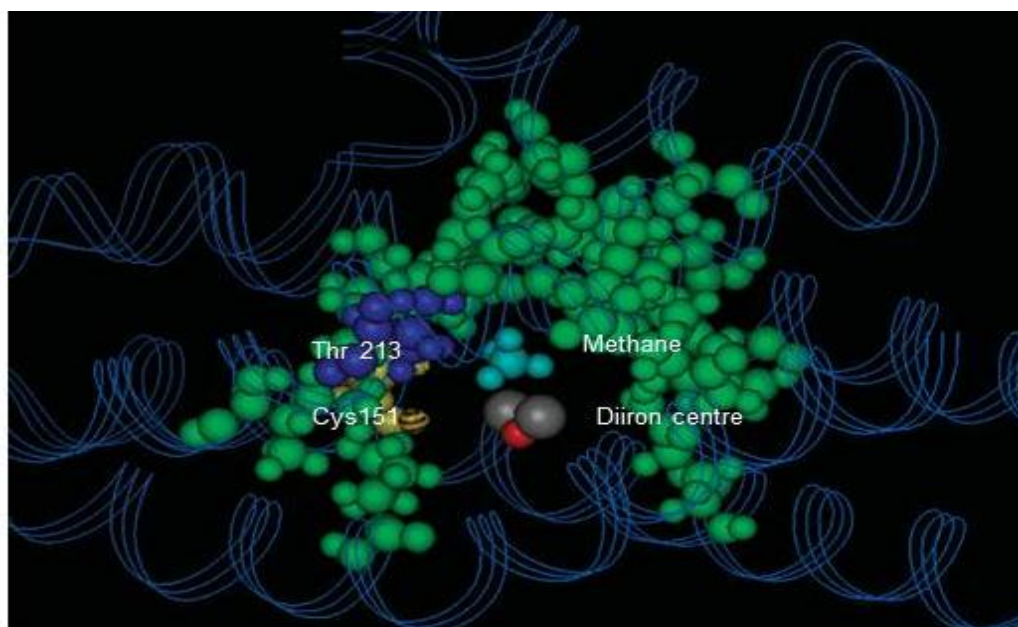


**Figure 4.1** The position of Cys151 and Thr213 near the diiron centre of sMMO where the proposed binding site for methane and other substrates lies.

The diiron centre is in silver/grey, and the bound methane molecule is shown in blue (George *et al.*, 1996).

#### 4.1.1 Residues corresponding to Thr 213 and Cys 151 in other diiron enzymes

In a comparative study between MMO and ribonucleotide reductase (RNR), Nordlund *et al.* (1992) found that the area around the diiron active site centre is similar in both and the corresponding residue to Cys151 in sMMO is Tyr122 in RNR. It has been proved that tyrosine 122 provides a stable tyrosyl radical with a critical role in initiating the reaction of reduction of ribonucleotides to deoxyribonucleotides by ribonucleotide reductase (Sjöberg, 1997). This result led to the suggestion of a similar role to Tyr122 for Cys151 in sMMO in possibly providing a cysteinyl radical during the oxidation cycle of sMMO (Nordlund *et al.*, 1992; Rosenzweig *et al.*, 1993; Feig *et al.*, 1994). Cys151 is conserved in all well studied sMMO enzymes (Smith *et al.*, 2002). The amino acid equivalent to Cys151 in alkene monooxygenase is glutamate or aspartate (Saeki and Furuhashi, 1994; Zhou *et al.*, 1999) and leucine in stearoyl-ACP desaturases. The monooxygenases that have glutamine in the same position as Cys151, such as toluene *ortho*-monooxygenase, are capable of oxidation of aromatic hydrocarbons, which may suggest that Cys151 has another role or may have not essential role in this site (Elango *et al.*, 1997). The amino acid Thr in position 213 of the  $\alpha$ -subunit of sMMO is the same in all known soluble monooxygenase enzymes with a diiron centre (SDIMOs) (Johnson and Olsen 1995; Zhou *et al.*, 1999). Substituting the amino acids Cys151, Thr213 and Ile217 around the active site in sMMO with long side chain amino acid such as Tyr122, Phe208 and Phe212 as in ribonucleotide reductase may make the

sMMO enzyme accommodate smaller substrates than it does as it has been proposed by [Green and Dalton \(1989\)](#).

#### 4.1.2 Mutagenesis of residues Cys151 and Thr213

Thr213 and its equivalents in related enzymes have been implicated in providing a proton to the active site via hydrogen bond forming during the monooxygenase oxidation reaction cycle ([Elango \*et al.\*, 1997](#); [Rosenzweig \*et al.\*, 1993](#)). In addition, the position of Thr213 in a  $\pi$ -turn in an  $\alpha$ -helix in both sMMO and cytochrome P-450 makes it a candidate in controlling the conformation of the active site of the enzymes ([Raag \*et al.\*, 1991](#)). Replacement of Thr by Ala in cytochrome P-450 via site- directed mutagenesis completely disrupted the conformation of the enzyme. However, this result may not be sufficient to determine the exact role of this residue because it is not clear whether the mutation affects the conformation of the enzyme, or catalytic cycle, or maybe both ([Raag \*et al.\*, 1991](#)). A similar result was obtained from a study by [Smith \*et al.\*, \(2002\)](#), when Thr 213 in sMMO was substituted with Ala, and no sMMO components of the mutant enzyme could be seen in SDS-PAGE indicating that the enzyme was destabilized and possibly inactivated by the mutation. However, the mutation of Thr213 to Ser yielded a mutant with activity towards naphthalene and the SDS-PAGE verified the presence of stable sMMO components that were purified subsequently by the same method applied for the wild type sMMO. The alteration of Thr 213 to Ala removed the O<sub>γ</sub> functional group whereas changing Thr213 to Ser conserved the O<sub>γ</sub> group. The fact that the presence of the O<sub>γ</sub> correlated with the presence of sMMO activity indicates

a critical role of O<sub>γ</sub> in the structure and possibly also for activity of the enzyme (Smith *et al.*, 2002). In the same study, Cys151 was replaced by glutamate via site-directed mutagenesis (as in alkene monooxygenase in *Rhodococcus rhodochrous*). Also, Cys151 was changed to tyrosine (as in ribonucleotide reductase). The new mutant C151Y was naphthalene negative and no sMMO components could be detected in SDS-PAGE, indicating a low level or unstable sMMO production. C151E, unlike C151Y, gave a strong naphthalene positive result with whole cells. However, the C151E strain did not show detectable sMMO subunits in the SDS-PAGE of the mutant soluble extract. Even though converting the Cys to Glu conserved the activity towards naphthalene, producing a free radical from glutamate is considered impossible due to the self-decarboxylation of the glutamyl radical (Nonhebel *et al.*, 1979). In a study at the corresponding position in toluene monooxygenase substitution of Gln141 with Cys (as in sMMO) showed that it preserved its activity (Pikus *et al.*, 1997). Although tyrosine has been shown to produce a free radical in ribonucleotide reductase (RNR) (which is not a monooxygenase) (Sjöberg, 1997), converting Cys151 in sMMO to tyrosine like RNR diminished its activity which may be due wholly or partially to instability of sMMO (Smith *et al.* 2002). As such one of the mutants (C151Y E114D) in the present study was designed and constructed in order to stabilize the hydroxylase subunits in the unstable C151Y mutant of sMMO.

## 4.2 Investigation of mutant C151S in the $\alpha$ -subunit of sMMO

As mentioned in the previous paragraph, the two mutants C151Y and C151E were well investigated by [Smith \*et al.\* \(2002\)](#). Another mutant C151S has been constructed by Smith and co-workers at University of Warwick previously. The mutant C151S was designed to probe the role of the cysteine residue at this position in providing a free radical or affecting the conformation and activity of the sMMO especially in accommodating large di- and tri-aromatic substrates. This mutant was constructed within pTJS175 and then transferred into the new expression system pT2MLY that contains a His-affinity tag in the  $\beta$ -subunit of the sMMO hydroxylase as mentioned in the Materials and Methods Chapter. Converting the amino acid Cys151 (which was implicated in providing a cysteinyl radical) from the thiol group (SH) into the amino acid serine with a hydroxyl group was based on the rationale that a hydroxyl residue could not provide any free radical ([Nonhebel \*et al.\*, 1979](#)) and would abolish the enzyme activity if a free radical at this position was essential. After the mutant was expressed in the new system it was shown to be naphthalene positive and was then tested with a number of mono-aromatic compounds namely toluene, ethyl benzene and mesitylene and di-aromatics namely naphthalene and biphenyl, since these compounds are only oxidized by sMMO and not by pMMO. Also mutant C151S was tested with the tri-aromatic compounds anthracene and phenanthrene that up to date have not been shown to be oxidized by the wild type or any of previous mutants such as mutants L110G, L110C, L110Y and L110R ([Borodina \*et al.\*, 2007](#)). These tests were performed in comparison to the wild type *Methylosinus trichosporium* OB3b and wild type sMMO with the new His-tag expression system.

### 4.3 Site-directed mutagenesis

Investigation of the specific role of different amino acids in sMMO can be achieved by site-directed mutagenesis. In the past, site-directed mutagenesis for sMMO was inapplicable owing to many reasons such as the lack of suitable host for protein expression (Borodina *et al.*, 2007). Many attempts to overcome this problem were made, hence West *et al.*, (1992) succeeded in expressing both protein B and C in an heterologous system, *E. coli*, whereas the hydroxylase could not be manipulated in such a system. Martin and Murrell (1995) were able to create the first homologous expression system by using a marker-exchange technique. In this method, part of *mmoX* gene was knocked-out and replaced with a kanamycin resistance cassette. The resulting sMMO<sup>-</sup> strain was named mutant F. Although it needs a long time and many manipulation steps, a similar technique had been used successfully by Khalifa, (2012) to create mutants in both *Ms. trichosporium* and *Mc. capsulatus*. Lloyd *et al.* (1999) developed a homologous system by complementation of mutant F with a broad host range plasmid harbouring the sMMO encoding genes with the native promoter. The resulting mutant was able to grow at high copper concentration with high sMMO activity that was comparable to the wild type. This system has been developed by Smith *et al.*, (2002) who used mutant F with a new vector system. The new system, created by site-directed mutagenesis, enabled this group to mutate some of the amino acids in the *mmoX* gene that encode  $\alpha$ -subunit of MMOH. This system was tested by mutagenesis of Thr213 and Cys151 which are the only hydrophilic amino acids around the active site that were implicated in providing a proton during the

oxidizing cycle of methane and other substrates at the diiron site (further details about these residues will be provided later on in this Chapter). The inflexibility and limitation of this system in mutagenesis of other amino acids in the sMMO components rather than the part of MmoX encoded by the sequence deleted from mutant F led to development of a more tractable and efficient system by Borodina *et al.* (2007). This study created a new strain that was named SMDM (Soluble Methane monooxygenase Deleted Mutant). SMDM is an OB3b strain from which a large part from the sMMO operon has been deleted to make this system more amenable and give more opportunities to investigate other residues in the *mmoXYBZD* genes (Figure 4.2). The system was validated by investigation of the role of Leu110 which was a candidate gate for substrate entry to the sMMO active site owing to its position close to the di-iron centre revealed by crystallographic studies (Rosenzweig *et al.*, 1997, Borodina *et al.*, 2007).

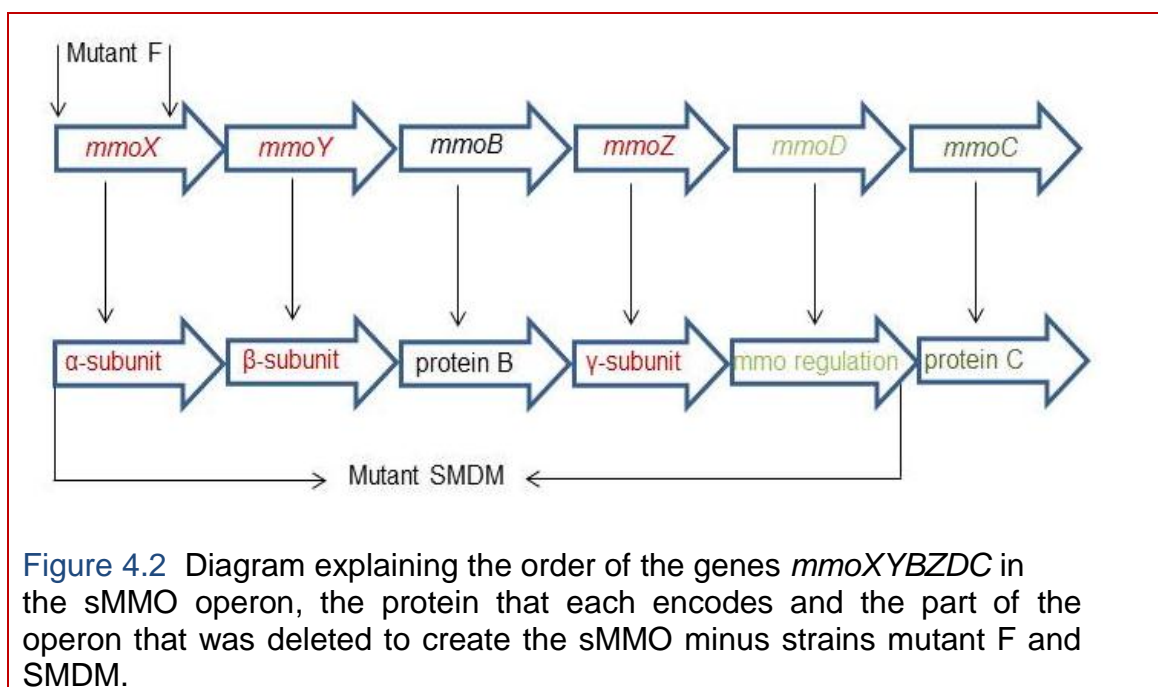


Figure 4.2 Diagram explaining the order of the genes *mmoXYBZDC* in the sMMO operon, the protein that each encodes and the part of the operon that was deleted to create the sMMO minus strains mutant F and SMDM.

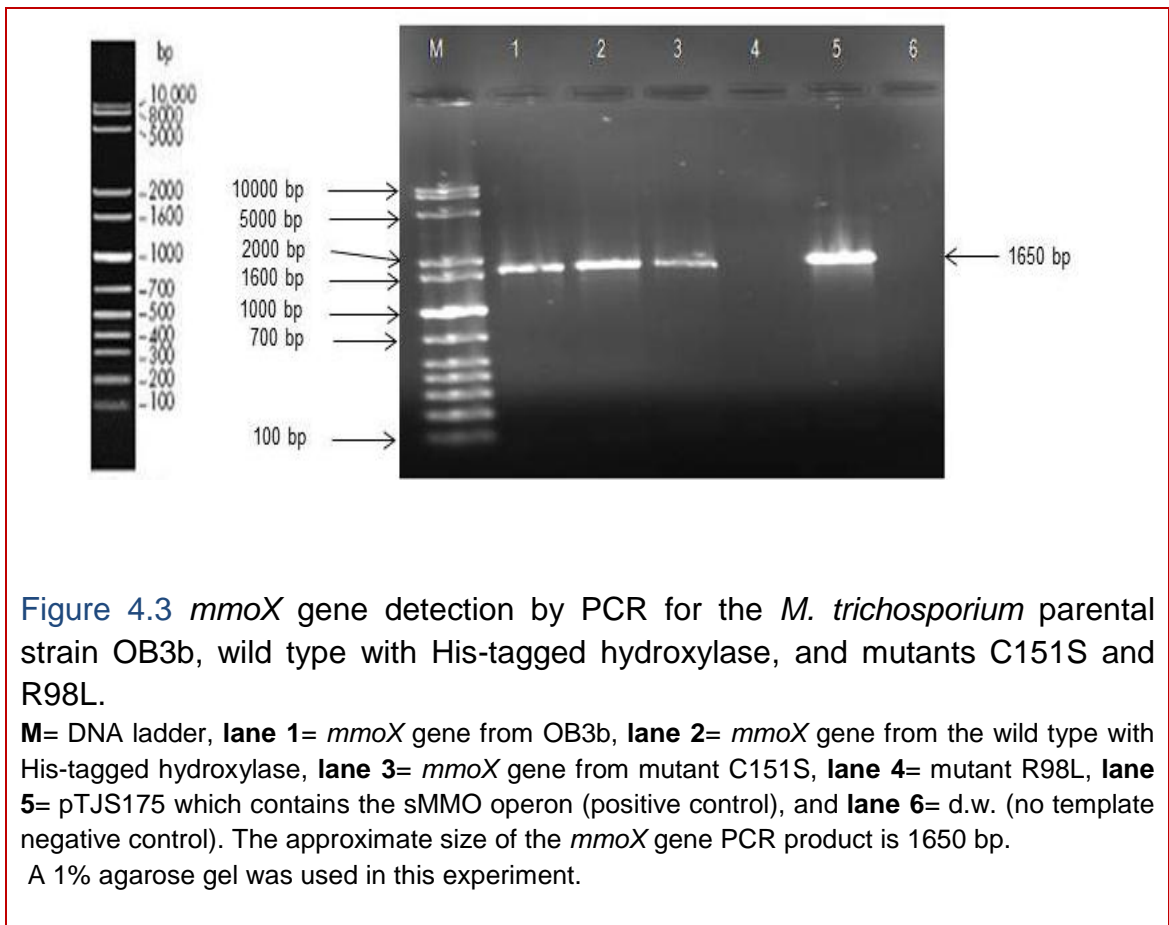
A new expression system pT2ML was developed by Nichol (2011) based on the previous system (Smith *et al.*, 2002). Two unwanted *Bam*HI sites and one *Nde*I site were removed from pTJS140 in two steps by overlap PCR to produce plasmid pTN2. 516 bp was then removed from the *mmoX* gene in pTJS175 by *Pst*I restriction sites to yield pDIDI, which was carried out in the same research group by Dr. M. Lock (Sheffield Hallam University). The sMMO operon was then cloned into pTN2 to produce pT2ML with inactive sMMO. A His-tag was then inserted into the end of the  $\beta$ -subunit to produce the new expression system pT2MLY.

In the present study, site-directed mutagenesis by overlapping PCR and using the new expression system pT2MLY were used to create new mutants. These techniques were used to introduce point mutations into the *mmoX* gene which was then transformed into *E. coli* S17.1. *E. coli* S17.1 with the mutated plasmid was then conjugated into the SMDM strain which resulted in constructing new mutant sMMO expressing strains.

#### **4.3.1 Characterization and naphthalene test for C151S**

In order to confirm the presence of the C151S mutant gene which is constructed before this study by site-directed mutagenesis (T.J. Smith personal communication), the *mmoX* gene that encodes the  $\alpha$ -subunit of the sMMO hydroxylase with the desired mutation was amplified from the engineered methanotroph strain and sequenced as follows; PCR was run by using *mmoX*-specific primers (two primers; *mmoX*- p1 (forward) and *mmoX*- p4 (reverse) were designed to cover most of *mmoX* gene) with total DNA from SMDM

pT2MLY C151S as the template alongside *Ms. trichosporium* OB3b, and *Ms. trichosporium* wild type with His-tagged hydroxylase (SMDM pT2MLY wt.) which is identical to C151S apart from the point mutation in codon 151. PCR products for positive samples were re-amplified and BSA was used to remove any inhibiting substances which might occur in the PCR amplification to obtain a clear band representing a sufficient amount of the gene for sequencing (Figure 4.3).



DNA was sequenced for the whole of the PCR product of the cloned mutant gene by using four primers to cover the gene; *mmoX*-specific primers and *mmoX* mutant primers (two primers were designed to cover the mutation in the area around the active site). The sequenced PCR product was then aligned with the wild type OB3b and wild type with His-tagged hydroxylase by performing a DNA BLAST search provided by the National Centre for Biotechnology Information Service (NCBI) (<http://www.ncbi.nlm.nih.gov/>). This showed that there were two mutations in the C151S mutant gene, one in codon 145 which is silent because it affects only the third (wobble) position of an Ile codon, while the mutation in codon 151 showed conversion of Cys to Ser (Figure 4.4). The second mutation was also made to change the restriction pattern of the gene to help in identify the mutant without sequencing.

```

•   OB3b           ACT CTT CTC GAC GGC CTC ACC CGC CTC GGC GOC GGC AAC AAG GTC CAT CCC CGC TGG GGC
•   WT            ACT CTT CTC GAC GGC CTC ACC CGC CTC GGC GOC GGC AAC AAG GTC CAT CCC CGC TGG GGC
•   C151S         ACT CTT CTC GAC GGC CTC ACC CGC CTC GGC GOC GGC AAC AAG GTC CAT CCC CGC TGG GGC
•
•   OB3b           GAG ACG ATG AAG GTG ATC TCG AAC TTC CTC GAG GTC GGC GAATATAAC GCG ATC GCG GCT
•   WT            GAG ACG ATG AAG GTG ATC TCG AAC TTC CTC GAG GTC GGC GAATATAAC GCG ATC GCG GCT
•   C151S         GAG ACG ATG AAG GTG ATC TCG AAC TTC CTC GAG GTC GGC GAATATAAC GCG ATC GCG GCT
•
•   OB3b           TGG GOC ATG CTT TGG GAC AGC GCC ACC GOC GOC GAG CAG AAG AAC GGC TAT CTC GOG CAG
•   WT            TGG GOC ATG CTT TGG GAC AGC GCC ACC GOC GOC GAG CAG AAG AAC GGC TAT CTC GOG CAG
•   C151S         TGG GOC ATG CTT TGG GAC AGC GCC ACC GOC GOC GAG CAG AAG AAC GGC TAT CTC GOG CAG
•
•   OB3b           GTG CTC GAC GAG ATT CGT CAC ACG CAT CAA TGC GGC TTC ATCAAT CACTAT TACTCCAAG
•   WT            GTG CTC GAC GAG ATT CGT CAC ACG CAT CAA TGC GGC TTC ATCAAT CACTAT TACTCCAAG
•   C151S         GTG CTC GAC GAG ATC CGT CAC ACG CAT CAA TGC GGC TTC ATCAAT CACTAT TACTCCAAG
•
•   OB3b           CATTAT CAC GAT CCG GOC GGC CACAAT GAC GOC CGT GCG ACG GCG GCG ATC GGT CCG CTG
•   WT            CATTAT CAC GAT CCG GOC GGC CACAAT GAC GOC CGT GCG ACG GCG GCG ATC GGT CCG CTG
•   C151S         CATTAT CAC GAT CCG GOC GGC CACAAT GAC GOC CGT GCG ACG GCG GCG ATC GGT CCG CTG
•
•   OB3b           TGG AAG GGC ATG AAG GCG GTC TTC GCG GAC GGC TTC ATC TCC GCG GAC GCG GTG GAG TGC
•   WT            TGG AAG GGC ATG AAG GCG GTC TTC GCG GAC GGC TTC ATC TCC GCG GAC GCG GTG GAG TGC
•   C151S         TGG AAG GGC ATG AAG GCG GTC TTC GCG GAC GGC TTC ATC TCC GCG GAC GCG GTG GAG TGC
•
•   OB3b           TCG GTC AAT CTG CAG CTG GTC GGC GAA GOC TGCTTCA CCAAT CCG CTC ATC GTC GCG GTC
•   WT            TCG GTC AAT CTG CAG CTG GTC GGC GAA GOC TGCTTCA CCAAT CCG CTC ATC GTC GCG GTC
•   C151S         TCG GTC AAT CTG CAG CTG GTC GGC GAA GOC TGCTTCA CCAAT CCG CTC ATC GTC GCG GTC
•
•   OB3b           ACC GAA TGG GCT TCG GCA AT GGC GAC GAG ATC ACG CCG ACC GTG TTC CTC TCG GTG GAG
•   WT            ACC GAA TGG GCT TCG GCA AT GGC GAC GAG ATC ACG CCG ACC GTG TTC CTC TCG GTG GAG
•   C151S         ACC GAA TGG GCT TCG GCA AT GGC GAC GAG ATC ACG CCG ACC GTG TTC CTC TCG GTG GAG
•

```

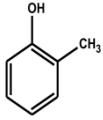
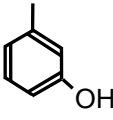
Figure 4.4 *mmoX* gene sequencing for mutant C151S compared to the parental wild type OB3b and wild type with His-tagged hydroxylase (WT). The red colour shows a silent mutation at the position encoding amino acid 145 to remove a restriction enzyme site. The orange colour shows the mutated amino acid Cys to Ser at 151.

## 4.4 Investigating the role of C151S in oxidation of aromatic compounds

### 4.4.1 The C151S mutant showed regioselectivity in oxidation of the monoaromatic hydrocarbon toluene

The four expected products from oxidation of toluene are benzyl alcohol, *p*-cresol, *m*-cresol, and *o*-cresol. Unlike many studies which showed that the main product from toluene oxidation by the parental wild-type strain *Ms. trichosporium* OB3b is benzyl alcohol, in the present study strain OB3b was found to oxidize toluene with the main product *o*-cresol (96.70%) followed by *p*-cresol (3.28%), and *m*-cresol (0.01%). The whole cells assay of mutant C151S revealed some alteration in regioselectivity by yielding different product percent from both the OB3b and wt. with His-tagged hydroxylase represented by *o*-cresol as a main product with percentage 99.99% and *p*-cresol (0.01%) with no *m*-cresol whereas wild type with His-tagged hydroxylase showed comparable products to OB3b (*p*-cresol, 2.33% and *m*-cresol 0.02%) as shown in (Table 4.1). After correction for differences of cell density, no statistically significant difference was observed in the amount of *m*-cresol produced by the mutant compared with the wild type OB3b ( $p > 0.05$ ). However, there was a significant difference in the amount of *p*-cresol and *o*-cresol produced between the C151S mutant and His-tagged wild type by using Kruskal-Wallis test (Conover-Inman) with ( $p < 0.05$ ) and ( $p < 0.01$ ) respectively (Figure 4.5). Also, there was a significant difference in *p*-cresol produced by C151S compared to OB3b ( $p < 0.05$ ).

**Table 4.1** Products distribution percent of toluene oxidation by C151S.

Strains	Product percentage %		
	 <i>p</i> -cresol	 <i>o</i> -cresol	 <i>m</i> -cresol
OB3b	3.28%	96.70%	0.01%
wt his-tag	2.33%	97.64%	0.02%
C151S	0.01%	99.99%	ND

The distribution of the products is shown as a percentage of the total products obtained from triplicate technical samples, i.e. three separate aliquots were taken from the same batch of fermentor grown bacteria for each strain. ND indicates no detectable product. The extracted products were analysed by GC-MS and mass spectra of the products were compared with those of authentic standards and the NIST (National Institute for Standards and Technology) list in the software that controls the GC-MS.

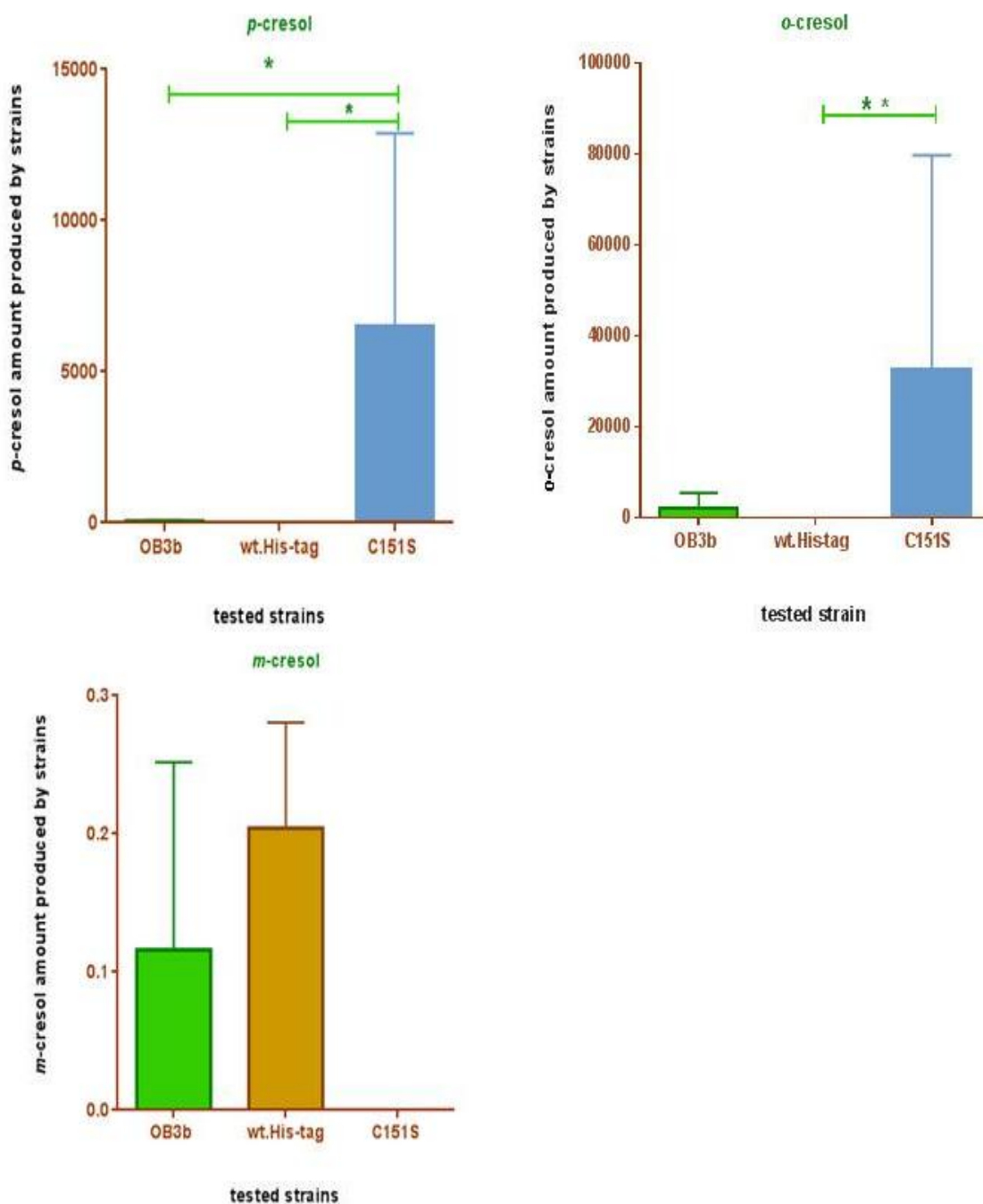


Figure 4.5 Statistical analysis of the toluene oxidation products (*p*-, *o*- and *m*-cresol) data for mutant C151S, OB3b and wild type with His-tagged hydroxylase. Statistical analysis was performed by applying the Kruskal-Wallis test (Conover-Inman).

Data from triplicate technical samples were obtained from injection and analysis of 1  $\mu$ l sample of extracted product by using GC-MS. The amounts of product are expressed in terms of the peak areas obtained from GC-MS.

Data presented as (Mean  $\pm$  S.E.M), statistical analysis: Kruskal-Wallis test (Conover-Inman).

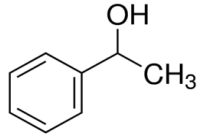
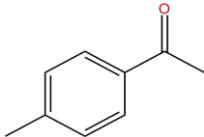
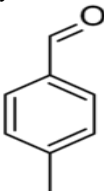
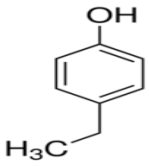
\* Significant at  $P < 0.05$ .

\*\* Significant at  $P < 0.01$ .

#### **4.4.2 Oxidation of ethyl benzene by C151S yields regiospecific products different from OB3b and His-tag wt.**

The oxidation of ethyl benzene has been found to produce different products depending on the strain is being tested (Nichol, 2011). In the present study when the 4-ethyl benzene was oxidized by wild type OB3b, four products were seen with 4-ethyl phenol being the main product (84.54%) followed by 1-phenyl ethanol, 4-methylbenzaldehyde, and phenyl methyl ketone with 9.81%, 4.04% and 1.59% abundance respectively (Table 4.2). Testing the wild type with His-tagged hydroxylase in this assay resulted in production of ethyl phenol with highest percentage abundance (72.63%) among the four products; 4-methylbenzaldehyde and 1-phenyl ethanol came after ethyl phenol with nearly comparable amount 13.78% and 13.57% respectively. No phenyl methyl ketone was detected among the products of the reaction catalysed by the wild type recombinant with His-tag. However, when C151S was investigated toward ethyl benzene, it produced only ethyl phenol and 1-phenyl ethanol with 81.57% and 18.42% abundance respectively (Table 4.2). No 4-methylbenzaldehyde or phenyl methyl ketone was detected as a product from ethyl benzene oxidation by mutant C151S. There was no significant difference between OB3b with wt. with His-tag MMOH and C151S for all four products (4-ethyl phenol, 1-phenyl ethanol, 4-methylbenzaldehyde and phenyl methyl keton) when it was compared statistically by using one Kruskal-wallis (Conover-Inam) test (Figure 4.6).

**Table 4.2** Distribution of products from oxidation of the monoaromatic ethyl benzene by parental methanotrophs OB3b, His-tag wild type and mutant C151S.

Strain	Product distribution percentage %				Relative activity percentage %		
	1-phenyl ethanol 	Phenyl methyl ketone 	4-methylbenzaldehyde 	4-ethyl phenol 	1-phenyl ethanol	4-methylbenzaldehyde	4-ethyl phenol
OB3b	9.81%	1.59%	4.04%	84.54%	100%	100%	100%
His-tag wt	13.57%	ND	13.78%	72.63%	13.59%	42.8%	8.6%
C151S	18.42%	ND	ND	81.57%	51.35%	ND	26.99%

ND refers to non-detectable product peak in GC-MS. Compounds were compared to the NIST list in the GC-MS.. The assay was performed for triplicate technical samples from the same batch of frozen cells of each strain. The relative activity was obtained by comparing the activity of the wild type with His-tag hydroxylase and the mutant to the parental wild type OB3b, which was considered to have 100% activity.

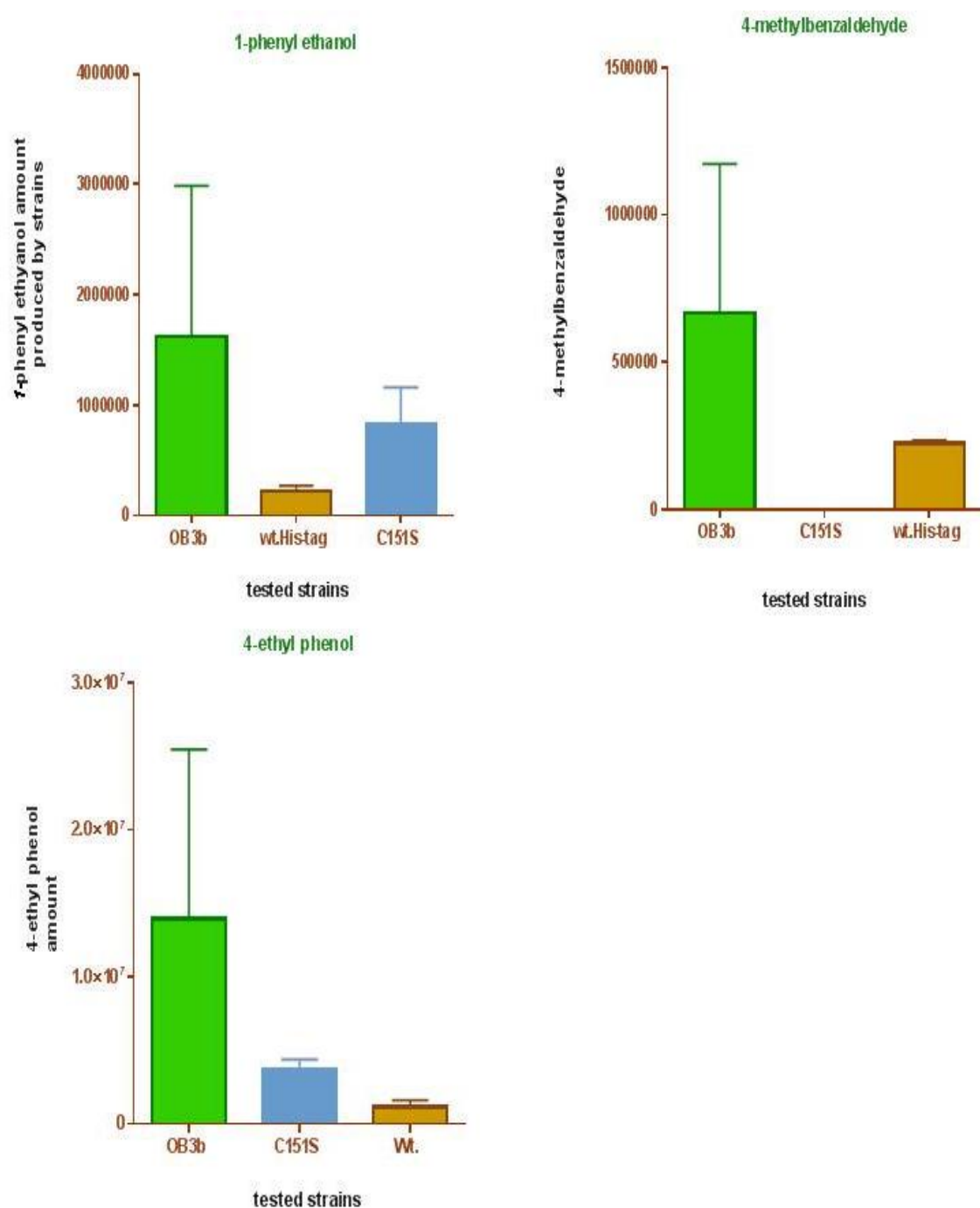


Figure 4.6 Comparing the raw data for products obtained from ethyl benzene oxidation by mutant C151S, the parental wild type OB3b and wild type with His-tag showing no significant difference between them at  $p < 0.05$ .

The significance of the results was calculated for the data of each product (peak area for each product). Data were obtained via analysing 1  $\mu$ l of the extraction from each assay via GC-MS. Assays were performed for triplicate technical samples.

Data presented as (Mean  $\pm$  S.E.M), statistical analysis: Kruskal-Wallis test (Conover-Inman).

#### 4.4.3 Oxidation and product distribution from naphthalene by C151S

The C151S mutant showed as strong naphthalene positive in both plate and liquid methods. To evaluate the production of naphthol and the regioselectivity of the enzyme, 5 ml culture of mutant cells were tested towards naphthalene for 48 h as detailed in the Materials and Methods Chapter. The product which was then analysed by GC-MS after being extracted with diethyl ether, revealed that the products from naphthalene oxidation were 1-naphthol (83.08%) and 2-naphthol (16.91%) (Figure 4.7, Table 4.3). This result was similar to the result obtained from wild type OB3b and not greatly different from the wild type with His-tagged hydroxylase which showed slightly more 1-naphthol (57.64%) than 2-naphthol (42.35%). No change in regioselectivity was observed for the C151S mutant compared to the wild type with His-tag or parental wild type OB3b. Also no new unexpected products were detected for this mutant. There was no statistically significant difference observed at level  $p < 0.05$  when compared to the product distribution of OB3b with C151S or between wild type with His-tagged hydroxylase with C151S by using Kruskal-Wallis (Conover-Inman) test.

**Table 4.3** Distribution of products 1-naphthol and 2-naphthol from naphthalene oxidation by mutant C151S.

strain	Product percentage %		Relative total activity %	
	1-naphthol	2-naphthol	1-naphthol	2-naphthol
OB3b	85.23%	14.76%	100%	100%
His-tag wt.	57.64%	42.35%	233.66%	265.91%
C151S	83.08%	16.91%	55.94%	81.07 %

Naphthalene oxidation assays were performed for triplicate technical samples from the same bacterial fermentor batch for each strain. The retention times for the products peaks were compared with authentic standard peaks for 1-naphthol and 2-naphthol. Relative total activities were calculated for mutant C151S compared to the parental wild type OB3b which is considered as 100% activity.

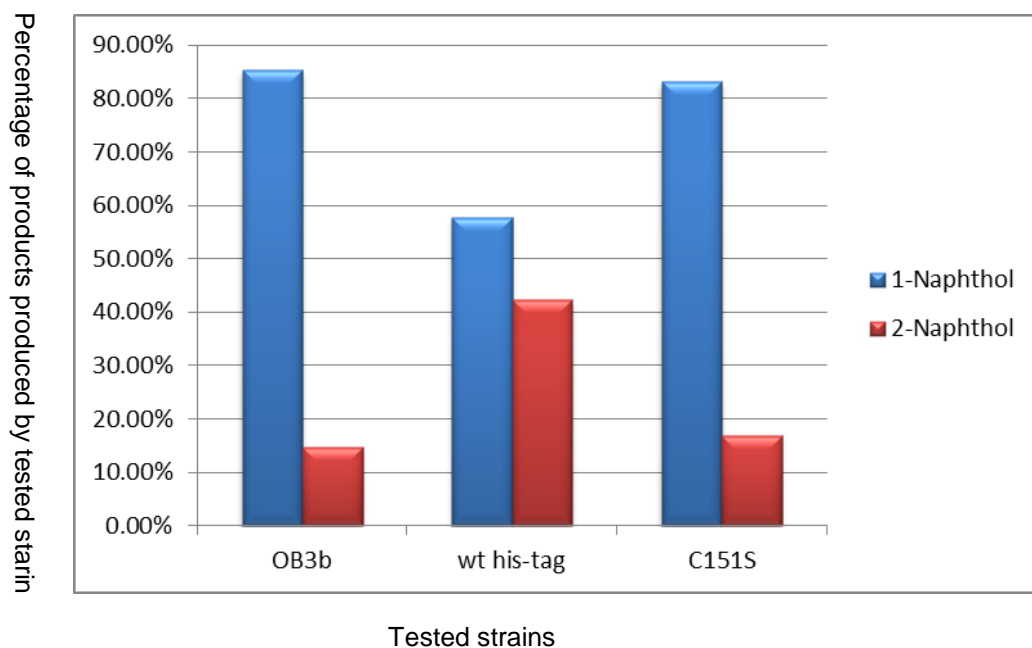


**Figure 4.7** Product distribution percentages from naphthalene oxidation by mutant C151S.

The percentage activity was calculated from three technical replicate samples from the same bacterial batch of each strain harvested from cells grown in the fermentor. The figure shows the same product distribution information presented in table 4.3 above.

#### **4.4.4 C151S showed no detectable activity toward mono-aromatic mesitylene, the di-aromatic hydrocarbon biphenyl, and tri-aromatics anthracene and phenanthrene**

Mutant C151S was also tested toward a monoaromatic compound with three side chains, 1, 3, 5-trimethyl benzene (mesitylene), and the di-aromatic compound biphenyl. The mutant C151S was shown not to have activity towards these substrates since measurable peaks could not be detected by using GC-MS. The biphenyl oxidation experiment was repeated with different incubation times, 48 h, 72 h, and 96 h, for the mutant C151S and also for the wild type OB3b and the wild type with His-tagged hydroxylase. Also mutant C151S was investigated to assay its ability to oxidize the tri-aromatic compounds such as anthracene and phenanthrene which to date have not been oxidized by OB3b or its mutants. Neither C151S nor OB3b nor wild type with His-tagged hydroxylase could oxidize either anthracene or phenanthrene after incubation for 48 h at 30°C according to the results obtained from GC-MS.

#### **4.4.5 Propylene oxidation assay for the C151S mutant showed the production of propylene oxide**

The propylene assay was performed for the soluble extract from the wild type with His-tagged hydroxylase as mentioned in the previous Chapter and it showed a detectable activity towards propylene. Due to the sensitivity of the

sMMO in the soluble extract to inactivation by various conditions, the propylene assay was performed for C151S in a whole cell suspension. The whole cell propylene oxidation assay was based on results from experiments that were done by Dr. Tim Nichol (member in Smith's group in BMRC), who used DTT as an inhibitor for pMMO in whole cells of the SMDM mutant (SMDM can grow on methane by using pMMO since it is OB3b of which a large part from sMMO has been deleted). The result revealed that using 5 mM DTT inhibited the activity of pMMO from SMDM whole cells towards propylene since no activity could be detected for this mutant compared to the SMDM without DTT (data not shown). Following this result, the propylene assay was performed for the C151S whole cells by using 5 mM DTT as inhibitor for pMMO. Any detected activity could then be attributed to sMMO activity. The mutant C151S showed an activity toward propylene, since there was a peak corresponding to propylene oxide, which appeared at the same retention time to an authentic standard of pure propylene oxide, when the extract were run on the GC (Figure 4.8). Product from a propylene assay was also analysed by GC-MS which showed a peak at the retention time 1.665 min, which was the same as for the pure propylene oxide and also was confirmed by comparison of the spectrum to the NIST list in the GC-MS. The activity was measured from the GC-MS data and compared with a standard curve of propylene oxide. Whole cells of C151S mutant were able to produce propylene oxide at  $1251 \text{ nmol}^{-1} \text{ min}^{-1} \text{ ml}^{-1}$ , compared with  $1825 \text{ nmol}^{-1} \text{ min}^{-1} \text{ ml}^{-1}$  for whole cell of the wild type OB3b and  $600 \text{ nmol}^{-1} \text{ min}^{-1} \text{ ml}^{-1}$  for the wild type with His-tagged hydroxylase. All assays were conducted in triplicate with the same batch of cells from each strain; the activities were corrected to a cell suspension  $\text{OD}_{600}$  of 5.. The activity for mutant C151S was

68% of the OB3b activity whereas it was 183% compared with the wild type with His-tagged hydroxylase.

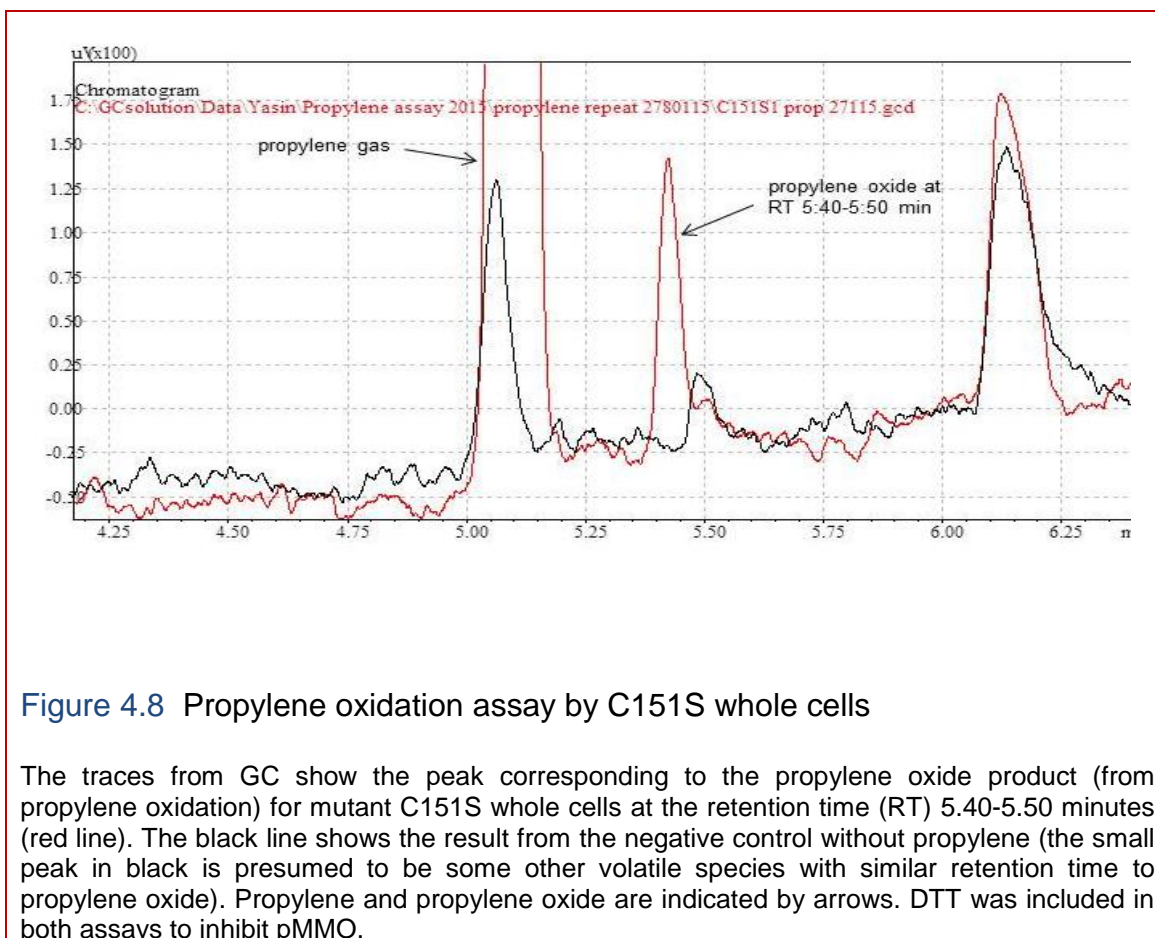


**Figure 4.8** Propylene oxidation assay by C151S whole cells

The traces from GC show the peak corresponding to the propylene oxide product (from propylene oxidation) for mutant C151S whole cells at the retention time (RT) 5.40-5.50 minutes (red line). The black line shows the result from the negative control without propylene (the small peak in black is presumed to be some other volatile species with similar retention time to propylene oxide). Propylene and propylene oxide are indicated by arrows. DTT was included in both assays to inhibit pMMO.

## 4.5 Discussion

To date the expression of soluble methane monooxygenase hydroxylase has been unsuccessful in heterologous systems. The expression of sMMO in a homologous expression system was a challenge due to obstacles which have been explained earlier in this thesis. These issues have been overcome by developing several related systems (Lloyd *et al.*, 1999; Smith *et al.*, 2002; Borodina *et al.*, 2007) including the last system by this group which shortens the cloning steps to one step by creating system pT2ML and then inserting the affinity His-tag in the  $\beta$ -subunit of the hydroxylase (pT2MLY) (M. Lock unpublished paper; Nichol, 2011) to enable the purification of the cloned hydroxylase in one step by using Ni-NTA affinity chromatography compared to the anion exchange chromatography and subsequent steps which were used in the previous studies. Activity for the wild type with His-tag has also been detected in purified protein from this system as mentioned previously in Chapter three.

Mutation of C151 in a previous study (Smith *et al.*, 2002) to evaluate the role of cysteine as a free radical provider during the sMMO catalytic cycle, resulting in inactive sMMO for mutant C151Y (which were mutated to tyrosine as in the ribonucleotide reductase) whereas mutation of cysteine to glutamic acid as in alkene monooxygenase of *R. Rhodochrous* B-276 produce an active sMMO. However, according to the result from the Smith *et al.* (2002) study, it seems that the role of this residue is not essential in providing a free radical. For this purpose, mutation of this amino acid to other amino acids is needed to generate more evidence to evaluate the role of this residue. Cysteine was mutated to serine that has a hydroxyl side chain group that is unlikely to supply a free

radical in contrast to the thiol group which was previously implicated in providing a free radical as in the tyrosine residue of RNR enzyme (Nordlund *et al.*, 1992). This mutant gene was expressed in the mutant F system (which is OB3b of which part from the hydroxylase  $\alpha$ -subunit gene was deleted) and then transferred to the new system pT2MLY by this group as mentioned previously. Also, approximately 550 bp were removed from the *mmoX* gene in pT2MLY which led to loss of the sMMO activity for this recombinant. As such any activity for *mmoX* must be due to the recombinant mutant.

The ability of C151S to grow on NMS agar plates with a minimum copper concentration or copper free medium in the present study may indicate the ability of this mutant to grow and consume methane by pMMO and then switch to the mutant soluble methane monooxygenase and continue to grow. Also this result may indicate that this residue has an important role other than providing the free radical implicated in the sMMO catalytic cycle. This is further supported by the oxidation of naphthalene by mutant C151S when it was grown on a plate, since naphthalene is known to be oxidized by sMMO and not by pMMO (Colby *et al.*, 1977).

It was intended in the present study not only to investigate the role that this residue might have in the catalytic cycle, but also it was aimed to increase the ability of this enzyme in oxidation of di- and tri-aromatic hydrocarbon compounds. When the mutant C151S was assayed toward the di-aromatic compound naphthalene, it showed no significant difference from the wild type OB3b or the wild type with His-tagged MMOH (Table 4.3).

The oxidation of mono-aromatic compound with one side chain such as toluene and ethyl benzene by this mutant showed some difference. The oxidation of

toluene by C151S yielded different product amounts from those produced by OB3b and wild type with His-tagged MMOH, with the *o*-cresol being the main product in mutant C151S with a significant difference from both OB3b and wild type with His-tag. A negligible amount of *p*-cresol and no *m*-cresol was detected for this mutant. Also the oxidation of ethyl benzene gave two products rather than the four that were produced by the OB3b and wild type with His-tagged MMOH. The products from toluene oxidation by mutant C151S may indicate that there is a small difference in the orientation that the mutant soluble methane monooxygenase holds this substrate in the active site

In a mutagenesis study for Thr201 in toluene 4-monoxygenase, [Pikus \*et al.\* \(2000\)](#) found that the mutation of Thr201 to Ala abolished the enzyme activity whereas mutation of Thr201 to Ser conserved the enzyme activity. This result was interpreted as showing that the amino acid Ser (which contains the side chain HOγ functional group) interacts with the binuclear iron centre and is believed to be essential in keeping the enzyme stable. The mutant C151S is in a close position to the diiron centre and the amino acid Ser has HOγ group which might have the same role in enzyme stability.

Propylene was used to evaluate the role of the C151S mutant in oxidation of a substrate with comparable conversion rate to methane when it is oxidized by methane monooxygenase. Also, it is known that propylene oxide is not a substrate for the second enzyme (methanol dehydrogenase [MDH]) in the methane oxidation pathway. Mutant C151S was positive in production of propylene oxide as mentioned previously, which may suggest that the sMMO is still fully active and this residue is not involved or it is not essential in radical chemistry. However, oxidation of methane by purified sMMO components from the C151S strain needs to be investigated to give a more reliable conclusion

concerning the involvement of this residue in radical chemistry of methane oxidation.

In terms of the other di- and tri-aromatic compounds there was no measurable activity toward biphenyl and mesitylene up to 96 h of incubation or with anthracene and phenanthrene up to 48 h. It was found that the OB3b and His-tag wild type had a measurable activity towards biphenyl, since OB3b produced (>97%) 4-hydroxybiphenyl, (0.16%) 2-hydroxybiphenyl and (0.38%) 3-hydroxybiphenyl. Mesitylene was also oxidized by the wild type OB3b in 1 h with 3, 5-dimethylbenzyl alcohol produced (> 99%), and a trace of 2, 4, 6-trimethylphenol (0.44%). However, no products were detected from mesitylene oxidation by OB3b when it was incubated for 24 h and 48 h (Nichol, 2011).

# Chapter 5: Investigating the role of hydrophobic and hydrophilic residues within and outside the hydroxylase active site.

---

## 5.1 Introduction

The diiron centre where the methane and other substrates are oxidized is deeply buried in the active site of the  $\alpha$ -subunit of the MMO hydroxylase (Rosenzweig *et al.*, 1997; Elango *et al.*, 1997). The substrate needs to pass through three hydrophobic cavities as well as the pore cavity to reach the active site from the protein surface (Rosenzweig *et al.*, 1997; Rosenzweig *et al.*, 1993; Whittington *et al.*, 2001(a); Whittington *et al.*, 2001(b); Sazinsky and Lippard 2005). The diiron centres of most monooxygenase enzymes are coordinated by four glutamate residues and two histidine residues. One of these glutamate residues provides a bridging carboxylate ligand (Rosenzweig *et al.* 1993). In addition, there are two hydroxides or one hydroxide and one water molecule that bind the diiron centre (Elango *et al.* 1997). The four glutamate residues Glu114, Glu243, Glu144 and Glu209 provide carboxylate group ligands to the diiron active centre. The presence of an environment with activated oxygen around the active sites of MMOH, RNR-R2 and  $\Delta$ 9-ACP was suggested as having an important role in formation of high-valent iron intermediates. The high-valent iron intermediate plays a role in the catalytic cycle of these enzymes which has been proved by spectroscopic studies (Lee *et al.*, 1993a; Lee *et al.*,

1993b; Liu *et al.*, 1994; Liu *et al.*, 1995; Shu *et al.*, 1997; Whittington and Lippard 2001). Moreover, structural studies for MMOH and RNR-R2 revealed that these enzymes have different conformations in the reduced and oxidized states which are characterized by a carboxylate shift in the glutamate residues around the active site. This carboxylate shift was observed in Glu243 in sMMO and also was seen in the R2 active site when it was compared in the oxidized and reduced forms between the native enzyme and the mutated D84E. This conformational change affects the Fe-Fe distances and might have an important role in opening some of the active sites and hence on the catalytic cycle of the enzymes (Whittington and Lippard 2001).

## 5.2 Construction of C151Y E114D and E114D

Considering the similarity between sMMO and RNR-R2, the amino acid in the corresponding site to Tyr122 in RNR is Cys151 in sMMO, as such Smith *et al.* (2002) mutated Cys 151 to Tyr. The resulting mutation (C151Y) did not produce an active MMOH, which might be due to the instability of the mutant enzyme, since no bands could be detected in SDS-PAGE. In *Ms. trichosporium* OB3b and *Mc. capsulatus* Bath the two Glu (114 and 209) are linked to the diiron centre, the His (147 and 242) are linked to two Asp (143 and 242) which have been suggested to make a pseudo-two-fold symmetrical complex that stabilizes the MMOH like RNR-R2 (Nordlund *et al.*, 1992). The rationale behind the mutation of Glu114 to Asp (E114D) in the mutated plasmid C151Y (double mutant) was to make sMMO more similar to RNR here, in an attempt to gain a stable hydroxylase containing the C151Y mutation, since the hydroxylase from C151Y single mutant was not produced in a detectable amount and proved to

be inactive (Smith *et al.*, 2002). At a structural level, the idea was to replace Glu with the less bulky Asp, to allow Tyr (bulkier than Cys) to be accommodated at this position (personal communication with Kristoffer Andersson). In addition, it was intended to mutate the Glu114 to Asp (single mutant E114D) to investigate the role of this residue in sMMO of *Ms. trichosporium* OB3b (Figure 5.1).

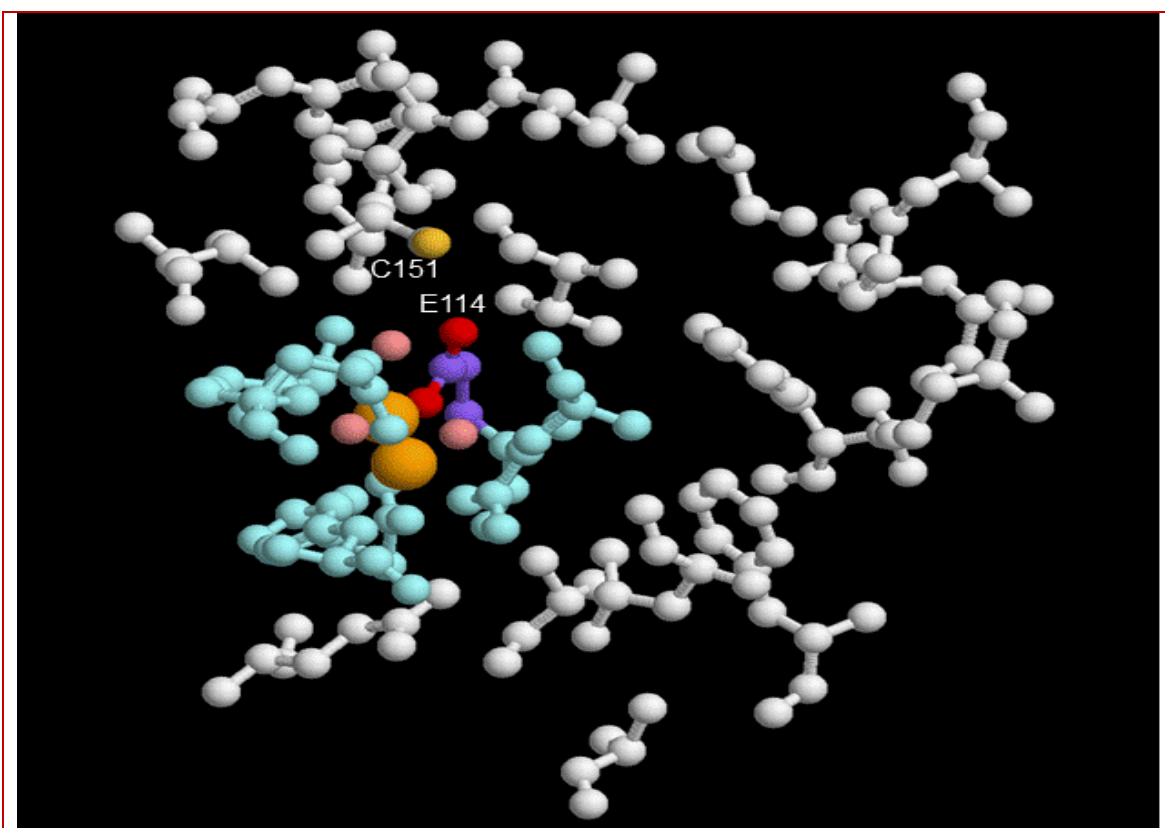


**Figure 5.1** The diiron centre of sMMO, and the position of residues E114 and C151.

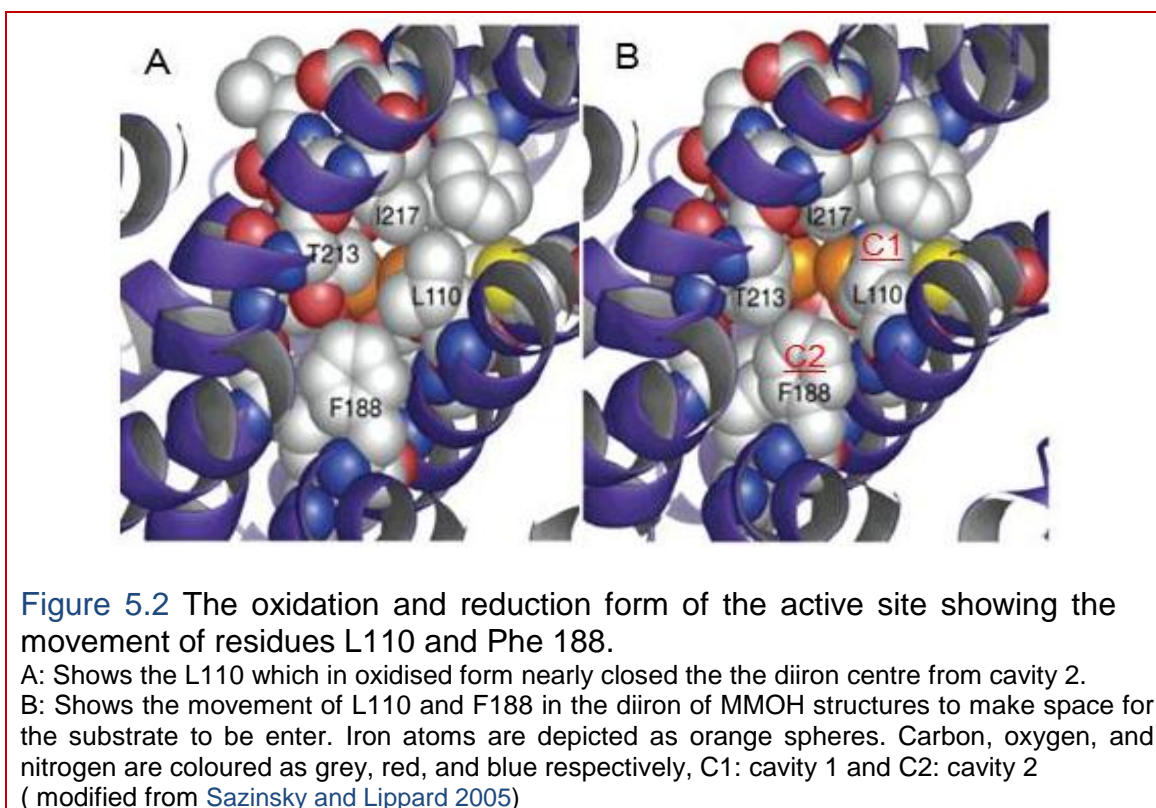
The iron atoms of the diiron site are shown in orange the associated water molecules in pink. The ligands of the diiron centre are shown in light blue, apart from the sidechain of Glu114, where the carboxylate oxygens are red and the rest of the sidechain purple. The sulfur atom of the C151 sidechain is yellow. The residues of the rest of the hydrophobic pocket adjacent to the diiron centre are shown in white. The image was conducted based on the structural studies on sMMO (Rosenzweig *et al.*, 1997; Elango *et al.*, 1997).

### 5.3 Mutagenesis of the proposed substrate gating residue Phe 188

The substrate binding site in MMOH is composed of hydrophobic residues and surrounded by hydrophilic residues. The hydrophobic side chains around the active site include Leu110, Phe188, and Phe292 (Rosenzweig *et al.*, 1997). Crystallographic studies suggested a role for L110 as a substrate gate to the active site since it is a residue with different positions in the structure between the oxidised and reduced states of the enzyme. This allosteric change leads to a connection between cavities within the protein, which is proposed to allow the entry of substrate and maybe egress of the product. However, previous mutagenesis to investigate the function of this residue showed that it has a role in the regioselectivity of the enzyme rather than as a gate for substrates (Borodina *et al.*, 2007). Another residue Phe188 was suggested to undergo a movement which may lead to the formation of a connection between cavities 1 and 2 and so Phe188 may work together with Leu110 in controlling the substrate gating (Rosenzweig *et al.*, 1997). A channel has been seen in the crystal structure of T4MO hydroxylase, which becomes closed upon binding of the equivalent of protein B to prevent the connection between internal (cavities 1 and 2) within T4MOH (Bailey *et al.*, 2008). A similar channel like-space has not been identified in the  $\alpha$ -subunit of MMOH. In contrast, hydrophobic residues were found including Leu110, Phe188 and Phe236, which were proposed to occupy this space preventing formation of such a channel. This adds another proposed role to L110 and Phe188 (McCormick and Lippard 2011). Nichol, (2011) mutated Phe188 to the smaller hydrophobic amino acid Ala, which produced a naphthalene positive mutant with a change in enzyme

regioselectivity towards aromatic substrates. Phe188 was also mutated to less hydrophobic residue Trp by Smith and co-workers, which inactivated the enzyme (manuscript in preparation). The rationale from this is to keep the hydrophobicity around the active site and to investigate the role of shorter residue amino acid in allowing the entry of large di- or tri-aromatic compounds to the active site.

Recently, it has been revealed via crystallography of the MMOH-protein B complex that the interaction between MMOH and protein B leads to a change in the conformation of MMOH causing a change in the orientation of residue Phe188. As a result, cavities 1 and 2 become joined leaving a sufficient channel between cavities 2 and 3 to permit gaseous substrates to access the active site (Lee *et al.*, 2013).



## 5.4 Mutants R98L, R98A and R98A S4G

The distance between the protein exterior and the diiron active site in the hydroxylase  $\alpha$ -subunit is about 12 Å (Sazinsky and Lippard 2006). Several cavities are implicated in forming the pathway for substrate entry and for products to leave the hydroxylase active site in the SDIMOs as well as permitting the movement of other moieties which are critical for substrate oxidation namely, electron, proton and molecular oxygen (McCormick and Lippard 2011). In one of the hydrophobic pockets on the way of the substrate into the active site, there is an ionic network which might form a rigid complex that limits the passage of the large molecules into the active site. In a previous work by Smith and co-workers (manuscript in preparation, Lock *et al*), mutant R98L was constructed to disrupt this ionic network. When the mutant R98L was assayed towards the diromatic substrate hydroxyphenyl, there was a change in the regioselectivity of mutated sMMO. Here this mutant was transferred to the new vector pT2MLY with the His-tag. Also, the mutant R98A was constructed, in which the ionic network was disrupted by converting of R98 to alanine, which is a hydrophobic residue with a short side chain. It was hypothesized that this mutant may permit access to the active site by larger di and triaromatic compounds than the R98L mutant. During the construction of R98A, the double mutant R98A S4G was produced due to an unintended second mutation.

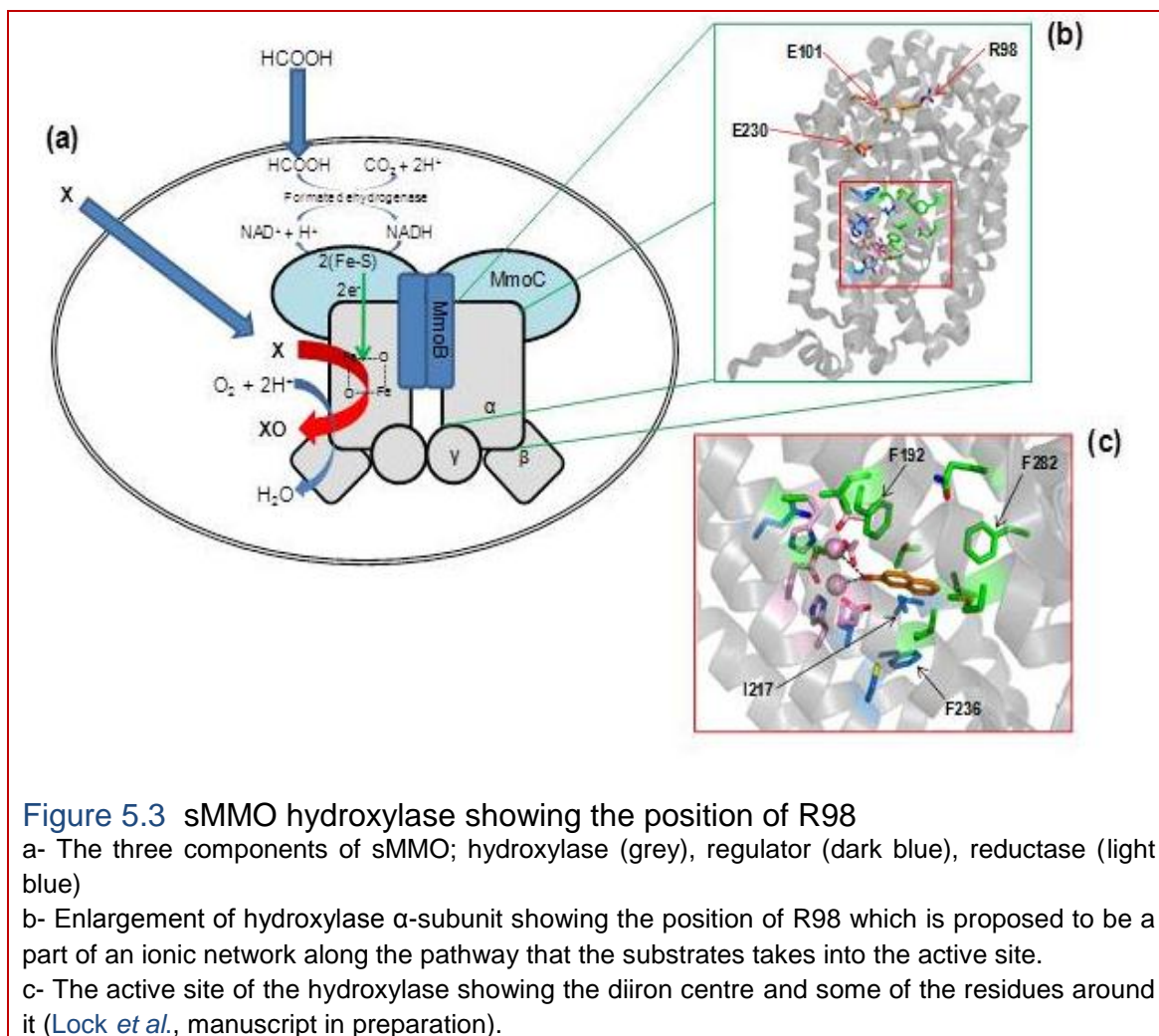


**Figure 5.3** sMMO hydroxylase showing the position of R98

a- The three components of sMMO; hydroxylase (grey), regulator (dark blue), reductase (light blue)

b- Enlargement of hydroxylase  $\alpha$ -subunit showing the position of R98 which is proposed to be a part of an ionic network along the pathway that the substrates takes into the active site.

c- The active site of the hydroxylase showing the diiron centre and some of the residues around it (Lock *et al.*, manuscript in preparation).

#### **5.4.1 Construction and cloning of mutants E114D C151Y, E114D, R98A and R98A S4G using vectors pTJS175 and pT2MLY**

Apart from the double mutant E114D C151Y which was constructed by using pTJS175 C151Y and pT2MLY, the other mutants (E114D, R98A and R98A S4G) were constructed by using pTJS175 and pT2MLY. All mutants were constructed using the four primers as described in Materials and Methods Chapter (Table 2.2).

Two PCRs were run, each one with two primers (the forward flanking primer *mmoX*- p1 with the reverse primer which contains the desired change and the reverse flanking primer *mmoX*- p4 was run with the forward mutation primer as described in Materials and Methods Section 2.3.5.) to create two PCR products; the first round of PCR produced products with approximate size 954 bp and 693 bp for the mutant R98A. In a similar manner, 1002 bp and 645 bp products were obtained from the primary PCRs for mutant E114D (Figure 5.4). The PCR products which are consistent with their predicted size were then purified from the gel to use as a DNA template to run an overlap PCR in the next step. The PCR product was purified before and after the overlap PCR to be ready for the next step.

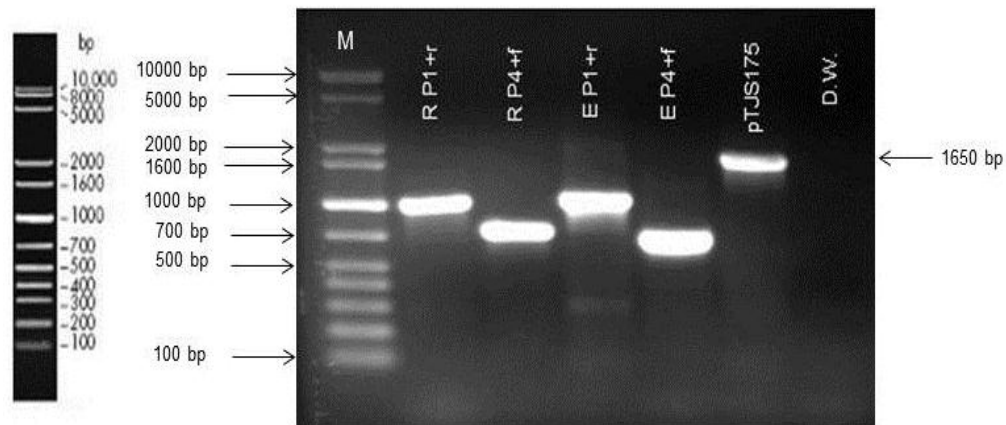


**Figure 5.4** Agarose gel (1%) showing the mutagenic PCRs

Two PCRs were run to construct each mutant, each PCR with two primers; the first PCR was run with one of the flanking forward primer (p1-*mmoX* primer) and a mutagenic reverse primer. The second PCR was run with the reverse flanking primer (p4-*mmoX* primer) and the appropriate forward mutagenic primer which was complementary to the reverse mutagenic primer.

**M**= DNA ladder.

PCR for construction of mutant R98A;

**Rp1+r**= PCR run using p1-*mmoX* forward flanking primer and mutagenic reverse primer (r).

**Rp4+f**= PCR run using p4-*mmoX* reverse flanking primer and mutagenic forward primer (f).

PCR for construction of mutant E114D and E114D C151Y

**Ep1+r**= PCR run using p1-*mmoX* forward flanking primer and mutagenic reverse primer (r).

**Ep4+f**= PCR run using p4-*mmoX* reverse flanking primer and mutagenic forward primer (f).

.

#### 5.4.2 Ligation of mutant *mmoX* genes into pJET 1.2

To achieve the ligation of the *mmoX* gene with pT2MLY, the overlap PCR should be digested with two restriction enzymes *Bam*HI and *Nde*I as mentioned previously. At the same time pT2MLY was digested with the same restriction enzymes and then purified from the gel. The large size of pT2MLY meant that the purified plasmid from the gel was present in only a very small amount which was not enough sometimes for a successful ligation. This caused a substantial challenge; because each time the cloning step failed it was necessary to repeat the overlap PCR and associated sequencing.

This problem was overcome by ligating the overlap PCR product into the high efficiency pJET1.2 cloning vector (Life technology) to produce pYYL1 (include the vector pJET1.2 with the overlap product). The ligation reaction was transformed into laboratory prepared competent *E. coli* S17.1. Colony PCR was performed to detect the putative mutated *mmoX* gene by using primers *mmoX*-p1 and *mmoX*-p4,

The transformed *E. coli* S17.1 which showed a band in the colony PCR with primers *mmoX*-p1 and *mmoX*-p4 was recultured in LB broth with the appropriate antibiotic (ampicillin  $100 \mu\text{g}^{-1} \text{ml}^{-1}$ ). A miniprep was done for the progeny plasmids (pYYL1) isolated from these transformed *E. coli* S17.1, which after digestion with *Bam*HI and *Nde*I revealed fragment of the expected size (~2974 bp) for pJET1.2 and the *mmoX* gene (~1650bp)(data not shown). PCR was performed with primers *mmoX*-p1 and *mmoX*-p4 for *mmoX* gene to confirm its presence in the new plasmid (Figure 5.5C).

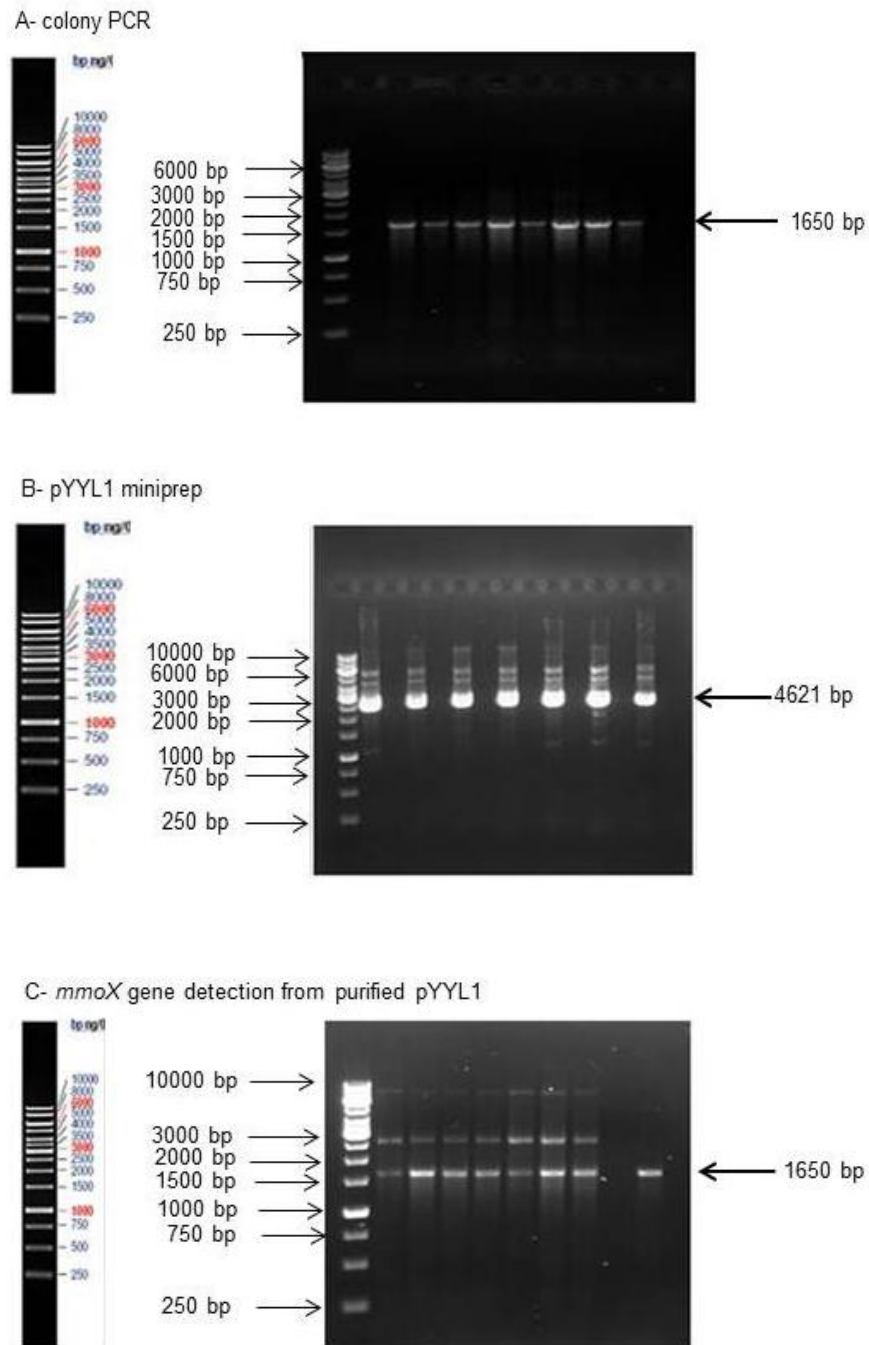


**Figure 5.5** Representative agarose gels (1%) showing cloning steps for the mutated *mmoX* genes in pJET1.2

**Gel A-** After transformation of the plasmid clones containing the R98A mutated *mmoX* genes within pJET 1.2 (pYYL1) into *E.coli* S17.1 competent cells, colony PCR was performed for selected colonies using primers *mmoX*-p1 and *mmoX*-p4. The PCR products were of the expected approximate size (~1650 bp) as shown in gel A.

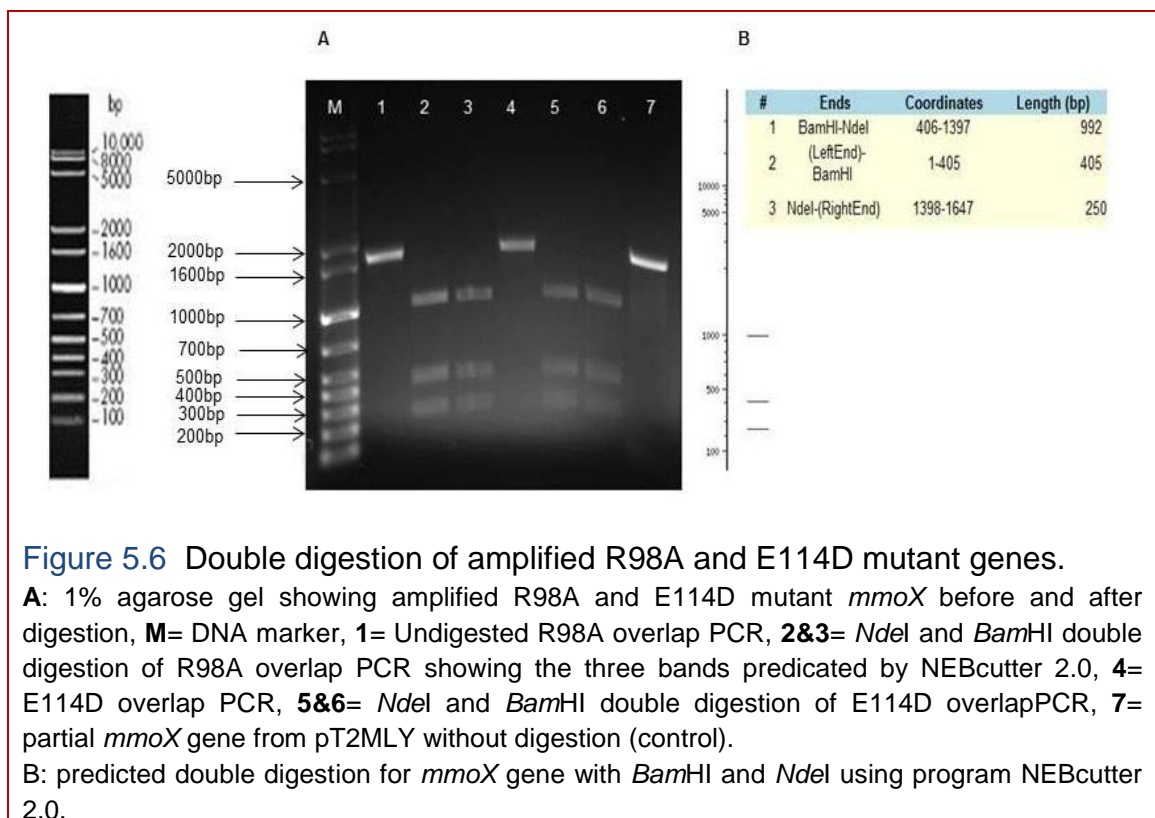
**Gel B-** Plasmid minipreps of the R98A mutant of pYYL1 from the transformed *E.coli* S17.1.

**Gel C-** PCR was performed to detect the mutated *mmoX* genes within the purified pYYL1 clones by using primers *mmoX*-p1 and *mmoX*-p4 which shows products of the expected size for *mmoX* gene.

Similar results were obtained for mutants R98A S4G, E114D, and E114D C151Y.

### 5.4.3 Double digestion of purified mutated *mmoX* gene with *Bam*HI and *Nde*I

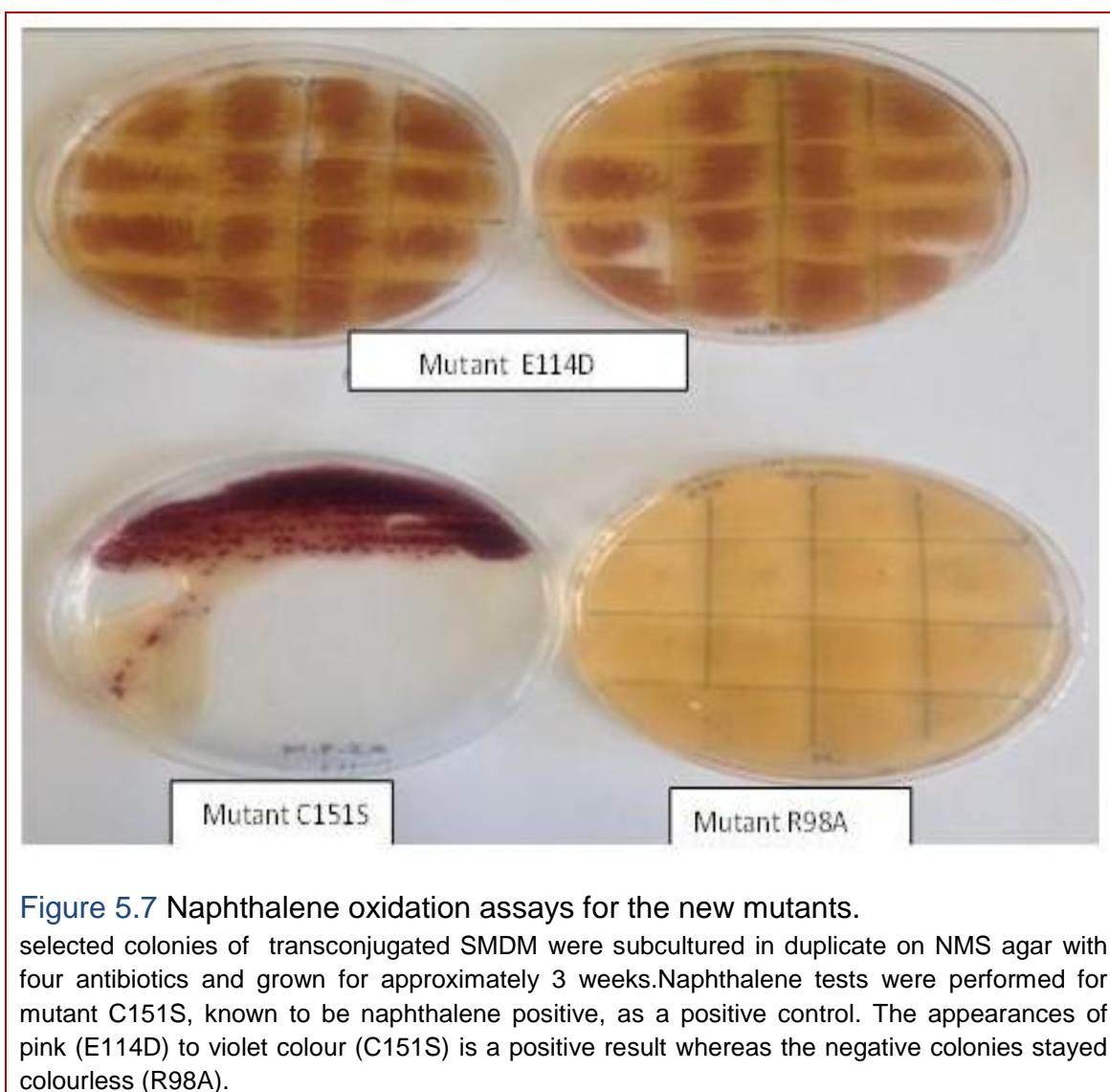
The mutated *mmoX* gene that was amplified from pYYL1 by PCR was gel purified by using the gel extraction kit (Qiagen) and then double digested with *Nde*I and *Bam*HI. The digested PCR product revealed three bands in the gel as intended and as predicted by conceptual digestion using NEB cutter version 2.0. The digested PCR product was compared with undigested PCR product (Figure 5.6 A&B respectively). The desired band which is about 992 bp was then excised from the gel and purified to be ready for ligation in the next step with pT2MLY double digested with the same restriction enzymes *Bam*HI and *Nde*I. The double digestion of pT2MLY was confirmed by the appearance of two bands; one of about 474 bp and the other part of the plasmid which was ~16893 bp.



#### 5.4.4 Cloning of mutant into His-tag expression plasmid pT2MLY

After purification of the band that contained the desired mutation (top band in lane 2, 3, 5, and 6 as shown in (Figure 5.6) from the double digested *mmoX* gene, the purified double digested gene was ligated by using the Quick Instant Ligation Kit (NEB) to pT2MLY that had been digested with same restriction enzymes (*NdeI* and *BamHI*). The ligation reaction was transformed into XL-10 Gold ultra-competent cells as described in the Materials and Methods Chapter, Section 2.4.1. Colony PCR was performed and the resulting plasmid containing the putative mutated gene was purified from the transformants and then sent for sequencing with four primers *mmoX*- p1, *mmoX*- p4, Seq-f and Seq-r (Table 2.2). After the sequence had been confirmed to show that the mutation was found at the intended site for each mutant and that there were no unwanted mutations, the purified mutated plasmids were transferred into *E. coli* S17.1 and then the mutated plasmids transferred from *E. coli* S17.1 into SMDM by conjugation as described in the Materials and Methods Chapter, Section 2.4.2. After growth on methane on NMS agar plates with four antibiotics for three weeks, the mutants were tested towards naphthalene, which gave a positive assay for mutant SMDM pT2MLY E114D and negative for mutants SMDM pT2MLY E114D C151Y and SMDM pT2MLY R98A. Colony PCR was run for the *mmoX* gene and then the PCR product was purified and sent for sequencing. Sequencing showed that SMDM pT2MLY E114D C151Y and SMDM pT2MLY E114D contained the desired mutation alone, whereas the intended R98A mutant contained another unplanned mutation in position 4 to produce a new double mutant SMDM pT2MLY R98A S4G. Construction of the

R98A mutant was repeated to gain the intended single mutant SMDM pT2MLY R98A, which was also negative in the naphthalene test. The mutants were further characterized by growing on NMS media with low copper to induce the production of sMMO, which was then assayed by the naphthalene oxidation plate test again. Positive results were obtained for E114D. E114D C151Y, R98A and R98A S4G were naphthalene negative (Figure 5.7).



The naphthalene negative mutant strains were further characterised by amplifying the *mmoX* gene from purified whole genomic DNA. The *mmoX* genes from all mutants were sequenced to confirm the results. The alignments from BLAST searches performed via the NCBI server (<http://blast.ncbi.nlm.nih.gov/Blast.cgi>) confirmed the presence of the intended mutations. The gene sequences obtained were conceptually translated into protein and the presence of the mutations is shown in alignments of the amino acid sequences below (Figure 5.8)

```

E114D    MAI S LATKAATDALKVNRAPVGVPEPQEVHKKWLQ S FNWDFKENRTKYPTKYHMANETKEQ F
F188W    MAI S LATKAATDALKVNRAPVGVPEPQEVHKKWLQ S FNWDFKENRTKYPTKYHMANETKEQ F
R98L     MAI S LATKAATDALKVNRAPVGVPEPQEVHKKWLQ S FNWDFKENRTKYPTKYHMANETKEQ F
OB3b     MAI S LATKAATDALKVNRAPVGVPEPQEVHKKWLQ S FNWDFKENRTKYPTKYHMANETKEQ F
C151S    MAI S LATKAATDALKVNRAPVGVPEPQEVHKKWLQ S FNWDFKENRTKYPTKYHMANETKEQ F
R98A     MAI S LATKAATDALKVNRAPVGVPEPQEVHKKWLQ S FNWDFKENRTKYPTKYHMANETKEQ F
R98A, S4G MAI G LATKAATDALKVNRAPVGVPEPQEVHKKWLQ S FNWDFKENRTKYPTKYHMANETKEQ F
E114D, C151Y MAI S LATKAATDALKVNRAPVGVPEPQEVHKKWLQ S FNWDFKENRTKYPTKYHMANETKEQ F
**

E114D    KVI AKEYARMEAAKDERQ FGTLLDGLTRLGAGNKVHP RWGETMKVISNFLEVG D YNAIAA
F188W    KVI AKEYARMEAAKDERQ FGTLLDGLTRLGAGNKVHP RWGETMKVISNFLEVG E YNAIAA
R98L     KVI AKEYARMEAAKDERQ FGTLLDGLTRLGAGNKVHP L WGETMKVISNFLEVG E YNAIAA
OB3b     KVI AKEYARMEAAKDERQ FGTLLDGLTRLGAGNKVHP RWGETMKVISNFLEVG E YNAIAA
C151S    KVI AKEYARMEAAKDERQ FGTLLDGLTRLGAGNKVHP RWGETMKVISNFLEVG E YNAIAA
R98A     KVI AKEYARMEAAKDERQ FGTLLDGLTRLGAGNKVHP A WGETMKVISNFLEVG E YNAIAA
R98A, S4G KVI AKEYARMEAAKDERQ FGTLLDGLTRLGAGNKVHP A WGETMKVISNFLEVG E YNAIAA
E114D, C51Y KVI AKEYARMEAAKDERQ FGTLLDGLTRLGAGNKVHP R WGETMKVISNFLEVG E YNAIAA
**

E114D    SAM L WDSATAAEQ KNGYLAQV LDEIRH THQ C AFINHYYSKHYHDPAGHNDARRTRAIGPL
F188W    SAM L WDSATAAEQ KNGYLAQV LDEIRH THQ C AFINHYYSKHYHDPAGHNDARRTRAIGPL
R98L     SAM L WDSATAAEQ KNGYLAQV LDEIRH THQ C AFINHYYSKHYHDPAGHNDARRTRAIGPL
OB3b     SAM L WDSATAAEQ KNGYLAQV LDEIRH THQ C AFINHYYSKHYHDPAGHNDARRTRAIGPL
C151S    SAM L WDSATAAEQ KNGYLAQV LDEIRH THQ S AFINHYYSKHYHDPAGHNDARRTRAIGPL
R98A     SAM L WDSATAAEQ KNGYLAQV LDEIRH THQ C AFINHYYSKHYHDPAGHNDARRTRAIGPL
R98A, S4G SAM L WDSATAAEQ KNGYLAQV LDEIRH THQ C AFINHYYSKHYHDPAGHNDARRTRAIGPL
E114D, C151Y SAM L WDSATAAEQ KNGYLAQV LDEIRH THQ Y AFINHYYSKHYHDPAGHNDARRTRAIGPL
**

E114D    WKG M KRV F A DGFISGDAVECSVNLQ LVGEACFTNPLIVAVTEWASANGDEITPTVFLSVE
F188W    WKG M KRV F A DGFISGDAVECSVNLQ LVGEACFTNPLIVAVTEWASANGDEITPTVFLSVE
R98L     WKG M KRV F A DGFISGDAVECSVNLQ LVGEACFTNPLIVAVTEWASANGDEITPTVFLSVE
OB3b     WKG M KRV F A DGFISGDAVECSVNLQ LVGEACFTNPLIVAVTEWASANGDEITPTVFLSVE
C151S    WKG M KRV F A DGFISGDAVECSVNLQ LVGEACFTNPLIVAVTEWASANGDEITPTVFLSVE
R98A     WKG M KRV F A DGFISGDAVECSVNLQ LVGEACFTNPLIVAVTEWASANGDEITPTVFLSVE
R98A, S4G WKG M KRV F A DGFISGDAVECSVNLQ LVGEACFTNPLIVAVTEWASANGDEITPTVFLSVE
E114D, C151Y WKG M KRV F A DGFISGDAVECSVNLQ LVGEACFTNPLIVAVTEWASANGDEITPTVFLSVE
**

```

**Figure 5.8** Deduced sequences of amino acid for the new mutants compared to the wild type OB3b and mutant C151S.

Black colour: the sequence of the wild type *mmoX*. Mutagenized positions are shown in orange type and indicated by two stars with the original amino acid shown in red type.

#### 5.4.5 Purification of His-tagged mutant hydroxylases

The soluble extracts which were obtained by means of the French pressure disrupter (part of which were loaded onto SDS-PAGE as shown in [Figure 5.9](#)) were loaded onto Ni-NTA columns and purified by following the steps described in Materials and Methods Chapter Section (2.6.2.2). The soluble extract and the purified His-tagged hydroxylases were analysed via 12% or 16% SDS-PAGE prepared as described Section 2.8. Chapter 2. The gel for the soluble extracts and the purified hydroxylase revealed an almost identical banding pattern to the wild type; with three bands for the purified hydroxylase corresponding to the three hydroxylase subunits  $\alpha$ ,  $\beta$ , and  $\gamma$  for the wild type and each of the mutants as shown in ([Figure 5.9](#)). Mutant E114D was grown on NMS plates with three antibiotics; streptomycin, spectinomycin and gentamycin with a thick streaking to gain enough biomass for the subsequent experiments. In addition to showing three bands in the SDS-PAGE referring to the hydroxylase subunits, there was a fourth band which can be seen in almost all samples. The purification and detection of hydroxylase subunits was performed alongside C151S and His-tag wild type as positive controls.

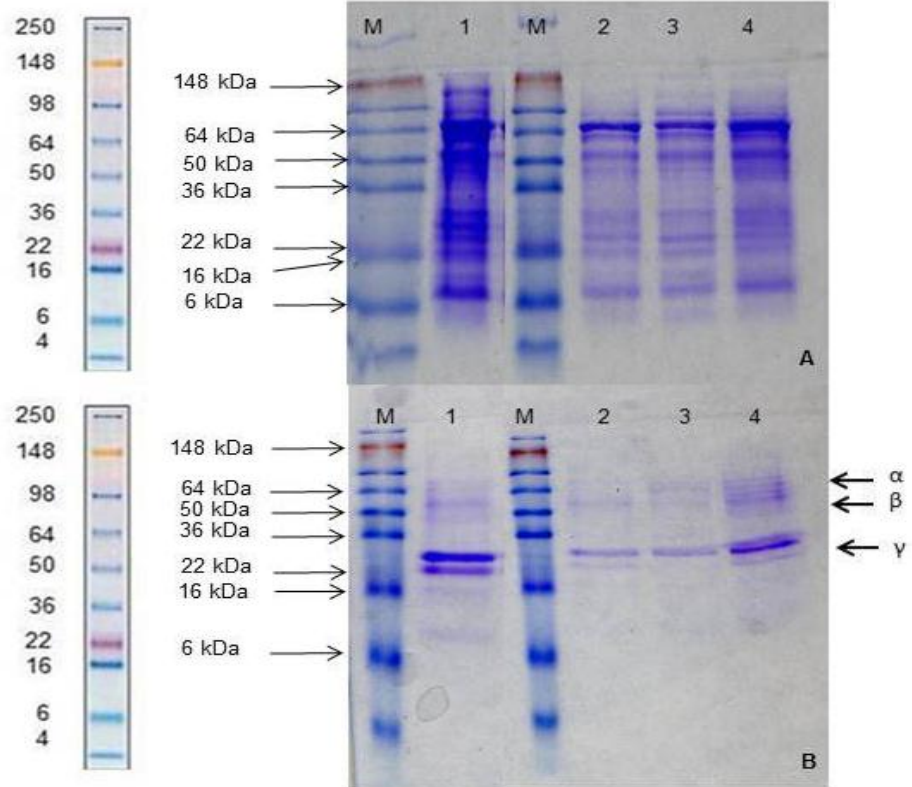


**Figure 5.9** The soluble extract and purified His-tagged hydroxylase from the mutants E114D and E114D C151Y compared to the His-tagged wild type and C151S mutant hydroxylases.

**Gel A:** Soluble extract from mutants E114D and E114D C151Y showing nearly identical banding patterns to one another and to the His-tagged wild type and mutant C151S.

**Gel B:** Purified His-tagged MMOH from the wild type and mutants shown in gel A. Each preparation showed three main bands corresponding to the  $\alpha$ -,  $\beta$ - and  $\gamma$ - subunits of the hydroxylase in addition to a fourth faint band. Both gels are 12% SDS-PAGE in buffer tris-glycine.

The order of the lanes is the same in both gels as follows: **M**= SeeBlue® plus2 pre-stained protein standard, **lane 1**=His-tagged wild type, **lane 2**= C151S, **lane 3**=C151Y E114D, **lane 4**= E114D

#### **5.4.6 No detectable naphthalene product in GC-MS for naphthalene positive E114D on NMS plates**

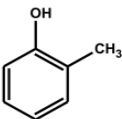
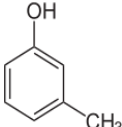
When the E114D mutant was tested for the oxidation of naphthalene on an NMS plate with three antibiotics; streptomycin, spectinomycin and gentamycin, it showed a positive result as explained previously (5.4.4). The E114D methanotroph strain expressing the mutant sMMO was then grown to high cell density on an NMS agar plate with three antibiotics with dense streaking of the bacteria on the whole area of plate. Then after switching from pMMO to sMMO, which was detected by the naphthalene oxidation assay on an NMS plate, the cells were harvested and resuspended in 25 mM MOPS pH 7.0 and kept at -80°C. Frozen cells were thawed and tested with naphthalene as the substrate and the products were analysed via GC-MS, which showed no recognizable peaks corresponding to either of the possible products from naphthalene monooxygenation (1-naphthol or 2-naphthol), even though the same strain was positive for the naphthalene oxidation when evaluated via the plate colorimetric test. Extending the incubation period from 48 h to 72 h and 96 h did not result in appearance of any products detectable via GC-MS (data not shown).

#### **5.4.7 Oxidation of toluene by the E114D mutant**

When the mono-aromatic compound toluene is used as a substrate to be oxidized by sMMO, hydroxylation can occur on three distinct positions on the ring or on the side chain. In the current study, when the toluene was oxidized for 48 h at 30°C by OB3b or the His-tagged wild type MMOH, the hydroxylation

was ring hydroxylation with no benzyl alcohol whereas *o*-cresol was the main product followed by *p*-cresol and *m*-cresol in a very small amount. When the E114D mutant was tested towards toluene, *p*-cresol was the only product observed with small activity. When the amounts of the products in the triplicate samples of the mutant E114D, wild type OB3b and His-tagged wild type hydroxylase were compared, there was no significant difference between them ( [Table 5.1](#)). When the assay was repeated using a different batch of E114D mutant cells, no measurable activity was found

**Table 5.1** Distribution of toluene oxidation products by E114D compared to OB3b and His-tag wild type.

Strains	Product percentage %		
	 <i>p</i> -cresol	 <i>o</i> -cresol	 <i>m</i> -cresol
OB3b	3.28%	96.70%	0.01%
wt his-tag	2.33%	97.64%	0.02%
E114D	100%	ND	ND

Oxidation of toluene by His-tagged wild type hydroxylase and mutant sMMO-expressing cells, monitored by GC-MS. Peaks were assigned using the NIST list in the PC connected to the GC-MS. ND indicates no detectable activity. The retention times for the peaks were also compared to authentic standards of the products. The OD<sub>600</sub> was corrected to 5 for all of the tested strains.

#### 5.4.8 E114D produced 1-phenyl ethanol from ethyl benzene

The mutant E114D was tested towards the monoaromatic hydrocarbon ethyl benzene in a reaction for 48 h at 30°C. Among the possible products from ring oxidation, only one product, 4-ethyl phenol was observed, whereas the oxidation of the side chain gave the compounds 4-methylbenzaldehyde, phenyl methyl ketone, and 1-phenyl ethanol. The wild type strain OB3b oxidized ethyl benzene giving the same 4 compounds mentioned above; 1-phenyl ethanol, phenyl methyl ketone, 4-methylbenzaldehyde and 4-ethyl phenol, with 4-ethyl phenol as the major product followed by 1- phenyl ethanol, 4-methylbenzaldehyde and then phenyl methyl ketone. The wild type with His-tag hydroxylase produced 4-ethyl phenol as the major product whereas 4-methylbenzaldehyde and 1-phenyl ethanol were produced in almost equal smaller amounts (Table 5.2). Ethyl benzene was oxidized to ethyl phenol as the major product and both 1-phenyl ethanol and 4-methylbenzaldehyde in nearly equal amounts. Phenyl methyl ketone was not detected as a product from ethyl benzene oxidation by the His-tagged wild type. Mutant E114D gave 1-phenyl ethanol as the sole detectable product from ethyl benzene oxidation with a low activity compared to the wild type OB3b and His-tagged wild type (Table 5.2). No statistically significant difference was observed among the mutant E114D, the wild type OB3b and wild type with His-tag hydroxylase. As stated previously, all assays were performed in triplicate.

**Table 5.2** Oxidation of ethyl benzene by mutant E114D, compared to the wild type OB3b and wild type with His-tagged hydroxylase.

Strain	Percent of products %				Relative activity %
	1-phenyl ethanol	phenyl methyl keton	4-methylbenzaldehyde	4-Ethyl phenol	1-phenyl ethanol
OB3b	9.81%	1.59%	4.04%	84.54%	100%
His-tag wt	13.57%	ND	13.78%	72.63%	13.59%
E114D	100%	ND	ND	ND	6.38%

Ethyl benzene oxidation products were identified on the trace from the GC-MS by comparison with the NIST list (1  $\mu$ l from the extraction was injected and analysed for each strain).

ND: indicates that no product could be detected in the the extraction when analysed on the GC-MS. Relative activity was obtained from technical triplicates from the same batch of frozen cell of strains compared to the activity of the wild type OB3b which was considered as 100% active and the OD<sub>600</sub> was corrected to 5

#### **5.4.9 Mutant E114D showed no activity towards the di-aromatic or tri-aromatic substrates in GC assays.**

Mutant E114D was also tested towards the diaromatic hydrocarbon biphenyl for 48 h at 30 °C and the result was analysed in GC-MS as detailed in the Materials and Methods Chapter (Section 2.6.6). All mutants in the present study, R98L, E114D, wild type OB3b and the His-tagged wild type hydroxylase (including C151S which was explained in Chapter 4), showed no activity that could be detected in GC-MS towards biphenyl even when the mutants, the wild type OB3b and His-tag wild type incubated with the substrate for longer time; 72 h and 96 h instead of 48 h. The mutant E114D was also assayed with the tri-aromatic hydrocarbons anthracene and phenanthrene, which also revealed the

mutant as non-active in towards these substrates. Control experiments were performed to compare the wild type OB3b and the His-tag wild type to the mutant. As observed previously, results for the wild type and the His-tag wild type were also negative towards these tri-aromatic substrates anthracene and phenanthrene.

## **5.5 Transformation of *E. coli* S17.1 with pT2MLY F188W and R98L and then conjugation with *Ms. trichosporium* SMDM**

Plasmids pT2MLY F188W and pT2MLY R98L were constructed by Dr. M. Lock in this research group. During the current study, the plasmids were sequenced to confirm the existence of the desired mutation within both of them and the absence of unwanted mutations. *E. coli* S17.1 were then transformed with pT2MLY F188W and pT2MLY R98L. Then the transformed *E. coli* S17.1 pT2MLY F188W and *E. coli* S17.1 pT2MLY R98L were conjugated with SMDM. A positive naphthalene test confirmed the activity of the His-tagged R98L mutant when expressed in the methanotroph. Total genomic DNA was extracted and PCR was performed with primers *mmoX*- p1 and *mmoX*- p4 to detect the *mmoX* gene. The purified amplified *mmoX* gene was sequenced, which revealed the desired mutation at position 98. After a naphthalene negative result for the F188W mutant, the conjugation was repeated three times. After that the whole genomic DNA was extracted and the *mmoX* gene was detected in mutant F188W by PCR with *mmoX*- p1 and *mmoX*- p4 (Figure 5.10). The PCR product was then sequenced and the mutation was observed at the intended site.

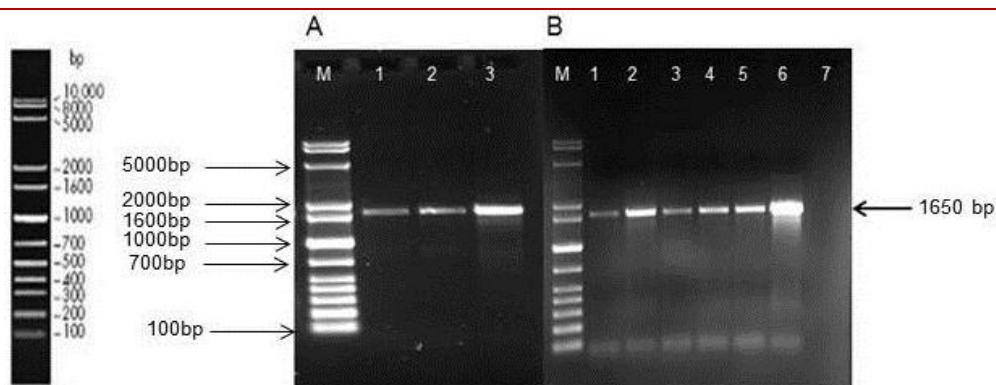


**Figure 5.10** Detection of *mmoX* gene in R98L and F188W methanotrophs exconjugants.

**Gel A:**

**M**= DNA ladder. **Lane 1&2**=PCR amplification of the *mmoX* gene from the R98L exconjugant using primers *mmoX*- p1 and *mmoX*- p4. **Lane 3**= pTJS175 plasmid DNA (positive control).

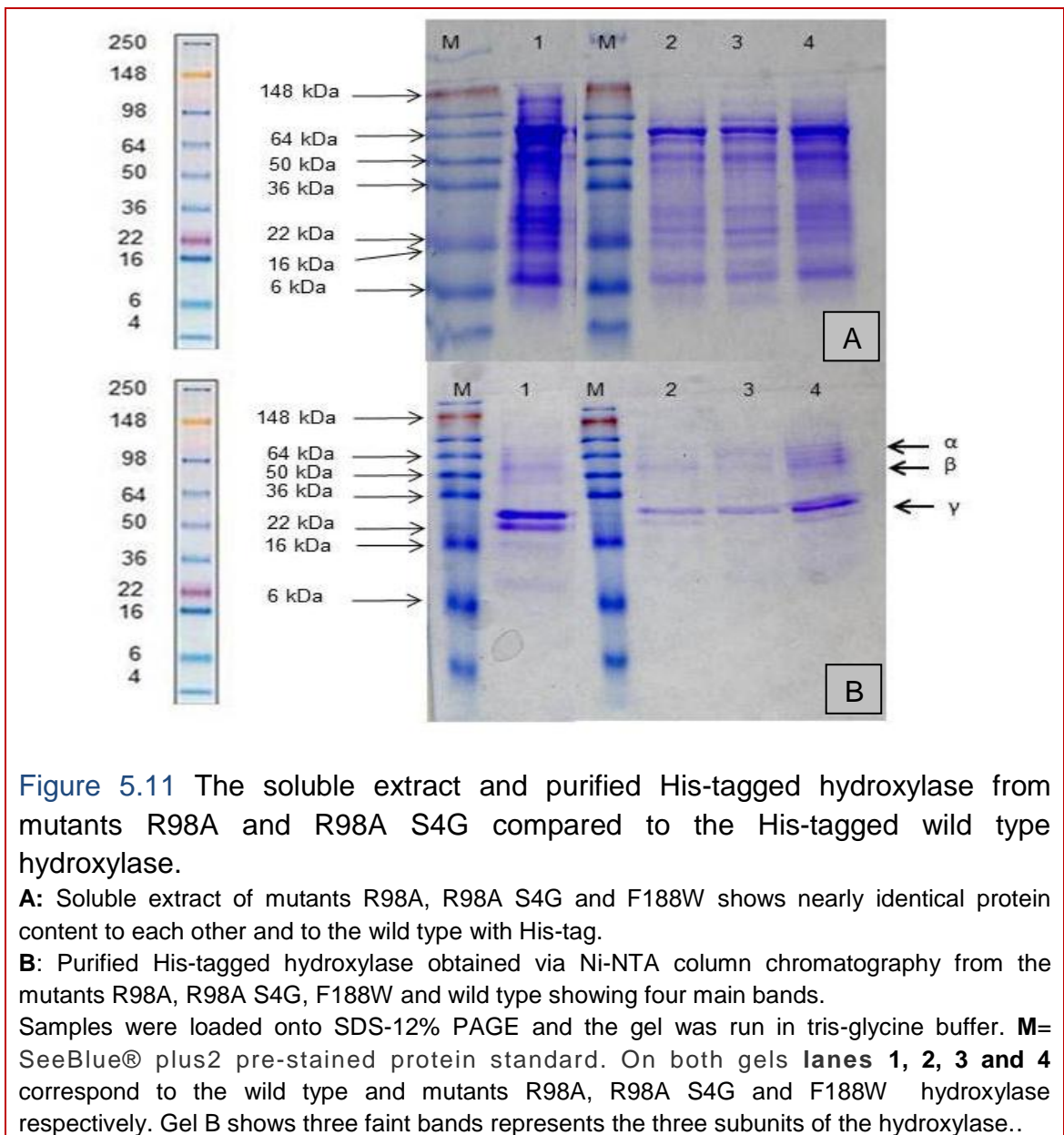
**Gel B:**

**M**=DNA ladder. **Lane 1-5**= PCR amplification of the *mmoX* gene from the F188W exconjugant using primers *mmoX*- p1 and *mmoX*- p4. **Lane 6**= pTJS 175 plasmid DNA (positive control), **7**= No DNA template (negative control).

### 5.5.1 Purification of the His-tag hydroxylase from mutants R98A and R98A S4G.

The naphthalene negative mutants were further characterized by *mmoX* gene detection PCR using primers; *mmoX*- p1 and *mmoX*- p4. The PCR products were excised and purified from an agarose gel and then sent for sequencing. The results from sequencing confirmed the change of Arg to Ala in the mutant R98A in addition to Ser to Gly change at position 4 for the double mutant R98A S4G. The mutants were grown in flask cultures with four antibiotics. After three weeks the harvested cells were broken to release the proteins. The soluble extract was prepared and samples loaded onto SDS-PAGE and the rest was loaded onto an Ni-NTA column. The purified His-tagged hydroxylase was also

loaded into 12% or 16% SDS-PAGE prepared as described in Materials and Methods Chapter. The His-tagged MMOH for each of the three His-tagged mutants R98A, R98A S4G, and F188W as well as the His-tag wild type each contained three bands corresponding to the three hydroxylase subunits  $\alpha$ ,  $\beta$ , and  $\gamma$  in addition to the fourth band explained previously (Figure 5.11).



## 5.5.2 Oxidation of naphthalene by mutant R98L and product distribution

The R98L mutant was tested for oxidation of naphthalene on an NMS plate with four antibiotics. Since the result was positive on the colorimetric plate test, the whole cell suspension was incubated with a few naphthalene crystals as described in the Materials and Methods Chapter (Section 2.6.4.). The ability of this mutant to oxidize naphthalene was assayed after incubation for 48 h at 30°C with naphthalene. The result from the GC-MS trace showed that there are two peaks corresponding to 1-naphthol and 2-naphthol, as was shown for the wild type OB3b and His-tag wild type. The R98L mutant produced more 1-naphthol than 2-naphthol in a ratio more similar to that produced by the His-tag wild type than that from the wild type OB3b (Table 5.3). When the original data for the triplicate samples for R98L were compared to the wild type OB3b and the His-tag wild type, no statistically significant difference was observed between them ( $p > 0.05$ ) by using Kruskal-Wallis (Conover-Inman) test.

**Table 5.3** Oxidation of naphthalene by mutant R98L and product distribution percentages.

Strain	Product percentage		Relative activity %	
	1-Naphthol	2-Naphthol	1-Naphthol	2-Naphthol
OB3b	85.23%	14.76%	100%	100%
wt. His-tag	57.64%	42.35%	155.77%	177.18%
R98L	57.86%	42.13%	61.88%	75.64%

The assays were performed in the same day. The retention time for the products was compared with authentic standards, and the identification confirmed by NIST list in the GC-MS. Relative activity was obtained from triplicate samples from the same batch of frozen cells of each strain and compared to the activity of the wild type OB3b. The relative activities are corrected to  $OD_{600} = 5$  for all samples.

### 5.5.3 Oxidation of ethyl benzene by the R98L mutant results in increased activity.

The activity for the whole cells of R98L towards the mono-aromatic substrate ethyl benzene was evaluated in a reaction mixture with ethyl benzene for 48 h at 30°C and then the extracted product was analysed via GC-MS. The result showed that the mutant, like the wild type, hydroxylated the ethyl benzene primarily on the ring. Oxidation of ethyl benzene showed that 4-ethyl phenol is the main product but with less activity than OB3b and His-tagged wild type. Some oxidation of the side chain by R98L was observed, producing 4-methylbenzaldehyde with an activity 7 times more than OB3b and 2 times more than the His-tag wild type. The other product from the side chain oxidation was 1-phenyl ethanol with a comparable product percentage to the wild type OB3b and less than the His-tag wild type. Finally, the fourth product was phenyl methyl ketone, which was detected in smaller relative amount compared to the OB3b (Table 5.4; Figure 5.12). The raw data for the triplicate samples for each of mutant R98L with OB3b and the His-tag were compared. The result showed that R98L produced 1-phenyl ethanol 13.3 times more than the His-tag wild type and 1.8 more than wild type OB3b. Although the product phenylmethyl ketone was not detected for the His-tagged wild type, the amount of this product from the R98L mutant was higher than the wild type OB3b by 1.6-fold. Also the R98L mutant oxidized the ethyl benzene to 4-methylbenzaldehyde with 6.2-fold greater yield than the His-tagged wild type and 2-fold more than OB3b. In contrast, the highest increase in yield was found in the oxidation of ethyl benzene to ethyl phenol with a 14-fold greater yield from mutant R98L than the His-tag wild type and 1.2-fold more than OB3b. However, there is no statistically

significant difference between mutant R98L compared to the wild type OB3b and His-tagged wild type when Kruskal-Wallis (Conover-Inman) test was applied to compare between them for all four products from ethyl benzene oxidation (Figure 5.13).

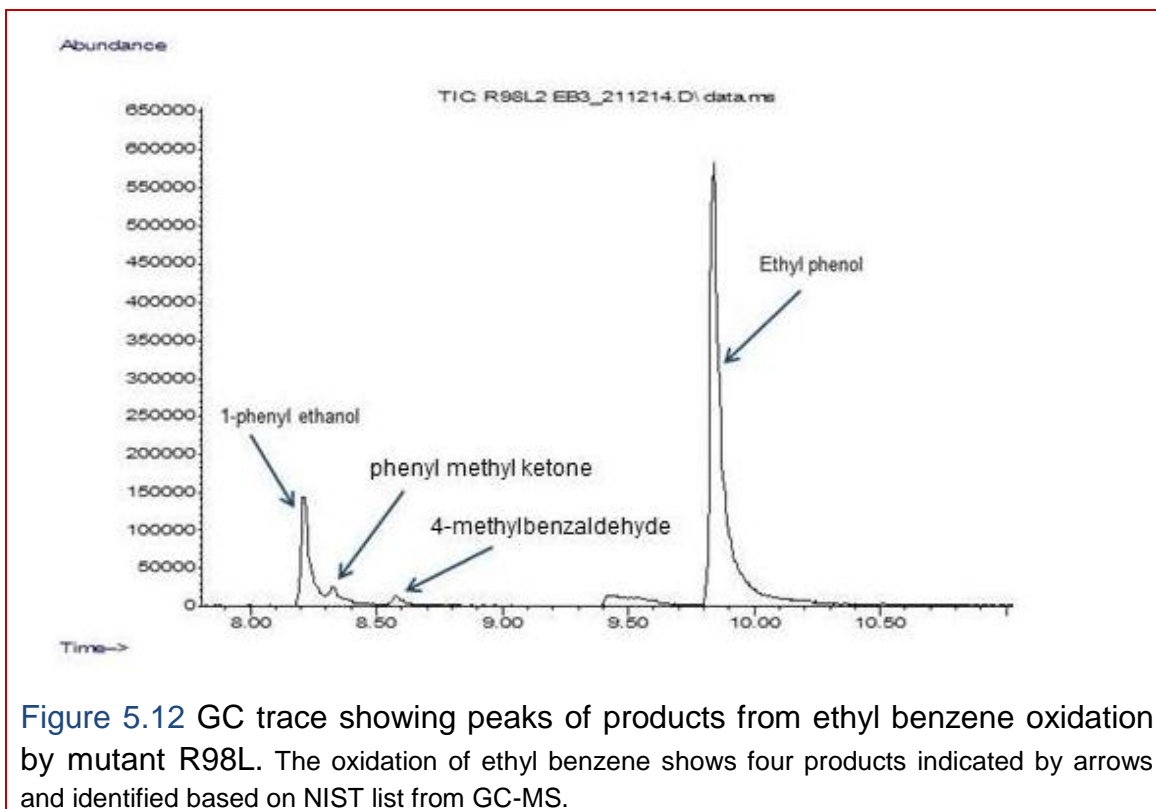


Figure 5.12 GC trace showing peaks of products from ethyl benzene oxidation by mutant R98L. The oxidation of ethyl benzene shows four products indicated by arrows and identified based on NIST list from GC-MS.

**Table 5.4** Distribution of products from ethyl benzene oxidation by OB3b, wild type with His-tagged hydroxylase and mutant R98L.

Strain	distribution of products %				Relative activity %			
	1-phenyl ethanol	phenyl methyl ketone	4-methylbenzaldehyde	4-Ethyl phenol	1-phenyl ethanol	phenyl methyl ketone	4-methylbenzaldehyde	4-Ethyl phenol
OB3b	9.81%	1.59%	4.04%	84.54%	100%	100%	100%	100%
His-tag wt	13.57%	ND	13.78%	72.63%	13.5%	ND	ND	8.63%
R98L	9.16%	1.23%	38.23%	51.36%	181.88%	83.98%	177.11%	121.05%

ND: indicates no detectable activity peak in GC-MS for specific product. The distribution of products shows the amount of each product as a percentage of total product produced by each strain. Compounds were compared to NIST list in the GC-MS. The relative activity was calculated by considering the activity for wild type OB3b as 100% active. The results were obtained from triplicate technical samples from the same batch of frozen cells for each strain and the OD<sub>600</sub> was corrected to 5.

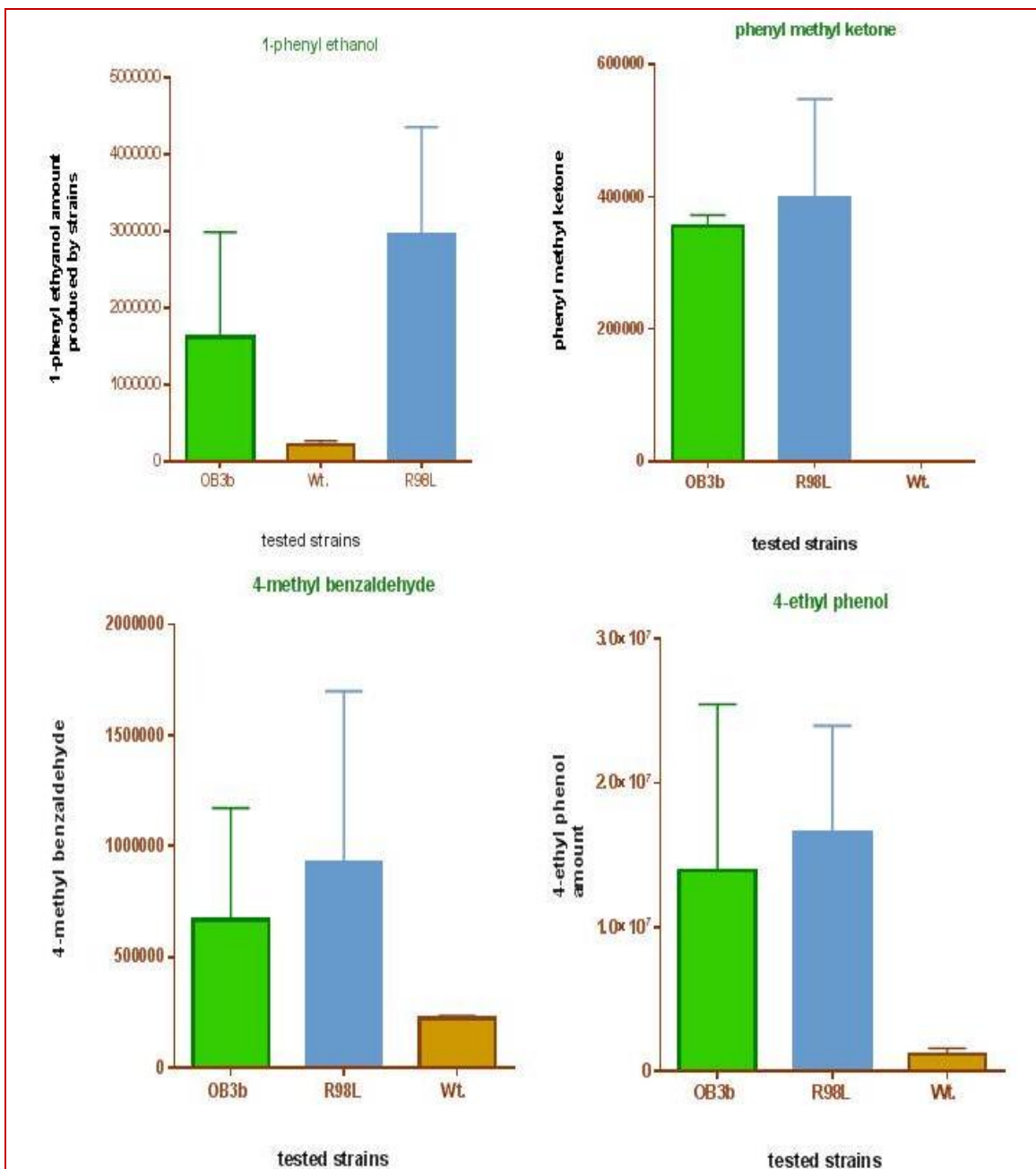


Figure 5.13 Comparing the original data for triplicate technical samples for mutants R98L with OB3b and wild type with His-tagged hydroxylase. No significant difference at level  $p < 0.05$  was detected among mutant R98L, OB3b and the wild type with His-tagged hydroxylase in product distribution from ethyl benzene oxidation. The original data were analysed via the Kruskal-Wallis statistical test (Conover-Inman) and data presented as (Mean  $\pm$  S.E.M.). The amounts of products were obtained by measuring the product peak areas from the GC-MS traces.

#### **5.5.4 No recognizable activity could be seen for R98L towards the tri-aromatic compound anthracene or phenanthrene**

The ability for the whole cells of the R98L mutant to oxidize tri-aromatic substrates was investigated by using anthracene and phenanthrene as a candidate substrates over 48 h at 30°C. Although R98L showed activity towards many substrates, similar to OB3b and His-tagged wild type, no detectable peak likely to indicate oxidation products of either phenanthrene or anthracene could be detected when the extracted assay reaction was injected onto the GC-MS.

## **5.6 Discussion**

### **5.6.1 Sequential ligation by using two plasmids for the mutated overlap PCR**

After constructing the overlap PCR by using high fidelity Phusion *Taq* polymerase to create the new mutants, sequential ligation was used. The overlapped PCR product firstly was ligated into a commercial plasmid pJET 1.2 to produce pYYL1. The mutated *mmoX* genes were sequenced after this cloning step to check for unwanted (PCR -derived) mutations. Working with a complex shuttle and expression vector with a very large size of more than 17 kb makes cloning of mutant genes a challenge, especially during the purification of such a large plasmid from gel electrophoresis after digestion with restriction enzymes. The pJET 1.2 was used in the present study to clone the overlap PCR product before transfer into the expression vector. This two step sequential cloning procedure was necessary, since cloning a low abundance combinatorial PCR product into a large vector did not give a high enough frequency of recombinants to be practicable. Cloning via pJET 1.2 allowed preparation of a large amount of the insert to gain a tolerable cloning frequency with the large plasmid.

### **5.6.2 Mutation of C151Y mutant to double mutant E114D C151Y**

In a previous study ([Smith \*et al.\*, 2002](#)) the amino acid cysteine 151 was mutated into tyrosine as in ribonucleotide reductase (RNR). The tyrosine at this position is known to provide a free radical required by RNR. The mutant C151Y

lost its activity due to forming an unstable hydroxylase. It was proposed that the mutation of the glutamic acid residue at site 114 to aspartic acid as in ribonucleotide reductase may result in stabilizing the hydroxylase by replacing the Glu with an amino acid with smaller side chain to give more space for Tyr. In the present study it was found that mutation of the glutamic acid 114 into aspartic acid in the mutant C151Y resulted in a more stable protein that could be visualized on SDS-PAGE. The mutant C151Y E114D was constructed within the system pT2MLY to allow purification by using a His-tag affinity column. The mutated C151Y E114D MMOH was purified in the present study by using the His-tag affinity column and was shown to be present via SDS-PAGE. The SDS-PAGE revealed that MMOH contains all three subunits but the cell expressing the mutant enzyme had no activity towards naphthalene. The presence of Cys 151, Thr 213 and Ile 217 in sMMO around the diiron centre instead of Tyr122, Phe208 and Phe212 in RNR enzyme may make sMMO able to accommodate larger substrates than RNR (Nordlund *et al.*, 1992). Replacing the cysteine at 151 with tyrosine might make the active site too narrow to accept di-aromatic substrates such as naphthalene.

### **5.6.3 Mutation of glutamic acid 114 to aspartic acid (mutant E114D)**

The single mutant E114D was created in this site by using the system pT2MLY. The oxidation of methane or the other substrates by MMOH is catalysed by the carboxylate-bridged dinuclear iron centre (Whittington *et al.*, 2001). It has been seen that there is a carboxylate shift during the oxidation and reduction of the diiron centre during the catalytic cycle of the enzyme. This shift may have an

important role in the enzyme mechanism; also the oxygen-rich area around the active site in MMOH is implicated in having a critical role by building a high-valent iron intermediate during the enzyme catalytic cycle (Lee *et al.*, 1993; Liu *et al.*, 1994; Liu *et al.*, 1995; Lee *et al.*, 1999; Shu *et al.*, 1997). These facts and crystallographic studies support the importance of the presence of residues such as glutamate to ligate the diiron centre (Whittington *et al.*, 2001). The mutation E114D in the current study was designed in order to introduce a change into the residues ligating the diiron centre whilst retaining the carboxylate group at this position. The shorter side chain of aspartic acid, compared with glutamic acid, might affect the way that the active site holds the substrate by changing in the geometry around the diiron centre. The mutant E114D was naphthalene positive unlike E114D C151Y, but the colour of the complex formed between the diazonium salt and the naphthol products was not as strong as it is for the wild type or mutant C151S as positive controls (Figure 5.7). The inactive mutant R98A was used as a negative control. When cells expressing the mutant E114D were assayed with naphthalene as the substrate, and the sample was analysed by GC-MS after solvent extraction, no peak could be seen in the GC-MS corresponding to 1- or 2-naphthol. This may be because this mutant oxidized the naphthalene to an unstable product or the amount of the naphthol product was not enough to be detected by GC-MS. The main and the only product from oxidation of toluene by this mutant was *p*-cresol.. The oxidation of another substituted mono-aromatic compound ethyl benzene by the E114D mutant showed only one product 1-phenyl ethanol with low activity. The detection of the single product from toluene and ethyl benzene may indicate that this mutant has increased regioselectivity with these

substrates. Alternatively, the amount of these products may be too small to detect or the product may be further oxidized.

This mutant showed no activity toward the more complex tri-aromatic compounds such as anthracene and phenanthrene which are not oxidized by the wild type OB3b or other studied sMMO mutants which may be due to the toxicity of these compounds for the bacteria.

#### **5.6.4 Activity of transconjugated R98L, F188W, R98A and R98A S4G**

A previous study was performed on mutant R98L ([Lock \*et al.\*, manuscript in preparation](#)) to investigate the effect of this mutation on the way that the substrate interacts with the active site. The mutant F188W was constructed in the same study. These mutants were subsequently transferred into the new expression system pT2MLY (personal communication with Nicol, Lock and Smith) and then cloned in *E. coli* (as part of the work described in this thesis) conjugated into the *Ms. trichosporium* SMDM expression host to further investigate these residues with the His-tag affinity system. In the previous study by this group, R98L showed a higher activity than OB3b towards toluene and an increase in regioselectivity towards biphenyl at the 4-position. A similar result was obtained in the current study; R98L showed an increased regioselectivity toward ethyl benzene with a greater proportion of 4-methylbenzaldehyde being produced than with the wild type OB3b and His-tag recombinant wild type. The present study showed that R98L was able to oxidise ethyl benzene to produce 13.3-fold more 1-phenyl ethanol than the His-tagged wild type. Also, from the

oxidation of ethyl benzene, mutant R98L was able to produce 4-ethyl phenol and 4-methylbenzaldehyde in 6.2-fold and 14-fold, respectively, greater yield than the His-tagged wild type. With naphthalene as the substrate, the R98L mutant gave a more similar percentage of 1- and 2- naphthol to that produced by the His-tag wild type than was observed with the original wild type strain *Ms. trichosporium* OB3b. The tri-aromatic compounds anthracene and phenanthrene appear to be too large to enter the active site for this mutant. The changing of Arg to Leu at position 98 may limit the entry of large substrate into the active site. An amino acid with a smaller side chain such as Leu is expected to change the nature of the ion network which may allow the substrate to enter and be held in the active site in a different way from the wild type OB3b. This effect might be seen more clearly when the Arg98 was mutated to Ala, which was done with the intention of increasing the space in the route of the substrate into the active site. Changing Arg98 to a smaller uncharged residue may result in a complete disruption to this ion network leading to a conformational change in the protein geometry. The result was an inactive mutant enzyme when it was tested towards naphthalene. In terms of the unintended double mutant R98A S4G, there is no clear role for the amino acid Ser at the beginning of the  $\alpha$ -subunit of the hydroxylase in the enzyme activity; as such it is suggested that there is no substantial effect of the presence of the second mutation for mutant R98A S4G (Figure 5.14).

The phenylalanine 188 is implicated in formation of the hydrophobicity layer around the active site. Unlike F188A which was constructed in a previous study (Nichol, 2011) and gave a positive naphthalene test in addition to showing some change in regioselectivity, mutation of phenylalanine 188 to the less hydrophobic though bulkier tryptophan resulted in an inactive enzyme when

tested with naphthalene. Crystallographic studies suggested a critical role for this residue in opening and closing the cavities around the active site with the aid of L110 (Rosenzweig *et al.*, 1997). It was also noticed that when protein B attached to the hydroxylase this led to changes in the orientation of F188 resulting in rearrangement of the helices within the enzyme and opening of cavities 1 and 2 to accommodate substrates (Lee *et al.*, 2013). This mutant needs to be tested further towards aliphatic substrates as it showed a stable hydroxylase exhibiting all three subunits in SDS-PAGE (Figure 5.11)

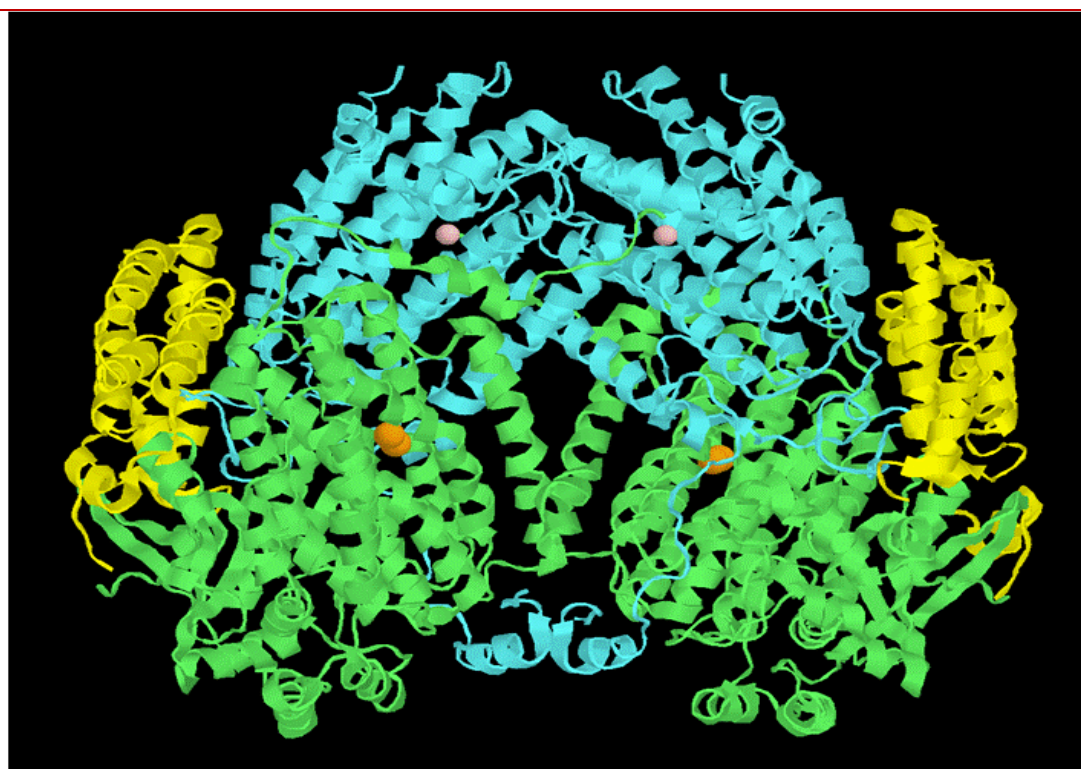


**Figure 5.14** Soluble methane monooxygenase hydroxylase showing the position of the S4G mutant. The alpha, beta and gamma subunits are shown in green, blue and yellow, respectively. The iron atoms of the two diiron sites are shown as orange spheres. The residue (S4G) near to the N- terminus of the alpha subunit as shown as a pink sphere (The position of S4 in sMMO was indicated in image conducted by other crystallographic study for Resenzweig *et al.*, 1997)

# Chapter 6: General discussion, summary and future work

---

## 6.1 Protein purification

### 6.1.1 Purification of hydroxylase

A large number of studies have been performed on purified soluble methane monooxygenase from various methanotrophic bacteria, and so it is considered that the wild type sMMO is a well characterized enzyme (Fox and Lipscomb 1989; Nakajima *et al.*, 1992; Woodland *et al.*, 1984; Grosse *et al.*, 1999; Patel *et al.*, 1987; Shen *et al.*, 1997; Rosenzweig *et al.*, 1997; Elango *et al.*, 1997; McDonald *et al.*, 1997; Shaofeng *et al.*, 2007; Shigematsu *et al.*, 1999). Soluble methane monooxygenase consists as mentioned previously of protein A (hydroxylase) with three subunits  $\alpha$ ,  $\beta$ , and  $\gamma$  with size 55, 43 and 23 kDa respectively. Protein B (16 kDa) and protein C (reductase) with size nearly 39 kDa. In the current study the soluble methane monooxygenase hydroxylase was purified in recombinant form with an attached His-tag. Three bands could be seen on SDS-PAGE corresponding to the hydroxylase subunits. Purification was performed by means of anion exchange chromatography followed by metal affinity chromatography using a modified protocol from Smith *et al.* (2002) and Shaofeng *et al.* (2007) with the addition of a metal affinity chromatography step after anion exchange. The hydroxylase is unstable and so some preservatives to stabilize it were added during the purification. Dithiothreitol was added to a concentration 5 mM to stabilize the hydroxylase. Shaofeng *et al.* (2007) found that increasing the concentration of DTT to 20 mM had an advantage not only in preserving the stability, but also led to improved hydroxylase activity by 18%. In

addition, it was noticed by [Shaofeng \*et al.\* \(2007\)](#) that adding other substances such as cysteine, and sodium thioglycolate during the purification could enhance the stability of the hydroxylase. For these reasons cysteine and thioglycolate were added to the buffers used for the purification of the reductase and hydroxylase in the current study.

It is well established that the diiron centre is critical for the catalytic cycle of the sMMO enzyme. A study by [Shen \*et al.\* \(1997\)](#) revealed different iron content of sMMO hydroxylase purified by two different methods; 3.78 mol/mol Fe by High performance liquid chromatography (HPLC) and 2.02 mol/mol by three step liquid chromatography (LC). This shows that different amount of iron may be lost during the purification protocol. However, this study found that the activity was not improved by adding 1-3 mM FeCl<sub>3</sub>. [Nakajima \*et al.\* \(1992\)](#) found that adding of Fe<sup>2+</sup> enhanced enzyme activity. In the present study during the purification, Fe (NH<sub>4</sub>)<sub>2</sub>(SO<sub>4</sub>)<sub>2</sub> was used as a source to provide iron. The His-tag affinity method has been chosen by Smith's group to facilitate the hydroxylase purification from soluble extract. Six Histidines were inserted in the β-subunit of the hydroxylase by using molecular techniques by this group to be used as a clamp to purify the protein in the Ni-NTA affinity column. This method showed a successful hydroxylase purification as it was explained in the result Chapter to have three bands by SDS-PAGE comparing to sMMO hydroxylase purified by anion exchange chromatography.

## 6.1.2 Purification of protein B

To achieve full sMMO activity, all three components of the enzyme are essential. Protein B has been found to have many important roles in addition to its role in coupling electron transfer from reductase to hydroxylase (Green and Dalton, 1989; Callaghan *et al.*, 2002; Lee *et al.*, 2013). Formation and accumulation of H<sub>2</sub>O<sub>2</sub> by sMMO was found to be toxic for the enzyme in the absence of protein B, therefore it was suggested that protein B is able to inhibit the formation of H<sub>2</sub>O<sub>2</sub> by sMMO (Froland *et al.*, 1992). Strangely, it was found that protein B showed a truncation that happens near the N-terminal, which leads to the production of inactive truncated proteins known as protein B' and B'' (Lloyd *et al.*, 1997; Pilkington *et al.*, 1990), though this, was not seen *in vivo* in *Ms. trichosporium*. However, constructing protein B with an affinity tag (glutathione S-transferase [GST]) fusion and then purifying from *E. coli* resulted in a stable protein B with a high activity, comparable or higher to that of the wild type protein B (WTB) from *Mc. capsulatus* (Lloyd *et al.*, 1997). Protein B of *Ms. trichosporium* fused with GST in plasmid pGEX-2T was used in the current study to obtain an active form of protein B and avoid truncation. The fused GST-protein B was then expressed in *E. coli* BL-21 after the plasmid construct had been characterized by restriction digestion as mentioned in Chapter 3 (Section 3.5.4.1.).

In a study on alkene monooxygenase coupling protein (AmoB), it was found that the GST-AmoB fusion was six times more active than wild type AmoB from *Rhodococcus rhodochrous* B-276 (Smith *et al.*, 1999). In the same study, cleavage of GST-AmoB with thrombin (which is a serine protease) was

attempted, which required omission of benzamidine (a serine protease inhibitor) from the cleaving buffer. Removing benzamidine from the buffer resulted in the loss of coupling protein activity, presumably because of the presence of contaminating proteases. Therefore, an attempt to cleave the GST from WTB (wild type protein B) in the current study has not been made to preserve its activity.

### 6.1.3 Purification of protein C

An attempt to purify protein C, the third component of sMMO which is a light sensitive protein, from *Ms. trichosporium* OB3b was also made during the present study. When the soluble extract was loaded onto the DEAE anion exchange column used in the purification (Chapter 3, Section 3. 5. 2. 1), it showed a peak corresponding to the reductase-containing fractions which appeared at 0.35 M NaCl (Smith *et al.*, 2002). The pooled samples were further purified by using Superdex 75 which also showed only one peak, corresponding to the reductase. The obtained sample was loaded onto SDS-PAGE which did not show any detectable band of protein, but when part of the sample was loaded onto a gel for silver staining (a more sensitive staining method than Coomassie blue for detecting a small amounts of protein), showed many faint bands in the gel which may indicate protein degradation during the purification. The presence of an activity for this sample when it was tested towards oxidation of cytochrom c supports the presence of protein C.

Various expression systems are under investigation in this group such as GST-MmoC in pGEX-2T. It is presumed that cleavage of GST from MmoC is important for reductase activity because in a study on AMO from *Rhodococcus*

*rhodochrous* B-276 (Smith *et al.*, 1999), it was found that cleavage of the GST-reductase fusion protein was necessary to obtain active reductase. As alternative to avoid the need for cleaving the fusion protein, the reductase of sMMO from *Ms. trichosporium* OB3b was cloned into one of the pET series vectors which included the presence of a poly histidine tag. It was hoped that use of a smaller tag would obviate the need for purification since the 6His-tag may be small enough to permit activity without cleavage.

During the present study, an alternative way that was used to obtain reductase was by exploiting the strain expressing sMMO with the mutation F282L in the hydroxylase, which was found to contain inactive hydroxylase but the other components of the sMMO were active. Mutant F282L was tested towards propylene and naphthalene to confirm its inactivity toward a range of substrates. Soluble extract from this mutant was used to provide protein B and C when His-tagged hydroxylase from the wild type or another mutant needed to be assayed.

#### **6.1.4 Activity of purified protein**

The purified His-tagged hydroxylase in combination with the protein B and C containing F282L soluble extract showed activity when it was tested toward propylene with product detection via GC, although this result was difficult to reproduce. The consistency in the preparation of active purified hydroxylase is hard to achieve even with enzyme purified with His-tag affinity column possibly due to many interacting reasons. The activity of the sMMO components was variable due to their being very sensitive to number of factors such as temperature. Shaofeng *et al.* (2007) found that the hydroxylase lost about 42%

of its activity when it was kept at 4°C for 48 h. In the same study it was noticed that the diiron centre was unstable and may be lost during the purification, which consequently affects the enzyme activity. Precautions against enzyme inactivation were taken in the current study, namely keeping the material on ice during the cell breakage and subsequent protein purification steps. Also the reducing agent DTT and the protease inhibitor benzamidine were added. The French pressure cell was chilled to 0-4 °C in the cold room before use and while it was being used it was kept on ice except when being pressurized in the press. Despite these precautions, it was found that the hydroxylase activity in purified hydroxylase was not consistent during the protein assay towards propylene.

The propylene oxidation assay was employed in the current study because, unlike the natural sMMO substrate methane, propylene oxide (the product of propylene oxidation) is not oxidized by the methanol dehydrogenase (MDH) enzyme in these bacteria and hence accumulates and can be detected subsequently by gas chromatography. The His-tag purified hydroxylase showed an activity with F282L as a source for protein B and C in various conditions as explained in Chapter 3. Carbon tetrachloride was used in the present study as a solvent to extract the product from propylene oxidation. Carbon tetrachloride was chosen as the extraction solvent because it is the only solvent known not to be oxidized by sMMO. The first batch used in the present study enabled clear results as supplied. Unfortunately, the subsequent batches from the same supplier contained a contaminating substance with the same GC retention time as the product propylene oxide. Thirteen different solvents were investigated as solvents for extraction of propylene oxide. These solvent were propan-2-ol, 1-pentanol, toluene, propan-1-ol, 1-butanone, acetonitrile, hexane, 2-phenyl

ethanol, 1-phenyl ethanol, mesitylene, ethyl benzene, benzyl alcohol and diethyle ether. Each of these solvents contained a substance with retention time similar to propylene oxide. An efficient solventless method named solid- phase microextraction (SPME) was investigated as an alternative method to detect the propylene oxide to avoid any peaks resulting from the solvent itself since in SPME the sample extracts directly into a retractable fused-silica fibre fixed into a needle (Vas and Vèkey 2004). The assay samples extracted by SPME showed a clear, well separated peak for some samples and an unresolved peak for others (Figure 3.11 A&B respectively). The retention time for propylene oxide extracted using SPME was confirmed with an authentic standard of propylene oxide extracted under the conditions by the SPME method. SPME requires warming the sample to the boiling point for the desired product to be evaporated, which becomes absorbed by the silica fibre, which can then be injected directly into the GC. This method is useful with a few samples since the injection is usually manual. However, running many samples at the same time may lead to problems with performing the extractions in a consistent way, especially with regard to consistency in warming of the samples and inaccuracies arising from saturation of the fiber with product after analysing large numbers of samples. However, optimizing the conditions for SPME for the propylene oxidation assay to overcome the problems mentioned above could enable a reproducible method in the future to obtain a well separated product peak, as well as excluding the use of a hazardous solvent such as CCl<sub>4</sub>. In addition, the inactivity obtained during testing the purified His-tagged hydroxylase could be attributed to the loss of iron during the purification steps, or from the buffer used in purification. An attempt to use imidazole rather than histidine in the elution buffer resulted in inactive hydroxylase (M.Lock personal

communication). A comparison study between hydroxylase purified by multi step method starting with DEAE anion exchange and His-tagged hydroxylase purified by Ni-NTA affinity chromatography is needed.

## **6.2 Mutants construction**

### **6.2.1 Using two cloning steps to facilitate cloning of mutants and minimise PCR-derived errors**

Site directed mutagenesis of a gene is used to change one or a small number of the encoded amino acids ([Heckman and Pease 2007](#)). The overlap extension PCR technique was used in the present study to achieve this to create new mutants by site-directed mutagenesis. Four primers were used; two flanked the two ends of *mmoX* gene whereas two complementary primers to each other contained the desired mutation and were also used to run two different primary PCRs. Then overlap extension PCR was performed as explained in detail in the Materials and Methods Chapter (Section 2.5.3). The overlap PCR product was sequenced before and after cloning to confirm the presence of the mutation in the desired position and then amplified in plasmid pJET 1.2 to proliferate the mutated gene. The digested mutated gene excised from the pJET 1.2 clone, was then cloned into the vector pT2MLY which had been digested with the same restriction enzymes. The plasmid pT2MLY was created in this group to minimize the cloning steps, remove unwanted restriction sites, making the cloning in one step and reducing the number of minipreps which were used in previous studies to screen all the growing mutants by doing colony PCR. Moreover, approximately 500 bp was excised from the *mmoX* gene in this vector, so any naphthalene positive result must be due to the presence of the

new mutated gene. Some mutants were naphthalene negative although they grew well in NMS media with a low amount of or free from added copper and also supplied with four antibiotics; streptomycin, spectinomycin, gentamycin and nalidixic acid. This experiment was confirmed by repeating a further three times. Since the mutants were able to grow on low copper NMS medium on methane as their sole source of carbon and energy it is likely that the mutated sMMO enzymes, although inactive toward the diaromatic hydrocarbon naphthalene, were able to support growth on methane. The fact the mutant methanotroph cells were resistant to streptomycin and spectinomycin was consistent with their having taken up the plasmid containing the mutant genes. This was confirmed by extracting the DNA, performing a PCR for the *mmoX* gene and then sequencing to confirm the presence of the intended mutation.

### **6.3 Mutation of Cys151 to Ser proved that the thiol group from cysteine is not essential for the oxidation of substrates tested in the present study**

The presence of amino acid cysteine 151 close to the sMMO active site in a position analogous to the tyrosine which is the free radical providing amino acid in ribonucleotide reductase makes this amino acid a candidate to have a similar role in radical chemistry in sMMO (Elango *et al.*, 1997; Nordlund *et al.*, 1992). C151 and the nearby hydrophilic residue T213 were investigated by Smith *et al.* (2002). Mutant C151E in this study showed a positive naphthalene test although no hydroxylase components could be seen on SDS-PAGE. Substitution of Cys 151 to Ser in the present study was predicted to abolish the enzyme activity due

to the absence of a thiol group in Ser. The mutation C151S has preserved activity toward a range of substrates, indicating that radical chemistry at this position is not essential for monooxygenase activity. At the same time the Ser has not produced any activity in the C151S mutant towards the tri-aromatic compounds anthracene and phenanthrene. Methane oxidation by C151S sMMO soluble extract needs to be investigated to confirm that the C151S mutant was grown relying on sMMO and not pMMO. In order to detect the methanol product from the sMMO in soluble extract it will be necessary to inhibit oxidation of methanol by methanol dehydrogenase.

#### **6.4 Mutants R98L, R98A and R98A S4G**

In a previous study, an attempt was made to increase the ability of sMMO in oxidation of large di- and tri-aromatic compounds, which resulted in a mutant R98L with 6-fold greater activity than the wild type in oxidation of the diaromatic hydrocarbon biphenyl (Lock *et al.*, manuscript in preparation). R98L was reconstructed in the new His-tagged expression system pT2MLY. The pT2MLY R98L was then transformed into *E. coli* S17.1 which was then conjugated with SMDM in the present study to compare its activity with the R98L mutant without the His-tag. Also His-tagged wild type was tested in parallel with this mutant. The pT2MLY R98L mutant showed a higher activity than His-tag wild type and wild type OB3b in oxidation of monoaromatic compounds, i.e. R98L showed higher activity than His-tagged wild type in oxidation of ethyl benzene yielding 1-phenyl ethanol, phenylmethyl ketone, a compound assigned by the GC-MS analysis software as 4-methylbenzaldehyde and 4-ethyl phenol in 13.3, 1.7, 6.2,

and 14-fold greater amount than wt. His-tag respectively. This result showed a similar trend to the result that was obtained from the previous work on R98L in oxidizing different mono- and di-aromatic substrates. Together these results revealed the importance of this amino acid and suggested that the mutant in which the ionic interaction is disrupted allows easier access of large substrates into the active site. The results also indicate that the disruption of the ion network in the mutant not only facilitates the entry of large substrates but also, presumably via a conformational change, perturbs the structure of the active site so as to alter the regioselectivity of the enzyme.

Another possible role for this residue was that it has a role in keeping the enzyme in an active conformation. Mutation of R98 to the smaller residue Ala was aimed at increasing the space to accommodate larger substrates such as tri-aromatic compounds and to disrupt the ion network. The resulting mutant R98A was inactive towards naphthalene. The presence of the desired mutant *mmoX* gene in the recombinant methanotroph was confirmed by PCR and DNA sequencing. It was also confirmed that the mutant MMOH was expressed since all three hydroxylase subunits were detected by SDS-PAGE. These results indicate that the R98A mutant enzyme is produced but it was inactive with naphthalene, presumably due to a conformational effect on naphthalene binding and / or activity of the diiron centre due to disruption of the ion network.

The double mutant R98A S4G was unplanned and resulted from an unwanted second mutation S4G during an attempt to construct the R98A mutant. It has been found that the fidelity of overlap PCR in avoiding unwanted mutations is approximately 98% and unplanned mutations can occur at frequency of around 1/4000 nucleotides (Ho *et al.*, 1989).

The R98A S4G mutant was inactive towards naphthalene even though all the hydroxylase subunits were seen in SDS-PAGE. This result is very similar to that obtained for the single mutant R98A. The amino acid Ser 4 is sited at the beginning of the MmoX polypeptide and from the crystallographic structure studies it seems that this residue is not involved in architecture of the enzyme or in holding the substrate in the active site. Also it is unlikely to be involved in formation of the ionic network or involving in formation hydrophobic cavity around the active site. Hence there is no evidence that this residue has a significant role in sMMO structure or activity.

## **6.5 Mutants E114D C151Y and E114D**

The mutation of Cys to Tyr in position 151 in the sMMO hydroxylase as in ribonucleotide reductase enzyme (which has been proven to provide free radical catalysis in that enzyme) resulted in an inactive mutant towards aromatic compounds such as naphthalene, which might be due the instability of hydroxylase or low level expression (Smith *et al.*, 2002). Mutation of Glu 114 to Asp (an amino acid with shorter carboxylate side chain) in the background of the C151Y mutation was intended to preserve nearly the same conditions in the active site and make space in the core of the protein for the large tyrosine residue in position 151 to preserve the stability of MMOH. The result was a double mutant E114D C151Y which was expressed in the His-tag system. The affinity purified double mutant C151Y E114D hydroxylase was stable, since three bands resembling the hydroxylase  $\alpha$ ,  $\beta$ , and  $\gamma$  subunits could be seen in SDS-PAGE, with an extra fourth faint band. The identification of the fourth band by mass spectrometry (data not shown, which done by Dr. Malcolm Lock in this

group) revealed that this band may have a run of histidine residues which cause to bind to the Ni-NTA column and then appear in the purified hydroxylase preparation.

Hence, it is likely that Asp at position 114 has an effect in conserving the architecture of the hydroxylase when Cys151 is converted to the bulkier Tyr and as such it stabilizes the hydroxylase for C151Y E114D. Although, the mutation of E144D in C151Y mutant resulted in a stable hydroxylase, the enzyme was still inactive towards naphthalene, which reflects the fact that the presence of tyrosine in this position does not mimic the tyrosine in the ribonucleotide reductase enzyme in providing a free radical involved in catalysis. Alternatively, it could produce a free radical not involved in catalysis.

Glu 114 has a role in the enzyme activity since the single mutant E114D was naphthalene positive and has activity towards monoaromatic compounds such as toluene but the activity was very low compared to the His-tag wt. and wild type OB3b as it was detailed in the results Chapter. This mutant showed no detectable activity in the GC-MS assay for naphthalene oxidation even though it was naphthalene positive on NMS agar plates. It is likely that the product from naphthalene oxidation is not abundant enough to be detected by the GC-MS assay.

It is appropriate to mention that for some aromatic substrate the reaction needs to be analysed after only a short period, such as mesitylene studied by [Nichol, \(2011\)](#), since the products observed from this substrate can be detected after incubation for only 30 minutes, but not after 24 h or 48 h incubation time. A similar phenomenon may explain the results from the mutant E114D where naphthol product from naphthalene oxidation could be detected after a short

time using the colorimetric assay but not using the GC-MS assay, where the reaction were incubated for longer. Indeed, it may be that the oxidation product could be detected from the mutants considered to be inactive with aromatic substrates if shorter incubation time was used. Nonetheless, these mutants must have substantially reduced activity since the wild type produced a detectable product under the same conditions. The products that are lost during the long incubation may be metabolized or lost because they are volatile.

Also from the previous crystallographic studies, it is likely that the substrate needs to pass through a number of cavities in the sMMO enzyme to reach the active site to be oxidised. Although many mutants during the mutagenesis studies have a comparable activity and some have higher than the wild type, such as R98L and C151S in the present study, changing one amino acid in the substrate access pathway may not be sufficient or the best way to allow larger substrates such as the triaromatic compounds anthracene and phenanthrene to enter to the active site. So it may be that changing more than one amino acid in the substrate entry pathway is needed to allow larger substrates to enter the active site and become oxidized.

## 6.6 Summary and future work

The present study has shed light on the role of several residues in the sMMO hydroxylase. Combining the outcomes from the present study with the results from previous studies, no critical role in free radical chemistry during the catalytic cycle can be assigned to Cys151. In particular the mutant C151S showed activity for some substrates even though it does not have thiol group (SH) in this residue which was implicated in the formation of a radical. Further mutation in this site might be useful to give more firm conclusions about the role of this residue near the diiron active site in MMOH.

The His-tag affinity purification system in sMMO hydroxylase, which was characterized in the present study for the first time, revealed promising results representing by an active purified hydroxylase when it was assayed under various conditions. All mutants in this study were cloned with this new affinity system for the sMMO hydroxylase. It is likely that new optimization conditions may enhance high and consistent activity for His-tagged MMOH. Further work is needed to gain a comparable activity of purified His-tagged MMOH compared to native enzyme.

Replacing the extraction solvent  $\text{CCl}_4$  for propylene oxide from propylene oxidation assay with solventless solid phase microextraction (SPME), resulted in a detectable activity peak on the GC reflecting the ability to use SPME as a new approach for measuring the amount of propylene oxide without needing to extract the product with an organic solvent. To the author's knowledge this is the first report to use this method to detect the propylene oxide produced by the sMMO enzyme. The handling of a high number of samples via this method may

be difficult. By overcoming this limitation, the SPME may become more applicable for this purpose to avoid any interaction between the products with the extraction solvent.

The present study also shed the light on the R98 residue which was not proposed by the authors of previous crystallographic studies to have a role in the sMMO activity. The R98L mutant showed activity up to 14 times more than the His-tagged wild type in oxidation of a mono-aromatic compound. It is proposed that the ionic network of which R98 is part is critical in limiting the access of large substrates into the active site although another factor, maybe the size of the active site itself prevents oxidation of triaromatic compounds. Another mutation in this residue may be needed for further investigation of the role of this residue.

Mutation of Glu114, which is one of residues that ligate the diiron centre, to Asp resulted in a less active sMMO compared to the wild type. The same mutation was proved to have a role in stabilizing the unstable hydroxylase containing the mutation C151Y from previous work in this group. No mutant from the present study was able to oxidize tri-aromatic compounds phenethrene and anthracene which may encourage future researchers to investigate more candidate amino acids from crystallographic studies or from comparing sMMO with other similar enzymes to construct single and multiple mutants to achieve this aim.

The mutant F188W showed a negative naphthalene result. From the previous crystallography studies, it was shown that during the formation of the complex between the MMOH and MMOB, both F188 and L110 move so as to open the channel into the active site somewhat. The previous single mutations at these two residues into amino acids with shorter side chains resulted in naphthalene

positive mutants such as F188A, L110C, and L110G. Based on these crystallography and mutation studies, a double mutation to reduce the size of both these amino acids may result in a mutant with a considerably more open passageway into the active site to permit the accomodation of large substrates such as phenanthrene and anthracene. The fact that the double mutation E114D C151Y yielded a stable hydroxylase indicates that, at least in principle, it is possible to make a double mutation of nearby residues without disrupting the stability of the enzyme.

# Appendixes

---

## Appendix 1 media preparation

### 1.1) Preparation of Nitrate Mineral Salts Medium (0.1mg/L $\text{CuSO}_4 \cdot 5\text{H}_2\text{O}$ )

#### Preparation of 1 x NMS Medium

- 100 ml 10 x NMS salts solution.
- 1 ml Sodium Molybdate solution
- 1 ml Trace Elements Solution.
- 0.1 ml Fe EDTA solution.
- Dilute up to 1 L sdH<sub>2</sub>O
- Autoclave at 15 psi for 15 minutes.

For NMS agar plates 1.5% bacteriological agar (wt/v) is added to the medium prior to autoclaving. When the NMS is cool enough to hold in the hand, aseptically add 10 ml phosphate buffer. If this is done too early the phosphate will precipitate out.

#### 10 x NMS salts solution

- 10 g  $\text{KNO}_3$
- 10 g  $\text{MgSO}_4 \cdot 7\text{H}_2\text{O}$  (4.8g  $\text{MgSO}_4$ )
- 2 g  $\text{CaCl}_2 \cdot 2\text{H}_2\text{O}$
- up to 1 L sdH<sub>2</sub>O

#### FE EDTA solution

- 3.8 g Fe EDTA
- up to 100 ml sdH<sub>2</sub>O
- 

#### Sodium Molybdate solution

- 0.5 g  $\text{NaMoO}_4 \cdot 2\text{H}_2\text{O}$

- up to 1 L sdH<sub>2</sub>O

#### **Trace elements solution**

- 0.1 g CuSO<sub>4</sub>·5H<sub>2</sub>O
- 0.5 g FeSO<sub>4</sub>·7H<sub>2</sub>O
- 0.4 g ZnSO<sub>4</sub>·7H<sub>2</sub>O
- 0.015 g H<sub>3</sub>BO<sub>3</sub>
- 0.05 g CoCl<sub>2</sub>·6H<sub>2</sub>O
- 0.25 g EDTA (di sodium salt)
- 0.02 g MnCl<sub>2</sub>·4H<sub>2</sub>O
- 0.01 g NiCl<sub>2</sub>·6H<sub>2</sub>O
- up to 1 L with sdH<sub>2</sub>O

Dissolve the above in the specified order in distilled water and dilute to 250 ml. Store in the dark (wrap around with Aluminium foil).

#### **Phosphate Buffer**

- 49.7 g Na<sub>2</sub>HPO<sub>4</sub>·26 g
- 39 g KH<sub>2</sub>PO<sub>4</sub>
- Up to 1 L sdH<sub>2</sub>O

pH should be 6.8 without altering. Sterilise by autoclaving in 100 ml aliquots and store at room temp.

#### **1.2) Liquid LB media:**

- 10 g Tryptone
- 5 g yeast extract
- 10 g NaCl
- 100 µl 5M NaOH
- up to 1 L sdH<sub>2</sub>O
- Autoclave at 15 psi for 15 minutes

For solid agar plates 1.5 % bacteriological agar (wt/v) is added to LB medium prior to autoclaving

### 1.3) SOC and NZY media

#### SOC Broth

(Prepared immediately before use)

- 2 ml of filter-sterilized 20 % (w/v) glucose or 1 ml of filter-sterilized
- 2 M glucose
- SOB medium (autoclaved) to a final volume of 100 ml

#### NZY media

- 10 g of NZ amine (casein hydroxylase)
- 5 g of yeast extract
- 5 g of NaCl

Deionized water to a final volume of 1 litre

The pH was adjusted to 7.5 and then autoclaved.

The following supplements were sterilized by filtration and added before using

- 12.5 ml of 1 M  $\text{MgCl}_2$
- 12.5 ml of 1 M  $\text{MgSO}_4$
- 20 ml of 20% (w/v) glucose (or 10 ml of 2 M glucose)

## Appendix 2 Buffer preparation

### 1.1) Preparation of buffers for genomic tip-20 protocol

#### B1 buffer

- 18.61 g Na<sub>2</sub>EDTA·2H<sub>2</sub>O
- 6.06 g Tris base
- 800 ml distilled water.
- 50 ml 10% Tween-20 solution (v/v)
- 50 ml 10% Triton X-100 solution. (v/v)
- Adjust the pH to 8.0 with HCl.
- Up to 1 L sdH<sub>2</sub>O

#### B2 buffer

- 286.59 g guanidine HCl
- 700 ml sdH<sub>2</sub>O
- 200 ml 100% Tween-20 (v/v)
- Up to 1 L sdH<sub>2</sub>O

#### QBT buffer

- 43.83 g NaCl,
- 10.46 g MOPS
- 800 ml distilled water.
- Adjust the pH to 7.0 with NaOH.
- Add 150 ml pure isopropanol
- 15 ml 10% Triton X-100 solution (v/v)
- Up to 1 L sdH<sub>2</sub>O

#### QC buffer

- 58.44 g NaCl,
- 10.46 g MOPS (free acid)
- 800 ml distilled water.
- Adjust the pH to 7.0 with NaOH.
- Add 150 ml isopropanol.
- Up to 1 L sdH<sub>2</sub>O

### **QF buffer**

- 73.05 g NaCl
- 6.06 g Tris base
- 800 ml distilled water.
- Adjust the pH to 8.5 with HCl.
- Add 150 ml pure isopropanol.
- Up to 1 L sdH<sub>2</sub>O

## **Appendix 3 SDS PAGE reagents and protocol**

### **RUNNING BUFFER**

- 7.2 g Glycine
- 1.5 g Tris
- 0.5 g SDS
- dH<sub>2</sub>O up to 500 ml

### **RESOLVING BUFFER (3 M Tris-HCl pH 8.8)**

### **STACKING BUFFER (0.5 M TrisHCl pH 6.8)**

### **RESOLVING GEL (12.5 %)**

- 4.84 ml 40 % acrylamide/bis solution
- 2.5 ml resolving buffer
- 2.65 ml H<sub>2</sub>O
- 0.1 ml 10 % glycerol (v/v)
- 0.1 ml 10 % SDS
- 0.5 ml 10 % APS (fresh made)
- 5 µl TEMED (add last)

### **STACKING GEL**

- 0.83 ml 40 % acrylamide/bis solution
- 1.36 ml stacking buffer
- 2.8 ml H<sub>2</sub>O
- 50 µl 10 % SDS(v/v)
- 50 µl 10 % glycerol (v/v)
- 0.5 ml 10 % APS (wt/v)
- 5 µl TEMED (add last)

### **SAMPLE BUFFER (2x) (gel loading)**

- 250 µl stacking buffer
- 200 µl 100% glycerol
- 80 µl 0.5% bromophenol blue
- 100 µl β-mercaptoethanol (100 %)
- 1.2 ml 10% SDS (wt/v)

### **STAIN SOLUTION**

- 450 ml methanol
- 450 ml sdH<sub>2</sub>O
- 100 ml glacial acetic acid
- 2.5 g Coomassie brilliant blue R

### **DESTAIN SOLUTION**

- 300 ml methanol
- 100 ml glacial acetic acid
- 600 ml sdH<sub>2</sub>O

### **SDS PAGE Protocol**

- clip together glass plates including rubber lining
- pour resolving gel until few mm below level of wells
- overlay gel with 700 µl ethanol or isopropanol
- after gel has set (~30 min) wash off ethanol with water and blot off excess
- assemble stacking gel and pour over resolving gel
- allow to set
- remove clips and rubber seal, assemble gel tank and add running buffer
- boil 10 µl sample for 10 min
- add 10 µl sample buffer to each sample
- run at 130 V 150 mA for 30 min turn to 150 V for 1h or until dye reaches bottom of gel.

## **Appendix 4 Ethanol free NADH preparation**

### **Preparation of 100mM NADH**

- 0.7635 g NADH
- 10 ml sdH<sub>2</sub>O
- Divide into 1 ml aliquots

### **Ether extraction of NADH**

- Add 250 µl diethyl ether to 1ml NADH
- Remove top layer
- Add 250 µl diethyl ether
- Remove top layer
- dry overnight in Eppendorf 5301 concentrator
- Add 1ml sdH<sub>2</sub>O and vortex till dissolved.

Store at in foil at -15°C, use within 1 week.

## References

**Abbruzzese, A., Park, M. H., & Folk, J. E.** (1986). Deoxyhypusine hydroxylase from rat testis. Partial purification and characterization. *The Journal of Biological Chemistry*, 261 (7), 3085-3089.

**Aberg, A., Hahne, S., Karlsson, M., Larsson, A., Ormo, M., Ahgren, A., & Sjoberg, B. M.** (1989). Evidence for two different classes of redox-active cysteines in ribonucleotide reductase of *Escherichia coli*. *The Journal of Biological Chemistry*, 264(21), 12249-12252.

**Al Hasin, A., Gurman, S. J., Murphy, L. M., Perry, A., Smith, T. J., & Gardiner, P. H.** (2009). Remediation of chromium (VI) by a methane-oxidizing bacterium. *Environmental Science & Technology*, 44(1), 400-405.

**Altarsha, M., Benighaus, T., Kumar, D., & Thiel, W.** (2009). How is the reactivity of cytochrome P450cam affected by Thr252X mutation? A QM/MM study for X= serine, valine, alanine, glycine. *Journal of the American Chemical Society*, 131 (13), 4755-4763.

**Andersson, K., Froland, W., Lee, S., & Lipscomb, J.** (1991). Dioxygen independent oxygenation of hydrocarbons by methane monooxygenase hydroxylase component. *Nouveau Journal De Chimie*, 15(6), 411-415.

**Anthony, C.** (1986). Bacterial oxidation of methane and methanol. *Adv. Microb. Physiol*, 27, 113-210.

**Anthony, C.** (1982). *Biochemistry of methylotrophs* Academic Press.

**Astier, Y., Balendra, S., Hill, H. A. O., Smith, T. J., & Dalton, H. (2003).** Cofactor-independent oxygenation reactions catalyzed by soluble methane monooxygenase at the surface of a modified gold electrode. *European Journal of Biochemistry*, 270 (3), 539-544.

**Baani, M., & Liesack, W. (2008).** Two isozymes of particulate methane monooxygenase with different methane oxidation kinetics are found in *Methylocystis* sp. strain SC2. *Proceedings of the National Academy of Sciences of the United States of America*, 105 (29), 10203-10208.

**Bailey, L. J., Acheson, J. F., McCoy, J. G., Elsen, N. L., Phillips Jr, G. N., & Fox, B. G. (2012).** Crystallographic analysis of active site contributions to regiospecificity in the diiron enzyme toluene 4-monooxygenase. *Biochemistry*, 51 (6), 1101-1113.

**Bailey, L. J., McCoy, J. G., Phillips, G. N., Jr, & Fox, B. G. (2008).** Structural consequences of effector protein complex formation in a diiron hydroxylase. *Proceedings of the National Academy of Sciences of the United States of America*, 105 (49), 19194-19198. doi:10.1073/pnas.0807948105 [doi]

**Balasubramanian, R., & Rosenzweig, A. C. (2007).** Structural and mechanistic insights into methane oxidation by particulate methane monooxygenase. *Accounts of Chemical Research*, 40 (7), 573-580.

**Balasubramanian, R., Smith, S. M., Rawat, S., Yatsunyk, L. A., Stemmler, T. L., & Rosenzweig, A. C. (2010).** Oxidation of methane by a biological dicopper centre. *Nature*, 465 (7294), 115-119.

**Basu, P., Katterle, B., Andersson, K., & Dalton, H.** (2003). The membrane-associated form of methane mono-oxygenase from *Methylococcus capsulatus* (Bath) is a copper/iron protein. *Biochem.J*, 369, 417-427.

**Behling, L. A., Hartsel, S. C., Lewis, D. E., DiSpirito, A. A., Choi, D. W., Masterson, L. R., Gallagher, W. H.** (2008). NMR, mass spectrometry and chemical evidence reveal a different chemical structure for methanobactin that contains oxazolone rings. *Journal of the American Chemical Society*, 130 (38), 12604-12605.

**Belova, S. E., Baani, M., Suzina, N. E., Bodelier, P. L., Liesack, W., & Dedysh, S. N.** (2011). Acetate utilization as a survival strategy of peat-inhabiting *Methylocystis* spp. *Environmental Microbiology Reports*, 3(1), 36-46.

**Belova, S. E., Irina, S. K., Bodelier, P. L., & Svetlana, N.** *Methylocystis bryophila* sp. nov., a Novel Facultatively Methanotrophic Bacterium from Acidic Sphagnum Peat, and Emended Description of the 2 Genus *Methylocystis* (ex Whittenbury *et al.*, 1970) Bowman *et al.* 1993 3.

**Bertoni, G., Bolognese, F., Galli, E., & Barbieri, P.** (1996). Cloning of the genes for and characterization of the early stages of toluene and o-xylene catabolism in *Pseudomonas stutzeri* OX1. *Applied and Environmental Microbiology*, 62 (10), 3704-3711.

**Bertoni, G., Martino, M., Galli, E., & Barbieri, P.** (1998). Analysis of the gene cluster encoding toluene/o-xylene monooxygenase from *Pseudomonas stutzeri* OX1. *Applied and Environmental Microbiology*, 64 (10), 3626-3632.

**Birnboim, H. C., & Doly, J.** (1979). A rapid alkaline extraction procedure for screening recombinant plasmid DNA. *Nucleic Acids Research*, 7(6), 1513-1523.

**Borgulya, J., Bruderer, H., Bernauer, K., Zürcher, G., & Prada, M. D.** (1989). Catechol-O-methyltransferase-inhibiting pyrocatechol derivatives: synthesis and structure-activity studies. *Helvetica Chimica Acta*, 72 (5), 952-968.

**Borodina, E., Nichol, T., Dumont, M. G., Smith, T. J., & Murrell, J. C.** (2007). Mutagenesis of the "leucine gate" to explore the basis of catalytic versatility in soluble methane monooxygenase. *Applied and Environmental Microbiology*, 73 (20), 6460-6467.

**Brandstetter, H., Whittington, D. A., Lippard, S. J., & Frederick, C. A.** (1999). Mutational and structural analyses of the regulatory protein B of soluble methane monooxygenase from *Methylococcus capsulatus* (Bath). *Chemistry & Biology*, 6(7), 441-449.

**Brazeau, B. J., & Lipscomb, J. D.** (2000). Kinetics and activation thermodynamics of methane monooxygenase compound Q formation and reaction with substrates. *Biochemistry*, 39 (44), 13503-13515.

**Brazeau, B. J., & Lipscomb, J. D.** (2003). Key amino acid residues in the regulation of soluble methane monooxygenase catalysis by component B. *Biochemistry*, 42 (19), 5618-5631.

**Brusseau, G. A., Tsien, H., Hanson, R. S., & Wackett, L. P.** (1990). Optimization of trichloroethylene oxidation by methanotrophs and the use of a colorimetric assay to detect soluble methane monooxygenase activity. *Biodegradation*, 1 (1), 19-29.

**Buolamwini, J. K.** (2000). Cell cycle molecular targets in novel anticancer drug discovery. *Current Pharmaceutical Design*, 6 (4), 379-392.

**Burrows, K. J., Cornish, A., Scott, D., & Higgins, I. J.** (1984). Substrate specificities of the soluble and particulate methane mono-oxygenases of *Methylosinus trichosporium* OB3b. *Journal of General Microbiology*, 130 (12), 3327-3333.

**Byrne, A. M., Kukor, J. J., & Olsen, R. H.** (1995). Sequence analysis of the gene cluster encoding toluene-3-monooxygenase from *Pseudomonas pickettii* PKO1. *Gene*, 154 (1), 65-70.

**Callaghan, A. J., Smith, T. J., Slade, S. E., & Dalton, H.** (2002). Residues near the N-terminus of protein B control autocatalytic proteolysis and the activity of soluble methane mono-oxygenase. *European Journal of Biochemistry / FEBS*, 269 (7), 1835-1843.

**Canada, K. A., Iwashita, S., Shim, H., & Wood, T. K.** (2002). Directed evolution of toluene ortho-monooxygenase for enhanced 1-naphthol synthesis and chlorinated ethene degradation. *Journal of Bacteriology*, 184(2), 344-349.

**Cardy, D. L., Laidler, V., Salmond, G. P., & Murrell, J. C.** (1991). Molecular analysis of the methane monooxygenase (MMO) gene cluster of *Methylosinus trichosporium* OB3b. *Molecular Microbiology*, 5 (2), 335-342.

**Carlson, J., Fuchs, J. A., & Messing, J.** (1984). Primary structure of the *Escherichia coli* ribonucleoside diphosphate reductase operon. *Proceedings of the National Academy of Sciences of the United States of America*, 81 (14), 4294-4297.

- Cavanaugh, C.** (1993). Methanotroph-invertebrate symbioses in the marine environment: ultrastructural, biochemical and molecular studies. *Microbial Growth on C*, 1, 315-328.
- Cerqueira, N. M., Fernandes, P. A., & Ramos, M. J.** (2007). Ribonucleotide reductase: a critical enzyme for cancer chemotherapy and antiviral agents. *Recent Patents on Anti-Cancer Drug Discovery*, 2 (1), 11-29.
- Cervantes, C., Campos-García, J., Devars, S., Gutiérrez-Corona, F., Loza-Tavera, H., Torres-Guzmán, J. C., & Moreno-Sánchez, R.** (2001). Interactions of chromium with microorganisms and plants. *FEMS Microbiology Reviews*, 25 (3), 335-347.
- Chan, S. I., Chen, K. H., Yu, S. S., Chen, C., & Kuo, S. S.** (2004). Toward delineating the structure and function of the particulate methane monooxygenase from methanotrophic bacteria. *Biochemistry*, 43 (15), 4421-4430.
- Chan, S. I., Lu, Y., Nagababu, P., Maji, S., Hung, M., Lee, M. M., Ng, K. Y.** (2013). Efficient Oxidation of Methane to Methanol by Dioxygen Mediated by Tricopper Clusters. *Angewandte Chemie*, 125 (13), 3819-3823.
- Chang, S., Wallar, B. J., Lipscomb, J. D., & Mayo, K. H.** (1999). Solution structure of component B from methane monooxygenase derived through heteronuclear NMR and molecular modeling. *Biochemistry*, 38 (18), 5799-5812.
- Chang, S., Wallar, B. J., Lipscomb, J. D., & Mayo, K. H.** (2001). Residues in *Methylosinus trichosporium* OB3b methane monooxygenase component B

involved in molecular interactions with reduced-and oxidized-hydroxylase component: a role for the N-terminus. *Biochemistry*, 40 (32), 9539-9551.

**Chan, S. I., & Yu, S. S.** (2008). Controlled oxidation of hydrocarbons by the membrane-bound methane monooxygenase: The case for a tricopper cluster. *Accounts of Chemical Research*, 41 (8), 969-979.

**Chen, C., Chen, K. H., Ke, S., Yu, S. S., & Chan, S. I.** (2004). Preparation and characterization of a (Cu, Zn)-pMMO from *Methylococcus capsulatus* (Bath). *Journal of Inorganic Biochemistry*, 98 (12), 2125-2130.

**Choi, D. W., Kunz, R. C., Boyd, E. S., Semrau, J. D., Antholine, W. E., Han, J. I., DiSpirito, A. A.** (2003). The membrane-associated methane monooxygenase (pMMO) and pMMO-NADH:quinone oxidoreductase complex from *Methylococcus capsulatus* Bath. *Journal of Bacteriology*, 185 (19), 5755-5764.

**Colby, J., & Dalton, H.** (1978). Resolution of the methane mono-oxygenase of *Methylococcus capsulatus* (Bath) into three components. Purification and properties of component C, a flavoprotein. *The Biochemical Journal*, 171 (2), 461-468.

**Colby, J., Stirling, D. I., & Dalton, H.** (1977). The soluble methane mono-oxygenase of *Methylococcus capsulatus* (Bath). Its ability to oxygenate n-alkanes, n-alkenes, ethers, and alicyclic, aromatic and heterocyclic compounds. *Biochem.j*, 165, 395-402.

**Cook, S. A., & Shiemke, A. K.** (1996). Evidence that copper is a required cofactor for the membrane-bound form of methane monooxygenase. *Journal of Inorganic Biochemistry*, 63 (4), 273-284.

**Csaki, R., Bodrossy, L., Klem, J., Murrell, J. C., & Kovacs, K. L.** (2003). Genes involved in the copper-dependent regulation of soluble methane monooxygenase of *Methylococcus capsulatus* (Bath): cloning, sequencing and mutational analysis. *Microbiology (Reading, England)*, 149 (Pt 7), 1785-1795.

**Culpepper, M. A., Cutsail III, G. E., Gunderson, W. A., Hoffman, B. M., & Rosenzweig, A. C.** (2014). Identification of the valence and coordination environment of the particulate methane monooxygenase copper centers by advanced EPR characterization. *Journal of the American Chemical Society*, 136 (33), 11767-11775.

**Dalton, H.** (1980). Oxidation of hydrocarbons by methane monooxygenases from a variety of microbes. *Advances in Applied Microbiology*, 26, 71-87.

**Dalton, H.** (2005). The Leeuwenhoek Lecture 2000 the natural and unnatural history of methane-oxidizing bacteria. *Philosophical Transactions of the Royal Society of London. Series B, Biological Sciences*, 360 (1458), 1207-1222.

**Dalton, H., & Stirling, D. I.** (1982). Co-metabolism. *Philosophical Transactions of the Royal Society of London. Series B, Biological Sciences*, 297 (1088), 481-496.

**Davies, S. L., & Whittenbury, R.** (1970). Fine structure of methane and other hydrocarbon-utilizing bacteria. *Journal of General Microbiology*, 61(2), 227-232.

**Davis, D., Kemp, D., Kroschwitz, J., & Howe-Grant, M.** (1991). Kirk-Othmer Encyclopedia of Chemical Technology.

De Montellano, Paul R Ortiz. (1986). Oxygen activation and transfer. *Cytochrome P-450* (pp. 217-271) Springer.

**Dedysh, S. N., Knief, C., & Dunfield, P. F.** (2005). *Methylocella* species are facultatively methanotrophic. *Journal of Bacteriology*, 187 (13), 4665-4670.

**Dever, J., George, K., Hoffman, W., & Soo, H.** (2005). Ethylene oxide. *Kirk-Othmer Encyclopedia of Chemical Technology*.

**Dijkhuizen, L., Levering, P., & De Vries, G.** (1992). The physiology and biochemistry of aerobic methanol-utilizing Gram-negative and Gram-positive bacteria. *Methane and methanol utilizers* (pp. 149-181) Springer.

**DiSpirito, A. A., Zahn, J. A., Graham, D. W., Kim, H. J., Larive, C. K.,**

**Derrick, T. S., Taylor, A.** (1998). Copper-binding compounds from *Methylosinus trichosporium* OB3b. *Journal of Bacteriology*, 180(14), 3606-3613

**Draths, K., & Frost, J.** (1991). Conversion of D-glucose into catechol: the not-so-common pathway of aromatic biosynthesis. *Journal of the American Chemical Society*, 113 (24), 9361-9363.

**Draths, K., & Frost, J.** (1995). Environmentally compatible synthesis of catechol from D-glucose. *Journal of the American Chemical Society*, 117 (9), 2395-2400.

**Dubbels, B. L., Sayavedra-Soto, L. A., Bottomley, P. J., & Arp, D. J.** (2009). *Thauera butanivorans* sp. nov., a C2-C9 alkane-oxidizing bacterium previously

referred to as '*Pseudomonas butanovora*'. *International Journal of Systematic and Evolutionary Microbiology*, 59 (Pt 7), 1576-1578.

**Dunfield, P. F., Yuryev, A., Senin, P., Smirnova, A. V., Stott, M. B., Hou, S., Ren, Y.** (2007). Methane oxidation by an extremely acidophilic bacterium of the phylum Verrucomicrobia. *Nature*, 450 (7171), 879-882.

**El Ghazouani, A., Baslé, A., Firbank, S. J., Knapp, C. W., Gray, J., Graham, D. W., & Dennison, C.** (2011). Copper-binding properties and structures of methanobactins from *Methylosinus trichosporium* OB3b. *Inorganic Chemistry*, 50 (4), 1378-1391.

**El Ghazouani, A., Basle, A., Gray, J., Graham, D. W., Firbank, S. J., & Dennison, C.** (2012). Variations in methanobactin structure influences copper utilization by methane-oxidizing bacteria. *Proceedings of the National Academy of Sciences of the United States of America*, 109 (22), 8400-8404.

**Elango, N. A., Radhakrishnan, R., Froland, W. A., Wallar, B. J., Earhart, C. A., Lipscomb, J. D., & Ohlendorf, D. H.** (1997). Crystal structure of the hydroxylase component of methane monooxygenase from *Methylosinus trichosporium* OB3b. *Protein Science*, 6 (3), 556-568.

**Elsen, N. L., Bailey, L. J., Hauser, A. D., & Fox, B. G.** (2009). Role for threonine 201 in the catalytic cycle of the soluble diiron hydroxylase toluene 4-monooxygenase. *Biochemistry*, 48 (18), 3838-3846.

**Erikstad, H., Jensen, S., Keen, T. J., & Birkeland, N.** (2012). Differential expression of particulate methane monooxygenase genes in the

verrucomicrobial methanotroph '*Methylacidiphilum kamchatkense*'

Kam1. *Extremophiles*, 16 (3), 405-409.

**Eriksson, M., Uhlin, U., Ramaswamy, S., Ekberg, M., Regnström, K., Sjöberg, B., & Eklund, H.** (1997). Binding of allosteric effectors to ribonucleotide reductase protein R1: reduction of active-site cysteines promotes substrate binding. *Structure*, 5 (8), 1077-1092.

**Feig, A. L., & Lippard, S. J.** (1994). Reactions of non-heme iron (II) centers with dioxygen in biology and chemistry. *Chemical Reviews*, 94(3), 759-805.

**Fishman, A., Tao, Y., & Wood, T. K.** (2004). Toluene 3-monooxygenase of *Ralstonia pickettii* PKO1 is a para-hydroxylating enzyme. *Journal of Bacteriology*, 186 (10), 3117-3123.

**Fox, B. G., Borneman, J. G., Wackett, L. P., & Lipscomb, J. D.** (1990). Haloalkene oxidation by the soluble methane monooxygenase from *Methylosinus trichosporium* OB3b: mechanistic and environmental implications. *Biochemistry*, 29 (27), 6419-6427.

**Fox, B. G., Froland, W. A., Dege, J. E., & Lipscomb, J. D.** (1989). Methane monooxygenase from *Methylosinus trichosporium* OB3b. Purification and properties of a three-component system with high specific activity from a type II methanotroph. *The Journal of Biological Chemistry*, 264 (17), 10023-10033.

**Fox, B. G., & Lipscomb, J. D.** (1988). Purification of a high specific activity methane monooxygenase hydroxylase component from a type II

methanotroph. *Biochemical and Biophysical Research Communications*, 154 (1), 165-170.

**Fox, B. G., Liu, Y., Dege, J. E., & Lipscomb, J. D.** (1991). Complex formation between the protein components of methane monooxygenase from *Methylosinus trichosporium* OB3b. Identification of sites of component interaction. *The Journal of Biological Chemistry*, 266 (1), 540-550.

**Fox, B. G., Shanklin, J., Ai, J., Loehr, T. M., & Sanders-Loehr, J.** (1994). Resonance Raman evidence for an Fe-O-Fe center in stearyl-ACP desaturase. Primary sequence identity with other diiron-oxo proteins. *Biochemistry*, 33 (43), 12776-12786

**Fox, B. G., Shanklin, J., Somerville, C., & Munck, E.** (1993). Stearyl-acyl carrier protein delta 9 desaturase from *Ricinus communis* is a diiron-oxo protein. *Proceedings of the National Academy of Sciences of the United States of America*, 90 (6), 2486-2490.

**Froland, W. A., Andersson, K. K., Lee, S. K., Liu, Y., & Lipscomb, J. D.** (1992). Methane monooxygenase component B and reductase alter the regioselectivity of the hydroxylase component-catalyzed reactions. A novel role for protein-protein interactions in an oxygenase mechanism. *The Journal of Biological Chemistry*, 267 (25), 17588-17597.

**Fuse, H., Ohta, M., Takimura, O., Murakami, K., Inoue, H., Yamaoka, Y., Omori, T.** (1998). Oxidation of trichloroethylene and dimethyl sulfide by a marine *Methylomicrobium* strain containing soluble methane monooxygenase. *Bioscience, Biotechnology, and Biochemistry*, 62 (10), 1925-1931.

**George, A. R., Wilkins, P. C., & Dalton, H.** (1996). A computational investigation of the possible substrate binding sites in the hydroxylase of soluble methane monooxygenase. *Journal of Molecular Catalysis B: Enzymatic*, 2 (2), 103-113.

**Gilbert, B., McDonald, I. R., Finch, R., Stafford, G. P., Nielsen, A. K., & Murrell, J. C.** (2000). Molecular analysis of the pmo (particulate methane monooxygenase) operons from two type II methanotrophs. *Applied and Environmental Microbiology*, 66 (3), 966-975.

**Giraud, E., Moulin, L., Vallenet, D., Barbe, V., Cytryn, E., Avarre, J. C., Sadowsky, M.** (2007). Legumes symbioses: absence of Nod genes in photosynthetic *bradyrhizobia*. *Science (New York, N.Y.)*, 316(5829), 1307-1312.

**Goan, Y. G., Zhou, B., Hu, E., Mi, S., & Yen, Y.** (1999). Overexpression of ribonucleotide reductase as a mechanism of resistance to 2, 2-difluorodeoxycytidine in the human KB cancer cell line. *Cancer Research*, 59 (17), 4204-4207.

**Green, P. N.** (1992). Taxonomy of methylotrophic bacteria. *Methane and methanol utilizers* (pp. 23-84) Springer.

**Green, J., & Dalton, H.** (1989). Substrate specificity of soluble methane monooxygenase. Mechanistic implications. *The Journal of Biological Chemistry*, 264 (30), 17698-17703.

**Green, J., & Dalton, H.** (1989). A stopped-flow kinetic study of soluble methane mono-oxygenase from *Methylococcus capsulatus* (Bath). *Biochem.J*, 259, 167-172.

**Green, J., Prior, S. D., & Dalton, H.** (1985). Copper ions as inhibitors of protein C of soluble methane monooxygenase of *Methylococcus capsulatus* (Bath). *European Journal of Biochemistry*, 153 (1), 137-144.

**Grosse, S., Laramée, L., Wendlandt, K. D., McDonald, I. R., Miguez, C. B., & Kleber, H. P.** (1999). Purification and characterization of the soluble methane monooxygenase of the type II methanotrophic bacterium *Methylocystis* sp. strain WI 14. *Applied and Environmental Microbiology*, 65 (9), 3929-3935.

**Hakemian, A. S., Kondapalli, K. C., Telser, J., Hoffman, B. M., Stemmler, T. L., & Rosenzweig, A. C.** (2008). The Metal Centers of Particulate Methane Monooxygenase from *Methylosinus trichosporium* OB3b. *Biochemistry*, 47 (26), 6793-6801.

**Hakemian, A. S., & Rosenzweig, A. C.** (2007). The biochemistry of methane oxidation. *Annu. Rev. Biochem.*, 76, 223-241.

**Hamel, P., & Girard, Y.** (1994). Synthesis of dephostatin, a novel protein tyrosine phosphatase inhibitor. *Tetrahedron Letters*, 35 (44), 8101-8102.

**Hanson, R. S., & Hanson, T. E.** (1996). Methanotrophic bacteria. *Microbiological Reviews*, 60 (2), 439-471.

**Haque, M. F. U., Kalidass, B., Bandow, N., Turpin, E. A., DiSpirito, A. A., & Semrau, J. D.** (2015). Cerium regulates expression of alternative methanol dehydrogenases in *Methylosinus trichosporium* OB3b. *Applied and Environmental Microbiology*, AEM. 02542-15.

**Hartog, J., & Wouters, W.** (1988). Flesinoxan hydrochloride. *Drugs Future*, 13, 31-33.

- Heckman, K. L., & Pease, L. R.** (2007). Gene splicing and mutagenesis by PCR-driven overlap extension. *Nature Protocols*, 2 (4), 924-932.
- Hoessel, R., Leclerc, S., Endicott, J. A., Nobel, M. E., Lawrie, A., Tunnah, P., Marko, D.** (1999). Indirubin, the active constituent of a Chinese antileukaemia medicine, inhibits cyclin-dependent kinases. *Nature Cell Biology*, 1 (1), 60-67.
- Hussein, G., Sankawa, U., Goto, H., Matsumoto, K., & Watanabe, H.** (2006). Astaxanthin, a Carotenoid with Potential in Human Health and Nutrition. *Journal of Natural Products*, 69(3), 443-449.
- Imai, M., Shimada, H., Watanabe, Y., Matsushima-Hibiya, Y., Makino, R., Koga, H., Ishimura, Y.** (1989). Uncoupling of the cytochrome P-450 cam monooxygenase reaction by a single mutation, threonine-252 to alanine or valine: possible role of the hydroxy amino acid in oxygen activation. *Proceedings of the National Academy of Sciences of the United States of America*, 86 (20), 7823-7827.
- Islam, T., Jensen, S., Reigstad, L. J., Larsen, O., & Birkeland, N. K.** (2008). Methane oxidation at 55 degrees C and pH 2 by a thermoacidophilic bacterium belonging to the Verrucomicrobia phylum. *Proceedings of the National Academy of Sciences of the United States of America*, 105 (1), 300-304.
- Jeschke, G.** (2012). DEER distance measurements on proteins. *Annual Review of Physical Chemistry*, 63, 419-446.
- Jiang, H., Chen, Y., Jiang, P., Zhang, C., Smith, T. J., Murrell, J. C., & Xing, X.** (2010). Methanotrophs: multifunctional bacteria with promising applications in

environmental bioengineering. *Biochemical Engineering Journal*, 49(3), 277-288.

**Jiang, Y., Wilkins, P. C., & Dalton, H.** (1993). Activation of the hydroxylase of sMMO from *Methylococcus capsulatus* (Bath) by hydrogen peroxide. *Biochimica Et Biophysica Acta (BBA)-Protein Structure and Molecular Enzymology*, 1163 (1), 105-112.

**Joe, Y. A., Wolff, E. C., & Park, M. H.** (1995). Cloning and expression of human deoxyhypusine synthase cDNA Structure-function studies with the recombinant enzyme and mutant proteins. *Journal of Biological Chemistry*, 270 (38), 22386-22392.

**Johnson, G. R., & Olsen, R. H.** (1995). Nucleotide sequence analysis of genes encoding a toluene/benzene-2-monooxygenase from *Pseudomonas* sp. strain JS150. *Applied and Environmental Microbiology*, 61 (9), 3336-3346.

**Jordan, A., & Reichard, P.** (1998). Ribonucleotide reductases. *Annual Review of Biochemistry*, 67 (1), 71-98.

**Kahng, H. Y., Byrne, A. M., Olsen, R. H., & Kukor, J. J.** (2000). Characterization and role of *tbuX* in utilization of toluene by *Ralstonia pickettii* PKO1. *Journal of Bacteriology*, 182 (5), 1232-1242.

**Kaiser, A.** (2012). Translational control of eIF5A in various diseases. *Amino Acids*, 42 (2-3), 679-684.

**Karlsson, A., Beharry, Z. M., Eby, D. M., Coulter, E. D., Neidle, E. L., Kurtz, D. M., Ramaswamy, S.** (2002). X-ray crystal structure of benzoate 1, 2-

dioxygenase reductase from *Acinetobacter* sp. strain ADP1. *Journal of Molecular Biology*, 318(2), 261-272.

**Kazlauskaitė, J., Hill, H. A. O., Wilkins, P. C., & Dalton, H.** (1996). Direct electrochemistry of the hydroxylase of soluble methane monooxygenase from *Methylococcus capsulatus* (Bath). *European Journal of Biochemistry*, 241 (2), 552-556.

**Khalifa, A.** (2012). Gene Regulation in Methanotrophs: Evidence from *Methylococcus Capsulatus* (Bath) and *Methylosinus trichosporium* (OB3b),

**Kim, S., Bae, W., Hwang, J., & Park, J.** (2010). Aerobic TCE degradation by encapsulated toluene-oxidizing bacteria, *Pseudomonas putida* and *Bacillus* spp.

**Kim, H. J., Graham, D. W., DiSpirito, A. A., Alterman, M. A., Galeva, N., Larive, C. K., Sherwood, P. M.** (2004). Methanobactin, a copper-acquisition compound from methane-oxidizing bacteria. *Science (New York, N.Y.)*, 305 (5690), 1612-1615.

**Kim, Y. S., Kang, K. R., Wolff, E. C., Bell, J. K., McPhie, P., & Park, M. H.** (2006). Deoxyhypusine hydroxylase is a Fe (II)-dependent, HEAT-repeat enzyme. Identification of amino acid residues critical for Fe (II) binding and catalysis [corrected]. *The Journal of Biological Chemistry*, 281 (19), 13217-13225.

**Kitmitto, A., Myronova, N., Basu, P., & Dalton, H.** (2005). Characterization and structural analysis of an active particulate methane monooxygenase trimer from *Methylococcus capsulatus* (Bath). *Biochemistry*, 44 (33), 10954-10965.

**Kolberg, M., Strand, K. R., Graff, P., & Andersson, K. K.** (2004). Structure, function, and mechanism of ribonucleotide reductases. *Biochimica Et Biophysica Acta (BBA)-Proteins and Proteomics*, 1699 (1), 1-34.

**Kopp, D. A., Berg, E. A., Costello, C. E., & Lippard, S. J.** (2003). Structural features of covalently cross-linked hydroxylase and reductase proteins of soluble methane monooxygenase as revealed by mass spectrometric analysis. *The Journal of Biological Chemistry*, 278 (23), 20939-20945.

**Korte, J. E., Hertz-Picciotto, I., Schulz, M. R., Ball, L. M., & Duell, E. J.** (2000). The contribution of benzene to smoking-induced leukemia. *Environmental Health Perspectives*, 108 (4), 333-339.

**Kühlbrandt, W.** (1988). Three-dimensional crystallization of membrane proteins. *Quarterly Reviews of Biophysics*, 21 (04), 429-477.

**Landa, A. S., Sipkema, E. M., Weijma, J., Beenackers, A. A., Dolfing, J., & Janssen, D. B.** (1994). Cometabolic degradation of trichloroethylene by *Pseudomonas cepacia* G4 in a chemostat with toluene as the primary substrate. *Applied and Environmental Microbiology*, 60 (9), 3368-3374.

**Large, P. J., & Bamforth, C. W.** (1988). *Methylotrophy and biotechnology* Longman Scientific & Technical; Wiley.

**Larsson, A., & Sjoberg, B. M.** (1986). Identification of the stable free radical tyrosine residue in ribonucleotide reductase. *The EMBO Journal*, 5 (8), 2037-2040.

**Leahy, J. G., Batchelor, P. J., & Morcomb, S. M.** (2003). Evolution of the soluble diiron monooxygenases. *FEMS Microbiology Reviews*, 27 (4), 449-479.

**Learmonth, D. A., & Freitas, A. P.** (2002). Chemical synthesis and characterization of conjugates of a novel catechol-o-methyltransferase inhibitor. *Bioconjugate Chemistry*, 13 (5), 1112-1118.

**Learmonth, D. A., Vieira-Coelho, M. A., Benes, J., Alves, P. C., Borges, N., Freitas, A. P., & Soares-da-Silva, P.** (2002). Synthesis of 1-(3, 4-dihydroxy-5-nitrophenyl)- 2-phenyl-ethanone and derivatives as potent and long-acting peripheral inhibitors of catechol-O-methyltransferase. *Journal of Medicinal Chemistry*, 45 (3), 685-695.

**Lee, S. K., Fox, B. G., Froland, W. A., Lipscomb, J. D., & Munck, E.** (1993). A transient intermediate of the methane monooxygenase catalytic cycle containing an FeIV FeIV cluster. *Journal of the American Chemical Society*, 115 (14), 6450-6451.

**Lee, S., & Lipscomb, J. D.** (1999). Oxygen activation catalyzed by methane monooxygenase hydroxylase component: proton delivery during the OO bond cleavage steps. *Biochemistry*, 38 (14), 4423-4432.

**Lee, S. J., McCormick, M. S., Lippard, S. J., & Cho, U. S.** (2013). Control of substrate access to the active site in methane monooxygenase. *Nature*, 494 (7437), 380-384.

**Lee, S. K., Nesheim, J. C., & Lipscomb, J. D.** (1993). Transient intermediates of the methane monooxygenase catalytic cycle. *The Journal of Biological Chemistry*, 268 (29), 21569-21577.

**Lee, W., Wood, T. K., & Chen, W.** (2006). Engineering TCE-degrading rhizobacteria for heavy metal accumulation and enhanced TCE degradation. *Biotechnology and Bioengineering*, 95 (3), 399-403.

**Lelieveld, J., Crutzen, P., & Brühl, C.** (1993). Climate effects of atmospheric methane. *Chemosphere*, 26 (1), 739-768.

**Lidstrom, M. E.** (2006). Aerobic methylotrophic prokaryotes. *The Prokaryotes: Volume 2: Ecophysiology and Biochemistry*, 618-634.

**Lieberman, R. L., & Rosenzweig, A. C.** (2004). Biological methane oxidation: regulation, biochemistry, and active site structure of particulate methane monooxygenase. *Critical Reviews in Biochemistry and Molecular Biology*, 39 (3), 147-164.

**Lieberman, R. L., & Rosenzweig, A. C.** (2005). Crystal structure of a membrane-bound metalloenzyme that catalyses the biological oxidation of methane. *Nature*, 434 (7030), 177-182.

**Lieberman, R. L., Shrestha, D. B., Doan, P. E., Hoffman, B. M., Stemmler, T. L., & Rosenzweig, A. C.** (2003). Purified particulate methane monooxygenase from *Methylococcus capsulatus* (Bath) is a dimer with both mononuclear copper and a copper-containing cluster. *Proceedings of the National Academy of Sciences of the United States of America*, 100 (7), 3820-3825.

**Lindner, A. S., Adriaens, P., & Semrau, J. D.** (2000). Transformation of ortho-substituted biphenyls by *Methylosinus trichosporium* OB3b: substituent effects on oxidation kinetics and product formation. *Archives of Microbiology*, 174 (1-2), 35-41.

**Lippard, S. J.** (2005). Hydroxylation of C-H bonds at carboxylate-bridged diiron centres. *Philosophical Transactions. Series A, Mathematical, Physical, and Engineering Sciences*, 363 (1829), 861-77; discussion 1035-40.

**Lipscomb, J. D.** (1994). Biochemistry of the soluble methane monooxygenase. *Annual Reviews in Microbiology*, 48 (1), 371-399.

**Liu, K. E., Johnson, C. C., Newcomb, M., & Lippard, S. J.** (1993). Radical clock substrate probes and kinetic isotope effect studies of the hydroxylation of hydrocarbons by methane monooxygenase. *Journal of the American Chemical Society*, 115 (3), 939-947.

**Liu, K. E., Valentine, A. M., Wang, D., Huynh, B. H., Edmondson, D. E., Salifoglou, A., & Lippard, S. J.** (1995). Kinetic and spectroscopic characterization of intermediates and component interactions in reactions of methane monooxygenase from *Methylococcus capsulatus* (Bath). *Journal of the American Chemical Society*, 117 (41), 10174-10185.

**Liu, K. E., Wang, D., Huynh, B. H., Edmondson, D. E., Salifoglou, A., & Lippard, S. J.** (1994). Spectroscopic detection of intermediates in the reaction of dioxygen with the reduced methane monooxygenase/hydroxylase from *Methylococcus capsulatus* (Bath). *Journal of the American Chemical Society*, 116 (16), 7465-7466.

**Liu, X., Zhou, B., Xue, L., Yen, F., Chu, P., Un, F., & Yen, Y.** (2007). Ribonucleotide reductase subunits M2 and p53R2 are potential biomarkers for metastasis of colon cancer. *Clinical Colorectal Cancer*, 6 (5), 374-381.

- Liu, Y., Nesheim, J. C., Paulsen, K. E., Stankovich, M. T., & Lipscomb, J. D.** (1997). Roles of the methane monooxygenase reductase component in the regulation of catalysis. *Biochemistry*, 36 (17), 5223-5233.
- Liu, Q., Chai, J., Moche, M., Guy, J., Lindqvist, Y., & Shanklin, J.** (2015). Half-of-the-Sites Reactivity of the Castor Delta 9-18:0-Acyl Carrier Protein Desaturase. *Plant Physiology*, 169 (1), 432-441.
- Lloyd, J. S., Bhambra, A., Murrell, J. C., & Dalton, H.** (1997). Inactivation of the regulatory protein B of soluble methane monooxygenase from *Methylococcus capsulatus* (Bath) by proteolysis can be overcome by a Gly to Gln modification. *European Journal of Biochemistry / FEBS*, 248 (1), 72-79.
- Lloyd, J. S., Finch, R., Dalton, H., & Murrell, J. C.** (1999). Homologous expression of soluble methane monooxygenase genes in *Methylosinus trichosporium* OB3b. *Microbiology (Reading, England)*, 145, 461-470.
- Lou, Y., Schwender, J., & Shanklin, J.** (2014). FAD2 and FAD3 desaturases form heterodimers that facilitate metabolic channeling in vivo. *The Journal of Biological Chemistry*, 289 (26), 17996-18007.
- Lou, Y., & Shanklin, J.** (2010). Evidence that the yeast desaturase Ole1p exists as a dimer in vivo. *The Journal of Biological Chemistry*, 285 (25), 19384-19390.
- Lund, J., Woodland, M. P., & Dalton, H.** (1985). Electron transfer reactions in the soluble methane monooxygenase of *Methylococcus capsulatus* (Bath). *European Journal of Biochemistry*, 147 (2), 297-305.

- Luo, M. F., Wu, H., Wang, L., & Xing, X. H.** (2007). Study on the structure and function of a stable methane-oxidizing mixed microbial consortium. *Wei Sheng Wu Xue Bao = Acta Microbiologica Sinica*, 47 (1), 103-109.
- Martin, H., & Murrell, J.** (1995). Methane monooxygenase mutants of *Methylosinus trichosporium* constructed by marker-exchange mutagenesis. *FEMS Microbiology Letters*, 127 (3), 243-248.
- Maugard, T., Enaud, E., Sayette, A. d. L., Choisy, P., & Legoy, M. D.** (2002).  $\beta$ -Glucosidase-Catalyzed Hydrolysis of Indican from Leaves of *Polygonum tinctorium*. *Biotechnology Progress*, 18 (5), 1104-1108.
- McCormick, M. S., & Lippard, S. J.** (2011). Analysis of substrate access to active sites in bacterial multicomponent monooxygenase hydroxylases: X-ray crystal structure of xenon-pressurized phenol hydroxylase from *Pseudomonas* sp. OX1. *Biochemistry*, 50 (51), 11058-11069.
- McDonald, I. R., Uchiyama, H., Kambe, S., Yagi, O., & Murrell, J. C.** (1997). The soluble methane monooxygenase gene cluster of the trichloroethylene-degrading methanotroph *Methylocystis* sp. strain M. *Applied and Environmental Microbiology*, 63 (5), 1898-1904.
- McMurry, T. J., & Groves, J. T.** (1986). Metalloporphyrin models for cytochrome P-450. *Cytochrome P-450* (pp. 1-28) Springer.
- Merkx, M., Kopp, D. A., Sazinsky, M. H., Blazyk, J. L., Müller, J., & Lippard, S. J.** (2001). Dioxygen activation and methane hydroxylation by soluble methane monooxygenase: a tale of two irons and three proteins. *Angewandte Chemie International Edition*, 40 (15), 2782-2807.

**Merkx, M., & Lippard, S. J.** (2002). Why OrfY? Characterization of MMOD, a long overlooked component of the soluble methane monooxygenase from *Methylococcus capsulatus* (Bath). *The Journal of Biological Chemistry*, 277 (8), 5858-5865.

**Merrick, M.** (1993). In a class of its own—the RNA polymerase sigma factor  $\sigma$ ; 54 ( $\sigma$ N). *Molecular Microbiology*, 10 (5), 903-909.

**Michel, H.** (1991). General and practical aspects of membrane protein crystallization. *Crystallization of Membrane Proteins*, 73-88.

**Miyaji, A., Kamachi, T., & Okura, I.** (2002). Improvement of the purification method for retaining the activity of the particulate methane monooxygenase from *Methylosinus trichosporium* OB3b. *Biotechnology Letters*, 24 (22), 1883-1887.

**Murray, L. J., & Lippard, S. J.** (2007). Substrate trafficking and dioxygen activation in bacterial multicomponent monooxygenases. *Accounts of Chemical Research*, 40 (7), 466-474.

**Murray, L. J., Naik, S. G., Ortillo, D. O., García-Serres, R., Lee, J. K., Huynh, B. H., & Lippard, S. J.** (2007). Characterization of the arene-oxidizing intermediate in ToMOH as a diiron (III) species. *Journal of the American Chemical Society*, 129 (46), 14500-14510.

**Murrell, J. C., McDonald, I. R., & Gilbert, B.** (2000). Regulation of expression of methane monooxygenases by copper ions. *Trends in Microbiology*, 8 (5), 221-225.

**Murrell, J., & Smith, T.** (2010). Biochemistry and molecular biology of methane monooxygenase. *Handbook of Hydrocarbon and Lipid Microbiology*, 1045-1055.

**Myronova, N., Kitmitto, A., Collins, R. F., Miyaji, A., & Dalton, H.** (2006). Three-dimensional structure determination of a protein supercomplex that oxidizes methane to formaldehyde in *Methylococcus capsulatus* (Bath). *Biochemistry*, 45 (39), 11905-11914.

**Nakajima, T., Uchiyama, H., Yagi, O., & Nakahara, T.** (1992). Purification and properties of a soluble methane monooxygenase from *Methylocystis* sp. *M. Bioscience, Biotechnology, and Biochemistry*, 56 (5), 736-740.

**Newman, L. M., & Wackett, L. P.** (1995). Purification and characterization of toluene 2-monooxygenase from *Burkholderia cepacia* G4. *Biochemistry*, 34 (43), 14066-14076.

**Nguyen, H. H., Elliott, S. J., Yip, J. H., & Chan, S. I.** (1998). The particulate methane monooxygenase from *Methylococcus capsulatus* (Bath) is a novel copper-containing three-subunit enzyme. Isolation and characterization. *The Journal of Biological Chemistry*, 273 (14), 7957-7966.

**Nguyen, H. H., Shiemke, A. K., Jacobs, S. J., Hales, B. J., Lidstrom, M. E., & Chan, S. I.** (1994). The nature of the copper ions in the membranes containing the particulate methane monooxygenase from *Methylococcus capsulatus* (Bath). *The Journal of Biological Chemistry*, 269 (21), 14995-15005.

**Nichol, T.** (2011). Mutagenic Studies into the Catalytic Versatility of Soluble Methane Monooxygenase (PhD thesis at Sheffield Hallam University).

**Nonhebel, D. C., Tedder, J. M., & Walton, J. C.** (1979). *Radicals* CUP Archive.

**Nordlund, P., Dalton, H., & Eklund, H.** (1992). The active site structure of methane monooxygenase is closely related to the binuclear iron center of ribonucleotide reductase. *FEBS Letters*, 307 (3), 257-262.

**Nordlund, P., & Eklund, H.** (1993). Structure and function of the Escherichia coli ribonucleotide reductase protein R2. *Journal of Molecular Biology*, 232 (1), 123-164.

**Nordlund, P., & Eklund, H.** (1995). Di-iron—carboxylate proteins. *Current Opinion in Structural Biology*, 5 (6), 758-766.

**Nordlund, P., Sjöberg, B., & Eklund, H.** (1990). Three-dimensional structure of the free radical protein of ribonucleotide reductase.

**Ogiso, T., Ueno, C., Dianou, D., Huy, T. V., Katayama, A., Kimura, M., & Asakawa, S.** (2012). *Methylomonas koyamae* sp. nov., a type I methane-oxidizing bacterium from floodwater of a rice paddy field. *International Journal of Systematic and Evolutionary Microbiology*, 62(Pt 8), 1832-1837.

**Olsen, R. H., Kukor, J. J., & Kaphammer, B.** (1994). A novel toluene-3-monooxygenase pathway cloned from *Pseudomonas pickettii* PKO1. *Journal of Bacteriology*, 176 (12), 3749-3756.

**Op den Camp, Huub JM, Islam, T., Stott, M. B., Harhangi, H. R., Hynes, A., Schouten, S., Dunfield, P. F.** (2009). Environmental, genomic and taxonomic perspectives on methanotrophic Verrucomicrobia. *Environmental Microbiology Reports*, 1 (5), 293-306.

**Park, J. H., Aravind, L., Wolff, E. C., Kaevel, J., Kim, Y. S., & Park, M. H.** (2006). Molecular cloning, expression, and structural prediction of deoxyhypusine hydroxylase: a HEAT-repeat-containing metalloenzyme. *Proceedings of the National Academy of Sciences of the United States of America*, *103*(1), 51-56.

**Park, M. H.** (2006). The post-translational synthesis of a polyamine-derived amino acid, hypusine, in the eukaryotic translation initiation factor 5A (eIF5A). *Journal of Biochemistry*, *139* (2), 161-169. doi:139/2/161 [pii]

**Patel, R. N., & Savas, J. C.** (1987). Purification and properties of the hydroxylase component of methane monooxygenase. *Journal of Bacteriology*, *169* (5), 2313-2317.

**Paulsen, K. E., Liu, Y., Fox, B. G., Lipscomb, J. D., Munck, E., & Stankovich, M. T.** (1994). Oxidation-reduction potentials of the methane monooxygenase hydroxylase component from *Methylosinus trichosporium* OB3b. *Biochemistry*, *33* (3), 713-722.

**Paulsen, K. E., Liu, Y., Fox, B. G., Lipscomb, J. D., Munck, E., & Stankovich, M. T.** (1994). Oxidation-reduction potentials of the methane monooxygenase hydroxylase component from *Methylosinus trichosporium* OB3b. *Biochemistry*, *33* (3), 713-722.

**Periana, R. A., Taube, D. J., Evitt, E. R., Loffler, D. G., Wentrcek, P. R., Voss, G., & Masuda, T.** (1993). A mercury-catalyzed, high-yield system for the oxidation of methane to methanol. *Science (New York, N.Y.)*, *259* (5093), 340-343.

**Pfluger, A. R., Wu, W., Pieja, A. J., Wan, J., Rostkowski, K. H., & Criddle, C. S.** (2011). Selection of Type I and Type II methanotrophic proteobacteria in a fluidized bed reactor under non-sterile conditions. *Bioresource Technology*, 102 (21), 9919-9926.

**Pham, M. D., Lin, Y., Van Vuong, Q., Nagababu, P., Chang, B. T., Ng, K. Y., Li, M. S.** (2015). Inactivation of the particulate methane monooxygenase (pMMO) in *Methylococcus capsulatus* (Bath) by acetylene. *Biochimica Et Biophysica Acta (BBA)-Proteins and Proteomics*,

**Pikus, J. D., Mitchell, K. H., Studts, J. M., McClay, K., Steffan, R. J., & Fox, B. G.** (2000). Threonine 201 in the diiron enzyme toluene 4-monooxygenase is not required for catalysis. *Biochemistry*, 39 (4), 791-799.

**Pikus, J. D., Studts, J. M., McClay, K., Steffan, R. J., & Fox, B. G.** (1997). Changes in the regiospecificity of aromatic hydroxylation produced by active site engineering in the diiron enzyme toluene 4-monooxygenase. *Biochemistry*, 36 (31), 9283-9289.

**Pilkington, S. J., & Dalton, H.** (1990). Soluble methane monooxygenase from *Methylococcus capsulatus* bath. *Methods in Enzymology*, 188, 181-190.

**Pol, A., Heijmans, K., Harhangi, H. R., Tedesco, D., Jetten, M. S., & den Camp, Huub JM Op.** (2007). Methanotrophy below pH 1 by a new Verrucomicrobia species. *Nature*, 450 (7171), 874-878.

**Prior, S. D., & Dalton, H.** (1985). The effect of copper ions on membrane content and methane monooxygenase activity in methanol-grown cells of *Methylococcus capsulatus* (Bath). *Microbiology*, 131(1), 155-163

**Que, L., & True, A. E.** (1990). Dinuclear iron-and manganese-oxo sites in biology. *Progress in Inorganic Chemistry: Bioinorganic Chemistry, Volume 38*, 97-200.

**Raag, R., Martinis, S. A., Sligar, S. G., & Poulos, T. L.** (1991). Crystal structure of the cytochrome P-450CAM active site mutant Thr 252 Ala. *Biochemistry*, 30 (48), 11420-11429.

**Ramanathan, V., Cicerone, R. J., Singh, H. B., & Kiehl, J. T.** (1985). Trace gas trends and their potential role in climate change. *Journal of Geophysical Research: Atmospheres (1984–2012)*, 90 (D3), 5547-5566.

**Reichard, P.** (1988). Interactions between deoxyribonucleotide and DNA synthesis. *Annual Review of Biochemistry*, 57 (1), 349-374.

**Ricke, P., Erkel, C., Kube, M., Reinhardt, R., & Liesack, W.** (2004). Comparative analysis of the conventional and novel pmo (particulate methane monooxygenase) operons from *Methylocystis* strain SC2. *Applied and Environmental Microbiology*, 70 (5), 3055-3063.

**Rocha-Rios, J., Bordel, S., Hernández, S., & Revah, S.** (2009). Methane degradation in two-phase partition bioreactors. *Chemical Engineering Journal*, 152 (1), 289-292.

**Rosenzweig, A. C., Brandstetter, H., Whittington, D. A., Nordlund, P., Lippard, S. J., & Frederick, C. A.** (1997). Crystal structures of the methane monooxygenase hydroxylase from *Methylococcus capsulatus* (Bath): implications for substrate gating and component interactions. *Proteins: Structure, Function, and Bioinformatics*, 29 (2), 141-152.

**Rosenzweig, A. C., Frederick, C. A., & Lippard, S. J.** (1993). Crystal structure of a bacterial non-haem iron hydroxylase that catalyses the biological oxidation of methane.

**Rosenzweig, A. C., Nordlund, P., Takahara, P. M., Frederick, C. A., & Lippard, S. J.** (1995). Geometry of the soluble methane monooxygenase catalytic diiron center in two oxidation states. *Chemistry & Biology*, 2 (6), 409-418.

**Rui, L., Kwon, Y. M., Fishman, A., Reardon, K. F., & Wood, T. K.** (2004). Saturation mutagenesis of toluene ortho-monooxygenase of *Burkholderia cepacia* G4 for Enhanced 1-naphthol synthesis and chloroform degradation. *Applied and Environmental Microbiology*, 70(6), 3246-3252. doi:10.1128/AEM.70.6.3246-3252.

**Rui, L., Reardon, K. F., & Wood, T. K.** (2005). Protein engineering of toluene ortho-monooxygenase of *Burkholderia cepacia* G4 for regiospecific hydroxylation of indole to form various indigoid compounds. *Applied Microbiology and Biotechnology*, 66(4), 422-429

**Saeki, H., & Furuhashi, K.** (1994). Cloning and characterization of a *Nocardia corallina* B-276 gene cluster encoding alkene monooxygenase. *Journal of Fermentation and Bioengineering*, 78 (6), 399-406.

**Sambrook, J., Fritsch, E. F., & Maniatis, T.** (1989). *Molecular cloning* Cold spring harbor laboratory press New York.

**Sazinsky, M. H., Bard, J., Di Donato, A., & Lippard, S. J.** (2004). Crystal structure of the toluene/o-xylene monooxygenase hydroxylase from

*Pseudomonas stutzeri* OX1. Insight into the substrate specificity, substrate channeling, and active site tuning of multicomponent monooxygenases. *The Journal of Biological Chemistry*, 279 (29), 30600-30610.

**Sazinsky, M. H., Dunten, P. W., McCormick, M. S., DiDonato, A., & Lippard, S. J.** (2006). X-ray structure of a hydroxylase-regulatory protein complex from a hydrocarbon-oxidizing multicomponent monooxygenase, *Pseudomonas* sp. OX1 phenol hydroxylase. *Biochemistry*, 45 (51), 15392-15404.

**Sazinsky, M. H., & Lippard, S. J.** (2006). Correlating structure with function in bacterial multicomponent monooxygenases and related diiron proteins. *Accounts of Chemical Research*, 39 (8), 558-566.

**Scanlan, J., Dumont, M. G., & Murrell, J. C.** (2009). Involvement of MmoR and MmoG in the transcriptional activation of soluble methane monooxygenase genes in *Methylosinus trichosporium* OB3b. *FEMS Microbiology Letters*, 301 (2), 181-187.

**Scharrenburg, G. v., & Frankena, J.** (1996). Biokatalyse helpt farmaceutische industrie bij asymmetrische synthese. *Chemisch Magazine*, 4, 284-286.

**Semrau, J. D., Chistoserdov, A., Lebron, J., Costello, A., Davagnino, J., Kenna, E., Lidstrom, M. E.** (1995). Particulate methane monooxygenase genes in methanotrophs. *Journal of Bacteriology*, 177 (11), 3071-3079.

**Semrau, J. D., DiSpirito, A. A., & Yoon, S.** (2010). Methanotrophs and copper. *FEMS Microbiology Reviews*, 34 (4), 496-531.

**Semrau, J. D., Jagadevan, S., DiSpirito, A. A., Khalifa, A., Scanlan, J., Bergman, B. H., Murrell, J. C.** (2013). Methanobactin and MmoD work in

concert to act as the 'copper-switch' in methanotrophs. *Environmental Microbiology*, 15(11):3077-86.

**Shanklin, J., & Somerville, C.** (1991). Stearoyl-acyl-carrier-protein desaturase from higher plants is structurally unrelated to the animal and fungal homologs. *Proceedings of the National Academy of Sciences of the United States of America*, 88 (6), 2510-2514.

**Shaofeng, H., Shuben, L., Jiayin, X., Jianzhong, N., Chungu, X., Haidong, T., & Wei, T.** (2007). Purification and biochemical characterization of soluble methane monooxygenase hydroxylase from *Methylosinus trichosporium* IMV 3011. *Bioscience, Biotechnology, and Biochemistry*, 71 (1), 122-129.

**Shen, R., Yu, C., Ma, Q., & Li, S.** (1997). Direct Evidence for a Soluble Methane Monooxygenase from Type I Methanotrophic Bacteria: Purification and Properties of a Soluble Methane Monooxygenase from *Methylomonas* sp. GYJ3. *Archives of Biochemistry and Biophysics*, 345 (2), 223-229.

**Shields, M. S., Montgomery, S. O., Chapman, P. J., Cuskey, S. M., & Pritchard, P. H.** (1989). Novel pathway of toluene catabolism in the trichloroethylene-degrading bacterium g4. *Applied and Environmental Microbiology*, 55 (6), 1624-1629.

**Shields, M. S., & Francesconi, S. C.** (1997). Microbial degradation of trichloroethylene dichloroethylenes and aromatic pollutants. *Biotechnology Advances*, 15(2), 556-556.

**Shu, L., Nesheim, J. C., Kauffmann, K., Munck, E., Lipscomb, J. D., & Que, L., Jr.** (1997). An Fe<sub>2</sub>IVO<sub>2</sub> diamond core structure for the key intermediate Q of methane monooxygenase. *Science (New York, N.Y.)*, 275 (5299), 515-518.

**Simon, R., Priefer, U., & Pühler, A.** (1983). A broad host range mobilization system for in vivo genetic engineering: transposon mutagenesis in gram negative bacteria. *Nature Biotechnology*, 1 (9), 784-791.

**Sirajuddin, S., & Rosenzweig, A. C.** (2015). Enzymatic oxidation of methane. *Biochemistry*, 54 (14), 2283-2294.

**Sirajuddin, S., Barupala, D., Helling, S., Marcus, K., Stemmler, T. L., & Rosenzweig, A. C.** (2014). Effects of zinc on particulate methane monooxygenase activity and structure. *The Journal of Biological Chemistry*, 289 (31), 21782-21794.

**Sjöberg, B.** (1997). Ribonucleotide reductases—a group of enzymes with different metallosites and a similar reaction mechanism. *Metal Sites in Proteins and Models* (pp. 139-173) Springer.

**Sluis, M. K., Sayavedra-Soto, L. A., & Arp, D. J.** (2002). Molecular analysis of the soluble butane monooxygenase from '*Pseudomonas butanovora*'. *Microbiology (Reading, England)*, 148, 3617-3629.

**Small, F. J., & Ensign, S. A.** (1997). Alkene monooxygenase from *Xanthobacter* strain Py2 purification and characterization of a four-component system central to the bacterial metabolism of aliphatic alkenes. *Journal of Biological Chemistry*, 272 (40), 24913-24920.

**Smith, D. D. S., & Dalton, H.** (1989). Solubilisation of methane monooxygenase from *Methylococcus capsulatus* (Bath). *European Journal of Biochemistry*, 182 (3), 667-671.

**Smith, M. T.** (1999). Benzene, NQO1, and genetic susceptibility to cancer. *Proceedings of the National Academy of Sciences of the United States of America*, 96 (14), 7624-7626.

**Smith, S. M., Rawat, S., Telser, J., Hoffman, B. M., Stemmler, T. L., & Rosenzweig, A. C.** (2011). Crystal structure and characterization of particulate methane monooxygenase from *Methylocystis* species strain M. *Biochemistry*, 50 (47), 10231-10240.

**Smith, T., J., & Dalton, H.** (2004). Biocatalysis by methane monooxygenase and its implications for the petroleum industry. *Studies in Surface Science and Catalysis*, 151, 177-192.

**Smith, T. J., Lloyd, J. S., Gallagher S. C., Fosdike, W. L. J., Murrell J. C. and Dalton, H.** (1999). Heterologous expression of alkene monooxygenase from *Rhodococcus rhodochrous* B-276. *Eur. J. Biochem.* 260, 446-452

**Smith, T. J., & Murrell, J. C.** (2011). Mutagenesis of soluble methane monooxygenase. *Methods in Enzymology*, 495, 135-147.

**Smith, T. J., & Murrell, J. C.** (2010). *Methanotrophs* Wiley Online Library.

**Smith, T. J., Slade, S. E., Burton, N. P., Murrell, J. C., & Dalton, H.** (2002). Improved system for protein engineering of the hydroxylase component of

soluble methane monooxygenase. *Applied and Environmental Microbiology*, 68 (11), 5265-5273.

**Song, W. J., McCormick, M. S., Behan, R. K., Sazinsky, M. H., Jiang, W., Lin, J., Lippard, S. J.** (2010). Active site threonine facilitates proton transfer during dioxygen activation at the diiron center of toluene/o-xylene monooxygenase hydroxylase. *Journal of the American Chemical Society*, 132 (39), 13582-13585.

**Song, W. J., Gucinski, G., Sazinsky, M. H., & Lippard, S. J.** (2011). Tracking a defined route for O (2) migration in a dioxygen-activating diiron enzyme. *Proceedings of the National Academy of Sciences of the United States of America*, 108 (36), 14795-14800.

**Spain, J. C., & Gibson, D. T.** (1991). Pathway for Biodegradation of p-Nitrophenol in a *Moraxella* sp. *Applied and Environmental Microbiology*, 57 (3), 812-819.

**Stafford, G. P., Scanlan, J., McDonald, I. R., & Murrell, J. C.** (2003). *rpoN*, *mmoR* and *mmoG*, genes involved in regulating the expression of soluble methane monooxygenase in *Methylosinus trichosporium* OB3b. *Microbiology (Reading, England)*, 149, 1771-1784.

**Stanley, S., Prior, S., Leak, D., & Dalton, H.** (1983). Copper stress underlies the fundamental change in intracellular location of methane mono-oxygenase in methane-oxidizing organisms: studies in batch and continuous cultures. *Biotechnology Letters*, 5 (7), 487-492.

**Stein, L. Y., Yoon, S., Semrau, J. D., Dispirito, A. A., Crombie, A., Murrell, J. C., Klotz, M. G.** (2010). Genome sequence of the obligate methanotroph *Methylosinus trichosporium* strain OB3b. *Journal of Bacteriology*, 192 (24), 6497-6498.

**Stoecker, K., Bendinger, B., Schoning, B., Nielsen, P. H., Nielsen, J. L., Baranyi, C., Wagner, M.** (2006). Cohn's *Crenothrix* is a filamentous methane oxidizer with an unusual methane monooxygenase. *Proceedings of the National Academy of Sciences of the United States of America*, 103 (7), 2363-2367.

**Stolyar, S., Costello, A. M., Peeples, T. L., & Lidstrom, M. E.** (1999). Role of multiple gene copies in particulate methane monooxygenase activity in the methane-oxidizing bacterium *Methylococcus capsulatus* Bath. *Microbiology (Reading, England)*, 145, 1235-1244.

**Takeguchi, M., Miyakawa, K., & Okura, I.** (1998). Purification and properties of particulate methane monooxygenase from *Methylosinus trichosporium* OB3b. *Journal of Molecular Catalysis A: Chemical*, 132(2), 145-153.

**Takeguchi, M., Miyakawa, K., & Okura, I.** (1999). The role of copper in particulate methane monooxygenase from *Methylosinus trichosporium* OB3b. *Journal of Molecular Catalysis A: Chemical*, 137 (1), 161-168.

**Tanaka, H., Arakawa, H., Yamaguchi, T., Shiraishi, K., Fukuda, S., Matsui, K., Nakamura, Y.** (2000). A ribonucleotide reductase gene involved in a p53-dependent cell-cycle checkpoint for DNA damage. *Nature*, 404 (6773), 42-49.

**Tate, S., & Dalton, H.** (1999). A low-molecular-mass protein from *Methylococcus capsulatus* (Bath) is responsible for the regulation of

formaldehyde dehydrogenase activity in vitro. *Microbiology (Reading, England)*, 145, 159-167.

**Tchawa Yimga, M., Dunfield, P. F., Ricke, P., Heyer, J., & Liesack, W.**

(2003). Wide distribution of a novel pmoA-like gene copy among type II methanotrophs, and its expression in *Methylocystis* strain SC2. *Applied and Environmental Microbiology*, 69 (9), 5593-5602.

**Theisen, A. R., Ali, M. H., Radajewski, S., Dumont, M. G., Dunfield, P. F.,**

**McDonald, I. R., Murrell, J. C.** (2005). Regulation of methane oxidation in the facultative methanotroph *Methylocella silvestris* BL2. *Molecular Microbiology*, 58 (3), 682-692.

**Thompson, G. M., Cano, V. S., & Valentini, S. R.** (2003). Mapping eIF5A

binding sites for Dys1 and Lia1: in vivo evidence for regulation of eIF5A hypusination. *FEBS Letters*, 555 (3), 464-468.

**Tinberg, C. E., & Lippard, S. J.** (2009). Revisiting the mechanism of dioxygen

activation in soluble methane monooxygenase from *M. capsulatus* (Bath): Evidence for a multi-step, proton-dependent reaction pathway. *Biochemistry*, 48 (51), 12145-12158.

**Torrissen, O., & Christiansen, R.** (1995). Requirements for carotenoids in fish

diets. *Journal of Applied Ichthyology*, 11(3-4), 225-230.

**Tukhvatullin, I. A., Gvozdev, R. I., & Andersson, K. K.** (2000). The structure

of the active center of beta-peptide membrane-bound methane monooxygenase (pMMO) from *Methylococcus capsulatus* bath. *Doklady Biochemistry* :

*Proceedings of the Academy of Sciences of the USSR, Biochemistry Section / Translated from Russian, 374 (1-6), 177-182.*

**Uhlin, U., & Eklund, H.** (1994). Structure of ribonucleotide reductase protein R1.

**Umezawa, K., Kawakami, M., & Watanabe, T.** (2003). Molecular design and biological activities of protein-tyrosine phosphatase inhibitors. *Pharmacology & Therapeutics*, 99 (1), 15-24.

**Van Beilen, J. B., Duetz, W. A., Schmid, A., & Witholt, B.** (2003). Practical issues in the application of oxygenases. *Trends in Biotechnology*, 21(4), 170-177.

**Vardar, G., Tao, Y., Lee, J., & Wood, T. K.** (2005). Alanine 101 and alanine 110 of the alpha subunit of *Pseudomonas stutzeri* OX1 toluene-o-xylene monooxygenase influence the regiospecific oxidation of aromatics. *Biotechnology and Bioengineering*, 92 (5), 652-658.

**Vas, G., & Vekey, K.** (2004). Solid-phase microextraction: a powerful sample preparation tool prior to mass spectrometric analysis. *Journal of Mass Spectrometry*, 39 (3), 233-254.

**Vigliotta, G., Nutricati, E., Carata, E., Tredici, S. M., De Stefano, M., Pontieri, P., Alifano, P.** (2007). *Clonothrix fusca* Roze 1896, a filamentous, sheathed, methanotrophic gamma-proteobacterium. *Applied and Environmental Microbiology*, 73 (11), 3556-3565.

**Vincent, J. B., Olivier-Lilley, G. L., & Averill, B. A.** (1990). Proteins containing oxo-bridged dinuclear iron centers: a bioinorganic perspective. *Chemical Reviews*, 90 (8), 1447-1467.

**Vorobev, A. V., Baani, M., Doronina, N. V., Brady, A. L., Liesack, W., Dunfield, P. F., & Dedysh, S. N.** (2011). *Methyloferula stellata* gen. nov., sp. nov., an acidophilic, obligately methanotrophic bacterium that possesses only a soluble methane monooxygenase. *International Journal of Systematic and Evolutionary Microbiology*, 61 (Pt 10), 2456-2463.

**Wallar, B. J., & Lipscomb, J. D.** (1996). Dioxygen activation by enzymes containing binuclear non-heme iron clusters. *Chemical Reviews*, 96 (7), 2625-2658.

**Wallar, B. J., & Lipscomb, J. D.** (2001). Methane monooxygenase component B mutants alter the kinetics of steps throughout the catalytic cycle. *Biochemistry*, 40 (7), 2220-2233.

**Walters, K. J., Gassner, G. T., Lippard, S. J., & Wagner, G.** (1999). Structure of the soluble methane monooxygenase regulatory protein B. *Proceedings of the National Academy of Sciences of the United States of America*, 96 (14), 7877-7882.

**Wang, W., Jacob, R. E., Luoh, R. P., Engen, J. R., & Lippard, S. J.** (2014). Electron transfer control in soluble methane monooxygenase. *Journal of the American Chemical Society*, 136 (27), 9754-9762.

**Wang, W., & Lippard, S. J.** (2014). Diiron oxidation state control of substrate access to the active site of soluble methane monooxygenase mediated by the

regulatory component. *Journal of the American Chemical Society*, 136 (6), 2244-2247.

**West, C. A., Salmond, G. P. C., Dalton, H., & Murrell, J. C.** (1992). Functional expression in *Escherichia coli* of proteins B and C from soluble methane monooxygenase of *Methylococcus capsulatus* (Bath). *Journal of General Microbiology*, 138 (7), 1301-1307.

**White, R. E., & Coon, M. J.** (1980). Oxygen activation by cytochrome P-450. *Annual Review of Biochemistry*, 49(1), 315-356.

**Whited, G. M., & Gibson, D. T.** (1991). Toluene-4-monooxygenase, a three-component enzyme system that catalyzes the oxidation of toluene to p-cresol in *Pseudomonas mendocina* KR1. *Journal of Bacteriology*, 173(9), 3010-3016.

**Whittenbury, R.** (1981). The interrelationship of autotrophy and methylotrophy as seen in *Methylococcus capsulatus* (Bath). *Microbial Growth on C1 Compounds*. Heyden, London, 181-190.

**Whittenbury, R., & Dalton, H.** (1981). The methylotrophic bacteria. *The prokaryotes* (pp. 894-902) Springer.

**Whittenbury, R., & Krieg, N.** (1989). Family IV. Methylococcaceae fam. nov. *Bergey's manual of systematic bacteriology* (pp. 256-261) Williams & Wilkins Baltimore.

**Whittenbury, R., Phillips, K. C., & Wilkinson, J. F.** (1970). Enrichment, isolation and some properties of methane-utilizing bacteria. *Journal of General Microbiology*, 61 (2), 205-218.

- Wolff, E. C., Lee, Y. B., Chung, S. I., Folk, J., & Park, M. H.** (1995). Deoxyhypusine synthase from rat testis: purification and characterization. *Journal of Biological Chemistry*, 270 (15), 8660-8666.
- Woodland, M. P., & Dalton, H.** (1984). Purification and characterization of component A of the methane monooxygenase from *Methylococcus capsulatus* (Bath). *The Journal of Biological Chemistry*, 259 (1), 53-59.
- Worsey, M. J., & Williams, P. A.** (1975). Metabolism of toluene and xylenes by *Pseudomonas putida* (arvilla) mt-2: evidence for a new function of the TOL plasmid. *Journal of Bacteriology*, 124 (1), 7-13.
- Yen, K. M., & Karl, M. R.** (1992). Identification of a new gene, tmoF, in the *Pseudomonas mendocina* KR1 gene cluster encoding toluene-4-monooxygenase. *Journal of Bacteriology*, 174 (22), 7253-7261.
- Yen, K. M., Karl, M. R., Blatt, L. M., Simon, M. J., Winter, R. B., Fausset, P. R., Chen, K. K.** (1991). Cloning and characterization of a *Pseudomonas mendocina* KR1 gene cluster encoding toluene-4-monooxygenase. *Journal of Bacteriology*, 173 (17), 5315-5327.
- Yoon, S., Im, J., Bandow, N., DiSpirito, A. A., & Semrau, J. D.** (2011). Constitutive expression of pMMO by *Methylocystis* strain SB2 when grown on multi-carbon substrates: implications for biodegradation of chlorinated ethenes. *Environmental Microbiology Reports*, 3 (2), 182-188.
- Zahn, J. A., & DiSpirito, A. A.** (1996). Membrane-associated methane monooxygenase from *Methylococcus capsulatus* (Bath). *Journal of Bacteriology*, 178 (4), 1018-1029.

**Zayed, A. M., & Terry, N.** (2003). Chromium in the environment: factors affecting biological remediation. *Plant and Soil*, 249 (1), 139-156.

**Zhou, B., Tsai, P., Ker, R., Tsai, J., Ho, R., Yu, J., Yen, Y.** (1998). Overexpression of transfected human ribonucleotide reductase M2 subunit in human cancer cells enhances their invasive potential. *Clinical & Experimental Metastasis*, 16 (1), 43-49.

**Zhou, B. S., Hsu, N. Y., Pan, B. C., Doroshov, J. H., & Yen, Y.** (1995). Overexpression of ribonucleotide reductase in transfected human KB cells increases their resistance to hydroxyurea: M2 but not M1 is sufficient to increase resistance to hydroxyurea in transfected cells. *Cancer Research*, 55 (6), 1328-1333.

**Zhou, N. Y., Jenkins, A., Chan Kwo Chion, C. K., & Leak, D. J.** (1999). The alkene monooxygenase from Xanthobacter strain Py2 is closely related to aromatic monooxygenases and catalyzes aromatic monohydroxylation of benzene, toluene, and phenol. *Applied and Environmental Microbiology*, 65 (4), 1589-1595.

**Zúñiga, C., Morales, M., Le Borgne, S., & Revah, S.** (2011). Production of poly- $\beta$ -hydroxybutyrate (PHB) by *Methylobacterium organophilum* isolated from a methanotrophic consortium in a two-phase partition bioreactor. *Journal of Hazardous Materials*, 190 (1), 876-882.

